~~NUREG/CR-4481~~
~~SAND85-2743~~

Note: This report was never published.

~~NUREG/CR-4481~~
~~SAND85-2743~~

Jocelyn

This document was never published, but it is the technical basis for the grouping of fission products in the MELCOR code.

Dana

Received
3/00

NUREG/CR-4481
SAND85-2743
R3, R4, R7

FISSION PRODUCT BEHAVIOR DURING SEVERE LWR ACCIDENTS: MODELING RECOMMENDATIONS FOR THE MELCOR CODE SYSTEM

Volume I: Fission Product Release From Fuel

D. A. Powers

Published: September 1988

Sandia National Laboratories
Albuquerque, NM 87185
Operated by
Sandia Corporation
for the
U.S. Department of Energy

Prepared for
Division of Reactor System Safety
Office of Nuclear Regulatory Research
U.S. Nuclear Regulatory Commission
Washington, DC 20555
Under Memorandum of Understanding DOE 40-550-75
NRC FIN No. A1339

ABSTRACT

Phenomena that influence fission product behavior during severe accidents at light water reactors are reviewed and recommendations for the modeling of these phenomena in the MELCOR code system are presented. Specifically, modeling recommendations are presented:

1. for the grouping of fission products into chemical classes;
2. for release of fission products from degraded fuel in-vessel, during high pressure ejection of melt from the vessel, during steam explosions, and as the result of core-concrete interactions;
3. for the condensation onto and evaporation of fission product vapors from structural and aerosol surfaces, and of steam onto and from aerosols;
4. for the agglomeration and deposition of aerosols; and
5. for the removal of fission product vapors and aerosols by emergency safety features (e.g., sprays, suppression pools, ice condensers, filters).

TABLE OF CONTENTS
Volume I

TABLE OF CONTENTS (cont.)

TABLE OF CONTENTS (cont.)

TABLE OF CONTENTS (cont.)

Volume II

LIST OF ILLUSTRATIONS

LIST OF ILLUSTRATIONS

LIST OF ILLUSTRATIONS

LIST OF TABLES

LIST OF TABLES

CHAPTER 1

INTRODUCTION

Probabilistic Risk Assessment. The probabilistic assessment of the risks of severe core damage accidents at a nuclear power plant is called a PRA. A PRA analysis identifies and delineates those combinations of events that can lead to a core melt accident, and estimates the frequency of occurrence of each such combination of events and of the consequences of each event combination.

The first two nuclear reactor PRAs, those for the Surry and Peach Bottom nuclear power plants, were performed as a part of the Reactor Safety Study [1] using analytical methods that were later implemented in the computer codes, MARCH [2], CORRAL [3], and CRAC [4]. During the last decade, user experience and peer reviews have identified serious deficiencies in this series of PRA codes including (1) inadequate or inconsistent treatments of important phenomena or plant features, (2) coding that does not easily permit the uncertainties associated with predictions obtained using these codes to be estimated, (3) code structures that do not facilitate incorporation of alternative or improved phenomenological representations, (4) interfaces that are poorly matched, and (5) poor documentation.

To overcome these deficiencies the Nuclear Regulatory Commission (NRC) initiated in 1982 a major multi-year program called MELCOR that has as its objective the development of a new system of risk assessment codes, the MELCOR Code System, which (1) models appropriately all phenomena essential to the description of severe Light Water Reactor (LWR) accidents, (2) provides credible predictions of the consequences of severe accidents, (3) permits meaningful estimates of the uncertainties associated with those predictions to be made, and (4) has a structure that facilitates the incorporation of new or alternative phenomenological models.

Architecture of the MELCOR Code System. The MELCOR code system will be structured, modular, integrated (matched interfaces), and portable (coded in ANSI FORTRAN 77). Discrete phenomena or groups of closely coupled phenomena will be coded in separate modules. This will facilitate modification or replacement of phenomenological representations. Modules will be variably dimensioned, which will allow system nodalization (compartmentalization) and the size of sets of ordinary differential equations (ODEs) to be easily changed. Because all parameter values will be externally accessible, sensitivity and uncertainty studies will be relatively convenient to perform with the MELCOR code system (at least by comparison to other PRA codes).

The MELCOR code system will have four structural levels: Level 1, executive control; Level 2, data management; Level 3, phenomenological representations; and Level 4, numerical implementations. Levels 3 and 4 are likely to be closely coupled. Ex-plant consequences (i.e., health effects and economic consequences) will be solved wholly separately from in-plant thermal-hydraulic processes and fission product behavior, which will be closely coupled but solved separately. For each time step, the solution for the thermal-hydraulic equations will be developed simultaneously for all control volumes (~15 for the reactor coolant system, ~10 for the containment building, ~1 for the auxiliary building). Then, using the thermal-hydraulic solution as input, the fission product behavior equations will be solved, one control volume at a time. Where necessary, the solution for fission product behavior from the previous time step will be used to support solution of the thermal-hydraulic equations during the current time step.

Phenomenological Assessments. In order to identify those phenomena essential to the description of severe LWR accidents (i.e., the set of phenomena that should be treated by the MELCOR Code System), a series of phenomenological reviews have been performed as part of (or in support of) the MELCOR Program. Reviews of thermal-hydraulic processes [5, 6] and ex-plant consequence phenomena [7-10] are reported elsewhere. This report presents the results of the review of fission product behavior conducted as a part of the MELCOR Program.

Fission Product Behavior. During the analysis of hypothetical severe accidents at Light Water Reactors, fission product behavior is modeled in order to develop realistic source terms as a starting point for the prediction of the ex-plant consequences of the accident. The essential features of an ex-plant source term are the masses and identities of the radioisotopes released from the failed LWR containment, their chemical and physical forms, and the heat and moisture content and release time and duration of the plume that contains them.

Specification of the masses, identities, and forms of the radioisotopes released to the environment upon containment failure requires (1) calculation of the rates of release of radioactive materials from overheated or molten fuel, (2) specification of the chemical and physical forms of the released radioactive materials (e.g., CsI vapor, aerosol of a given chemical composition), (3) calculation of their rates of transport through and deposition and resuspension within the primary system and the containment, and (4) specification of changes in their chemical and physical forms during transport, deposition, or resuspension. Accordingly, this report will discuss the processes (release, agglomeration, deposition, resuspension), species (vapors, aerosols), and physical states (gas-borne, deposited or condensed on surfaces, suspended or dissolved in water), that must be treated in order to develop source terms adequate for the calculation of ex-plant consequences. Determination of the heat and moisture content and the release time and duration of the radioactive plume will not be discussed, since these quantities are generally not calculated by the fission product behavior portions of severe accident risk analysis codes.

Processes. Review of pertinent literature including documentation for published fission product behavior codes suggests that the processes listed in Table 1.1 should be treated by the fission product behavior modules of the MELCOR code system. When a process listed in Table 1.1 can take place by different mechanisms, Table 1.1 also lists those mechanisms that make significant contributions to its rate. This review concluded that adequate mathematical representations are available for each mechanism and process that should be treated by the MELCOR code system.

Species and States. Because the rate of change with time of the mass of a species (vapor or aerosol) in a state (location within a control volume) can be appropriately represented by an ordinary differential equation comprised of terms which give the contribution of individual rate processes to the total rate of change of the species, the MELCOR fission product behavior equations will consist of a set of ordinary differential equations. Since a separate ODE is required to describe each species in each state in which it can exist, detailed descriptions of fission product behavior (descriptions that involve many species and many states) can easily produce fission product behavior ODE sets that are very large (~500 ODEs). Since routine MELCOR calculations probably will be unacceptably slow if the fission product ODE set cannot be held to something like 50 ODEs, this report will also present the technical basis for adequately modeling fission product behavior using a number of species and states that produces an ODE set of approximately 50 ODEs (as few as 25 for scoping calculations; as many as 100 for sensitivity calculations).

Report Organization. Reduction of the size of the MELCOR fission product ODE set to a computationally tractable size, by limiting the number of species and states modeled by the MELCOR code system, is examined in Chapters 2 and 7 of this report. Chapters 3 through 6 review the rate processes that significantly influence fission product behavior and recommend a representation for each process.

Table 1.1

Fission Product Processes

Species	Process
Fission Product Vapors	Release from Fuel
	Chemical Reactions
	Gas Phase (gas-borne)
	Solution Phase (dissolved in water)
	Solid Phase (on surfaces)
	Condensation on Aerosols and Surfaces
	Brownian Diffusion
	Turbulent Diffusion
	Evaporation from Aerosols and Surfaces
	Intercompartment Flow
	Removal by Engineered Safety Features
	Sprays
	Ice Condensers
	Suppressions Pools
	Filters
	Fans
	Decay Heat
Aerosols	Formation
	Gas-to-Particle Conversion
	Mechanical Aerosolization
	Agglomeration
	Brownian Coagulation
	Turbulent Coagulation
	Gravitational Coagulation
	Deposition on Surfaces (walls, equipment)
	Brownian Diffusion
	Turbulent Diffusion
	Gravitational Settling
	Thermophoresis
	Diffusiophoresis
	Resuspension from Surfaces
	Intercompartment Flow
	Removal by Engineered Safety Features
	Sprays
	Ice Condensers
	Suppression Pools
	Filters
	Fans
	Decay Heat
Steam	Condensation on Aerosols
	Evaporation from Aerosols

Chapter 2 begins with an examination of radioactive decay and isotope effects, then develops the case for reducing the number of species modeled by neglecting isotope effects and grouping chemical elements into classes, and finally recommends a set of element classes for use in the modeling of in- and ex-vessel release processes. In-vessel release processes are then discussed in Chapter 3 and ex-vessel processes in Chapter 4. Chemical reactions of vapors and natural vapor deposition processes, and natural deposition processes for aerosols and aerosol agglomeration mechanisms are reviewed in Chapter 5. Removal of gas-borne species by Engineered Safety Features (ESFs) is discussed in Chapter 6. Chapter 7 examines methods for modeling aerosol agglomeration and recommends a method for use in the MELCOR code system, discusses the number of aerosol species required by the recommended agglomeration method, and then presents the technical basis for reduction of the fission product behavior ODE set to a tractable size by limiting the number of states modeled and by further reduction of the number of species modeled by combination of the chemical classes developed in Chapter 2 into components.

Lastly, for convenience this report has been divided into two volumes: Volume I, Fission Product Release From Fuel, and Volume II, Vapor and Aerosol Processes. Thus, Chapters 1 through 4 are presented in Volume I and Chapters 5 through 7 in Volume II.

REFERENCES

1. U. S. Nuclear Regulatory Commission, Reactor Safety Study - An Assessment of Accident Risks in U.S. Commercial Nuclear Power Plants, WASH-1400 (NUREG-75/014), October 1975.

2. R. O. Wooton and H. I. Avci, MARCH (Meltdown Accident Response Characteristics) Code Description and User's Manual, BMI-2064 NUREG/CR-1711 Battelle Columbus Laboratories, Columbus, OH, October 1980.

3. P. C. Owzarski and A. K. Postma, CORRAL Code User's Guide Addendum to Appendix J of Appendix VII of the Reactor Safety Study - An Assessment of Accident Risks in U. S. Commercial Nuclear Power Plants, WASH-1400 (NUREG-75/014), October 1975.

4. L. T. Ritchie, J. D. Johnson, and R. M. Blond, Calculations of Reactor Accident Consequences, Version 2 (CRAC2): Computer Code User's Guide, NUREG/CR-2326, SAND81-1994, Sandia National Laboratories, Albuquerque, NM, February 1983.

5. G. G. Weigand, et al., Thermal-Hydraulic Process Modeling in Risk Analysis: An Assessment of the Relevant Systems, Structures, and Phenomena, NUREG/CR-3986, SAND84-1219, Sandia National Laboratories, Albuquerque, NM, August 1984.

6. S. R. Greene, Realistic Simulation of Severe Accidents in BWRs -- Computer Modeling Requirements, NUREG/CR-2940, ORNL/TM-8517, Oak Ridge National Laboratories, Oak Ridge, TN, April 1984.

7. R. M. Ostmeyer and J. C. Helton, Exposure Pathways Models for Accidental Radiological Releases, Sandia National Laboratories, Albuquerque, NM (in preparation).

8. G. E. Runkle and R. M. Ostmeyer. An Assessment of Dosimetry Data for Accidental Radionuclide Releases, NUREG/CR-4185, SAND85-0283 Sandia National Laboratories, Albuquerque, NM, August 1985.

9. J. S. Evans et al., Health Effects Model for Nuclear Power Plant Accident Consequence Analysis, NUREG/CR-4214, SAND85-7185, Sandia National Laboratories, Albuquerque, NM, July 1985.

10. R. P. Burke, et al., Economic Risks of Nuclear Power Reactor Accidents, NUREG/CR-3673, SAND84-0178 Sandia National Laboratories, Albuquerque, NM, April 1984.

CHAPTER 2

ISOTOPES, ELEMENTS, AND CHEMICAL CLASSES

2.1. An Introductory Description of Severe Accident Source Terms and This Chapter

Severe accidents at commercial nuclear power plants would involve damage to the reactor fuel, emissions of radioactivity, and general plant conditions more drastic than those considered in the design and safety analysis of the plants. Great interest has developed in severe reactor accidents since the publication of the Reactor Safety Study [1] and the mild, but still beyond-design-basis, accident at the Three Mile Island Generating Station [2]. The interest arises because there is the possibility the severe reactor accidents could lead to the uncontrolled release of radioactivity from a nuclear power plant which would have life-threatening consequences and produce long-term property damage. Because of this possibility, severe reactor accidents make the largest contribution to the risk that must be associated with the use of nuclear power [3].

Accidents of sufficient severity to produce dire consequences have never occurred in U.S. commercial nuclear power plants. The progression and consequences of these accidents can only be estimated in analytic studies.

Analytic studies of severe reactor accidents consist of several key elements:

1. The probability that a severe reactor accident might be initiated is estimated.

2. The phenomena that arise in a severe accident are described and calculations made to determine if and when uncontrolled release of radioactivity will occur.

3. The amount of radioactive material that might escape the plant is calculated.

4. The consequences of exposing people and property to the radioactivity expelled from the plant is estimated.

The lack of experience with severe reactor accidents has made exercises of this type difficult and the results uncertain. Strong biases have been built into the analytic studies so that any errors in the analyses will accrue toward overpredicting the severity of accidents that go beyond the design basis of the plants.

Past analyses of severe accidents have come under substantial criticism because of feelings that the conservatism of the analyses to err~~or~~ on the side of overpredicting accident severity has been carried too far. There is a perception that modern nuclear power plants may be better able to cope with even the severest accidents than has been admitted in the past. The relatively inconsequential events associated with the accident at Three Mile Island Unit #2 have bolstered the confidence that natural processes have been neglected which will substantially reduce the amount of radioactive material inflicted on the environment, even if accident phenomena lead to containment failure.

The assessments of accident phenomena and the estimates of radioactivity release are the elements of severe accident analyses that appear to embody the greatest conservatism that can be removed by further, more careful study. The further studies of these elements may allow engineering bounds on the calculations to be replaced by realistic evaluations based on mechanistic, physical processes. Many research programs are now underway to provide the greater understanding of severe accident phenomena and the behavior of radioactivity necessary to conduct more realistic analyses.

This document addresses the subject of radioactivity behavior during severe accidents. Analysis of the behavior of radioactive materials during severe accidents begins by dividing the behavior into several elements:

1. Release of radioactive material from the reactor fuel so it can be transported.

2. Transport of the radioactive material to locations where it can escape the confines of a reactor plant.

3. Behavior of the radioactive material while it awaits development of a pathway out of the plant or the chance to follow such a pathway.

The first of these elements of severe accident analysis, release of radioactive materials from the reactor fuel, can be further classified in terms of (a) release from fuel within the reactor vessel, and (b) release from fuel that has escaped the reactor vessel. The processes that lead to "in-vessel" and "ex-vessel" release are discussed in Chapters 3 and 4 of this document.

Before delving into the release and transport processes, it is useful to establish what materials are released and how much of each material might be present during a reactor accident. Establishing the inventories of materials that might be released in a reactor accident is the first objective of this chapter. It is found that there are many radionuclides whose release ought to be of interest. Further, nonradioactive species from structural materials, control rods, fuel cladding, and the like may be vaporized and may form aerosols during an accident. Since vapors of these nonradioactive species should affect behavior of the radionuclides, their release, too, is of interest. Quite clearly, the number of releasable materials that could be of interest gets quite large. Tracking the behavior of all these materials could strain the capacity of even the largest computer models. Consequently, definition of a basis for categorizing and simplifying the materials released during a severe accident is a second objective of this chapter.

2.2. Definitions of Radioactive Materials

Radioactive materials are produced by a variety of processes during normal operations of nuclear power plants:

A. Fission

Unstable nuclei can spontaneously fragment to produce, usually, two daughter isotopes that may also have unstable nuclei. Some important isotopes and their half-lives for spontaneous fissioning are:

Isotope	Half-Life for Spontaneous Fissioning*
${}^{236}_{92}U$	73.6 y
${}^{238}_{92}U$	8×10^{15} y
${}^{240}_{94}Pu$	1.2×10^{11} y
${}^{244}_{96}Cm$	1.4×10^{7} y
${}^{252}_{98}Cf$	66 y
${}^{256}_{100}Fm$	2.4 h

---

* Abbreviations used in this report in connection with half-lives are: year = y; days = d;, hours = h; minutes = m; seconds = s

Far more important than spontaneous fissioning is the fissioning of unstable nuclei brought on by neutron bombardment. Fissile nuclei in commercial light water reactors are:

$$^{235}_{92}U,\ ^{239}_{94}Pu,\ ^{241}_{94}Pu,\ \text{and}\ ^{233}_{92}U$$

Normally, fissioning of a nucleus is thought to be a "binary" process that produces two daughter nuclei. But, once in about 200-500 normal, binary, fission events a third particle is formed [4-6]. More rarely, four or more nuclei are formed during fissioning. Alpha particles are the most common additional nuclei formed in higher order fission processes. But, other nuclei can be formed. Comparative yields (normalized to the ^{4}He yield set equal to 100) of nuclei for higher order fissioning of ^{252}Cf are listed below [6]:

^{1}H	1.1
^{2}H	0.63
^{3}H	6.42
^{3}He	0.008
^{4}He	100
^{6}He	1.95
^{8}He	0.06
Li	0.126
Be	0.156

Ternary fissioning is such a rare event it is normally neglected. But, it is obvious ternary fissioning can be a source of tritium.

Products of fissioning are not simply described. These products will be discussed in the section below dealing with inventories.

B. Beta Decay

The nuclei produced by fissioning are typically quite unstable and radioactively decay. The most important decay process involves emission of an electron ($^{0}_{-1}e \equiv \beta^{-}$), a neutrino, and often a gamma ray. This is called beta decay and it results in increasing the atomic number of the decaying isotope by one, with no change in the mass number. Some of the important decay chains initiated by nuclear fissioning in light water reactor fuels are shown in Figure 2.1. Beta decay chains initiated by processes other than fissioning are shown in Figure 2.2. Note that naturally occurring isotopes can undergo beta decay. Some of these processes are listed in Figure 2.2.

C. Other Decay Processes

Other nuclear decay reactions are (a) emission of a gamma ray (γ), (b) emission of a positron ($\beta+$) and an antineutrino, and (c) emission of an alpha particle ($\alpha = {}^{4}_{2}He$). Four decay chains of importance to light water reactor safety are shown in Figures 2.3-2.6. These are the (a) uranium decay chain, (b) the thorium decay chain, (c) the actinide decay chain, and (d) the synthetic neptunium decay chain.

Decay processes of various natures are continually being discovered. For instance, in 1983 a two proton decay reaction was first discovered [7]:

$$ {}^{22}_{13}Al \xrightarrow[\beta+]{} {}^{22}_{12}Mg \xrightarrow[2p]{} {}^{20}_{10}Ne $$

D. Neutron Capture

Absorption of a neutron does not necessarily lead to fissioning of a nucleus. The unstable isotope created by absorption of a neutron can instead decay by other processes.

Within light water reactor fuel, neutron capture is responsible for formation of transuranic elements. Some example reactions and the decay processes set off by these reactions are:

$$ {}^{239}_{94}Pu + n \rightarrow {}^{240}_{94}Pu + \gamma $$

$$ {}^{238}_{92}U + n \rightarrow {}^{239}_{92}U + \gamma $$

$$ {}^{240}_{94}Pu + n \rightarrow {}^{241}_{94}Pu + \gamma \xrightarrow[\beta-]{} {}^{241}_{95}Am $$

$$ {}^{241}_{95}Am + n \rightarrow {}^{242}_{95}Am + \gamma \xrightarrow[\beta-]{} {}^{242}_{96}Cm $$

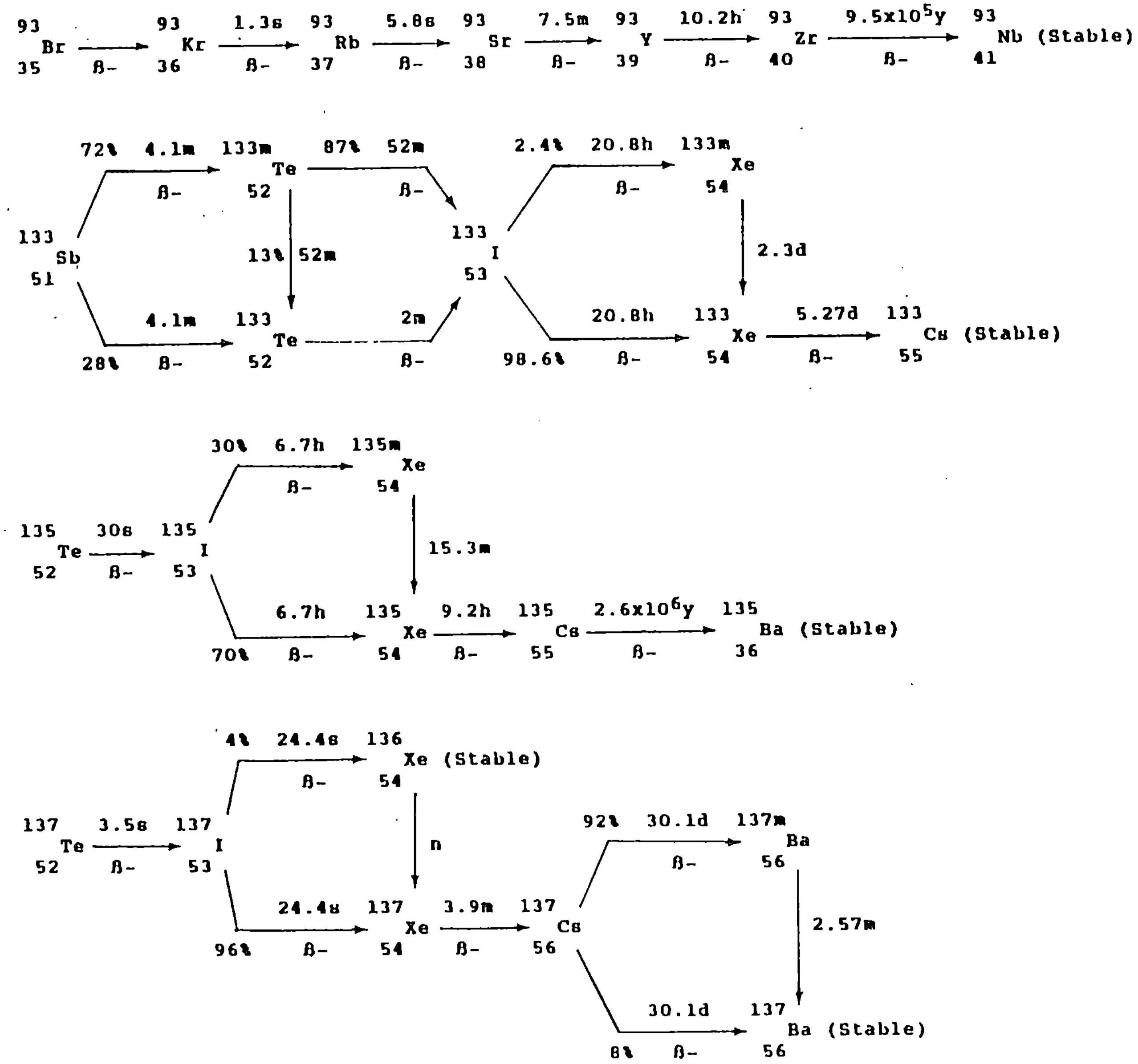

Figure 2.1. Some Important Beta Decay Reactions (Half-Lives Indicated Above Arrows to Products)

A. Neutron Capture Initiation

$$^{239}_{92}\mathrm{U} \xrightarrow[\beta^-]{23\mathrm{m}} {}^{239}_{93}\mathrm{Np} \xrightarrow[\beta^-]{2.3\mathrm{d}} {}^{239}_{94}\mathrm{Pu}$$

$$^{241}_{94}\mathrm{Pu} \xrightarrow[\beta^-]{15\mathrm{y}} {}^{241}_{95}\mathrm{Am}$$

$$^{242}_{95}\mathrm{Am} \xrightarrow[\beta^-]{} {}^{242}_{96}\mathrm{Cm}$$

$$^{234}_{90}\mathrm{Th} \xrightarrow[\beta^-]{24\mathrm{d}} {}^{234}_{91}\mathrm{Pa} \xrightarrow[\beta^-]{1.1\mathrm{m}} {}^{234}_{92}\mathrm{U}$$

$$^{94}_{40}\mathrm{Zr} \xrightarrow{n} {}^{95}_{40}\mathrm{Zr} \xrightarrow[\beta^-]{65\mathrm{d}} {}^{95}_{41}\mathrm{Nb} \xrightarrow[\beta^-]{35\mathrm{d}} {}^{95}_{42}\mathrm{Mo}\ \text{(Stable)}$$

B. Naturally Occurring Isotopes

$$^{14}_{6}\mathrm{C} \xrightarrow[\beta^-]{5770\mathrm{y}} {}^{14}_{7}\mathrm{N}\ \text{(Stable)}$$

$$^{40}_{19}\mathrm{K}\ \text{(nat'l. abund. = 0.0118\%)} \xrightarrow[\beta^-]{1.3\mathrm{x}10^{9}\mathrm{v}} {}^{40}_{20}\mathrm{Ca}\ \text{(Stable)}$$

$$^{48}_{2}\mathrm{Ca}\ \text{(nat'l. abund. = 0.18\%)} \xrightarrow[\beta^-]{2\mathrm{x}10^{16}\mathrm{y}} {}^{48}_{21}\mathrm{Sc} \xrightarrow[\beta^-]{41\mathrm{h}} {}^{48}_{22}\mathrm{Ti}\ \text{(Stable)}$$

$$^{87}_{37}\mathrm{Rb}\ \text{(nat'l. abund. = 27.85\%)} \xrightarrow[\beta^-]{4.7\mathrm{x}10^{10}\mathrm{y}} {}^{87}_{38}\mathrm{Sr}\ \text{(Stable)}$$

Figure 2.2 Beta Decay Chains Initiated by Processes Other Than Fissioning

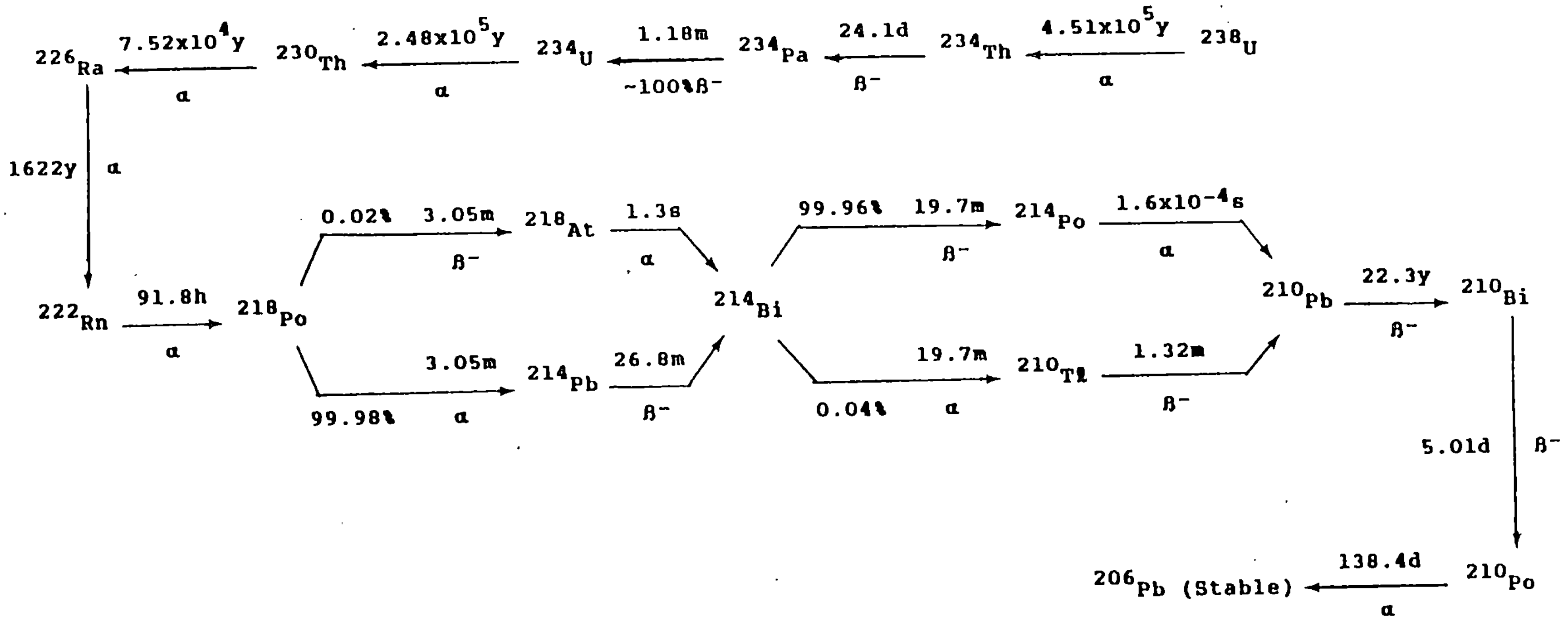

Figure 2.3. The Uranium Decay Series

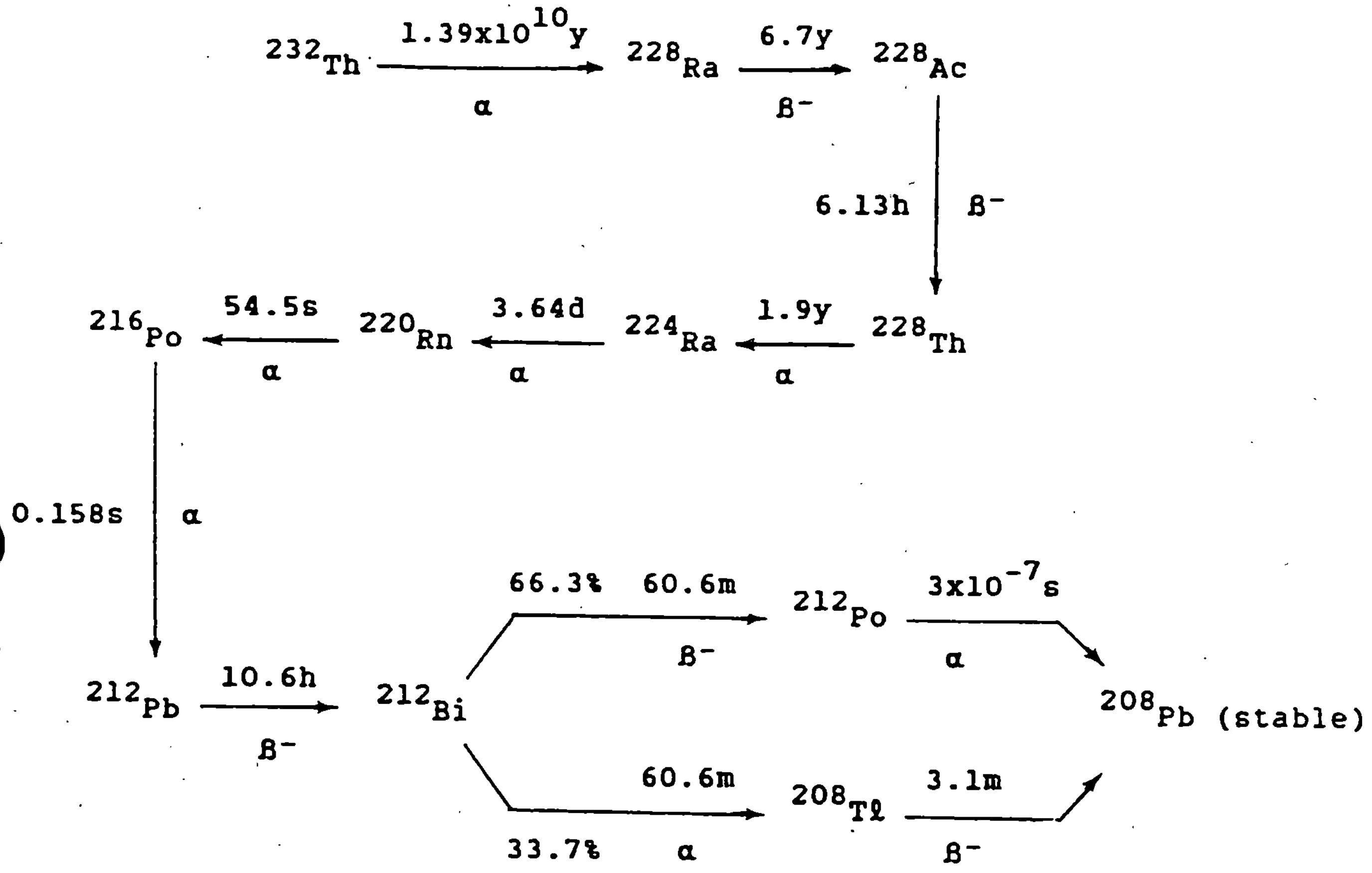

Figure 2.4. The Thorium Decay Series

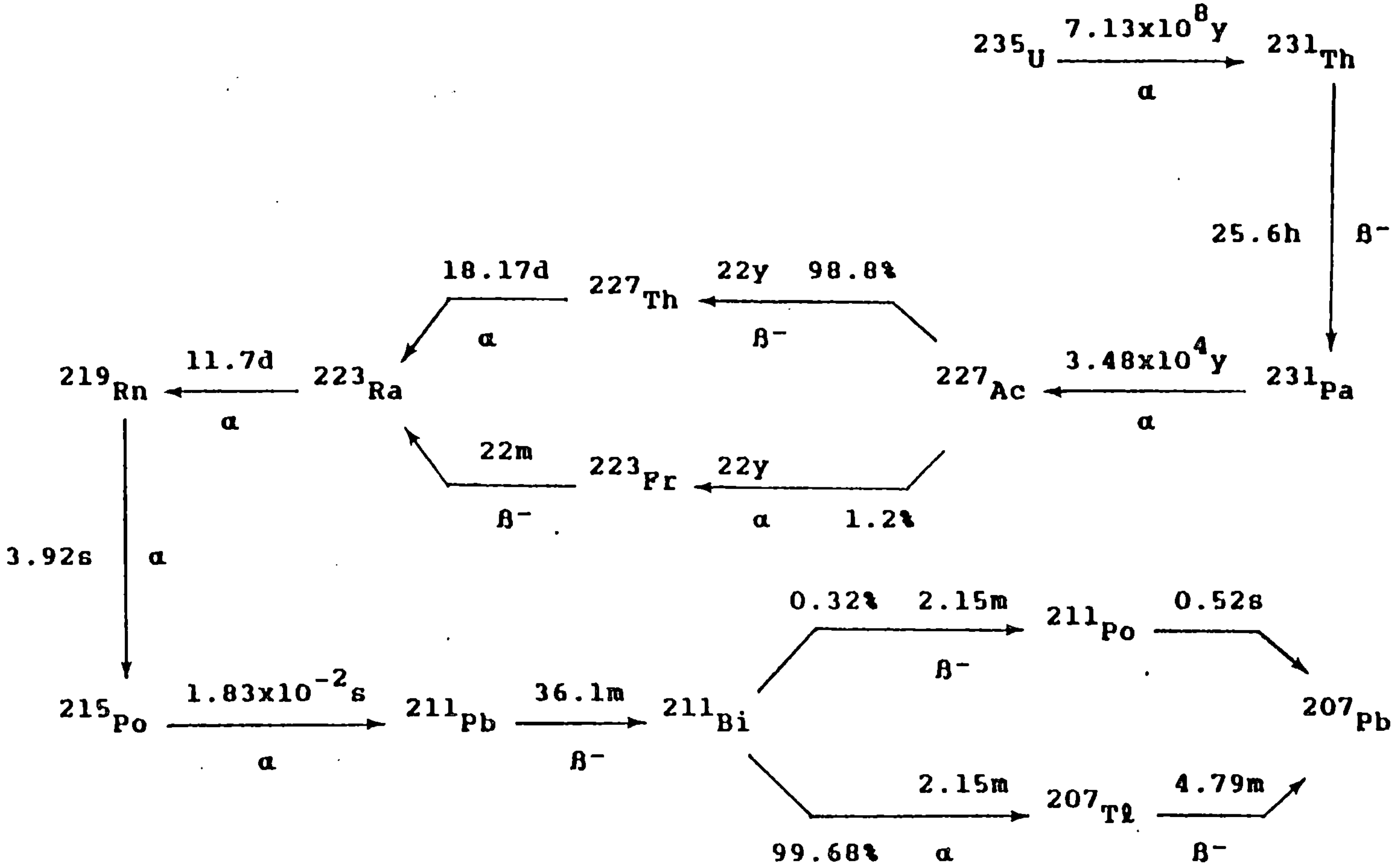

Figure 2.5. The Actinium Decay Series

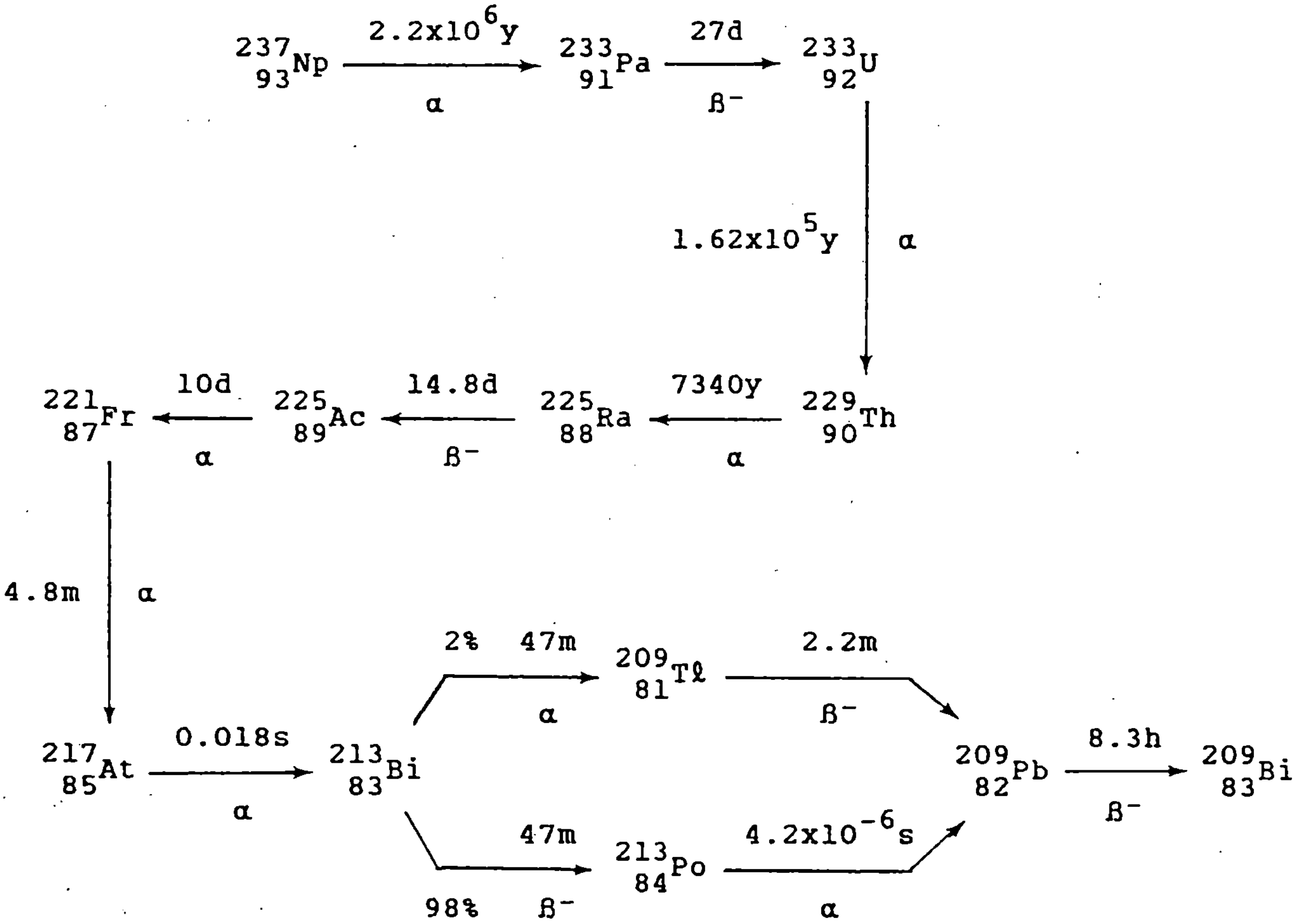

Figure 2.6 Neptunium Decay Chain

Neutron capture is responsible for making structural materials in a reactor radioactive. The ability of structural materials to capture a neutron depends on the "neutron capture cross section" of isotopes in the material. These cross sections depend on the energy of the neutron. For light water reactors, so-called thermal neutrons--energies on the order of kT, where k is the Boltzmann constant and T is the absolute temperature--are of greatest interest. Thermal neutron capture cross sections for isotopes of structural materials in light water reactors are listed in Table 2.1.

Absorption of neutrons by structural elements can produce unstable nuclei. Some of the radioactive products of neutron capture by structural materials are also shown in Table 2.1 along with the half-lives and decay processes of these product isotopes.

Generation of radioactive species in structures by neutron capture is probably not important for severe accident analyses. At shutdown, radioactive species in structures in a PWR core with a fuel burnup of 33,500 MWd/ton will decay at a rate of about 3×10^7 curies. Fission products and actinides in the fuel will decay at a rate of about 2×10^{10} curies.

Most of the radioactivity of structures comes from the isotopes [8]:

^{51}Cr	19% of curies at shutdown
^{56}Mn	39% of curies at shutdown
^{55}Fe	4% of curies at shutdown
^{60m}Co	12% of curies at shutdown
^{95}Zr	9% of curies at shutdown
^{95}Nb	8% of curies at shutdown
^{117m}Sn	5% of curies at shutdown

Activation products produced in some types of concrete that could be of interest are $^{63}Ni(t_{1/2} = 100y)$, $^{54}Mn(t_{1/2} = 0.85y)$, $^{152}Eu(t_{1/2} = 13y)$, $^{41}Ca(t_{1/2} = 10^5 y)$, $^{39}Ar(t_{1/2} = 270y)$, and $^{14}C(t_{1/2} = 5700Y)$.

E. Other Capture Reactions

Besides neutrons, capture of alpha particles and electrons can produce new unstable isotopes. Some example reactions are:

Table 2.1

Thermal Neutron Capture Cross Sections for Elements Found in Reactor Structures

Isotope	Natural Abundance (%)	Cross Section* (Barns)	Product Isotope	Half-Life	Decay Process
^{50}V	0.24	~200	^{51}V		
^{51}V	99.76	4.5	^{52}V	3.77m	β-
^{50}Cr	4.31	17	^{51}Cr	27.8d	β-
^{52}Cr	83.76	0.8	^{53}Cr		
^{53}Cr	9.55	18	^{54}Cr		
^{54}Cr	2.38	0.38	^{55}Cr	3.5m	β-
^{55}Mn	100	13.3	^{56}Mn	2.58h	β-
^{54}Fe	5.82	2.5	^{55}Fe	2.7y	Electron capture
^{56}Fe	91.66	2.7	^{57}Fe		
^{57}Fe	2.19	2.5	^{58}Fe		
^{58}Fe	0.33	1.0	^{59}Fe	45d	β-
^{59}Co	100	18	^{60}Co	5.27y	β-, γ
^{58}Ni	67.88	4.4	^{59}Ni	8x10^{4}y	Electron capture
^{60}Ni	26.23	2.6	^{61}Ni		
^{61}Ni	1.19	2	^{62}Ni		
^{62}Ni	3.66	15	^{63}Ni	92y	β-
^{64}Ni	1.08	1.6	^{65}Ni	2.56h	β-, γ
^{107}Ag	51.82	40	^{108}Ag	2.4m	β-, Electron capture
^{109}Ag	48.18	84	^{110}Ag	249d	β-
^{110}Cd	12.39	0.2	^{111m}Cd	49m	γ
^{111}Cd	12.75	?	^{12}Cd		
^{112}Cd	24.07	0.03	^{113m}Cd	14y	β-, γ
^{113}Cd	12.26	27,000	^{114m}Cd		
^{114}Cd	28.86	1.24	^{115}Cd	43d	β-, γ
^{116}Cd	7.58	1.4	^{117}Cd	3.2h	β-
^{113}In	4.28	63	^{114}In	50d	γ
^{115}In	95.72	200	^{116m}In	54m	β-
^{112}Sn	0.96	1.3	^{113}Sn	113d	Electron Capture
^{116}Sn	14.3	0.006	^{117m}Sn	14d	γ
^{118}Sn	24.03	0.01	^{119m}Sn	250d	γ
^{120}Sn	32.85	0.14	^{121}Sn	75y	β-
^{122}Sn	4.92	0.2	^{123}Sn	40m	β-
^{124}Sn	5.94	0.204	^{125m}Sn	9.4m	β-
^{90}Zr	51.46	0.1	^{91}Zr		
^{91}Zr	11.23	1	^{92}Zr		
^{92}Zr	17.11	0.2	^{93}Zr	9.5x10^{5}y	β-
^{94}Zr	17.40	0.1	^{95}Zr	65d	β-, γ
^{96}Zr	2.80	0.1	^{97}Zr	17h	β-

---

* These cross-sections do not take into account resonance adsorption. Such resonances are approximately accounted for by increasing the cross-sections by 45%.

$$^{238}_{92}U + \alpha \rightarrow {}^{241}_{94}Pu + n$$

$$^{239}_{94}Pu + \alpha \rightarrow {}^{242}_{96}Cm + n$$

$$^{195}_{79}Au + {}^{\circ}_{-}e \rightarrow {}^{195}_{78}Pt \quad .$$

Precisely speaking, the term fission product should be reserved for the daughter isotopes produced during fissioning and possibly the isotopes produced by the beta decay chains initiated by the fissioning. Here, however, the term "fission product" will be used to mean any radioactive material, regardless of how or where it was produced.

2.3. Inventories

A. Radioactive Materials

The first step in estimating the release of fission products is to determine the inventory of fission products available for release. It will be shown in later sections that inventory does, in fact, affect the release rate. Fortunately, calculation of the fission product inventory has become a well-developed technology.

If fissioning of the ^{235}U isotope were a homolytic process, the nuclear reaction would be

$$^{235}_{92}U + n \rightarrow 2 \; {}^{118}_{46}Pd$$

Rather than yielding two palladium isotopes, the ^{235}U fissioning yields a wide variety of isotopes. The probability that fissioning will yield a particular isotope is bimodally distributed with respect to the atomic mass number of the isotope. Peaks in the distribution occur for atomic mass numbers of 137 and 97. The distribution does depend slightly on the energy of the neutrons causing the fissioning. The fissioning yields for ^{235}U subjected to thermal neutrons are plotted against the mass number of the product isotope in Figure 2.7.

Fission yield also depends on the fissile isotope. The fission yields for ^{235}U and ^{239}Pu are compared in Table 2.2. Entries in the table are the probabilities in percent that fission will yield the indicated material. Since each fission

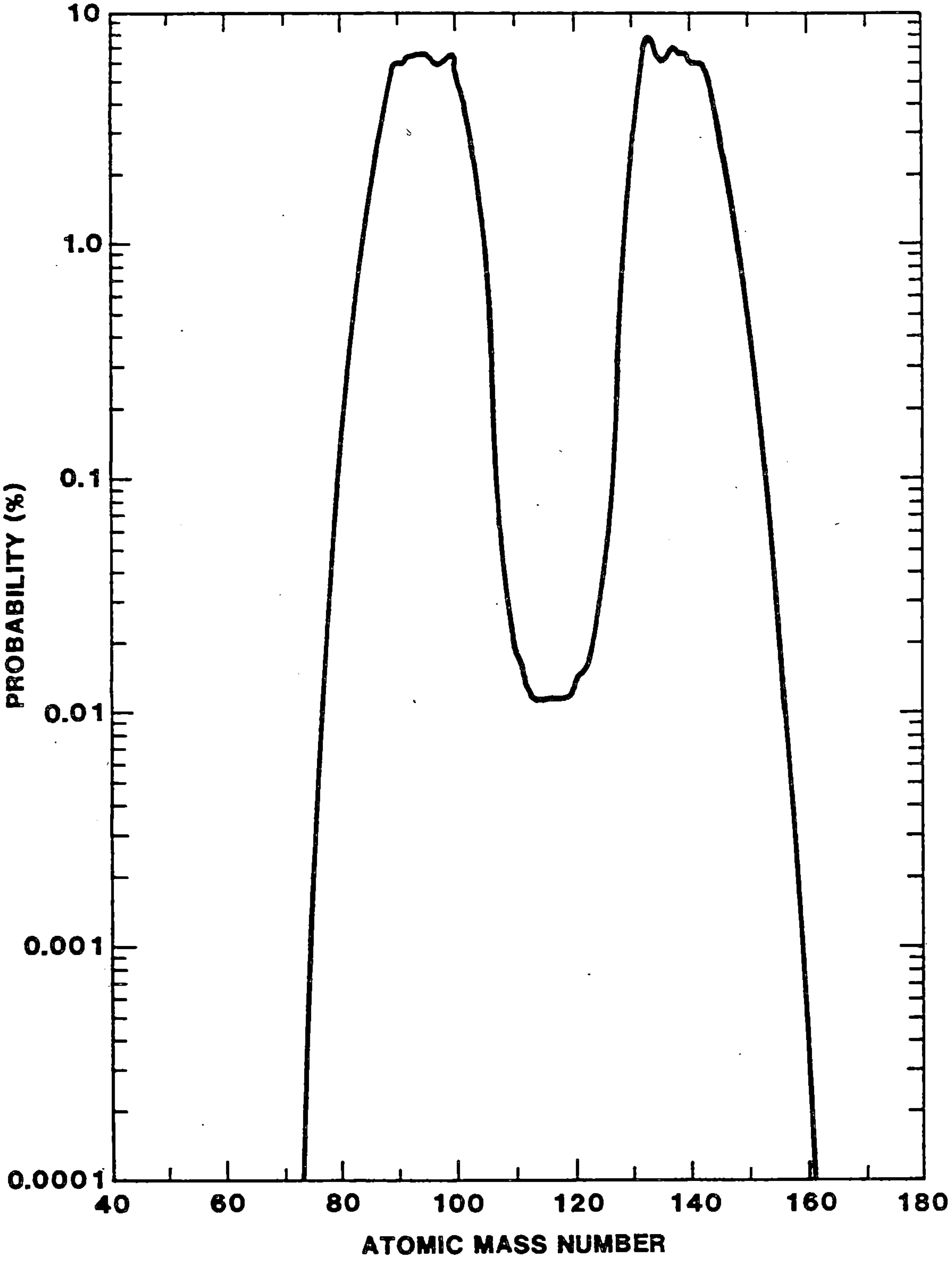

Figure 2.7. Fission Yields for ^{235}U

Table 2.2

Comparison of Fission Yields From $^{235}_{92}U$ and $^{239}_{94}Pu$ [9].

Fission Product Group	Yield (%) from $^{235}_{92}U$	Yield (%) from $^{239}_{94}Pu$
Zr, Nb	29.8	20.4
Y, La, Ce, Pr, Nd, Po, Sm, Eu, Ga	53.4	47.1
Ba, Sr	14.9	9.6
Mo	24.0	20.3
Ru, Te, Rh, Pd	26.3	51.6
Cs, Rb	22.6	18.9
I, Te	1.2	7.0
Xe, Kr	25.1	24.8

event yields two daughter products, the columns in Table 2.2 each sum to 200 percent. Notable features of the comparison of ^{235}U and ^{239}Pu fissioning are (1) the higher yield of metals (Ru, Te, Rh, Pd) in ^{239}Pu fissioning and (2) lower yields of both the Ba,Sr and the Zr,Nb groups.

To determine the absolute amounts of fission products in a reactor core requires:

1. The extent of fissioning and capture that has taken place.
2. The enrichment of the fuel in fissile isotopes.
3. The time and power history over which fissioning took place.

The need to know how much fissioning took place is obvious since the absolute isotope yield is the product of the probability a fission event will produce the isotope times the number of fission events. The irradiation history of fuel is usually reported in terms of "burnup," which includes both fissioning and capture.* Unfortunately, the fuel in reactor cores does not burn up uniformly. The burnup history of fuel assemblies in the Three Mile Island Core just prior to the accident are shown in Figure 2.8 (only one quarter of the core is shown in this figure; the rest of the core and the burnup histories of fuel assemblies in the rest of the core are symmetrically related about the centerlines shown in figure).

As a rough rule, burnup decreases with distance from the center of the core. This is because neutrons that would have been captured or would have continued the nuclear chain reaction if they were generated deep within the core have more of a chance to escape unproductively when they are generated near the perimeter of the core. Fission product inventories would of course vary, approximately, as do the burnups throughout the core.

---

* There are two conventional units of burnup. Percent burnup is the amount of fuel atoms destroyed by both capture and fission. Thus 1-percent burnup means that 10 kg of uranium have been converted in 1 metric tonne of fuel metal atoms. The other unit is megawatt days thermal per metric tonne of uranium. Conversion between the units is difficult because capture creates fissile plutonium that can act as a fuel. A 1-percent burnup corresponds to 6760 MWd/t U, if credit for the plutonium is not taken and 7765 MWd/t U if credit is taken.

4008	3512	3091	3187	2513	3206	3675	2479
3511	3234	3316	2965	2988	2927	2885	2107
3099	3280	3026	2974	2471	2835	3074	1713
3185	2971	2996	2675	2729	2395	2281	
2511	2991	2502	2736	2349	2129	1404	
3204	2902	2808	2410	2128	1494		
3672	2911	3048	2280	1403			
2478	2106	1711					

Figure 2.8. Burnup of TMI Fuel Rods in Megawatt Days per Metric Tonne Uranium [10]

The variations in burnup are not smooth functions of distance from the center of the core because the fuel is not uniformly enriched in fissile ^{235}U. The initial enrichment of fuel assemblies in the Three Mile Island Core are shown in Figure 2.9. (Again, only one quarter of the core is shown.) The fueling pattern consists of an outer ring of highly enriched material (2.96 percent ^{235}U). Within this ring there are alternating assemblies of medium enrichment (2.64 percent ^{235}U) and low enrichment (1.98 percent ^{235}U) fuel assemblies. The isotopic distributions of fission products in these fuel elements will be different even if burnup were the same. Powers [11] has used these differences in isotopic abundances in both uranium and plutonium to infer from samples of released material the damage pattern to the TMI core.

The time duration over which a level of burnup occurs affects the fission product inventories because the daughter isotopes of fissioning and the products of neutron capture are unstable and radioactively decay. Progress along the decay chains described above is a strong function of time and so, too, is the isotopic mix of fission products.

Reinspection of the decay chains described above and the complicated nature of products of the fission process, as well as the complexities described above concerning irradiation history and enrichment, should be enough to persuade even the most dogged that calculations of inventories is a complicated activity. Fortunately, the problem has been avidly pursued and is particularly susceptible to computer solution. Within the United States, the computer code ORIGEN has become an especially popular tool for solving the fission product inventory problem [12]. The basic algorithm solves systems of coupled, moderately stiff differential equations. A typical version of ORIGEN tracks the evolution of 1064 isotopes with half-lives greater than 1 second [8]. It is backed by an extensive library of nuclear data concerning half-lives, branch decay probabilities, and capture cross sections. Output is provided in terms of gram atoms, curies, and thermal power.

Other codes besides ORIGEN exist to solve the same problem. The CINDER code has been mentioned in the literature [13]. The British codes RICE and FISPIN are also available. Proprietary codes of reputably outstanding sophistication are apparently held by reactor vendors.

These computer models do not explicitly treat the radial distribution problem described above. Nor do they consider axial variations in fission product inventories that should parallel the axial power distribution in the core.

2.64%	1.98%	1.98%	2.64%	1.98%	2.64%	2.64%	2.96%
1.98%	1.98%	2.64%	1.98%	2.64%	1.98%	2.64%	2.96%
1.98%	2.64%	1.98%	2.64%	1.98%	2.64%	2.96%	2.96%
2.64%	1.98%	2.64%	2.96%	2.64%	1.98%	2.96%	
1.98%	2.64%	1.98%	2.64%	1.98%	2.96%	2.96%	
2.64%	1.98%	2.64%	1.98%	2.96%	2.96%		
2.64%	2.64%	2.96%	2.96%	2.96%			
2.96%	2.96%	2.96%					

Figure 2.9. Enrichment Pattern of Fuel in the TMI Unit 2 Core [10]

B. Justification of Elemental Phenomenological Source Terms

The same considerations that demonstrate the complexities of calculating the fission product inventories also demonstrate that there are a lot of fission products. The fission products are isotopes of a much smaller number of elements. It has become traditional to analyze the severe accident source term in terms of the behavior of the elements rather than the isotopes. When analyses progress to the point radiological concerns need to be addressed, the isotopic abundances in the elements released from the fuel are assumed to be the same as they would have been in the fuel were there no release. That is, the assumption is made that there are no effects on release or behavior, save inventory changes by radioactive decay, that arise because of different isotopes.

An alternative to this traditional approach would be to develop models of release and behavior that are peculiar to each isotope. This alternative would increase, of course, the labor involved in the development of severe accident source term models.

Isotopic difference could affect the behavior of fission products in three ways:

1. Isotopic differences could affect the chemical processes in which fission products engage by altering chemical equilibria.
2. Isotopic differences could affect the rates of chemical reaction.
3. Transmutation of the elements by radioactive decay could alter the release rates or behavior of fission products.

A definitive proof that none of the effects are important would be difficult to formulate. Below, evidence is presented that the first two effects are likely to be insignificant. The third effect, transmutation, is shown to be considerable only for a few particular cases. Because of these occasional transmutation effects, the traditional approach to source term modeling in terms of elements rather than isotopes may not be universally acceptable. But, because the transmutation effects are rare and because neither the thermodynamics nor kinetics of different isotopes are significantly different, it may not be necessary to adopt the alternative of isotopically based source term models.

The chemical processes that affect fission product release and behavior can be identified by systematically examining chemical equilibria. Are these chemical equilibria significantly different for the isotopes of a given element?

Consider two general equilibrium reactions, one involving the isotope A and the other the isotope A*:

$$AB + C \rightleftarrows AC + B \qquad K = \frac{[AC]\ [B]}{[AB]\ [C]}$$

$$A^*B + C \rightleftarrows A^*C + B \qquad K^* = \frac{[A^*C]\ [B]}{[A^*B]\ [C]}$$

The isotopic distortion of the equilibrium is shown by the ratio of the equilibrium constants:

$$K/K^* = \frac{[AC]\ [A^*B]}{[A^*C]\ [AB]}$$

But this ratio is just the equilibrium constant for the isotopic exchange reaction:

$$A^*C + AB \rightleftarrows A^*B + AC$$

This equilibrium constant is given by

$$K_{ex} = \frac{F_{A^*B}\ F_{AC}}{F_{A^*C}\ F_{AB}}$$

where F_i = the partition function of the species i. The partition function of the ith species is given by [14]:

$$F_i = \frac{g_{el}^{(i)} g_{nucl}^{(i)}}{S_i} \left[\frac{(2\pi m_i kT)^{3/2}}{h^3}\right] \left[\frac{22.627\pi^{7/2} I_i^{\ 1/2} (kT)^{3/2}}{h^3}\right] f_{vib}^{(i)}$$

where $g_{el}^{(i)}$ = electronic contribution to the partition function

$g_{nucl}^{(i)}$ = contribution to the partition function from nuclear spins

m_i = mass of the ith species

I_i = moment of inertia of the i^{th} species

k = Boltzmann's constant

h = Plank's constant

$$f_{vib}^{(i)} = \pi_j \left[\frac{\exp(-h\nu_j/2kT)}{1 - \exp(-h\nu_j/kT)} \right]$$

ν_j = frequency of the j^{th} vibration

s_i = symmetry number of the i^{th} species.

Isotopic substitution of one element in the i^{th} species will leave, of course, the symmetry of the species unaltered. Similarly, isotopic substitution does not alter $g_{el}^{(i)}$. Nuclear masses are so much greater than electronic masses for the isotopes of interest in reactor accident analyses that electronic motions are little altered when the nuclear mass is changed by one or two atomic mass units (amu).

The partition function for nuclear spin in the species AB can be cast in the form

$$g_{nucl}^{AB} = g_{nucl}^{(A)} \; g_{nucl}^{(B)}$$

Similar expressions can be written for the species A*B, AC, and A*C. Chemical process can almost never affect nuclear spin so the term $g_{nucl}^{(A)}$ is the same whether the atom A is in the species AB or the species AC.

If the species AB is considered a diatomic species composed of atom A and molecular fragment B, then

$$I_{AB} = \left(\frac{M_A M_B}{M_A + M_B} \right) \left(r_{eq}^{(AB)} \right)^2$$

where $r_{eq}^{(AB)}$ = equilibrium bond length between A and B. Since electronic motions are unaffected by isotopic substitution,

$$r_{eq}^{(AB)} = r_{eq}^{(A*B)}$$

Then, the equilibrium constant for the isotopic exchange reaction is given by

$$\frac{K}{K^*} = \left(\frac{M_{A^*B}}{M_{AB}}\right)^{3/2}\left(\frac{M_{AC}}{M_{A^*C}}\right)^{3/2}\left(\frac{I_{A^*B}I_{AC}}{I_{AB}I_{A^*C}}\right)^{1/2}\left(\frac{f^{A^*B}_{vib}}{f^{AB}_{vib}}\,\frac{f^{AC}_{vib}}{f^{A^*C}_{vib}}\right)$$

$$= \frac{M_{A^*B}}{M_{AB}}\;\frac{M_{AC}}{M_{A^*C}}\;\frac{f^{A^*B}_{vib}}{f^{AB}_{vib}}\;\frac{f^{AC}_{vib}}{f^{A^*C}_{vib}}$$

If the diatomic approximation for the species is again assumed, then there will be but one vibration for each species. The frequency of that vibration is given by

$$\nu_i = \sqrt{\frac{f_i}{m_i}}$$

where f_i is the force constant. Since the force constant is dictated by the chemical bonding, the force constant is essentially unaffected by isotopic substitution. Quite clearly a 1 to 2 percent change in m_i makes a very modest change in the vibrational frequency if m_i is large. At elevated temperatures the exponential terms in the vibrational contribution to the partition function can be linearized. Then,

$$\frac{K}{K^*} = \left(\frac{M_{A^*B}}{M_{AB}}\right)^{3/2}\left(\frac{M_{AC}}{M_{A^*C}}\right)^{3/2}$$

Clearly, for massive isotopes K*/K deviates little from unity. That is, equilibria are little affected by isotopic abundances.

The next question is whether the approach to equilibrium is sensitive to isotope effects. Melander [15] has presented an extensive review of isotope effects on chemical reaction rates. Nearly all analyses of these effects evolve from H. Eyring's [16] transition state theory of elementary chemical reaction rates.*

---

* Elementary chemical reactions are the actual microscopic, molecular transformations that take place in a chemical process. They are nearly never known except for simple systems that have attracted academic interest. Elementary reactions seldom bear much resemblance to the reactions defined from the stoichiometry of the process.

In this theory, molecular collisions give rise to an energetic, but metastable, transition complex:

$$AB + C \rightarrow [ABC] \rightarrow AC + B$$

After a brief induction period, the reactants AB and C come into dynamic equilibrium with the transition complex:

$$AB + C \rightleftarrows [ABC]$$

The rate at which products are produced depends on the concentration of the transition complex ABC. Analysis of the change in concentration brought on by isotopic substitution is just an equilibrium analysis much like that above. The reaction rate, given the concentration of ABC or A*BC, is a vibrational analysis. As the temperatures increase the ratio of the rates of reaction of A*B and AB approaches:

$$\frac{R_{A*B}}{R_{AB}} = \left[\frac{\frac{1}{M_{A*B}} + \frac{1}{M_{A*C}}}{\frac{1}{M_{AB}} + \frac{1}{M_{AC}}}\right]^{1/2}$$

It is apparent that for atomic masses on the order of 100, the ratio of rate constants will vary little with changes in mass of one or two units in comparison to the general uncertainty of the elementary reaction rate constant.

Thus, isotopes should participate in similar chemical reactions at similar rates. The existence of isotopes need not lead to formulation of isotopically based source term models.

There is a subtle feature of the isotope affect on release kinetics that is not addressed by this analysis. Some elements produced by fission will have both long and short half-life isotopes. Long-lived isotopes borne in the fuel lattice will have an opportunity during the course of reactor operation to migrate and accumulate at the grain boundaries. Short-lived isotopes will not have this opportunity. As a result, once an accident begins, there will be a greater fraction of long-lived isotopes at the grain boundary than short-lived isotopes. If transport through the fuel grains poses a major limitation on the rate of release, then long-lived isotopes of the element will escape more rapidly from the fuel than short-lived isotopes, at least until the inventory of long-lived isotopes accumulated at grain boundaries has been depleted. This effect will be greatest for the more volatile isotopes.

Transmutation by radioactive decay does depend on the isotope in question, in terms both of the rate and the nature of the product. It is easy to imagine situations in which an isotope decays to an element with radically different chemical character and consequently radically different behavior during a severe accident. For instance, consider these situations:

1. The isotope of interest is the product of radioactive decay of a noble gas. The isotope of interest is released from the fuel at a rate much slower than the rate of release of the noble gas. Nevertheless, this isotope will appear in the emissions from the core during an accident to an extent dictated by the radioactive decay of released noble gas.

2. The element of interest is quite volatile and is expected to be released quite rapidly from the fuel. But, a fraction of the element is produced by decay of a fairly refractory species that is not released from the fuel. Then, release of the element of interest may persist long after conditions of the fuel are well beyond those expected to lead to quantitative release. The persistent release is the result of decay of the refractory species and prompt release of the decay products.

Though these situations can be imagined, it is important to ascertain their significance before investing in the labor of developing isotopically based source term models.

At first blush, the situations in which radioactive decay might affect fission product behavior mostly involve highly volatile species--the noble gases and, perhaps, iodine. The most important decay processes involving the noble gases and iodine are the ß-decay chains.

For radioactive decay to have a significant bearing on the source term, three conditions must be met:

1. The inventory of the decaying isotope must be high enough to have a perceptible effect.

2. The decay process must occur to a significant extent during the time frame of interest.

3. The decay process must not be so rapid that it is largely complete before any significant release can take place.

Let G be the inventory of the decaying element and H the inventory of the element that is the product of the decay process of interest. Let Co be the inventory of the decaying isotope and $t_{1/2}$ be the half-life of this isotope. Co' is the inventory of the product of decay, were decay to go instantaneously to completion. Assume that an error of E in the release fraction of an isotope is barely tolerable. Then, decay processes need to be considered to avoid an excessive error, when

$$Co/G > E$$

and

$$\frac{0.693\ t(min)}{-\ln\left[1-\frac{EG}{Co}\right]} \leq t_{1/2} \leq \frac{0.693\ t(max)}{-\ln\left[1-\frac{EG}{Co}\right]}$$

or

$$Co'/H > E$$

and

$$t_{1/2} \leq \frac{0.693\ t(max)}{-\ln\left[1-\frac{EH}{Co'}\right]}$$

where t(max) is the maximum time of interest and t(min) is the time from reactor scram to the onset of significant fission product release.

Isotopes in the portion of the ß-decay chain involving Te, I, Xe, and Cs are shown in Table 2.3. The half-lives of the isotopes and typical inventories in fuel irradiated to about 33,000 MWd/t are also shown in the table. The inventories in this table are provided in the form of decay rates. Any other unit, such as thermal power, dose, or moles, might be used. To scan these isotopes for instances of transmutation effects that might have a significant impact on source term behavior, it was assumed that

$$E = 0.1$$

$$t(min) = 1200$$

$$t(max) = 80,000$$

The isotopes ^{132}Te and ^{134}Te meet the criterion for concern over radioactive decay effects in source term models. Williams [17] has discussed the effect of ^{132}Te and the ex-vessel source term. If Te is not released in-vessel because it has bound chemically to unoxidized zircaloy clad, it is available

Table 2.3

The ß-Decay Series Involving Te, I, Xe, and Cs Isotopes

Tellurium			Iodine			Xenon			Cesium		
Atomic Mass (amu)	$t_{1/2}$ (s)	Co (10^{5}Ci)	Atomic Mass (amu)	$t_{1/2}$ (s)	Co (10^{5}Ci)	Atomic Mass (amu)	$t_{1/2}$ (s)	Co (10^{5}Ci)	Atomic Mass (amu)	$t_{1/2}$ (s)	Co (10^{5}Ci)
127	$3.3x10^{4}$	72.8	127	Stable							
127m(a)	$9x10^{6}$	0.2									
129	4038	250	129	$5x10^{14}$	$2x10^{-5}$	129m(c)	$6.9x10^{5}$	$7x10^{-3}$			
						129	Stable				
131	1500	761	131	$7x10^{5}$	867	131m	$1x10^{6}$	5.4			
						131	Stable				
131m(b)	$1x10^{5}$	65.5									
132	$2.8x10^{5}$	1259	132	8280	1277						
133	120	1044	133	$7.5x10^{4}$	1832	133	$4.6x10^{5}$	1833	133	Stable	
133m	3780	692									
134	2520	1514	134	3180	2011	134	Stable		134	$6.9x10^{7}$	116.9
135	18	792	135	$2.4x10^{4}$	1728	135	$3.3x10^{4}$	344	135	$6x10^{13}$	$1.9x10^{-4}$
136	21	445	136	86	810	136	Stable		136	$1x1x10^{6}$	35.6
			137	24	837	137	234	1681	137	$9.5x10^{8}$	65.3
						138	1020	1579	138	1932	1670
						139	41	1246	139	570	1645
						140	17	866	140	66	1510

---

a. Only 2 percent of the ^{127m}Te decays by ß- emission. The rest decays by emission of a γ ray to yield ^{127}Te.

b. 52 percent of the ^{131m}Te decays by ß- emission. The rest decays by emission of a γ ray to yield ^{131}Te.

for release ex-vessel. Ex-vessel release of Te is slow because of the low chemical activity of the element when dissolved in metals. Iodine release ex-vessel is expected to be quite rapid. Because of the decay of ^{132}Te, there is the potential of prolonged ex-vessel iodine release into the containment atmosphere. This release rate is essentially the rate of Te decay since iodine is so promptly purged from the fuel ex-vessel.

Similarly, protracted release of iodine can occur in-vessel if ^{134}Te binds to clad or structures within the reactor vessel. As the tellurium isotope decays, iodine is produced and possibly released even if conditions have long been established that should have allowed rapid, quantitative expulsion of all iodine.

Several iodine isotopes meet the criterion for consideration. But, there seem to be no radical consequences of iodine transmutation to xenon. This transmutation can probably be adequately handled by inventory adjustments with time.

Decay of ^{133}Xe and ^{135}Xe meet the criterion for consideration. The decay of ^{133}Xe is to the stable cesium isotope and so can be treated simply by inventory adjustment. Decay of ^{135}Xe does yield a radioactive cesium isotope. Because of the decay, there will always be some cesium suspended in the reactor atmosphere if there was xenon release from the fuel. But, because the half-life of xenon is very long, the amount of cesium will not be large.

Within the decay series examined here only the ^{132}Te and perhaps the ^{134}Te isotopes seem to deserve attention that could not be supplied by source term models based on the chemistry of the element and neglecting transmutation. A few other examples of significant transmutation effects in radioactive source term behavior are known. Decay of ^{140}Ba to ^{140}La and its effect on ex-vessel release is such an example.

So few instances of transmutation effects make it difficult to consider going to the difficulty of developing isotopically based source term models. It would be better to treat in an ad hoc manner the instances where transmutation effects are important and do so within the context of source term models based on the elements.

C. Elemental Inventories of Fission Products

Inventories of fission products for a pressurized water reactor with end-of-life fuel are shown in Table 2.4. Inventories for 30 minutes, 1 hour, 4 hours, and 1 day after scram of the reactor are listed in the table. These inventories are just examples to provide an indication of the order of magnitude of the inventories likely to be encountered in reactor accident analyses. The reactor core for the example was assumed

Table 2.4
Fission Product Inventories* for a PWR Core

	Amount (gram moles) After Decaying for			
Element	30 Min	1 Hour	4 Hours	1 Day
Tritium	1.123	1.123	1.123	1.122
Ge	0.321	0.321	0.321	0.321
As	0.105	0.105	0.105	0.104
Se	45.13	45.13	45.13	45.14
Br	17.50	17.50	17.49	17.48
Kr	294.1	294.1	294.0	294.0
Rb	272.0	272.0	272.0	272.0
Sr	717.6	717.6	717.4	716.8
Y	366.3	366.3	366.2	365.9
Zr	2439	2349	2439	2439
Nb	37.4	37.4	37.4	37.4
Mo	1995	1995	1996	1996
Tc	510.3	510.3	510.4	511.0
Ru	1265	1265	1265	1265
Rh	230.5	230.5	230.6	231.0
Pd	545.4	545.4	545.4	545.7
Ag	27.38	27.39	27.39	27.42
Cd	32.04	32.04	32.04	32.06
In	0.751	0.751	0.752	0.754
Sn	21.71	21.71	21.70	21.70
Sb	7.852	7.844	7.825	7.778
Te	203.5	203.5	203.3	202.8
I	103.6	103.6	103.3	102.3
Xe	2380	2380	2380	2381
Cs	1237	1237	1237	1238
Ba	629.2	629.1	629.0	628.4
La	548.8	548.8	548.7	548.6
Ce	1276	1276	1276	1276
Pr	477.0	477.0	477.1	477.5
Nd	1532	1532	1532	1533
Pm	67.59	67.60	67.61	67.68
Sm	179.5	179.5	179.5	179.6
Eu	53.35	53.35	53.36	53.42
Gd	23.67	23.67	23.68	23.73
Tb	0.565	0.565	0.566	0.566
Dy	0.276	0.276	0.276	0.277
Ho	0.021	0.021	0.021	0.021
Er	0.004	0.004	0.004	0.004
Np	126.3	126.1	125.1	118.7
Pu	2333	2334	2335	2341
Am	16.81	16.82	16.82	16.85
Cm	5.277	5.278	5.278	5.278

---

*Inventories in this table were taken from Reference 8.

to consist of 89.1 metric tons of uranium. The burnup of the fuel was 33,500 MWd/ton uranium produced over 3 years on an 80 percent duty cycle. For more details on the calculations see Reference 5.

D. Need to Consider Nonradioactive Inventories

The consideration of inventories would stop after the amounts of radioactive materials were defined if the classic pathways [1] to defining source term were followed. This is acceptable in bounding estimates, in which mitigation of the phenomenological source term is not mechanistically evaluated. As outlined in the introductory material, this is not now an acceptable procedure. Source terms developed now and in the future will have to meet the needs of mechanistic calculations of fission product behavior after the fission products have escaped the fuel. The detailed description of the behavior of fission products released from the fuel are to be found in Chapter 5 of this document. Two of the most important features of the behavior are:

1. Fission product vapors can condense to form aerosols which can subsequently grow, sediment, or deposit on primary system structures and not escape either into containment or into the environment.
2. Fission product vapors can react with structural materials and be bound so they cannot escape into the containment or the environment.

Both of these processes have the potential of substantially reducing the fraction of the radionuclides released from the fuel that eventually escape the reactor plant.

Temperatures and conditions in the reactor core conducive to the vaporization of fission products are equally conducive to the vaporization of nonradioactive materials from the core. The extent of vaporization of nonradioactive materials that occurs while fission products are being vaporized directly affects the post-release behavior of the fission products. In particular, vaporization of nonradioactive materials will have a direct bearing on the efficacy of the two source term mitigation processes mentioned above.

Consider a situation in which a well-stirred atmosphere initially contains 10 g/m^3 of radioactive particles. These particles will be lost from the atmosphere by a variety of processes--diffusion to the walls, settling, etc. At the relatively high concentrations considered here and the relatively high concentrations of interest for reactor accident analyses, gravitational settling of the particles is the dominant mechanism of particle loss from the atmosphere. Settling is an especially efficient process because the particles agglomerate. In a well-stirred atmosphere the particles settle more rapidly with increasing particle size. The rate of loss of particles depends on a variety of factors such as the particle shape and density. A typical example of the variation in the concentration of material in the atmosphere with time is shown as a dashed line in Figure 2.10. After about 2 hours the mass concentration in the atmosphere has fallen to 1 g/m^3. After about 34 hours the concentration is only 0.01 g/m^3.

Now consider a situation in which the well-stirred atmosphere initially contains 10 g/m^3 of nonradioactive aerosol in addition to 10 g/m^3 of radionuclides. Though interest focuses on the radionuclides, the nonradioactive particles also agglomerate both with other nonradioactive particles and with radionuclide particles. The rate of agglomeration varies with nearly the square of the particle number concentration irrespective of the radioactivity of the particles [18]. More rapid loss of radionuclides from the atmosphere would be expected. This is, in fact, what occurs. The solid line in Figure 2.10 is the time dependence of radioactive material concentration in the atmosphere when the nonradioactive particles are present. In this case the concentration of radioactive species falls to 1 g/m^3 after only 1.5 hours. The concentration is less than 0.01 g m^3 after only 25 hours.

In reactor accident situations, the effects of nonradioactive particles may be even more severe than depicted in the hypothetical example described above. The inventory of nonradioactive species available for release during an accident will be shown, below, to be very large. Particle concentrations in the atmosphere from these nonradioactive sources can be several times the concentrations of particles formed from radionuclides. The dotted line in Figure 2.10 is for a situation in which the initial mass concentration in the atmosphere is 100 g/m^3, of which 10 g/m^3 is radionuclides. In this case, it takes only 0.5 hours to reduce the suspended radioactivity by a factor of 10 and only 2.5 hours to reduce it by a factor of 100.

Clearly, to take into account mitigation of radionuclide release by aerosol processes, it is necessary to know the release of nonradioactive species. Because nonradioactive species come from sources other than the fuel, release models distinct from those used for radionuclides may be needed. The generation of aerosols from nonradioactive materials can exceed aerosol generation from radionuclides by well over an order of magnitude.

Next, consider an example of fission product vapors reacting with structures. Sallach et al. [19] have found that tellurium vapors react rapidly with structural steel such as type 304 stainless steel. They have also found that Te vapors will

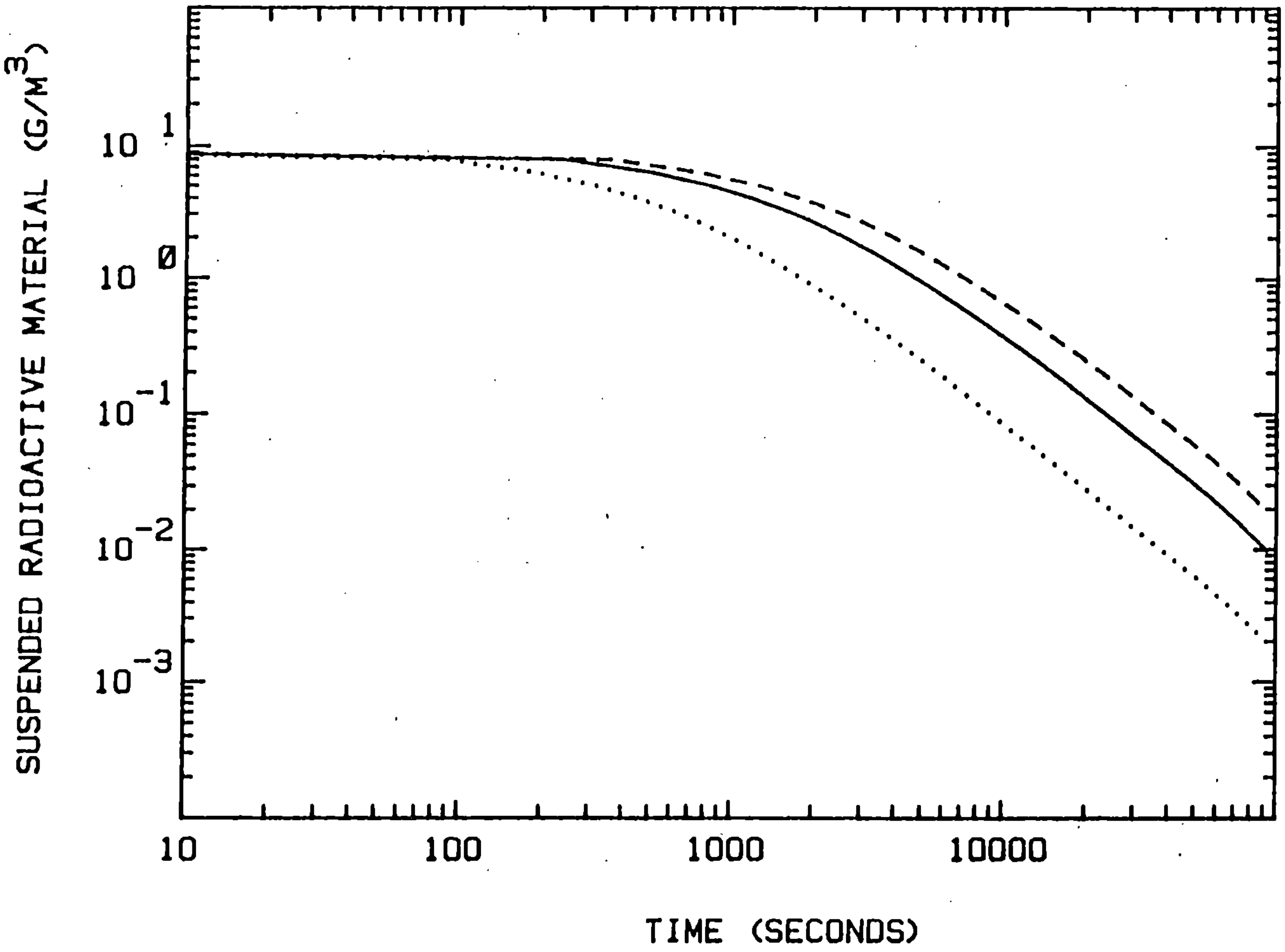

Figure 2.10. Effect of Nonradioactive Aerosols on the Time Dependence of the Concentration of Radioactive Aerosols. Dashed line is for radionuclides only. Solid line is for radionuclides and an equal amount of nonradioactive material. Dotted line is for a case in which radionuclides make up only 10% of the initial aerosol mass.

react rapidly with silver, which might be present in the primary system atmosphere because precious metal control rod alloys are vaporizing. Clearly, a competition for Te vapors can exist. The Te vapors can react with structural metals, and consequently, not become part of the radiological source term. Or, the Te vapors can react with silver aerosols and remain part of the source term provided aerosol processes are neglected.

The fate of Te vapors depends on the availability of surfaces --either structural or aerosol--for reaction. In Figure 2.11, the fraction of Te that has reacted with silver aerosol rather than structural steel, and consequently, remains a part of the source term, is shown as a function of the silver aerosol concentration. For this calculation the aerosol was assumed to consist of 1 µm particles and the steel was assumed to be present as the walls of an 18-inch diameter pipe. This figure shows that the mitigative effect of fission product release caused by fission product reactions with structures can be prevented to a significant extent if reactive aerosols are present along with the fission products. Since the aerosols produced by vaporization of nonradioactive materials can be chemically quite reactive toward fission products, the magnitude and timing of the vaporization must be known if the fate of the fission products is to be properly described.

E. Inventories of Nonradioactive Materials

The arguments made above demonstrate how important it is to develop source terms for nonradioactive species likely to be vaporized from the reactor core. There are some essential differences between the fission product source term and the nonradioactive source term. The most important of these is that the nonradioactive sources are not intimately associated with a heat source. The attentions concerning the nonradioactive sources should then focus on the most volatile constituents since it is likely that the host matrix for these constituents will be cool, at least relative to fuel. Some care must be exercised in making this discrimination among nonradioactive materials in the core, since materials that might appear refractory readily react in the high-temperature, high-pressure steam environment of a reactor to yield volatile products.

Because the nonradioactive materials are not typically associated with a heat source, the contribution of these materials to the aerosol emissions from a reactor core during an accident are difficult to define. Inventories of volatile materials that can make these contributions are not defined simply by the masses of nonradioactive host materials in and adjacent to the core. Some other means, preferably mechanistic calculation, must be found to determine if the host material gets hot enough for its volatile constituents to contribute to the aerosol emissions. Whether and how much of the host materials

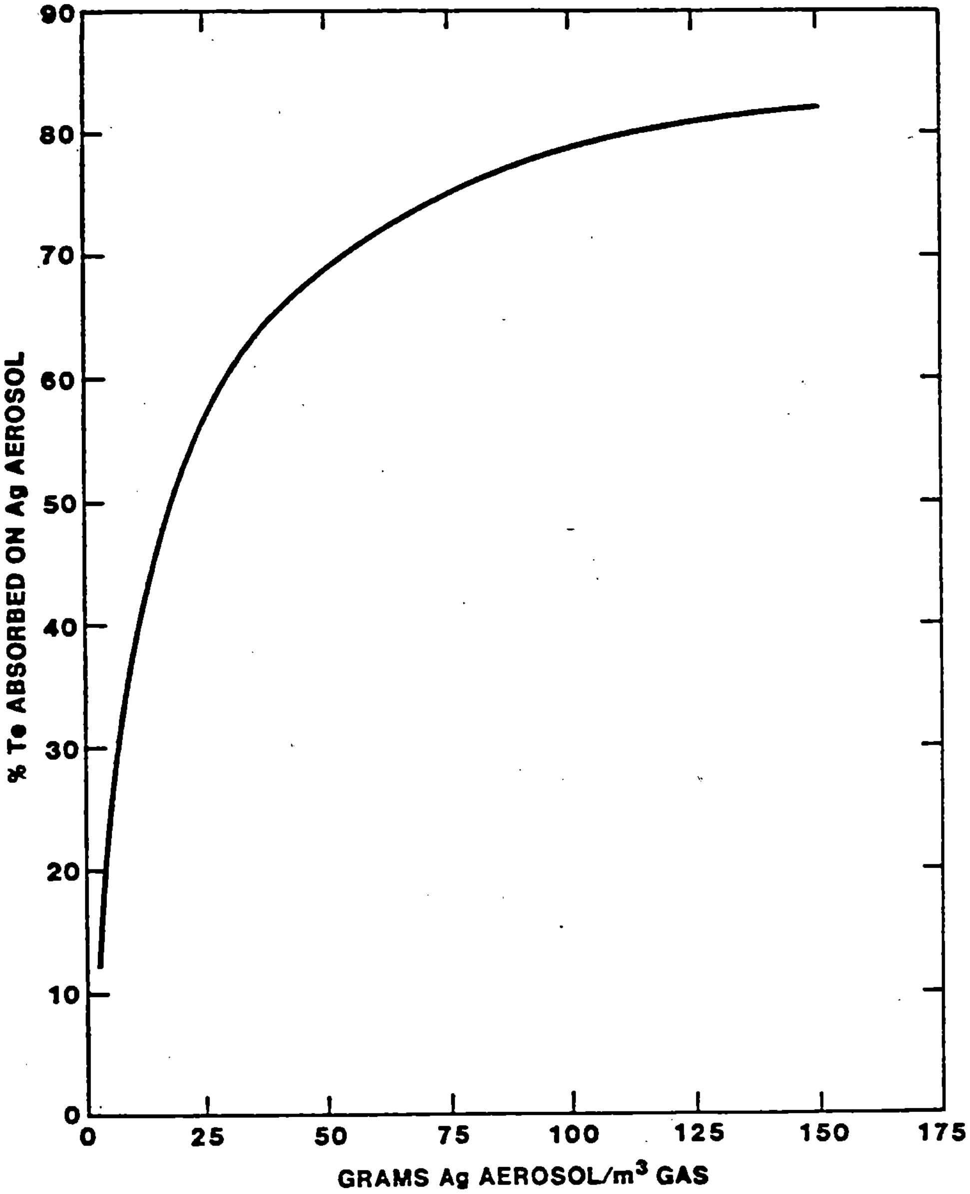

Figure 2.11. Competition Between Reaction of Te with Steel and Reaction of Te with Silver Aerosols

participate in the vaporization process will depend on the heat-up and melting of the reactor fuel. The behavior of the fuel, in turn, will depend on the nature of the particular accident in question.

Considerations made to date indicate that the nonradioactive materials most likely to be vaporized from the core are:

1. Alloying agents in the fuel cladding.
2. Precious metal control rod alloys.
3. Products of steam reaction with boron carbide or borosilicate glass control rod materials.
4. Volatile alloy constituents or impurities in the structural steels of the reactor.

Fuel cladding in nearly all light water reactors is either Zircaloy 2 or Zircaloy 4 (stainless steel cladding on the fuel in San Onofre Unit 1 is a well-known exception). The compositions of these alloys are:

Weight Percent of Trace Elements in Zircaloy 2 and 4

Element[a]	Zircaloy 2	Zircaloy 4
Sn	1.5	1.5
Fe	0.12	0.2
Cr	0.10	0.10
Ni	0.05	-

[a] Balance of alloy mass is Zr and < 150 ppm Hf.

Tin is the most volatile constituent of the clad. In a typical pressurized water reactor there will be 250 kg of tin. In a boiling water reactor there might be as much as 905 kg of tin that can participate in the vaporization process. Other constituents of the clad could contribute only about 1/10 as much to the aerosol as tin. Chromium is moderately volatile when in the metallic state (boiling point = 2938 K) or in the highly oxidized hexavalent state (boiling point of CrO_3 = 600 K). The volatility of chromium is significantly depressed when the trivalent state of chromium is stable.

Iron is not especially volatile, except at quite high temperatures. In oxygen both Fe(g) and FeO(g) are important gas species. In steam FeOH(g) and $Fe(OH)_2$(g) can form. The gas species FeO(OH)(g) has been hypothesized.

Nickel vaporizes primarily as a metal.

Many pressurized water reactors use an alloy of silver, indium, and cadmium as a control rod material. A typical inventory of this control rod alloy in a large pressurized water reactor is:

Silver (Ag)	2365 kg
Indium (In)	442 kg
Cadmium (Cd)	147 kg

All constituents of this alloy are volatile. A rather thorough thermochemical analysis of the vaporization of this alloy has been done recently [20]. As the alloy is heated within the control rod sheath, quite high partial pressures of Cd are produced:

Temperature (K)	Cadmium Partial Pressure (atm)
1000	0.015
1200	0.129
1400	0.598
1600	1.898
1800	4.671
2000	9.634

Pressure from the cadmium as well as pressurization of the helium fill gas in the rod can cause the control rod clad to rupture [21, 22]. Once evaporation can take place the cadmium is preferentially distilled from the alloy. Subsequent evaporation from the Ag-In alloy requires higher temperatures and is not congruent. The rate of vaporization may be controlled in a reactor accident by heat input to the alloy.

Both pressurized water reactors and boiling water reactors use B_4C control rod materials or borosilicate glass burnable poisons. The predominant neutron absorption reaction is

$$^{10}_{5}B + n \rightarrow {}^{7}_{3}Li + \alpha$$

so that after some period of operation, the rods contain lithium. A typical boiling water reactor would contain 530 kg of boron. A pressurized water reactor might contain 82 kg boron and 137 kg SiO_2.

In steam, boron reacts according to the stoichiometry [23]:

$$B_4C + 6H_2O \rightarrow 2B_2O_3 + C + 6H_2$$

The product B_2O_3 will also react with steam to produce boric acid vapors (H_2BO_2 and H_3BO_3). Reactions of these boric acids with fission products are of concern. For instance, the reaction

$$HBO_2 + CsI \rightarrow HI + CsBO_2$$

is suspected as a means of creating vapor phase iodine in the primary system.

Silicates will also vaporize at high temperatures. The vaporization process can be described by the reactions such as:

$$SiO_2(c) + H_2 \rightarrow H_2O + SiO(g)$$

$$SiO_2(c) + 2H_2O \rightarrow Si(OH)_4(g) \quad .$$

Silica, too, is reactive toward CsI, yielding a silicate and free iodine [23].

Compositions of important structural alloys found in nuclear reactors are listed in Table 2.5. It is not possible _a priori_ to say how much of a contribution constituents of these alloys could make to aerosol emissions during a severe accident. The contribution depends on the heating of the steel, which in turn depends on the nature of the core meltdown process. The vaporization of Mn, Mo, Si, S, and P will make the earliest contributions. Vaporization of the major alloy constituents has been discussed above. If reactive vaporization is neglected, then the vapor pressure of 304 stainless steel is given by [24]:

$$\log P(\text{atms}) = 6.1210 - 18{,}836/T(K)$$

and the vapor pressure of 316 stainless steel is given by:

$$\log P(\text{atms}) = 6.1127 - 18{,}868/T(K) \quad .$$

The vaporization of neither alloy is congruent.

F. Chemical Classification of the Elements for Source Term Models

There are about 1000 isotopes that are of interest for severe accident source term models. From the preceding discussions it is apparent that the source term models need not be constructed to explicitly predict release and behavior of so many isotopes. Rather, the models can be constructed to predict the behavior of some 100 elements. This factor of 10 reduction in the effort needed to develop source term models is important. The effort needed to describe release and behavior of 100 elements may still be too much for many applications. Even if the list of elements to be explicitly treated were pared of elements with low inventories in the reactor core, only about a factor of two reduction in the source term modeling effort would be achieved.

Table 2.5

Compositions of Important Structural Alloys (weight percent)

Alloy	Fe	Cr	Ni	Mn	Mo	Other Elements
304 Stainless	bal	18-20	8-10.5	2	-	0.08 C; 0.045 P; 0.03 S; 1 Si
308 Stainless	bal	19-21	10-12	2	-	0.08 C; 0.045 P; 0.03 S; 1 Si
309 Stainless	bal	22-24	12-15	2	-	0.2 C; 0.045 P; 0.03 S; 1 Si
316 Stainless	bal	16-18	10-14	2	2-3	0.08 C; 0.045 P; 0.03 S; 1 Si
Inconel 600	8	15.5	76	0.5		0.08 C; 0.008 S 0.25 Cu

To further reduce the magnitude of the source term model development effort, another approximation must be introduced. Historically, the additional approximation is to group the elements into chemically similar categories and explicitly treat only one element from each category in the source term model. This is exactly the type of approximation used in the Reactor Safety Study [1]. Seven chemical categories were defined as listed below:

1. Noble Gases: Xe, Kr
2. Halogens: I, Br
3. Alkali metals: Cs, Rb
4. Alkaline earths: Sr, Ba

5. Tellurium group: Te, Se, Sb

6. Transitional metal group: Ru, Mo, Pd, Rh, Tc

7. Lanthanides: La, Nd, Eu, Y, Ce, Pr, Pm, Sm, Np, Pu, Zr, Nb, U, Th

The underlined element in each of the above groups was taken to be the representative of that group. It was this representative element that was actually treated in the Reactor Safety Study source term model. The behaviors of other elements were assumed to be similar to that of the group representative.

All chemical categorizations of the elements require some subjective discrimination between the similarities and differences in the chemistries of the elements. The chemistries of all elements are indeed different. The differences can be amplified or muted depending on the chemical environment and the process of interest.

Consider, as an example of the difficulties of chemical categorization of the elements, the noble gases. The very, very weak chemical interactions of Xe and Kr leads nearly all analysts to group these elements and treat them as one species. Certainly for the purposes of estimating the behavior of noble gases at very high temperatures this is an acceptable approximation. Were the attentions switched to the consideration of filtered vents with activated charcoal trapping of the noble gases, grouping of the noble gases Xe and Kr would not be acceptable. Xenon will absorb efficiently on activated charcoal even at surprisingly high temperatures. Krypton, on the other hand, absorbs on charcoal only at low temperatures that would be difficult to maintain in an environment expected to develop during a severe reactor accident. Most schemes for filtered venting with noble gas trapping are found wanting because of the chemical differences between krypton and xenon which in other contexts are negligible.

It is apparent then that any categorization of the elements will be specific to a given process and will reflect only some subset of the properties of the elements. As a broader base of information and analysis develops, it will not be surprising if exceptions are found or paradoxes develop from the categorizations.

The groupings for the noble gases, halogens, and alkali metals developed for the Reactor Safety Study are defensible. As noted above, grouping of the noble gases can fail for situations radically different than the high temperature environments usually of interest in source term modeling. Chemical bonding of bromine and iodine are somewhat different but these differences are usually manifest at only low temperatures or in an aqueous medium. Grouping of the alkali metals is particularly acceptable. Even in sophisticated chemical studies Cs and Rb are considered to have nearly identical chemistries.

Difficulties with the Reactor Safety Study categorization begin to appear in the alkaline earth group. Barium and strontium have qualitatively similar chemistries. But, in quantitative features they are somewhat different. Barium is more easily reduced from the oxide to the metal than strontium. Barium typically exhibits higher vapor pressures than does strontium. The Reactor Safety Study authors recognized these quantitative differences, apparently, and in many cases explicitly treated both elements. For most purposes the quantitative differences between the behavior of Sr and the behavior of Ba may not be of sufficient significance to warrant separate treatment of the elements. For situations involving release of the elements from fuel some conservatism can be introduced by selecting barium rather than strontium as the group representative.

The remaining chemical categories defined in the Reactor Safety Study (the Tellurium, Transition Metal, and Lanthanides Groups) are most difficult to rationalize. These categorizations ignore both quantitative and qualitative differences in chemistry. Tellurium and certainly selenium are essentially nonmetals. Antimony, on the other hand, is a main group metal. Te and Se will react with metals much as does sulfur to form covalent compounds. Antimony will alloy with metals. When antimony does form a compound with a metal compound, it is typically an intermetallic with metal-metal bonding. There seems to be little reason to expect release of antimony to parallel the release of tellurium and selenium in all of the wide variety of chemical circumstances created by severe reactor accidents. The differences in chemistry during transport of antimony and tellurium released from the fuel ought to be even more obvious.

Ruthenium, palladium, and rhodium are platinoids, notable for their lack of reactivity and refractory qualities. Molybdenum and technetium are early transition elements with a rich oxide chemistry that can develop at the oxygen potentials liable to be present around reactor fuel during a severe accident. There seems to be no reason to expect all these elements to behave similarly during release from the fuel or during transport.

Actinides, lanthanides, and early transition metals, Nb and Zr, are lumped into the Reactor Safety Study's "Lanthanide" Group. Thereby, the release of practically nonvolatile zirconium is presumed similar to uranium despite the fact uranium can form quite volatile hexavalent species such as UO_3 and $UO_2(OH)_2$.

The conservative approach utilized in the Reactor Safety Study focused on release of radionuclides and largely neglected natural processes that might mitigate this release. Consequently, there was little need in the Reactor Safety Study to consider release of nonradioactive species. As noted above, modern source term analyses do not neglect mitigation and consequently cannot neglect release of the nonradioactive species during a severe accident. These nonradioactive species must then be included in any categorization of the elements.

An alternative to the chemical categorization of elements used in the Reactor Safety Study is shown in Tables 2.6 and 2.7. This 13-category scheme incorporates the more important nonradioactive species likely to be vaporized during a severe accident. It repairs some, but by no means all, of the chemistry approximations made in the Reactor Safety Study.

The categorization of the noble gases, alkali metals, alkaline earths, and halogens done in the Reactor Safety Study is retained in this alternate scheme. The only change has been to declare barium the representative of the alkaline earth group. Were the categorization to be used for purposes other than release from the fuel, the representative of the alkaline earth group might be selected to be strontium because of the decay of ^{140}Ba.

Explicit addition of sodium and potassium to the alkali metals has been noted. Also, calcium and magnesium have been added to the alkaline earth groups. These additions have been made to accommodate the release from concrete during ex-vessel interactions of core debris.

Tellurium and selenium constitute a single group in the scheme. Antimony has been incorporated into one of the two Main Group categories.

The Main Group categories are added to accommodate releases of control rod alloy species and tin from the Zircaloy clad. The Main Group elements exhibit a wide range of volatilities. For instance, cadmium boils at 1040 K whereas tin boils at 2543 K. Consequently, the Main Group elements have been split into two categories. Cadmium is taken as the representative of the more volatile Main Group category. Tin, rather than silver, is taken as the representative of the less volatile Main Group elements.

The choices for representatives of the two Main Group categories have been made based on expectations concerning accident analyses. It would be expected that during severe accidents in pressurized water reactors that the control rods would rupture and expel cadmium. There is so much cadmium, and it would be released so suddenly, it will be important to consider explicitly in accident analyses. Silver, too, might be released from the

Table 2.6

Classification of the Elements into Chemically Similar Groups

Group Name	Representative Element	Elements in the Group
Noble gases	Xe	He, Ne, Ar, Kr, Xe, Rn, He, Ne
Alkali metals	Cs	Li, Na, K, Rb, Cs, Fr, Cu
Alkaline earths	Ba	Be, Mg, Ca, Sr, Ba, Ra
Halogens	I	F, Cl, Br, I, At
Chalcogens	Te	O, S, Se, Te, Po
Platinoids	Ru	Ru, Rh, Pd, Re, Os, Ir, Pt, Au, Ni
Transition Metals I	Mo	V, Cr, Fe, Co, Mn, Nb, Mo, Tc, Ta, W
Tetravalents	Ce	Ti, Zr, Hf, Ce, Th, Pa, U, Np, Pu
Trivalents	La	Al, Sc, Y, La, Ac, Pr, Nd, Pm, Sm, Eu, Gd, Tb, Dy, Ho, Er, Tm, Yb, Lu, Am, Cm, Bk, Cf
Uranium	U	U
Main Group I	Cd	Cd, Hg, Zn, As, Sb, Pb, Tl, Bi
Main Group II	Sn	Ga, Ge, In, Sn, Ag
Boron	B	B, Si, P

Table 2.7

Alphabetical Listing of the Elements and Their Classification

Element	Group	Representative
Actinium	Trivalents	La
Aluminum	Trivalents	La
Americium	Trivalents	La
Antimony	Main Group I	Cd
Argon	Noble Gases	Xe
Arsenic	Main Group I	Cd
Astatine	Halogens	I
Barium	Alkaline Earths	Ba
Berkelum	Trivalents	La
Berylium	Alkaline Earths	Ba
Bismuth	Main Group I	Cd
Boron	Boron	B
Bromine	Halogens	I
Cadmium	Main Group I	Cd
Calcium	Alkaline Earths	Ba
Californium	Trivalents	La
Carbon	Tetravalents	Ce
Cerium	Tetravalents	Ce
Cesium	Alkali Metals	Cs
Chlorine	Halogens	I
Chromium	Transition Metals	Mo
Cobalt	Transition Metals	Mo
Copper	Alkali Metals	Cs
Curium	Trivalents	La
Dysprosium	Trivalents	La
Einsteinium	Alkaline Earths	Ba
Erbium	Trivalents	La
Europium	Trivalents	La
Fermium	Alkaline Earths	Ba
Fluorine	Halogens	I
Francium	Alkali Metals	Cs
Gadolinium	Trivalents	La
Gallium	Main Group II	Sn
Germanium	Main Group II	Sn
Gold	Platinoids	Ru
Hafnium	Tetravalents	Ce
Helium	Noble Gases	Xe
Holmium	Trivalents	La
Hydrogen	Noble Gases	Xe

Table 2.7 (continued)

Alphabetical Listing of the Elements and Their Classification

Element	Group	Representative
Indium	Main Group II	Sn
Iodine	Halogens	I
Iridium	Platinoids	Ru
Iron	Transition Metals	Mo
Krypton	Noble Gases	Xe
Lanthanum	Trivalents	La
Lithium	Alkali Metals	Cs
Lead	Main Group I	Cd
Lutetium	Trivalents	La
Magnesium	Alkaline Earths	Ba
Manganese	Transition Metals	Mo
Mercury	Main Group I	Cd
Molybdenum	Transition Metals	Mo
Neodymium	Trivalents	La
Neon	Noble Gases	Xe
Neptunium	Tetravalents	Ce
Nickel	Platinoids	Ru
Niobium	Transition Metals	Mo
Nitrogen	Noble Gases	Xe
Osmium	Platinoids	Ru
Oxygen	Chalcogens	Te
Palladium	Platinoids	Ru
Phosphorus	Boron	B
Platinum	Platinoids	Ru
Plutonium	Tetravalents	Ce
Polonium	Chalcogens	Te
Potassium	Alkali Metals	Cs
Prasedymium	Trivalents	La
Promethium	Trivalents	La
Protactinium	Tetravalents	Ce
Radium	Alkaline Earths	Ba
Radon	Noble Gases	Xe
Rhenium	Platinoids	Ru
Rhodium	Platinoids	Ru
Rubidium	Alkali Metals	Cs
Ruthenium	Platinoids	Ru

Table 2.7 (continued)

Alphabetical Listing of the Elements and Their Classification

Element	Group	Representative
Samarium	Trivalents	La
Scandium	Trivalents	La
Selenium	Chalcogens	Te
Silicon	Boron	B
Silver	Main Group II	Sn
Sodium	Alkali Metals	Cs
Strontium	Alkaline Earths	Ba
Sulfur	Chalcogens	Te
Tantalum	Transition Metals	Mo
Technetium	Transition Metals	Mo
Tellurium	Chalcogens	Te
Terbium	Trivalents	La
Thallium	Main Group I	Cd
Thorium	Tetravalents	Ce
Thulium	Trivalents	La
Tin	Main Group II	Sn
Titanium	Tetravalents	Ce
Tungsten	Transition Metals	Mo
Uranium	Uranium	U
Vanadium	Transition Metals	Mo
Xenon	Noble Gases	Xe
Ytterbium	Trivalents	La
Yttrium	Trivalents	La
Zinc	Main Group I	Cd
Zirconium	Tetravalents	Ce

control rod alloy. But, the alloy will be quite fluid and should promptly drain from the heated core regions so releases will be minimized. Tin from the fuel clad will be present in both pressurized and boiling water reactors. The tin will remain intimately associated with degrading fuel. It will then be necessary to explicitly consider tin release.

The platinoids are grouped. Ruthenium is taken to be the representative of this group because of its radiological consequences if it appears in the radiological source term. Some caution is necessary in the use of this representative. Rhodium can have greater volatility than ruthenium in the steam/hydrogen environment of the primary system during a severe accident. Nickel is included in the platinoid group because of this element's low volatility in steam and hydrogen atmospheres.

A new group is formulated of the early transition elements. These elements are readily oxidized in steam and hydrogen environments. The oxidized forms of these elements tend to be volatile. Molybdenum is chosen to be the representative of the group because of the diversity of its chemistry and the radiological importance of this element. Structural elements iron and manganese are included in the group, though it would not be difficult to rationalize a separate category for these elements. The structural element chromium is included in the group because of the similarity of its chemistry to that of the representative of the group, Mo.

Uranium could easily be incorporated in the early transition metal group. Because of the actinide contraction, uranium exhibits chemistry quite similar to that of molybdenum. In particular, the hexavalent state of uranium is quite volatile. But, because of the obvious importance of distinct, explicit, treatment of uranium during severe reactor accidents, a separate category is reserved for this element.

The lanthanides and actinides are split into two categories, the trivalent elements and the tetravalent elements. The tetravalents favor, even at high temperatures, the cubic fluorite structure of UO_2. Consequently, the activity and volatility of these elements dissolved in UO_2 remains low.

The trivalent elements favor the various hexagonal structures and dissolve in UO_2 only at the expense of some loss of stability. This loss of stability is reflected by somewhat higher than expected volatility. Yttrium is included with the trivalents, though it is assuredly a transition element. Because of the lanthanide contraction, the chemistry of yttrium is amazingly similar to that of lanthanum.

, it is not in the trivalents in table 2.6

At first glance, it might seem unreasonable to place plutonium among the trivalents. It is, after all, present as tetravalent PuO_2 in reactor fuel. But at elevated temperatures plutonium exhibits a distinct tendency to reduce to the trivalent state.

Finally, a separate group is set aside for boron. This category is important only if large amounts of boron or borosilicate glass are present in the core. Silicon and phosphorous are included in the group because these elements, too, reactively vaporize in steam.

Because of its subjective nature and its dependence on chemical circumstances that are poorly known, chemical categorization will never be an entirely satisfactory approximation. Categorizations, and certainly the selection of the representative element from each group, ought to change as more knowledge develops concerning severe accidents.

Alternatives to chemical categorization have been suggested. Powers [25] has developed a procedure for allocating scarce research resources to the study of fission products that is based on the attributes of the fission products rather than the similarities of their chemistries. The elements are rank-ordered in terms of several attributes. Powers chose (1) inventory, (2) decay rate, (3) thermal power, (4) melting point, and (5) radiological consequences. Ties are allowed in the ranking to account for uncertainty. The ranks within each attribute group are summed for each element. These sums can be multiplied by penalty functions to account for risk adverse or cost adverse tastes. The rank sums are themselves ranked in rank order until (1) resources are exhausted, (2) the marginal rate of return has fallen to a sufficient level that greater utility is obtained by turning to the next lower rank, or (3) attentions have gone to ranks low enough that the elements are known to be unimportant. An example of this type of rank ordering is shown in Table 2.8.

The rank-ordering procedure has not received universal endorsement and has not been adopted here.

Another procedure that has been suggested is to assume various releases of elements, use the CRAC code [26] to determine the consequences of the release, and from these consequences determine which fission products are most important. Unfortunately, this procedure is exceptionally laborious. It requires a great deal more knowledge concerning chemical form and nature of the release than is typically available. Finally, the results change with different assumptions concerning the consequence code.

Table 2.8

Importance Ranking of Radionuclides in Terms of Inventory, Dose Curies, and Mobility

Rank	Element at Indicated Time After Scram		
	1 Hour	1 Day	100 Days
1	Cs	I	Zr
2	I	Te	U
3	Te	Cs	Pr
4	Rb	Xe	Nb
5	Ba	Ba	Cs
6	Mo	Pr	Ce
7	Pr	Mo	Rh
8	La	Ce	Y
9	Np	Zr	Sr
10	Xe	Nb	Fe
11	Sn	Np	Ru
12	Sr	La	Te
13	Nb	Sn	Ba
14	Y	Rh	Ni
15	U	Tc	Cr
16	Tc	Sr	Xe
17	Ce	Nd	^3H
18	Zr	Y	Kr
19	Sb	U	Sn
20	Br	Ru	Pm
21	Kr	Sm	Cm
22	Rh	Sb	Se
23	Nd	Pd	Rb
24	Ru	Cr	Cd
25	Mn	Ag	Zn

2.4 Recommendations for MELCOR

From the preceding discussions the following recommendations for the development of MELCOR are formulated:

1. Radionuclide inventories ought not be calculated within MELCOR. Rather, these inventories should be calculated with one of the specialized codes such as ORIGEN. A set of default values should be included in MELCOR.

2. It is desirable that provision be made in MELCOR to have radical and axial variations in the inventories of the radionuclides.

3. Elemental release models rather than isotopic release models can be used in MELCOR. It is possible that one exception to this general rule is the release of ^{132}I and ^{132}Te.

4. Release of nonradioactive species as well as release of radionuclides will have to be considered in MELCOR. This may necessitate separate release models for fuel, cladding, structural materials, and control rods.

5. The many elements susceptible to release during a severe accident may be grouped into 13 categories. The release and behavior of members of a given category is then described by the release and behavior of a single representative element in the category. The categorization recommended here is shown in Table 2.6 and an alphabetical cross index is provided in Table 2.7.

References

1. USNRC, Reactor Safety Study: An Assessment of Accident Risks in US Commercial Nuclear Power Plants, WASH 1400, NUREG 75/04, October 1975.

2. J. G. Kemeny, Chairman, Report of the President's Commission on The Accident at Three Mile Island, and L. Jaffe, Head, Reports of the Technical Assessment Task Force, Vol. 1, October 1975.

3. R. S. Denning, "Reduction in Reactor Risk by the Mitigation of Accident Consequences," Proc. ANS/ENS Topic Meeting on Thermal Reactor Safety, Knoxville, TN, April 1980, CONF-800403, Vol. 1, p. 189.

4. N. Feather, "Ternary Fission--a Review," Proc.. 2nd IAEA Symposium on the Physics and Chemistry of Fission, Vienna, 28 July-1 August 1969, International Atomic Energy Agency, 1969.

5. R. A. Nobles, Phys. Rev. 126 (1962) 1508.

6. S. W. Cooper, et al., Phys. Rev. 154 (1967) 1193.

7. M. D. Cable, J. Honkanen, E. C. Schloemer, M. Ahmed, J. W. Ewidd, Z. Y. Chou and J. Cerny, Phys. Rev. C 30 (1984) 1276.

8. D. E. Bennett, Sandia-ORIGEN User's Manual, NUREG/CR-0987, SAND79-0299, Sandia National Laboratories, Albuquerque, NM, October 1979.

9. D. R. Olander, Fundamental Aspects of Nuclear Reactor Fuel Elements, UC-796, TID 26711, 1975.

10. Personal Communication to D. A. Powers from T. P. Suchocki (GPU) dated 6 June 1978.

11. D. A. Powers, "Plausible Conditions of the TMI-2 Core," Transactions ANS 34 (1980) 563.

12. A. G. Croff, ORNL-5621, Oak Ridge National Laboratory, 1980.

13. "Radionuclide Release and Transport," Chapter 8 in PRA Procedures Guide, Volume 1, NUREG/CR-2300, January 1983.

14. T. L. Hill, An Introduction to Statistical Thermodynamics, Addison Wesley Pub. Co., 1960.

15. L. Melander, Isotope Effects on Reaction Rates, The Ronald Press Co., NY, 1960.

16. S. Gladstone, K. J. Lalder, and H. Eyring, The Theory of Rate Processes, McGraw-Hill Book Co., 1961.

17. D. Williams, "Effects of Radioactive Decay Chains on Source Terms," Appendix C in R. J. Lipinski, et al., Uncertainty in Radionuclide Release Under Specific LWR Accident Conditions Volume II: Analyses, SAND84-0410/2, Sandia National Laboratories, Albuquerque, NM, October 1984.

18. L. D. Reed, J. A. Gieseke, and H. Jordan, Effects of Radiation on Aerosol Behavior, BMI-NUREG-1943, Battelle Columbus Laboratory, Columbus, Ohio, December 1975.

19. R. L. Sallach, C. J. Greenholt, and A. R. Taig, Chemical Interactions of Tellurium Vapors with Reactor Materials, NUREG/CR-2921, SAND82-1145, Sandia National Laboratories, Albuquerque, NM, March 1984.

20. D. A. Powers, Behavior of Control Rods During Core Degradation: Pressurization of Silver-Indium-Cadmium Control Rods, NUREG/CR-4401, SAND85-0469 Sandia National Laboratory, Albuquerque, NM.

21. S. Hagan, KfK 2750, pp. 4300-4362, Kernforschungs-zentrum Karlsruhe, November 1978.

22. G. W. Parker, G. E. Creek, and A. L. Sutton, Jr., "Influence of Variable Physical Process Assumptions on Core Melt Aerosol Release," Proc. Int'l Mtg. on Thermal Reactor Safety, Chicago, IL, NUREG/CP-0027, Vol. 2, p. 1078, 1983.

23. R. M. Elrick and R. A. Sallach, Quarterly Report for The Advanced Reactor Safety Research Program, NUREG/CR-2679, SAND82-0904, Sandia National Laboratories, Albuquerque, NM.

24. C. S. Kim, Thermophysical Properties of Stainless Steels, ANL-75-55, Argonne National Laboratory, September 1975.

25. D. A. Powers, unpublished results.

26. L. T. Ritchie, J. D. Johnson, and R. M. Blond, Calculation of Reactor Accident Consequences, Version 2, NUREG/CR-2326, SAND81-1994, Sandia National Laboratories, Albuquerque, NM, February 1983.

CHAPTER 3

RELEASE OF FISSION PRODUCTS AND GENERATION OF AEROSOLS DURING THE IN-VESSEL PHASES OF A SEVERE REACTOR ACCIDENT

3.1 An Introduction to the In-Vessel Source Term and the Objectives of this Chapter.

Severe reactor accidents are, by definition, accidents in which the reactor fuel and clad are heated to the point that they suffer significant damage. Typically, this damage is presumed to progress through complete melting of the core and extensive reaction of the fuel cladding with steam.

The cladding on the fuel is often considered to be the first, and in some respects, the most important barrier to release of radionuclides from the reactor core. As soon as the cladding is damaged, radionuclide release begins. Volatile radionuclides such as Xe, Kr, Cs and I can be nearly quantitatively expelled from the fuel during core degradation within the reactor vessel. Once radionuclides have escaped the fuel there is at least the possibility that they may escape the power plant. The volatile radionuclides, so extensively released during core degradation, are also among the most radiologically consequential. A great deal of the attention in severe reactor accident analyses is devoted to determining the release and behavior of these volatile radionuclides. Over 70% of the discussion of severe accident source terms presented in the Reactor Safety Study [1] is devoted to the escape of volatile fission products from degrading reactor fuel. In some very simplified discussions of severe reactor accidents, there has been the implication that release of cesium and iodine from degrading reactor fuel is indeed the entire, substantive source term of radioactivity. Though this simplification is grossly in error, it is true the release of Cs and I from degrading reactor fuel is an important aspect of severe accidents.

The approach toward the severe accident source term taken in the Reactor Safety Study was intended to be "conservative." That is, errors in the analysis were to accrue on the side of overestimating the extent of fission product release--especially the release of volatile radionuclide both from the fuel and from the plant. Recently, and especially since the accident involving fuel degradation at Three Mile Island, the treatment of radionuclide release presented in the Reactor Safety Study has been questioned [2,3]. Most of the criticism has suggested that the models developed for the Reactor Safety Study may have been too conservative. These models neglect natural phenomena that would reduce the amount of radioactive material escaping the fuel that could escape the plant. Criticism that the

Reactor Safety Study may have been nonconservative has also appeared. Criticisms of the analyses done for the Reactor Safety Study have focused on release of radioactivity from the plant. But, in every case, the alternate considerations have been based on different portrayals of radionuclide release from the reactor fuel.

Criticisms of the Reactor Safety Study have prompted the initiation or continuation of many analytic and experimental research programs. A recent survey [4] identified 15 major programs to characterize release of radionuclides from reactor fuel as well as several programs to define the behavior of these radionuclides after release. Several analytic efforts that utilize results of the research to define new severe accident source terms have appeared [5-8]. A consistent thrust in all of the recent work has been to relate in a more mechanistic manner the release of radioactive species from the fuel to phenomena taking place during core degradation. That is, generic release estimates applicable to a wide variety of accidents at a wide variety of plants are being abandoned. In the place of these generic releases are models that are sensitive to features specific to the plant and the accident in question.

Development of mechanistic models of release is a formidable task. The diversity of radionuclides and nonradioactive species that are of interest has been discussed in the preceding chapter. Release of these species is an inherently chemical process. So, release models ought to be sensitive to those features of severe reactor accidents that ought to affect chemistry--notably temperature, pressure, and atmosphere composition. Release is also a transport process, so release models ought also to be sensitive to those features of severe accidents that affect transport--such as gas flow velocities, core geometry, fuel microstructure and clad state.

The definition of severe reactor accidents has progressed considerably since the time of the Reactor Safety Study. Small-break accidents and accidents initiated by power transients have been found to be much greater contributors to the potential risks of nuclear power plants (see, for example, References 9 and 10). Further, it has been found desirable to know not just the potential release of radioactivity, but also how the release varies from one type of accident to another. An indication of the range of variation of accident features that ought to affect release during accidents of interest today is provided in Table 3.1. Flow velocities through the core can vary by 2 to 3 orders of magnitude. Pressures can vary by 2 orders of magnitude. Fuel burn-up can vary by an order of magnitude. Local gas compositions can vary by several orders of magnitude. These wide variations in accident features ought then to cause variations in release of some significant nature.

Table 3.1

Features of Severe Reactor Accidents that Ought to Affect Release

Feature	Typical Range
System Pressure	2 - 170 atmosphere
Maximum Core Temperature	2200 - 3100 K
Heatup Rate of Core	~ 0 - 50 K/s
Flow Velocities Through the Core	1 - 200 cm/s
Extent of Clad Oxidation	20 - 100%
Ratio of Hydrogen to Steam in the Atmosphere	0 - 10^{10}
Fuel Burnup	1000 - 33000 MWd/ton
Time from Scram to Core Melting	1 - 32 hours

Developments have taken place since the time of the Reactor Safety Study in the analyses of radionuclide behavior after release from the fuel as well as in the description of the release process. Some of these developments are described in Chapters 5 and 6 of this report. A key input to the tools for analysis of radionuclide behavior is the timing of radionuclide release. That is, it is no longer adequate to know what is released and how much is released. It is also necessary to know when radioactive and nonradioactive species are released and how fast they are released.

It is clear, then, that models of radionuclide release must be much more sophisticated than those adequate for the Reactor Safety. Essential aspects of modern release models are:

1. The models must be sensitive to those features of plants and accidents that make various accidents different. Generic tables of release are inadequate.

2. Release models must be of mechanistic sophistication compatible with descriptions of subsequent phases of severe accident analyses. That is, seldom will it be adequate to simply assert an integral release fraction without defining the timing and chemical form of the release.

3. Both radioactive species and nonradioactive species must be considered in the definition of release models.

The objective of this chapter is first to describe the technology available for developing models of release from reactor fuel during core degradation. Meeting this objective will require reviewing some of the fundamental aspects of the release process. The second objective of the chapter is to discuss models that have been developed and used to describe release from the reactor fuel. An attempt is made to critically review these models in light of the discussions of the fundamentals of release. Finally, an objective of the chapter is to specify a release model for the MELCOR code that is at once of sufficient sophistication to meet the essential needs for modern reactor accident analyses yet simple enough to fit within the space and execution requirements of a systems code.

3.2 Nomenclature

Despite criticisms of the work, the framework created for the Reactor Safety Study is useful for describing release of radionuclides and nonradioactive species during in-vessel phases of an accident. As set down in the Reactor Safety Study and subsequently modified [11] release in-vessel can be divided into four regimes:

1. Gap Release
2. Diffusion Release
3. Meltdown Release
4. Fragmentation and Oxidation Release

Some sense of the magnitudes in each of these release stages is provided in Table 3.2.

As fuel heats, gases within the fuel rod pressurize. At the same time the clad itself weakens. If the ambient atmosphere is at low pressure, the clad will balloon and rupture. Even if this does not occur, eventually the clad ruptures. During normal operation and during early phases of the accident, radionuclides escape the fuel and collect between the fuel pellet and the fuel clad. When the clad ruptures this collected material can suddenly escape the fuel rod. This gap release of radioactivity can itself be divided into two steps--sudden release during depressurization of the rod and slower release as vapors in the fuel/clad gap diffuse to the point of clad rupture. This release was explicitly considered in the Reactor Safety Study. It is given only limited discussion here. Quite frankly this release is small. It is so rapid that it probably does not require detailed modeling. Uncertainty in gap release pales in comparison to uncertainties in release during subsequent stages of a reactor accident.

Table 3.2

Estimates Made in the Reactor Safety Study [1] of Radioactivity Release During In-Vessel Stages of a Severe Accident

Element	Fraction of the Core Inventory That Escapes the Fuel During[a]			
	Gap Release	Diffusion Release[b]	Meltdown Release	Fragmentation Release[c]
Xe, Kr	0.030	-	0.870	0.9
I, Br	0.017	-	0.883	0.9
Cs, Rb	0.050	-	0.760	-
Te, Se, Sb	0.0001	-	0.150	0.6
Sr, Ba	1×10^{-6}	-	0.100	-
Ru, Mo, Pd, Rh, Tc	-	-	0.030	0.9
Nd, La, Eu, Y, Ce, Pr, Pm, Sm, Np, Pu, Zr, Nb	-	-	0.003	-

(a) Leach release in-vessel was not considered.

(b) Diffusion release estimates were split between Gap release and Meltdown release.

(c) Indicates fraction of the inventory remaining in fragmented fraction of the fuel that is released. Release was presumed in the Reactor Safety Study to be due to oxidation of dispersed debris.

The fuel continues to heat following clad rupture. During this stage radionuclides migrate to the surfaces of the fuel and can escape into the fuel/clad gap. From this gap, the radionuclides can escape the fuel rod. This phase of release was not explicitly included in the Reactor Safety Study analyses. It was defined shortly after the study was published [11]. It has been a regime of great interest and is discussed here.

Further heating of the fuel can lead to melting. Formation of a liquid phase can take place in two ways. Clearly, the fuel or the products of fuel interaction with ZrO_2 produced by steam oxidation of the clad can melt. Nominal temperatures for melting of fuel and UO_2/ZrO_2 mixtures are 3140 K and 2800 K, respectively. Also the clad can melt. But, it has been found that melting clad can interact strongly with the fuel to form materials that start to melt at temperatures as low as 2170 K [12]. Melting of mixtures of ZrO_2, Zr, and UO_2 is often called "liquefaction" to distinguish it from melting of the fuel itself. For most purposes this distinction is useful only for specifying temperature and timing. An attempt is made here to retain this distinction.

Liquefaction of the $ZrO_2/Zr/UO_2$ mixture has also been called "eutectic formation." Since it manifestly is not the "formation of a eutectic," this nomenclature is avoided.

It is possible during the course of an accident that high temperature core debris will interact with liquid water. This might occur if molten or fragmented fuel fell from the core region of the reactor into the water-filled lower plenum of the reactor. It might also occur if water were deliberately injected into the vessel in an attempt to terminate an accident.

The interaction of molten fuel with water can lead to a steam explosion. In the Reactor Safety Study steam explosions were thought to expel finely fragmented debris into oxidant-rich atmospheres. Vigorous oxidation of the debris was estimated to cause extensive radionuclide release. This oxidation release is discussed extensively in Chapter 4 in connection with ex-vessel release and is not treated here.

Fuel/coolant interactions can be benign in the sense that fragmentation of the fuel is not violent and does not involve broad dispersal of the debris. Still this fragmentation can affect fission product release. A very high surface area is created. Rapid flows of steam across the surfaces take place. These conditions are conducive to rapid radionuclide release especially if the debris is still quite hot. Some discussion of release from fragmented fuel is presented in this chapter.

If the fuel is fragmented but not completely quenched by interaction with water, continued release of radionuclides can occur. Until the bed of debris begins to melt, release during this stage of the accident is similar to the diffusion release defined above, though the geometry is quite different. This situation of release from a debris bed can be reached by means other than fuel/coolant interactions. The differences in geometry of debris beds and intact fuel rods lead to differences in the methods for predicting release which are discussed here.

Finally, if the fuel is quenched, radionuclide release can occur by leaching into the surrounding liquid water. This type of release has not been a serious concern in accident analyses in the past and is not discussed here. The interested reader is referred to the discussion of ex-vessel leaching release in Chapter 4 and the relevant literature [13-16].

One other note on nomenclature refers to the use of the terms "fission product" and "radionuclide." As stated in Chapter 2, these terms are used interchangeably here even though it is known that not all the radioactive material available in a reactor is produced as a result of fissioning of uranium or plutonium nuclei. The terms are also used to refer to the stable isotopes formed in the decay chains of some important isotopes. This nomenclature ought not to cause confusion.

3.3 Fundamentals of the Release Process

Release during core degradation is just the conversion of a material in the core to an airborne material (leaching is ignored here). This process can occur by either mechanical means or as a result of chemical processes that convert a condensed species into a vapor species.

Mechanical aerosol formation does occur during core degradation. Lorenz et al. [17] have observed that a small amount of "dust" is expelled from fuel rods when the clad balloons and ruptures. Analyses show this material to be fuel with particle sizes between 5 and 50 µm. Brockmann and Stalker [18] have observed that coarse particulate is evolved when zircaloy clad is burned in air. The sizes and shapes of these particles could be rationalized only in terms of mechanical comminution of the condensed products of Zr oxidation. It is not difficult to imagine that rapid oxidation of cladding by steam could also produce coarse particulate. Parker et al. [19] have observed that when pressurized control rods rupture an alloy of silver and indium is sprayed about. Mitchell et al. [20] have shown these alloy droplets can have aerosol dimensions. Finally, violent fuel/coolant interactions could produce aerosol-sized particles of water and core debris (see Chapter 4).

In general, release by mechanical mechanisms of aerosol formation is of a sudden, transitory nature during core degradation. The products of the mechanical processes are coarse and would remain airborne for only short periods of time. Compositions of the mechanically produced particulate reflect the bulk composition of the parent material. That is, they are neither enriched nor depleted of radionuclides.

Continuing release of material from the core comes from vaporization--that is, from condensed-to-vapor phase transitions. Vaporization is responsible for most of the radionuclide release during core degradation and may be responsible for most of the total mass release. Vapors, when they condense, form very fine particles which can remain suspended for long periods of time. These particles can be quite enriched relative to the parent material in radionuclides.

Vaporization can be a simple unary process such as:

$$[AB]_{UO_2} \rightarrow AB\ (gas)$$

or

$$[AB]_{UO_2} \rightarrow A\ (gas) + B\ (gas)$$

where the symbol $[\ ]_{UO_2}$ means the condensed species is in the fuel lattice. Vaporization can also be a complex process involving reactions of the condensed species with ambient gases (predominantly H_2 and H_2O) to form a volatile species. Examples of these more complex vaporization processes are:

$$UO_2(c) + 2H_2O \rightarrow UO_2(OH)_2(gas)$$

$$BaZrO_3(c) + H_2O \rightarrow Ba(OH)_2(gas) + ZrO_2(c)$$

$$[CeO_2]_{UO_2} + 2H_2 \rightarrow Ce(gas) + 2H_2O$$

Regardless of their natures, all vaporization processes have some features in common. The driving force for vaporization and the maximum extent of vaporization are specified by differences between existing conditions and thermochemical equilibrium conditions. The rate of vaporization or, equivalently, the rate of approach to equilibrium is limited by kinetic or mass transport factors. The thermochemistry and kinetic factors of release are described in the subsections below.

A. Thermodynamics of Vaporization

Consider the vaporization of a species A from a host lattice. A particular vaporization process might be

$$[A]_{host} \rightarrow A_i(gas)$$

where A_i is some vapor form which may be distinct from the chemical form A dissolved in the host lattice. The driving force for this process is proportional to the difference between the equilibrium partial pressure of A_i in the ambient atmosphere and the actual partial pressure:

$$i^{th} \text{ driving force} \propto [P_i(eq) - P_i(t)]$$

$P_i(eq)$ = equilibrium partial pressure of A_i

$P_i(t)$ = actual partial pressure of A_i at time t

Since $[A]_{host}$ can vaporize by a variety of processes, the total driving force for vaporization of $[A]_{host}$ is given by:

$$\text{driving for release of } [A]_{host} = \sum_{j=1}^{N} [P_j(eq) - P_j(t)]\, K_j \quad \text{where}$$

where the K_js are proportionality factors and the summation is over all vapor species formed by A.

As a specific example, the vaporization of barium oxide dissolved in a UO_2 lattice is examined. Some vaporization reactions of barium oxide into an atmosphere of steam and hydrogen are:

$$[BaO]_{UO_2} \rightarrow BaO(gas)$$

$$[BaO]_{UO_2} + H_2 \rightarrow Ba(gas) + H_2O$$

$$[BaO]_{UO_2} + 1/2\ H_2 \rightarrow BaOH(gas)$$

$$[BaO]_{UO_2} + H_2O \rightarrow Ba(OH)_2(gas)$$

Then the driving force for barium oxide vaporization is:

$$K_{BaO}\,[P_{BaO}(eq) - P_{BaO}(t)] + K_{Ba}\,[P_{Ba}(eq) - P_{Ba}(t)]$$

$$+ K_{BaOH}\,[P_{BaOH}(eq) - P_{BaOH}(t)]$$

$$+ K_{Ba(OH)_2}[P_{Ba(OH)_2}(eq) - P_{Ba(OH)_2}(t)]$$

There are several features of vaporization processes that are revealed by examining the driving force expression. First, the driving force varies with time. As the actual concentration of the vapor forms approaches the equilibrium concentration (concentrations are related to partial pressures), the driving force, and consequently, the rate of vaporization go to zero. In a flowing system, such as steam/hydrogen mixtures flowing through a reactor core, the driving force for vaporization is spatially dependent. The driving force can be high at the flow entrance where the ambient vapor concentration of species is low. The driving force falls then along the flow path as the ambient concentration of the vapor species builds up toward equilibrium.

A second obvious feature of vaporization is that the driving force for vaporization increases with the number of vapor species that can form. Analyses that omit species with high equilibrium partial pressures can err badly.

Finally, it is essential, obviously, to know the equilibrium partial pressures. The equilibrium partial pressures determine the maximum extent of vaporization as well as figuring in the driving force for vaporization.

Consider again the vaporization of the hypothetical species $[A]_{host}$. The equilibrium partial pressure of A_i is given by:

$$\Delta G_i(T) = -RT\,\ell n\,[\phi_i P_i(eq)/\gamma_A X_A]$$

where $\Delta G_i(T)$ = standard state free-energy change for the vaporization process

T = absolute temperature

ϕ_i = fugacity coefficient of the i^{th} vapor species

γ_A = activity coefficient of A in the host material

X_A = mole fraction of A in the host material

R = gas constant

The values of $\Delta G_i(T)$ are typically available for most species of interest for reactor accident analyses [21]. If A can be present in only one host material, then X_A can be determined from inventories. When A can partition among several condensed host materials there is an additional problem of determining X_A in each phase. Discussion of this problem is deferred until later in this section.

The activity and fugacity coefficients that appear in the equilibrium are seldom known. There are limited data available for the activity coefficients of binary systems that show the activity coefficients can be functions of the system temperature, composition and pressure. Similarly, data for well-known gases show the fugacity coefficients are dependent on temperature, pressure, and properties of the vapor species.

The dichotomy between the simple elegance of the thermodynamic description of vaporization and the difficulty of implementing this description has been known for a long time. There has been quite a lot of effort expended to model the activity and fugacity coefficients for complicated systems. The experience gleaned from the use of these models provides a data base on their applicable range. These models will be the subject of discussion in the balance of this subsection.

Activity and fugacity coefficients as used above are measures of the deviation from ideality of condensed and vapor phases, respectively. These deviations from ideality arise because the molecular interactions, whether repulsive or attractive, are not the same in mixtures as they are in some pure reference state. It would seem obvious, intuitively, that since interactions among molecules are weak in the gas phase, that deviations from ideality would also be small in the gas phase. Extensive studies over the last 100 years have allowed descriptions to be formulated of even these small deviations from ideality in gases. It is conventional to express the descriptions in the form of an equation of state. Most of the popular models can be expressed in the form:

$$Z = \frac{PV}{RT} = \frac{V}{RT}\left\{\frac{RT}{(V-b)} - \frac{\theta\ (V-\eta)}{(V-b)\ (V^2+\delta V+\varepsilon)}\right\}$$

where $\theta = RT(\delta - \alpha)$

$\eta = (\beta - \varepsilon)/(\delta - \varepsilon)$

The value of Z, often called the "compressibility factor," for an ideal system would be one for all pressures and temperatures. When the system deviates from ideality, Z becomes a function of both pressure and temperature. Values for the parameters in various forms of the equation of state shown above are listed in Table 3.3. To make the models as useful as possible for the widest varieties of fluids, it has been traditional to express functional forms of the models in terms of the so-called "reduced variables":

$$T_r = T/T_c \text{ and } P_r = P/P_c$$

where T_c = critical temperature

P_c = critical pressure

This is quite useful for well-characterized gases. Unfortunately, most of the gaseous species of interest for the purposes of reactor safety are not well characterized and the critical temperatures and pressures have never been measured. Even methods to estimate these critical constants require data about the gases that are not known, in general. With the critical constants known, the equation of state must be fit to data to determine quantitative values for the parameters. Usually adequate data for the species of interest in severe accident analyses are not available.

Another popular equation of state is the Virial Expansion:

$$Z = 1 + B/V + C/V^2 + D/V^3 + \dots$$

In the nomenclature of Table 3.3, the parametric values in this equation of state can be written as:

$$B = b - \theta/RT \qquad C = b^2 - \theta b/RT + \theta\ (\delta + \eta)/RT$$

$$D = b^3 - \theta b^2/RT + \theta b(\delta + \eta)/RT - \theta(\delta^2 - \varepsilon + \eta\delta)/RT$$

The Virial Expansion is of particular interest since it, unlike the empirical equations of state in Table 3.3, has some theoretical significance. The relationship between the parameter B and molecular interactions is well known [32]. Whereas the detailed molecular properties are seldom known, they can sometimes be guessed. A Virial equation of state truncated after the B/V term is often quite accurate until:

$$P > [T/2]\ [\Sigma\ y_i P_c(i)/\Sigma\ y_i T_c(i)]$$

Table 3.3

Popular Equations of State

Model Name and Year It Was First Suggested	Parameters			
	θ	η	δ	ε
Van der Waals (1873)	a	b	o	o
Berthelot (1900)	a/T	b	o	o
Clausius (1880)	a/T	b	2C	C^2
Redlich-Kwong (1949)	$a/T^{1/2}$	b	b	o
Wilson[1]	$\theta_w(T)$	b	b	o
Peng-Robinson[2] (1976)	$\theta_{PR}(T)$	b	2b	$-b^2$
Lee-Erbar-Edminster[3] (1973)	$\theta_L(T)$	(T)	b	o

1. $P_c\theta_w(T)/R^2T_c{}^2 = 0.4275[1 + (1.57 + 1.62\,\omega)\,(T_r^{-1} - 1)\,T_r]$

2. $P_c\theta_{PR}(T)/R^2T_c{}^2 = 0.4275[1 + (0.480+1.574\omega-0.776\omega^2)(1 - T_r^{1/2})]^2$

3. $P_c\theta_L(T)/R^2T_c{}^2 = 0.45725[1 + (0.37464+1.542266\omega-0.2699\omega^2)\,(1 - T_r^{1/2})]^2$

where y_i = mole fraction of the species i in the gas phase. Once an equation of state is known, the fugacity coefficients can be calculated from:

$$\Phi_i = \exp\left\{\frac{1}{RT}\int_V^{\infty}\left[\frac{\partial P}{\partial n_i}\right]_{T,V,n_{j\neq i}} - \frac{RT}{V}dV - \ln Z\right\}$$

Again, what is simple in concept is difficult to implement, and the lack of appropriate data can make it impossible. Fortunately, the deviations from ideality do become small at high temperatures if the system is far from the critical point and pressures are low. The assumptions of ideality become questionable for fission product vapors only near the upper limit of pressures encountered in reactor accidents ~150 atmospheres.

Theoretically, an equation of state should provide the information necessary to correct nonidealities in the condensed phase as well as the gas phase. Even in the simplest systems, this is difficult to achieve. Consequently, an entirely different formalism has developed for dealing with the condensed phase.

Activity coefficients for the condensed phase are not confidently rationalized away as can be fugacity coefficients. Thermodynamic laws do show that the pressure dependence of the activity coefficients can be separated from the compositional and temperature dependencies. A general expression of the pressure-dependence of condensed phase activity coefficients is:

$$\gamma_i(P) = \gamma_i(P_{REF}) \exp\left[\int_{P_{REF}}^{P} \frac{V_i}{RT}\, dP\right]$$

where P = pressure of interest

P_{REF} = reference pressure where the activity coefficient is known

V_i = partial molar volume of the species i in the mixture

The reference pressure is usually 1 atmosphere. Partial molar volumes of species in a mixture are seldom known. It has become common to assume partial molar volumes are equal to the molar volumes of the pure species and that the partial molar volumes are independent of pressure. This assumption can only be made if conditions are well removed from the critical point.

With these assumptions the pressure dependance of activity coefficients is given by

$$\gamma_i(P) = \gamma_i(P_{REF}) \exp [V_i(P-P_{REF})/RT]$$

This expression shows that activity coefficients increase with pressure. The factor of increase is called the Poynting correction factor. Poynting correction factors for a species with a partial molar volume of 50 cm^3/mole at temperatures of 1000, 2000, and 3000 K are plotted against pressure in Figure 3.1. Most species of interest here would have even smaller partial molar volumes and, consequently, smaller correction factors. Clearly, for systems of interest for reactor safety analyses, the pressure correction of activity coefficients is not especially important.

Quite a variety of models have been developed to describe the compositional and temperature dependence of activity coefficient. The simplest model is, of course, that of the ideal mixture:

$$\gamma_i(P_{REF}) = 1 \quad \text{for all i and T}$$

This model should represent the asymptote that mixtures approach as temperatures increase.

More exotic models to describe activity coefficients at lower temperatures are summarized in Table 3.4. It is not difficult to reach a point at which these empirical models cannot be used because of the lack of data. Models that are based on binary interactions are attractive because the necessary parametric data can be extracted from binary phase diagrams which are far more abundant than detailed activity data. Powers [22] has used the Wilson equation to describe activities in the Ag-In-Cd mixture. Powers and Brockmann [23] have used regular solution models in their model of fission product release during core debris interactions with concrete.

Return now to the example of barium oxide vaporization. Some insight into the vaporization of this species can be obtained by examining the quantity:

$$\Sigma = P_{BaO}(eq) + P_{Ba}(eq) + P_{BaOH}(eq) + P_{Ba(OH)_2}(eq)$$

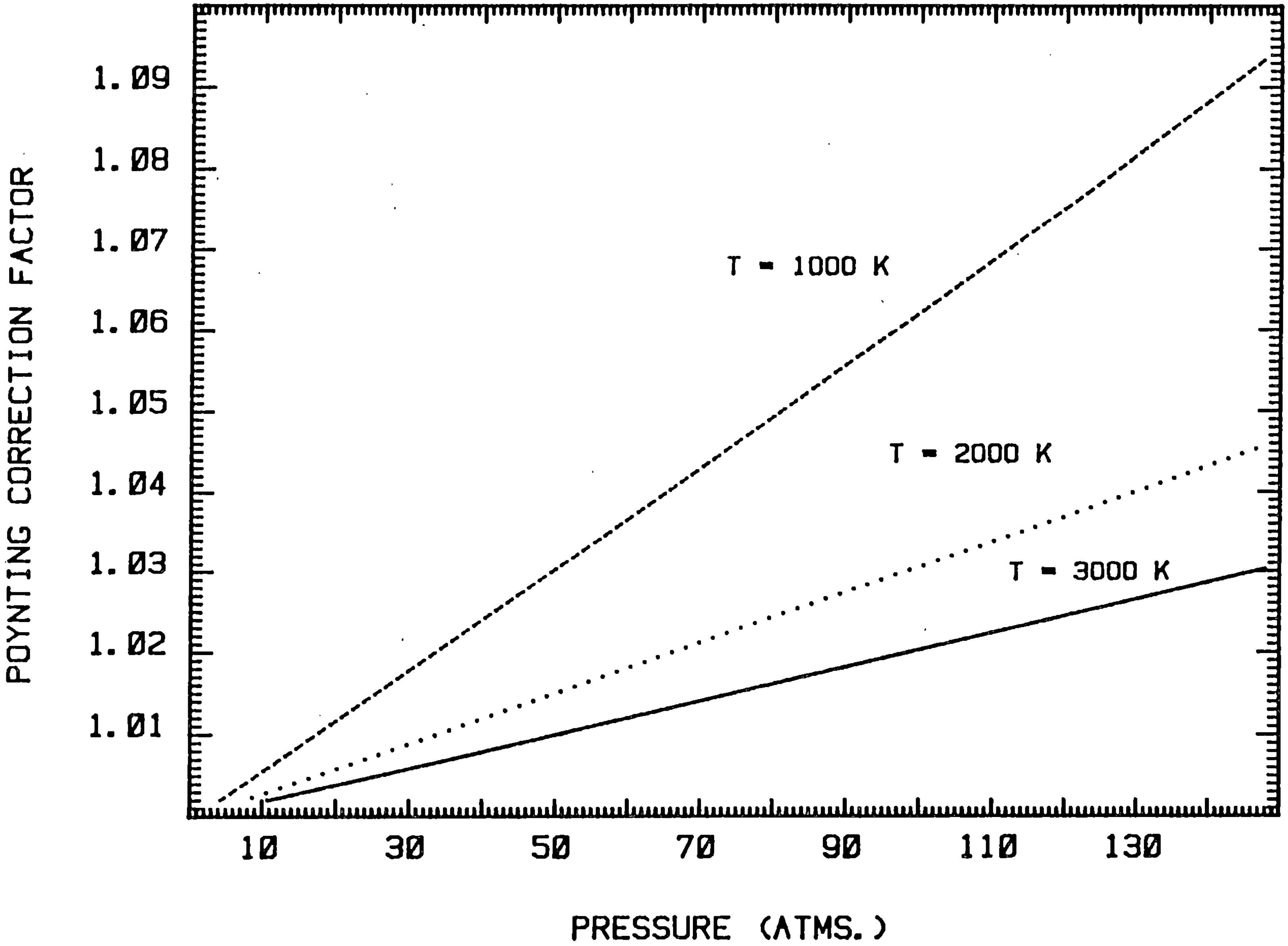

Figure 3.1. Poynting Correction Factors for Several Temperatures as a Function of Pressure.

Table 3.4

Popular Models for Activity Coefficients

Model	$RT\ \ell n\ [\gamma_k\ (P_{REF})]$
Ideal	0
Regular Binary	$B\ (1 - X_k)^2$
Wilson	$RT \left\{ 1 - \ell n\ [\sum_{j=1}^{N} X_j\ A_{k_j}] - \sum_{i=1}^{N} \left[\frac{X_i\ A_{ik}}{\sum_{j=1}^{N} X_j\ A_{ij}} \right] \right\}$ where $A_{ij} = \exp\ [-(\lambda_{ij} - \lambda_{ii})/RT]\ (V_j/V_i)$ and $\lambda_{ij} = \lambda_{ji}$
NRTL	$RT \left\{ \sum_{j=1}^{N} \left[\frac{X_j \tau_{jk} A_{jk}}{\sum_{\ell=1}^{N} X_\ell\ A_{\ell k}} \right] + \sum_{i=1}^{N} \left[\frac{X_i\ A_{ki}}{\sum_{\ell=1}^{N} X_\ell\ A_{\ell i}} \right] \left[\tau_{ki} - \sum_{j=1}^{N} \left[\frac{X_j\ \tau_{ji}\ A_{ji}}{\sum_{\ell=1}^{N} X_\ell\ A_{\ell i}} \right] \right] \right\}$ $\tau_{ji} = (\lambda_{ji} - \lambda_{ii})/RT \qquad A_{ji} = \exp\ (-\alpha_{ji}\ \tau_{ji}) \qquad \alpha_{ij} = \alpha_{ji}$
UNIQUAC	$RT\ (\ell n\ \gamma_k^c + \ell n\ \gamma_k^R)$ where $\ell n\ \gamma_k^c = 1 - \phi_k/X_k + \ell n\ [\phi_k/X_k] - \frac{Z}{2}\ q_k\ (1 - \frac{\phi_k}{\theta_k} + P_n\ (\frac{\phi_k}{\theta_k}))$ $\ell n\ \lambda_k^R = q_k \left[1 - \ell n\ (\sum_{j=1}^{N} \theta_j A_{jk}) - \sum_{i=1}^{N} \left(\frac{\theta_i A_{ki}}{\sum_{j=1}^{N} \theta_j A_{ji}} \right) \right]$ $A_{ji} = \exp\ [-\frac{(\lambda_{ji} - \lambda_{ii})}{RT}] \qquad \phi_i = \frac{X_i\ r_i}{\sum_{j=1}^{N} X_j\ r_j} \qquad \theta_i = X_i q_i / \sum_{j=1}^{N} X_j q_i$

From the discussions above, it is apparent that when ideality is assumed in both the gas and condensed phases then:

$$\Delta G_{BaO}(T) = - RT \ln \left[\frac{P_{BaO}(eq)}{X_{BaO}} \right]$$

$$\Delta G_{Ba}(T) = - RT \ln \left[\frac{P_{Ba} \; P_{H_2}}{X_{BaO} \; P_{H_2O}} \right]$$

$$\Delta G_{BaOH}(T) = - RT \ln \left[\frac{P^2_{BaOH}}{X_{BaO} \; P_{H_2}} \right]$$

$$\Delta G_{Ba(OH)_2}(T) = - RT \ln \left[\frac{P_{Ba(OH)_2}}{X_{BaO} \; P_{H_2O}} \right]$$

Thus,

$$\Sigma = X_{BaO} \left\{ K_{BaO} + K_{Ba} \left[\frac{P_{H_2O}}{P_{H_2}} \right] + K_{BaOH} \; P_{H_2}^{1/2} + K_{Ba(OH)_2} P_{H_2O} \right\}$$

where K_i are proportionality factors that are functions of temperature. It is obvious that the vaporization of barium oxide will depend on its concentration in the host material. It also depends on the composition of the ambient gas. The variations in partial pressures of the various barium-bearing species as a function of the P_{H_2}/P_{H_2O} ratio at 2000 K and a total pressure of 10 atmospheres are shown in Figure 3.2. In preparing this figure the chemistry of water and hydrogen at high temperatures was also recognized:

$$H_2 \rightleftarrows 2H$$

$$H_2O \rightleftarrows H_2 + 1/2 \; O_2$$

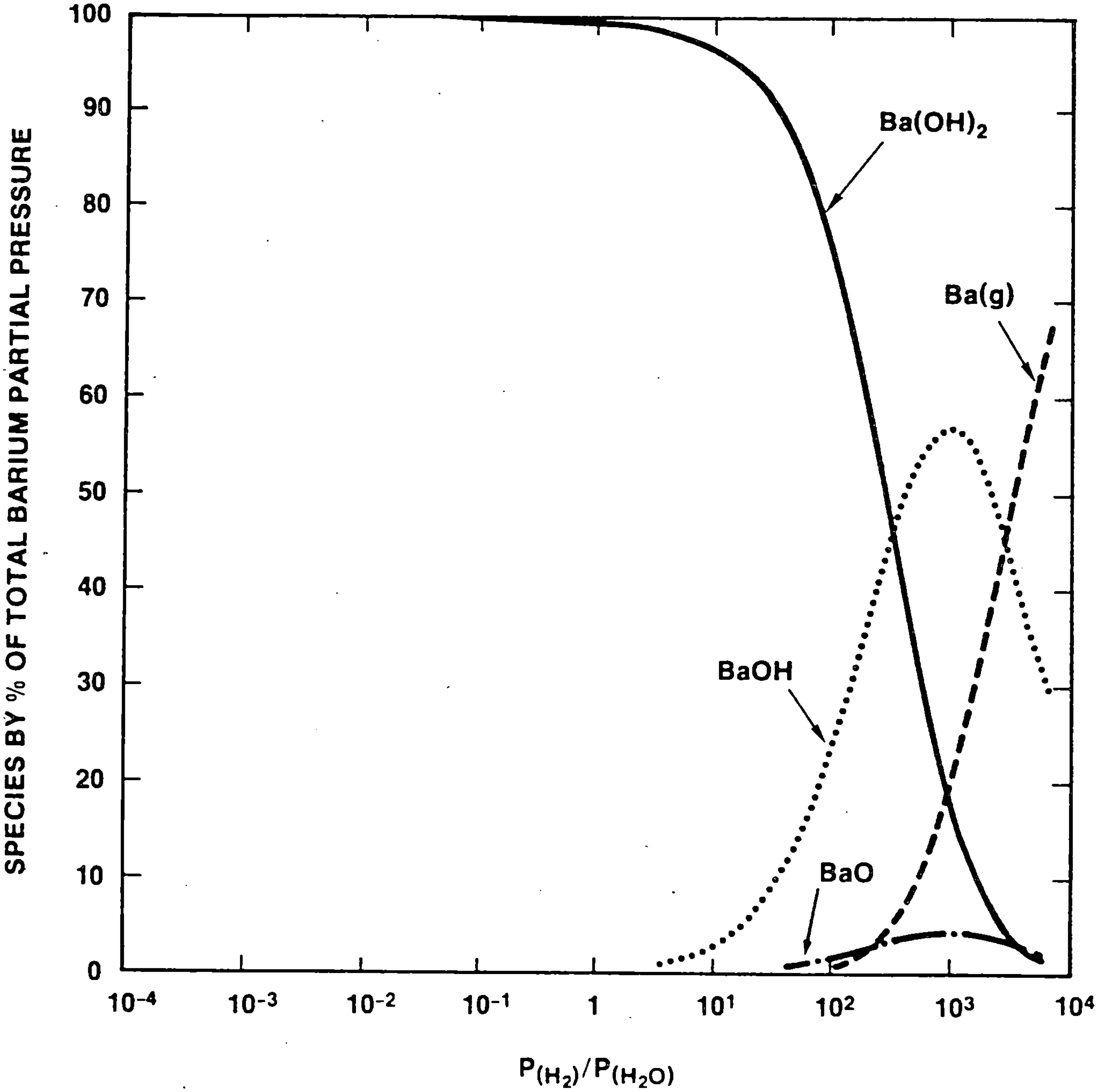

Figure 3.2. Vapor Species Produced at 2000 K and a Total Pressure of 10 Atmospheres by Vaporization of Barium Oxide as a Function of P_{H_2}/P_{H_2O}.

$$O_2 \rightleftarrows 2O$$

$$H_2O \rightleftarrows 1/2\ H_2 + OH$$

$$2H_2O \rightleftarrows HO_2 + 3/4\ H_2$$

The results in Figure 3.2 make it apparent that tabulated values of vapor pressures as functions of temperature only are of little value in the analysis of severe accident source terms. The vaporization should be a function of the ambient gas composition. It should also be apparent that within a reactor core the driving force for vaporization may change since the gas composition changes due to reactions such as the steam oxidation of the zircaloy clad on the fuel.

The analyses done for the Reactor Safety Study did consider effects of gas composition on vaporization though the final release fractions were independent of these considerations. However, the analyses done for the Reactor Safety Study restricted attention to oxidation reduction reactions of the type

$$MO_X(\text{gas}) + X\ H_2 \rightleftarrows M(\text{gas}) + X\ H_2O$$

Thus, for the barium oxide example the formalism of the Reactor Safety Study would yield:

$$\Sigma_{RSS} = [K_{BaO}P_{BaO}(eq) + K_{Ba}P_{Ba}(eq)]\ X_{BaO}$$

A comparison of Σ and Σ_{RSS} is presented in Figure 3.3. The comparison shows that a more complete description of the chemistry can yield higher driving forces for the vaporization of species than might be anticipated from the analyses done in the Reactor Safety Study. Higher driving forces do not necessarily translate into higher extents of release. But, the potential certainly exists for releases much higher than those predicted in the Reactor Safety Study. This possibility, if realized, would be, of course, quite contrary to the "conventional wisdom" that releases predicted in the Reactor Safety Study conservatively bound the actual releases during severe accidents.

The difficulty with the approach used in the Reactor Safety Study is that important vapor phase species were neglected. Vapor phase hydroxides figured prominently in the discussion above for BaO vaporization. The vaporization of many other species can be enhanced by vapor phase hydroxide formation. A general reaction expression for vapor phase hydroxide formation can be:

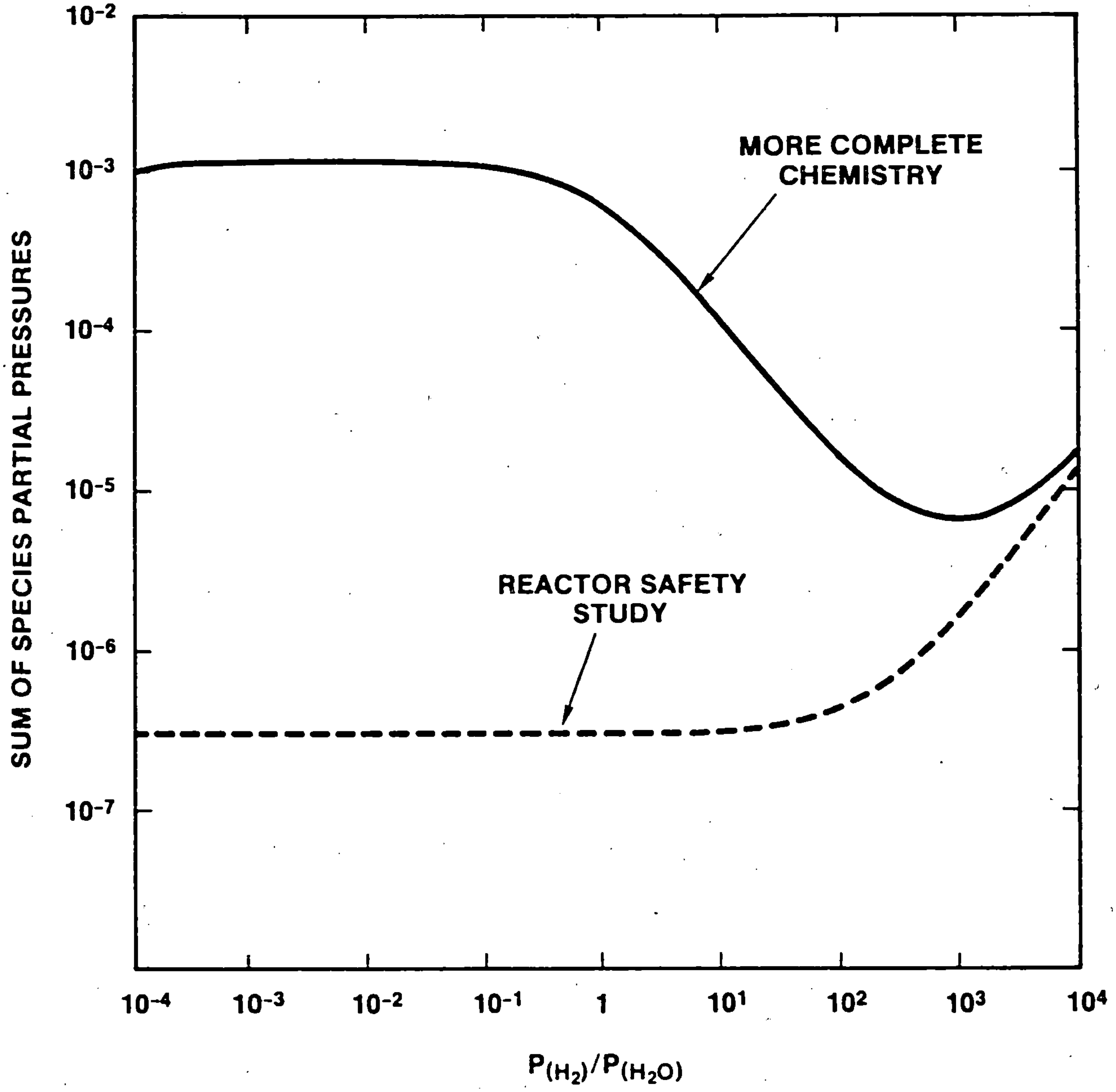

Figure 3.3. Σ and Σ_{RSS} for Barium Oxide Vaporization as a Function of P_{H_2}/P_{H_2O} at 2000 K and a Total Pressure of 10 Atmospheres. Σ is shown as the solid line. Σ_{RSS} is shown as a dashed line.

$$MO_y^{(c)} + n\ H_2O \rightleftarrows MO_{(y-n)}(OH)_{2n}(g)$$

and the corresponding equilibrium expression is:

$$\Delta G(T) = -\ RT\ \ell n \left[\frac{P_{MO_{(y-n)}(OH)_{2n}}}{X_{MO_y} P^{n}_{H_2O}}\right]$$

Consideration of vapor-phase hydroxides is hampered by lack of data. High-temperature chemical studies are usually done in refractory metal furnaces. Because these refractory metals are easily oxidized, the conditions conducive to vapor-phase hydroxide formation have been carefully avoided. By far, the greatest amount of work on vapor-phase hydroxides has been done in the geologic field and in the study of nuclear fallout. What studies have been done show that vapor-phase hydroxides will be important for many of the species of interest for source term development. A list of known vapor-phase hydroxides is presented in Table 3.5. Attempts have been made to predict the existence of vapor phase hydroxides for elements that have not been studied experimentally [21i].

Two other classes of vapor species that were not considered extensively in the development of the source terms for the Reactor Safety Study are the vapor-phase hydrides and mixed-vapor species. A general reaction for the formation of vapor-phase hydrides is

$$MO_y(g) + (y + z/2)\ H_2 \rightleftarrows MH_z(g) + y\ H_2O$$

$$\Delta G(T) = -\ RT\ \ln \left[\frac{P_{MH_2}\ P^{y}_{H_2O}}{P_{MO_y}\ P^{(y+z/2)}_{H_2}}\right]$$

Hydride formation clearly depends on temperature and the absolute pressures of both steam and hydrogen. The importance of vapor-phase hydrides has not been explored in any significant way to date. Based on inspection of the terms in the free-energy equation above, it would be expected that the contributions to the gas phase made by hydrides would vary markedly over the course of an accident as well as among various accident sequences.

Table 3.5

Some Vapor Species That Were Not Considered in the Reactor Safety Study

Fission Produce Category	Representative Element	Significant Vapor-Phase Hydroxide	Suspected Vapor-Phase Hydride
Alkali Metals	Cs	CsOH, $(CsOH)_2$	
Alkaline Earths	Ba	BaOH, $Ba(OH)_2$	BaH, SrH
Halogens	I		HI
Chalcogens	Te	TeO(OH)	H_2Te
Platinoids	Ru	RhO(OH)	
Early Transition Elements	Mo	$MoO_2(OH)_2$ $CrO_2(OH)_2$	
Tetravalents	Ce		
Trivalents	La	LaO(OH) $La(OH)_2$	
Uranium	U	$UO_2(OH)_2$	
Main Group Metals	Cd, Sn	InOH, $In(OH)_2$ SnOH, $Sn(OH)_2$	SnH, SbH_3
Boron	B	H_3BO_3, HBO_2	

Mixed-vapor species are those made of two or more atoms whose vaporization is of interest. These species have not been extensively studied. CsI(g) is the only well-recognized example. Vapor-phase tellurides such as AgTe, SnTe, and SbTe are known but seldom have been taken into consideration in the formulation of source terms. The efficiency with which mixed-vapor species transport fission products will lead to greater interest in these species as results of integral fission product release tests become available and attempts are made to rationalize these results.

Another class of species that has not been considered in the past is ions. Thermal ionization of vapors seldom is a major consideration in typical thermochemical analyses at temperatures less than 2800 K. Ionization would not be important in accident analyses, except that chemistry is taking place in the reactor in an intense radiation field. Though ions formed by the intense radiation are unstable, the continuing exposure to radiation assures that ions are reformed. Thus, a meta-stable equilibrium concentration of ions may well exist in the ambient atmosphere.

Insufficient analyses of the effects of ionizing radiation on chemistry have been undertaken to know if it is an effect of importance. What data are available show that it may be important for iodine and CsI chemistry [33].

Several chemical processes important to the analysis of fission product vaporization have been mentioned to this point. It is useful to examine how well these processes can be analyzed given that the data available are uncertain. The quantitative expression of the equilibria mentioned above can be written in the general form:

$$f = \frac{P_{H_2}^{a}}{P_{H_2O}^{b}} \exp(-\Delta G/RT)$$

where f is the quantity to be calculated and the partial pressures of hydrogen and steam are provided, but are uncertain, as is the temperature. The quantity ΔG is derived from tabulations and also may be uncertain. The uncertainty in the quantity f derived from these uncertain data, if cross-terms are neglected, is given by:

$$\left[\frac{\delta f}{f}\right]^2 = a^2 \left[\frac{\delta P_{H_2}}{P_{H_2}}\right] + b^2 \left[\frac{\delta P_{H_2O}}{P_{H_2O}}\right]^2 + \left[\frac{\Delta G}{RT}\right]^2 \left\{ \left[\frac{\delta \Delta G}{\Delta G}\right]^2 + \left[\frac{\delta T}{T}\right]^2 \right\}$$

It can be assumed that partial pressures calculated for severe accident scenarios might be 100 percent in error and temperatures might be 10 percent in error. Then

$$\left[\frac{\delta f}{f}\right]^2 \qquad a^2 + b^2 + \left(\frac{\delta \Delta G}{RT}\right)^2 + \frac{(\Delta G)^2}{(RT)} 10^{-2}$$

Rather high quality free-energy data from the various tabulations will be uncertain to about RT and a typical value of ΔG might be ηRT. Then

$$\left[\frac{\delta f}{f}\right]^2 \qquad a^2 + b^2 + 1 + 10^{-2} \eta^2$$

where η is a small integer as are a and b.

This derivation illustrates several points:

1. Uncertainties in even the best thermodynamic data place a constraint on the accuracy of calculated vapor-phase speciation of about 100 percent.
2. Temperatures produced by even crude thermal analyses of the core meltdown process do not have a tremendous influence on the relative uncertainty in calculated speciation of the vapor.
3. By far and away the greatest source of uncertainty in the vapor-phase speciation comes from the uncertainties in steam and hydrogen partial pressures.

Because the equilibrium speciation of the gas phase plays such an important role in determining the driving force for vaporization, the quality of steam and hydrogen partial pressure calculations is of essential concern. The current state of the art in making these calculations places a very big constraint on the quality of fission product source term calculations. Even so, neglect of these vapor phase speciation issues can lead to errors in the vapor pressures on the order of 10^3 to 10^5 percent, as illustrated by the discussion of Ba vaporization.

To this point, the analysis of thermochemistry has been done by explicitly stating the chemical reactions of interest and evaluating each of these reactions. A key point in the discussions has been the importance of including all the major species. Such a procedure can easily become overwhelming as the number of elements and species grows. A somewhat more formalized procedure is obviously needed.

A variety of procedures for analyses of multicomponent chemical equilibria have been developed over the past years [24-30]. These procedures often are based on minimizing the total free-energy, G, of a system where

$$G = \Sigma\, n_i \mu_i \quad .$$

$$\mu_i = G_f(i) + RT\, \ell n\, X_i \gamma_i \text{ for condensed phases}$$

$$\mu_i = G_f(i) + RT\, \ell n\, P_i \phi_i \text{ for vapors}$$

n_i = moles of the i^{th} species

subject to mass balance constraints:

$$\sum_{\text{all species}} n_i a_{i,e} = B_e \quad \text{for } e = 1 \text{ to } E$$

where $a_{i,e}$ = number of atoms of element e in the i^{th} species

B_e = moles of element e in the system

E = number of elements in the system

and non-negativity constraints:

$$n_i \geq 0 \quad \text{for all } i.$$

The problem as stated is an N dimensional constrained optimization with linear equality and inequality constraints. A little manipulation of the equations can reduce the dimensionality to E+1. This nearly always has to be done. Practical methods for solving nonlinear optimization problems rarely are feasible for dimensions greater than 100. Species of importance in calculation of phenomenological source terms can easily exceed 300 in number [23].

Direct search and sequential linear programming techniques have been used to solve the optimization problem in the past. Descent techniques are now almost exclusively used. Some of the more popular descent methods are:

1. STEEPEST DESCENT: Approach to a solution is guaranteed by the first order steepest descent method. The method is not widely used in specialized codes because the rate of convergence to a solution becomes infinitely slow as the solution is approached. Conservation of mass to any specified accuracy is possible at the expense of increasing number of iterations. The method is attractive because it is robust with respect to initial solutions for the iterative procedure and the programming is simple. The method is used in the PUFF code [31]. Muir has used a modification of the steepest descent method in the CORCON model of core debris interactions with concrete [24]. The method must be programmed with an arbitrary criterion for terminating the iterations and it will yield only approximate answers. The answers can be thermodynamically incorrect because they do not conform necessarily to the Gibbs Phase Rule.

2. SECOND ORDER STEEPEST DESCENT: Many of the problems of the first order steepest descent method are solved by the second order, or Newtonian, steepest descent method. Convergence to an exact solution that does obey the Gibbs Phase Rule is theoretically possible. In practice, however, the second order method has its own set of problems. Some of these have been described in a recent review [25]. The most germane is that convergence to a solution is guaranteed only if the initial solution for the iterative procedure is within a prescribed neighborhood of the exact solution. With increasing complexity of the problem, the allowed neighborhood can become quite small. This is a serious problem even for stand-alone implementations of the method and would be catastrophic for systems codes using equilibria calculations. Programming of the method is very complicated.

   Second order methods are widely used. Second order steepest descent is the basis of the RAND Code [26]. The most up-to-date implementations of the method are the FLUEQU code [27] and the SOLGASMIX Code [28,29]. The implementation in FLUEQU is of particular interest since this code provides a steepest descent routine to generate an acceptable initial solution for the second order iterations. SOLGASMIX has been used in the release estimates done for the IDCOR program [8,32]

3. OTHER DESCENT METHODS: Conjugate gradient, variable metric, and projected gradient methods are all being researched as methods to solve equilibrium problems.

Results to date suggest that only the projected gradient method offers great advantages over the more conventional descent techniques. The advantage of the projected gradient method lies in its ability to handle mixtures that deviate significantly from ideality. This may not be a tremendously important feature for source term calculations since data necessary to describe strongly nonideal mixtures are not available and ideal mixtures are usually assumed.

An alternative to descent methods for solving complex chemical equilibria problems is the so-called "equilibrium constant method" developed by Brinkley [30]. This method involves converting the optimization problem into a set of coupled nonlinear equations. To reduce the dimensionality of the problem, the nonlinear equations are formulated in terms of a set of "basis" species that are nearly always the most abundant species in the system. The equations are usually solved by a Newton-Raphson method.

This method has lost popularity because of the complexity of programming necessary to define suitable basis species for arbitrary problems. This may not be a severe restriction in codes used to repetitively solve a single problem. The equilibrium constant method is used in the VANESA model of aerosol generation during core debris/concrete interactions [23]. For in-vessel phases of an accident, the conditions of the system change enough and are different enough from accident scenario to accident scenario that coding for basis state definition may be needed.

Regardless of the equilibrium calculation method used there are several well-characterized test problems that can be used to assure the validity of the modeling [31]. A completely gas phase problem (pyrolysis of propane) and a heterogeneous problem (iron ore reduction) are particularly useful tests.

The thermodynamic nature of vaporization defines the maximum extent of vapor formation that could occur if time were allowed for the system to equilibrate. A simple method of using this thermodynamic formulation of the vaporization problem could be developed. Steam and hydrogen gases flowing past the melting core could be assumed to equilibrate with the core. These gases would then emerge from the core saturated with the vaporizing species. Simply knowing the saturation partial pressures of the vapor species and the flow rate of steam and hydrogen would be enough to determine estimates of release rates of fission products and nonradioactive materials from the core. Integration of the release rate would yield release fractions.

The saturated gases emerging from the core would produce the maximum amount of aerosol when they cooled sufficiently to initiate condensation of vapor. This in turn would maximize the natural mitigation of the release by aerosol processes of sedimentation and deposition. Saturated gases would maximize the rate of vapor reactions with structural materials. Large quantities of nonradioactive materials will, of course, accentuate deposition of radionuclide in the reactor coolant system and the reactor containment.

There is no reason to believe that maximizing the estimates of vapor release from the reactor core by relying on thermodynamic calculations of vaporization will lead to an upper bound on the radiological source term. There are, in fact, good reasons to believe the assumption of saturation is not conservative.

The approach to equilibrium is, then, an essential aspect of the problem of fission-product vaporization, even when only bounding approximations are sought. Since the approach to equilibrium is always from below, real gases emerging from the core will not be saturated in vapor. Condensation of this vapor will not lead to maximum aerosol production and natural mitigation of the releases by aerosol processes will not be maximized.

B. Phase Distribution of Fission Products

The composition of condensed phases play important roles in both the thermodynamics and kinetics of vaporization. Were there a single, condensed phase present during reactor accidents, the effects of composition would be easily handled. The initial composition would be known from the inventories and the time evolution of the condensed phase would be a direct consequence of the release process. When more than one phase is present, then volatile materials could exchange between phases as well as vaporize. This, too, would pose no major difficulty if the condensed phases and the gas phase were all in mutual equilibrium. At equilibrium, the equilibrium partial pressures of vaporous species are the same over all condensed phases. Condensed phase equilibrium is harder to achieve, unfortunately, than is equilibrium between a condensed and a vapor phase. Equilibrium is achieved by movement of species from regions of excessive concentration to regions of deficient concentration (Note that this does not mean movement from regions of high to regions of low concentration. The terms "excessive" and "deficient" refer to free-energies of the species, not their concentrations). Quite clearly, this movement is slower when it is from one condensed phase to another than when it is to or from a gas phase over a condensed phase.

There are situations in a reactor accident when the duration of condensed phase disequilibrium is the item of principle interest. The process of core melting is a prime example. Equilibrium has not been achieved during this melting process, else progression of the melting would cease.

Because condensed phase composition plays such an important role in vaporization, it is necessary to include analysis of the variations in phase composition even when equilibrium has not been achieved. A generally useful assumption to make in multiphase, dynamic, vaporization problems is that gas phases will equilibrate with condensed phases even when the condensed phases are not in equilibrium with each other. This assumption was made to good use in the CORCON model of core-debris interactions with concrete [24] and the VANESA model of ex-vessel aerosol generation [23].

During severe reactor accidents there are several points at which compositional relationships between several condensed phases, and possible disequilibrium in these compositions, are of great interest for the vaporization problem:

1. The fuel itself can be composed of several phases
2. The cladding and the fuel are not necessarily in equilibrium
3. The fuel melting stage, by definition, involves liquid and solid phases
4. Once melting is complete there are at least two phases present--a metallic liquid and an oxidic liquid.

If the disequilibrium produced by the fission process is negligible, then reactor fuel during normal operation is probably an equilibrium* system. The fuel has been hot for a long time during normal reactor operations so there has been an opportunity for disequilibrium features to anneal. This may not be entirely true for such things as grain growth and fuel sintering, which are slow because of the refractory nature of reactor fuel. But, for chemical mixture effects that are important to the issues of vaporization, the assumption of equilibration of the fuel is probably accurate.

---

* Equilibrium fuel here is used in a chemical thermodynamics sense. "Equilibrium" fuel is a term that also arises in the discussion of the extent of fuel irradiation. This alternate definition ought not be confused with the chemical equilibrium discussed here.

Equilibration of the fuel does not make that fuel single phase. The possible presence of fission gas bubbles entrapped in the fuel has been mentioned and is discussed further below. The fission products of a condensed nature may also cluster together and not dissolve in the fuel. Postirradiation examinations of the fuel show that there are at least three distinct phases in the fuel:

1. A METALLIC PHASE: This phase is composed of the more noble metals. Some compositions of the metallic inclusions, which are typically a few hundred micrometers in size, in UO_2 fuel are [50,51]:

   (a) 60 a/o Mo; 24 a/o Ru; 16 a/o Tc
   (b) 55 a/o Mo; 22 a/o Ru; 17 a/o Tc; 6 a/o Rh

   where a/o means atom percent.

   The elemental yields of the above fission products would typically be: 50 a/o Mo; 30.6 a/o Ru; 12.8 a/o Tc; 6.4 a/o Rh.

2. AN ALKALINE EARTH PHASE: This phase contains Ba, Sr, and Zr and probably is an alkaline earth zirconate. The phase may exist at low operating temperatures because of the low solubility of Ba and Sr ions in UO_2. At high temperatures of accident transients, this phase may be absorbed into the fuel lattice.

3. THE FLUORITE PHASE: This is the phase with the fuel and most of the fission products.

In addition to these phases, there have been reports of CsI crystals and Te on the surface of spent fuel [3]. A UPd_3 phase has been reported [52].

This phase partitioning of the fuel does not affect the thermodynamics of vaporization from the fuel since it is an equilibrium system. Quite obviously, it may affect the kinetics of vaporization if the rate-controlling factor is condensed phase mass transport.

An interesting problem that seems not to have been examined systematically is how the phase partitioning of the fuel varies with temperature. The most obvious species to undergo changes with temperature is molybdenum. If, at elevated temperatures, it can be stabilized in the fuel matrix as MoO_2, the molybdenum might be extracted from the metallic inclusions.

The clad on the reactor fuel and the fuel are usually separated by a very narrow physical gap. This can prevent the clad from chemically equilibrating with the fuel which, in fact, is probably desirable. But this disequilibrium can affect fission product release. Fission products rejected from the fuel can react and bind with the clad. The release of Te may be particularly sensitive to this type of reaction with the clad.

The disequilibrium between the fuel and the clad becomes a far more serious problem when temperatures reach the point the cladding can melt. Zirconium can reduce UO_2 and even dissolve it. There is evidence that the process can occur in the solid state [54] but it becomes most dramatic when the clad melts. The process of fuel attack dramatically lowers the temperature at which fuel "melts," and dramatically alters the chemical environment of fission products. The essential features of the process have been studied in some depth by workers at the Kernforschungszentrum Karlsruhe. The essential steps of the process are [55]:

1. As $Zr(\ell)$ extracts oxygen from the fuel, the wetting of fuel by clad improves and the extraction process accelerates.
2. When the local oxygen concentration in the fuel has reached the lower phase boundary of the UO_{2-x}/U system, the formation of liquid uranium causes the fuel matrix to desinter.
3. Fuel particles become entrained in the melt and are rapidly consumed to form a homogeneous (U,Zr)O melt.

This process is discussed in much greater detail elsewhere in this document. Unfortunately, no experimental investigations of the process have examined the behavior of fission products during the attack. Though phase diagrams of the U-O-Zr system have been developed [56], they have not been reduced to a thermochemical characterization that would permit analytic examinations of fission product behavior.

The simple formation of liquid in contact with its solid form may not at first appear to cause phase partitioning of trace impurities such as fission products. In fact, it does, and is the basis of "zone refining" of materials. Consider a simple binary system in which both the solid and the liquid are ideal mixtures. Then the partitioning of the impurity between the solid and the liquid phases is given by:

$$\Delta H_m (1 - T/T_m) + RT \ln (y/x) = 0$$

where ΔH_m = heat of fusion of the impurity

T_m = melting point (K) of the impurity

T = absolute temperature

y = mole fraction of the impurity in the liquid phase

x = mole fraction of the impurity in the solid phase

This simple model allows some conclusions of the effects of species properties on the phase partitioning:

1. partitioning increases with decreasing heat of fusion
2. partitioning increases with the temperature and decreases with increasing melting point of the species of interest.

Partitioning between a liquid and a solid phase will have its greatest effect on the rate rather than the ultimate extent of vaporization if that rate is controlled by condensed phase mass transport. The analysis above suggests that those species most susceptible to phase partitioning are the less refractory and usually more volatile species. Analysis with models that do not require ideal mixture behavior shows that some refractory species such as Ba and Sr are quite sensitive to phase partitioning.

As melting of the core progresses to completion, substantial amounts of structural steel are melted. The precise ratio of steel and fuel in the resulting melt depends very much on the nature of the core meltdown process. Some bounding estimates have been made [57]. Since steel and molten fuel are largely immiscible, there is the possibility of fission products partitioning between the two phases.

The partitioning of fission products between molten steel and molten UO_2 has been studied experimentally [58]. Results of these studies are shown in Table 3.6. Unfortunately, the partitioning experiments were done in an inert environment. The partitioning would be expected to be a strong function of the oxygen potential of the ambient atmosphere.

The effects of atmosphere composition and pressure of phase partitioning between steel and UO_2 can be estimated at least qualitatively by considering the exchange reaction between the phases to be

$$[MO_x]_{oxide} + xH_2 \rightleftarrows [M]_{metal} + xH_2O$$

Table 3.6

Experimental Partition Coefficients For Species Between UO_2 and Iron

Species	Wt % in UO_2	Wt % in Fe
Zr*	93.8 - 95.6	6.2 - 4.4
ZrO_2	93.6 - 97.3	6.4 - 2.7
Y_2O_3	93.8 - 97.4	6.2 - 2.6
La_2O_3	100	û 10^{-4}
CeO_2	97.1	2.9
PrO_2	92.4 - 96.5	7.6 - 3.5
SrO	99.4 - 99.5	0.6 - 0.5
BaO	97.8 - 98.6	2.2 - 1.4
Ru	8.7 - 5.9	91.3 - 94.1
Mo	6.2 - 7.7	93.8 - 92.3
Nb_2O_5	98.9 - 76.9	1.1 - 23.1
Nb	36.4 - 55.7	63.6 - 44.3

* time dependent

where MO_x is a fission product in the oxide form dissolved in the fuel melt and M is the fission product in the metallic state dissolved in the steel melt. Then the partitioning is given by:

$$- \Delta G_f(MO_x) + x\Delta G_f(H_2O) = RT \ln \left[\frac{P_{H_2}}{P_{H_2O}}\right] - RT \ln \left[\frac{\gamma_m X_m}{\gamma_o Y_o}\right]$$

where $\Delta G_f(i)$ = free-energy of formation of the i<u>th</u> species

P_j = partial pressure of species j

γ_m = Activity coefficient of the metallic fission product in the metal

X_m = mole fraction of the metallic fission product in the metal

γ_o = activity coefficient of the oxidic form of fission product in the fuel melt

Y_o = mole fraction of the oxidic fission product in the fuel melt.

C. Kinetics of Vaporization

The need to consider the kinetics of the vaporization process introduces substantial complications in the analysis of radionuclide release. The data requirements expand considerably and the sources of data become quite sparse. But, even an approximate treatment of vaporization kinetics is more realistic than *a priori* assumption of equilibrium.

The rate limitations to vaporization are due to:

1. Transport of vaporizing species in the condensed phase to a free surface.
2. The time required for the condensed-to-vapor phase change of a surface species.
3. The transport of vapors away from the surface.

The potential always exists for one or more of these three processes to limit the rate of vaporization. Two other processes can be rate controlling for some vaporization processes:

4. Transport of reactants such as H_2 or H_2O to the free surface where they convert the condensed species into a volatile chemical form.

5. The rate of heterogeneous reaction at the surface.

The discussions below concentrate on the first three of the rate controlling processes. (The last two processes are more specialized and all information to date suggests they proceed rapidly during release from reactor fuel.) These rate limitations operate in series, so the slowest will control the overall rate of vaporization. Some simplification of the analysis is possible if one of the above limitations can be selected as rate controlling. Though this is frequently done, it is not a wise procedure. The range of conditions that develop in a given reactor accident scenario or among different accident scenarios is sufficiently broad that it is very likely the rate-controlling step varies.

The first rate-controlling step cited above alludes to one very important feature of the kinetics of vaporization--it depends on the amount of free surface area that is available. The amount of free surface area that can participate in the vaporization process depends, of course, on the nature of core degradation processes. These processes are beyond the scope of this chapter. But, it must be emphasized that data on the variation in the available free surface area is essential input to any kinetic analysis.

To further define the information needs that must be met to conduct a kinetic analysis of vaporization, a simple development is carried out below.

Consider a host material, say UO_2, containing a vaporizing species at an initial concentration of X_b mole fraction. For the species to vaporize, it must be at a free surface. In UO_2, there are a variety of means for a species to get to a free surface. Obviously, it can diffuse. It might also nucleate as a bubble in the UO_2 grains or be part of a bubble. This bubble can diffuse to a free surface. The determination of how species migrate in UO_2 grains has been an area of active research for many years. This topic is discussed at greater length below in connection with the GRASS, FASTGRASS and similar models. For the moment assume that the migration of a species to a free surface can be characterized by a mass-transport coefficient, k_ℓ. Then, the rate at which the species migrate to a free-surface is given by:

$$\frac{1}{A}\frac{dn_s}{dt} = k_\ell(X_b - X_s)$$

where A = free surface area

n_s = moles of vaporizing species transported to the free surface

X_s = the concentration of vaporizing species at the surface

k_ℓ = mass transport coefficient.

Estimating the mass transport coefficient, k_ℓ, is beyond the intent of the simple discussions here. It is determined in reactor accident situations by the behavior of the fuel during the core meltdown process. There are several useful correlations for estimating k_ℓ and others can be derived by analogy with heat transport to the surface.

Quite clearly, the rate of condensed phase mass transport can limit the rate of vaporization. Since the rate is proportional to concentration, at low concentrations this rate can become slow--approaching infinitely slow. Thus, especially for those species released to a significant extent, condensed phase mass transport must be recognized as a limit to the vaporization process.

At the surface, vaporization is driven by a force proportional to the difference between the partial pressure in equilibrium with a mixture of the surface composition, $P_s(eq)$, and the actual partial pressure, P_g. The quantitative expression of the rate of phase change at the surface is often given as:

$$\frac{1}{A}\frac{dn_v}{dt} = \frac{44.33}{(MT)^{1/2}}\,[P_s(eq) - P_g] \, .$$

where n_v = moles of species vaporized

M = molecular weight of the vapor species

This is just the Hertz-Knudsen vaporization rate expression. Derivation of this expression requires the assumption that a surface species is nearly gaslike. This might seem a severe assumption. Certainly, evaporation rates from single crystals are often slower than would be expected from the Langmuir expression by factors of 0.1 to 10^{-6} [34]. Metals seem to obey the Hertz-Knudsen vaporization expression well [35]. Other surfaces with pores and cracks or crystals with high defect concentrations approach to within a factor of 2 the Hertz-Knudsen expression [34]. Even this deviation can be attributed to failure to properly account for back pressure from vaporized species.

A somewhat superior expression for the rate of surface vaporization that takes into account the necessary difference between the surface temperature, T_s, and the gas temperature, T_g, is [36]:

$$\frac{1}{A}\frac{dn_v}{dt} = \frac{2\alpha}{2-\alpha}(4-\pi)\frac{1}{(2\pi M)^{1/2}}\left[\frac{P_s(eq)}{(RT_s)^{1/2}} - \frac{P_g(T_s)^{1/2}}{(RT_g)^{1/2}}\right]$$

where α is a correction factor that is often near unity though it can become quite small. For the simple derivation here, the Hertz-Knudsen expression will be used. It has been found adequate for a number of systems analogous to release during core degradation. For instance, Ward [37] found it adequate for analyzing vaporization of Mn, Cu, and Cr from iron at 1850 K.

Continued vaporization will occur only if vapor species are swept away from the surface. The rate at which this occurs is given by:

$$\frac{1}{A}\frac{dn_g}{dt} = \frac{k_g}{RT}(P_g - P_b)$$

where n_g = moles of vapor species removed

k_g = gas phase mass transport coefficient

P_g = partial pressure of the vapor above the vaporization surface

P_b = partial pressure of the vapor in the bulk gas

R = gas constant.

Again, the estimation of the mass transport coefficient k_g is beyond the scope of this work. Providing the information necessary to calculate this mass transport coefficient is an essential product of calculations of the core degradation process. There are many correlations from which approximate mass transport coefficients can be derived. For instance, natural convection above a flat plate in laminar flow conditions gives a mass transport coefficient of [38]:

$$k_g = \frac{0.14}{M} \frac{\rho^{7/6} D_{AB}^{2/3}}{P} \left[\frac{K}{c_p}\right]^{1/12} \left[\frac{g\beta}{\mu} \frac{\Delta T}{L}\right]^{1/4}$$

where M = molecular weight of the gas

ρ = density of the gas

P = total pressure of the gas

D_{AB} = diffusion coefficient of the vapor in the gas phase

K = thermal conductivity of the gas

c_p = heat capacity of the gas

g = gravitational force

L = length of surface

μ = viscosity of the gas

β = $1/T$

Other correlations of this type are discussed later in this chapter.

When mass transport in the gas phase is through the pore structure of the UO_2 pellets, then an approximate expression for k_g is

$$k_g = \frac{D_{AK}}{r}$$

where D_{AK} = Knudsen diffusion coefficient for the vapor species

$$= \frac{4}{3} \left[\frac{8RT}{\pi M_A}\right]^{1/2} K_o$$

r = radius of the pellet

Two common expressions for K_o are available [39]:

(1) $K_o = \varepsilon(d/4)$

where ε = porosity of the pellet

d = diameter of the pores

(2) $\frac{1}{K_o} = \frac{128}{9} n_d \frac{\tau}{\varepsilon} r_{gr}^2 (1 + \pi/8)$

where $n_d = 3(1-\varepsilon)/4\pi r_{gr}^3$

$\tau/\varepsilon = D_{AB}/D_{AB}(eff)$

$D_{AB}(eff) = D_{AB}^{-1} + D_{AK}^{-1}$

D_{AB} = diffusion coefficient of the vapor in the ambient gas

r_{gr} = grain radius

τ = tortuosity of pathway

All correlations of a suitable type involve the diffusion coefficient of the vapor in the gas phase. This diffusion coefficient has not been measured for most of the vapors of interest to the discussions here. Fortunately, the diffusion of gases is far better understood than diffusion in condensed phases. Theories have been developed that relate the diffusion coefficients of gases to the molecular properties of these gases [40]. Unfortunately, these theories require data that are not usually available for vapors of interest here. Some useful approximate descriptions of the gas phase diffusion coefficients include the Gilliland equation [41]:

$$D_{AB} = \frac{0.0043T^{3/2}}{P\left[V_A^{1/3} + V_B^{1/3}\right]^2}\left[\frac{1}{M_A} + \frac{1}{M_B}\right]^{1/2}$$

where V_i = the molar volume of the ith gas phase species when condensed,

Recently, Singh and Singh suggested [42]:

$$D_{AB} = \frac{1.79\text{x}10^{-3} T^{1.622}}{P\left[V_A^{1/3} + V_B^{1/3}\right]^2} \left[\frac{1}{M_A} + \frac{1}{M_B}\right]^{1/2}$$

At steady state, the rates at which a vaporizing species is transported to the surface, vaporizes, and is swept away must all be equal:

$$\frac{dn_s}{dt} = \frac{dn_v}{dt} = \frac{dn_g}{dt} = \dot{N}$$

Then, with a little manipulation, the rate of vaporization, $\dot{N}$, is given by:

$$\frac{\dot{N}}{A}\left[\frac{(MT)^{1/2}}{44.33} + \frac{RT}{k_g} + \frac{P_b(eq)}{X_b k_\ell}\right] = P_b(eq) - P_g$$

where $P_b(eq)$ = the equilibrium partial pressure of vapor over a mixture of composition X_b.

This simple development of the kinetics of vaporization was carried out to illustrate the features of a system that affect its vaporization. In summary, these factors are:

1. temperature
2. absolute pressure
3. flow conditions both in the melt and in the gas phase
4. surface area
5. condensed phase composition
6. equilibrium behavior of the system.

Notice that the first four of these essential quantities are not, in general, determined by the vaporizing system. These factors must be supplied. Condensed-phase composition is an essential feature that is, after being initialized, affected by vaporization. If there is but one condensed phase, then the composition of that phase is determined by vaporization. If there are several condensed phases then the equilibrium among these phases and the kinetics of approach for this equilibrium also affect the phase compositions. Finally, the equilibrium thermodynamics of the condensed-to-vapor phase transition, which has to appear in the kinetics because it defines the driving force for vaporization, is an essential part of the vaporization problem.

This simple development of vaporization kinetics also serves to show how rate control of the process can be affected by the conditions of the system. The first term within the brackets of the above rate expression refers to surface vaporization. The form of the term shows that when temperatures are very high and the vaporizing species have large molecular weights, surface vaporization becomes rate controlling. This situation could be expected late in an accident, when meltdown has advanced quite far and temperatures have reached the point where high molecular weight species such as the second row transition metals, actinides, and lanthanides are volatile.

Finally, the explicit appearance of composition in the third term shows that as vaporization progresses, mass transport in the condensed phase becomes increasingly important as a rate-controlling process. Condensed phase mass transport must eventually always become the rate controlling step if the vaporization process continues long enough.

Quite clearly, it is not possible to "legislate" a single rate-controlling step for vaporization.

The rate-controlling processes discussed above do not exhaust the possible sources of rate control. For instance, vaporization is an endothermic process. The heat required to produce a mole of vapor can vary from about 9 kcal to more than 130 kcal. Due to an inability to supply heat to the structures, structural materials in a reactor core can be subject to vaporization rate control. It has been suggested that heat supply may be the rate controlling step in vaporization of silver and indium from control rod materials [22].

D. Condensation and Nucleation

The condensation of vapors is an essential part of radionuclide transport through the reactor coolant system. As such, it is treated in greater detail elsewhere in this document (see Chapter 5). A brief discussion of the condensation of vapors to form aerosols is included here because this process can affect the rates of vaporization from a condensed phase. For the purposes of this discussion, the interest is focused on the homogeneous nucleation of particles from the vapor. For these discussions only species that condense congruently will be considered. Where condensation involves decomposition or reaction of the vapor, the problems of analyzing nucleation are much harder. Unfortunately, incongruent nucleation is also important in reactor safety analyses.

As a gas is cooled or chemical conditions are altered, a point is reached where the vapor is saturated with respect to the pure condensed phase. At this point the vapor can begin to heterogeneously condense on other condensed phases--particularly solid, structural materials. If the gas is cooled at such a fast rate that the condensation rate cannot keep the gas saturated, the gas becomes supersaturated. It is possible then the condensed species could homogeneously nucleate to form aerosols. But, since the free-energy of tiny particles produced by nucleation is increased by surface effects, some high level of supersaturation is necessary before spontaneous nucleation can begin. Even when this level of supersaturation is achieved, there are kinetic barriers that must be crossed to relieve the supersaturated condition. Once nucleation begins, then the vapors in the gas are presented additional surface area for condensation. A competition for the excess vapor in the gas is set up between condensation on structures and condensation on the nuclei.

It is immediately obvious why the issue of homogeneous nucleation is important for the analysis of severe accident source terms. Condensation of vapors on solid surfaces removes these vapors at least temporarily from the inventory of vapors that will contribute to any radiological source term. Vapors that nucleate and vapors that condense on the nuclei remain, at least temporarily, potential contributors to the radiological source term. The questions to be addressed in this section concerning homogeneous nucleation are:

1. what level of supersaturation must be achieved before nucleation can begin?

2. what size are the nuclei?

3. how fast do the nuclei grow?

The thermodynamic condition for equilibrium between a vapor and a condensed phase is equality of the respective free-energies. When the condensed phase is present as a perfectly flat, deep pool, this condition defines the equilibrium vapor pressure. When the condensed phase is present as a finite body such as a small droplet, the curvature of the surface decreases the free-energy of the condensed phase. Consequently, a vapor pressure higher than the equilibrium vapor pressure is necessary to establish a metastable equilibrium with the condensed phase. If the effects of pressure-volume work can be ignored--they are usually small--the partial pressure of vapor, P, in equilibrium with a small droplet of radius r is:

$$\ln (P/P_{eq}) = \ln (S) = \frac{2V\sigma}{rRT}$$

where P_{eq} = normal equilibrium vapor pressure

V = molar value of the condensed vapor

σ = surface tension of the condensed vapor

R = gas constant = 82.06 cm^3/mole-K

The equilibrium defined here is clearly unstable toward fluctuations in either P or r.

This thermodynamic criterion is not enough to characterize the nucleation problem. It is necessary to also know the rate at which nuclei of radius r form. The problem is solved by defining conditions for which the rate of nucleation is detectably large.

Two important theories of nucleation exist. The rate of nucleation of particles of size r in both theories is given by

$$\frac{dn(r)}{dt} = Z\left[\frac{PN_A}{RT}\right]^2 \left[\frac{2\sigma}{\pi}\frac{MW}{N_A}\right]^{1/2} V \exp[-\xi]$$

where MW = molecular weight of condensed species

N_A = Avogadro's number

$$\xi = \frac{16}{3}\left[\frac{V_{molar}}{N_A}\right]^2 \left[\frac{\sigma}{kT}\right]^3 \frac{1}{[\ln(S)]^2}$$

k = Boltzmann's constant

Z = parametric discussed below

For practical purposes, it is convenient to assume the nucleating droplets are monodisperse with a radius given by

$$r = \frac{2V\sigma}{RT\ \ell n(S)}$$

Also, the practical, observable, nucleation rate is usually taken to be 1 nuclei per cubic centimeter per second. This definition of a critical nucleation rate closes the problem. The definition is arbitrary, but nucleation rates are so sensitive to the supersaturation ratio, S, that selection of the critical rate is not especially important [46].

The two theories for the homogeneous nucleation rate differ in their treatment of the parameter Z in the above rate expression. In the classic Becker-Doring theory [47], the parameter Z is taken to be 1. This theory has proved quite successful in the analysis of water nucleation and the nucleation of other species that hydrogen bond in the condensed phase.

A more recent development of homogeneous nucleation, the Lothe-Pound theory, takes $Z = 10^{17}$ [48] or 10^{12} [46]. Nucleation of species that do not hydrogen bond typically fall between the predictions of the Becker-Doring and Lothe-Pound.

A parametric difference of 10^{17} or 10^{12} in two theories might seem of serious consequence. In fact, the only significant difference between the two theories is the prediction of the critical supersaturation, which are typically different by a factor of 3 or 4 in the two theories. This deamplification of the effect of the value of Z is because of the sensitivity of the nucleation rate expression. This same difference in the predicted supersaturation would be caused by about a 20 percent change in the value of σ, the surface tension of the condensed material (see Figure 3.4). Uncertainties of 20 percent in surface tension are quite possible since the surface tensions of core materials have not been definitely measured.

Whether a condensing species behaves according to the Becker-Doring theory or the Lothe-Pound theory seems to depend on the surface structure of the condensate. Those species that can orient themselves on the surface to minimize the unsatisfied bonding potential behave in accordance to the Becker-Doring theory. Hydrogen bonding species--such as water or alcohols--are especially good examples of Becker-Doring condensates. Condensing species that cannot, by optimal orientation on the condensate surface, minimize unsatisfied bonding potentials follow the Lothe-Pound theory. Intuitively, there seems to be an extra energy driving force for condensation for these species that is brought on by the advantages of utilizing the unsatisfied

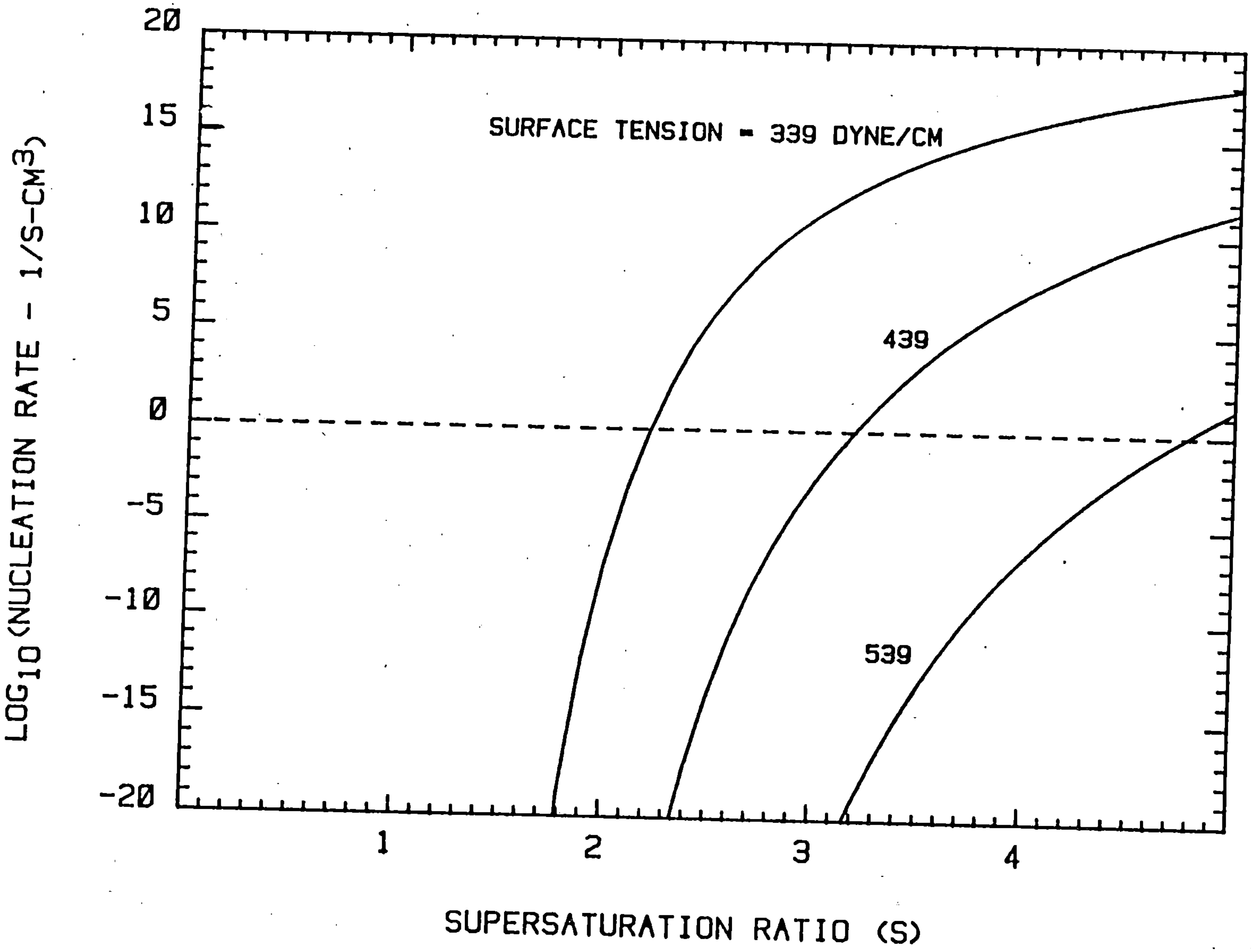

Figure 3.4. Nucleation Rate of Tin at 2000 K as a Function of the Supersaturation of the Vapor. Curves are marked by the assumed surface tension of liquid tin.

bonding potential of species on the surface. Consequently, lower supersaturations are required to initiate nucleation of Lothe-Pound condensate.

Metal vapors cannot, by orientation on the surface of a condensate, relieve unsatisfied bonding potentials. Consequently, condensation of metallic vapors such as Ag, Te, and Cd would be expected to follow the Lothe-Pound theory quite closely.

Condensation of compounds is not as easily predicted. Strongly ionic compounds such as CsI would retain long-range bonding potentials at the surface of a condensate regardless of the orientation of the surface molecules. Condensation of these strongly ionic compounds would be expected to more closely follow the Lothe-Pound theory than the Becker-Doring theory. Covalent compounds, such as Ag_2Te, could, by orientation, relieve some unsatisfied bonding potential. Similarly, vapor-phase hydroxides could achieve some stability by orientation to take advantage of hydrogen-bonding interactions. These species may approach the Becker-Doring model of condensation.

It appears, then, that for reactor safety analyses, condensation properties of vapors produced during heat-up and melting of the core could span the entire range bounded by the Becker-Doring and Lothe-Pound theories. In the absence of definitive information on the condensation of particular species or obvious behavior expecting, such as for metal vapors, the two bounds must be recognized. The most apparent difference between the bounds is that the Lothe-Pound theory predicts that lower supersaturations are required to initiate nucleation than does the Becker-Doring theory.

Fortunately, the question of the condensation behavior of vapors during nuclear reactor accidents will probably not be too severe. The rate at which vapors are carried out of the hot core region into cooler environments is fast enough for most accident scenarios that supersaturations high enough to satisfy the more stringent requirements of the Becker-Doring theory are quickly achieved. When this is not the case, the competitive process of condensation on structures will probably dominate and the homogeneous nucleation question becomes mute.

The description of nucleation presented here is for homogeneous nucleation and neglects the presence of any foreign bodies. In the environment created during a nuclear reactor accident, foreign bodies that will affect nucleation processes will be present in abundance. Notably, gaseous ions created by the intense flux of radiation can be important nucleation sites. Russel [53] has discussed the theories of nucleation in the presence of gaseous ions. Again, the effects are of theoretical importance but these effects are not overwhelmingly large in comparison to the effects of uncertainties in surface tension, or uncertainties caused by co-condensation of vapors.

The treatment of nucleation has also neglected thermal effects associated with condensation. Clement [125] has shown that the heat liberated during condensation can have an important effect on the competition between nucleation of vapors and condensation of vapors on structures.

Once the nuclei form, if supersaturation has not been relieved, the nuclei grow either by condensation of vapor or by agglomeration. The rate of growth by vapor condensation is given by

$$\frac{dm(r)}{dt} = \frac{4\pi r^2 P}{(2\pi MRT)^{1/2}} (M/N_A)$$

where m(r) is the mass of nuclei of radius r. Growth by agglomeration of nuclei is a more complex problem. While small, the nuclei can be treated as a pseudo-gas. When the nuclei become macroscopic in size ($r \sim 10^{-2}$ μm), then the growth process is probably more accurately described by models of aerosol agglomeration.

The preceding development of homogeneous nucleation was restricted to pure vapors and condensed phases. The problem of mixed condensation involving two or more vapor species is a good deal more complex. Camp [49] is currently developing descriptions of this process.

Even without detailed results for multi-component condensation several important points can be seen. First, from the analyses for pure vapors, it is obvious that surface tension of the condensed phase is an important parameter in determining when a species will nucleate. Since surface tensions do not correlate in a simple way with vapor compositions, there is no reason to suspect that the composition of aerosols will reflect the composition of the vapors. This is especially true when speciation of vapors and aerosols are of interest. Some species that are quite stable in the gas phase are quite unstable in the condensed phase. Gaseous hydroxides such as $Ba(OH)_2$ and LaOH are good examples of this.

Second, the onset of condensation is brought about by supersaturation of the vapor. Supersaturation can arise from changes in temperature. It can also arise when there is a sudden change in the chemical conditions. Consider the barium oxide vapor pressures discussed above. Suppose vaporization of barium oxide were taking place in a hydrogen rich gas brought about by steam reacting with zircaloy. In hydrogen, the barium partial pressure over barium oxide is quite high. As barium-bearing vapors passed across the boundary layer, they would encounter more oxidizing conditions as steam constitutes more of the gas phase. The equilibrium partial pressure over barium oxide is much lower in the steam-hydrogen mixtures than in nearly pure hydrogen. Consequently, the vapors could be supersaturated and could condense in the boundary layer.

This phenomenon of vapor condensation in the boundary layer is commonly encountered in the ferrous metallurgy [43]. A "fog line" is frequently observed a few millimeters above steel melts. This fog line is created by the condensation of alloy constituents vaporized from the melt. The vaporization of these alloy constituents increases sharply when a fog line appears and exacts a fairly stiff economic penalty, since alloy constituents lost by vaporization are usually quite expensive relative to iron.

Hills and Szekely [44] have found that if the concentration of the vapor is low so it is negligible in the bulk fluid, then the factor of enhancement of the vaporization accompanying fog line formation is approximately:

$$\frac{\Delta H_v}{RT_s}\left[1 - (T_b/T_s)\right]$$

where ΔH_v = heat of vaporization

T_s = temperature of the vaporizing surface

T_b = bulk gas temperature.

When these conditions are not met a more accurate expression, that compares well with data [45] for the factor of vaporization enhancement is [44]:

$$\frac{\dfrac{\Delta H_v}{C_p}\left[\dfrac{P_s(eq)}{RT_s} - \dfrac{P_b(eq)}{RT_b}\right] + (T_s - T_b)}{\dfrac{\Delta H_v}{c_p} + \dfrac{RT_s^3}{\xi\, P_s(eq)}\left[\dfrac{P_s(eq)}{RT_s} - \dfrac{P_b(eq)}{RT_b}\right]}$$

where

$P_b(eq)$ = equilibrium partial pressure of the vapor (pure) at the bulk temperature

c_p = heat capacity

$$\xi = - T_s \ln[P_s(eq)] + T_s \frac{\Delta S_v}{R}$$

ΔS_v = entropy of vaporization.

E. Summary of the Fundamentals of Vaporization Processes.

The preceding review of the fundamentals of vaporization ought to convince anyone that there are significant complications in estimating the release of radioactive and nonradioactive species during core degradation. A model that pursued each of the topics raised in the review to any depth would be an imposing creation--far too large to be accommodated in a systems code such as MELCOR. No such extensive model has yet been devised. The MELCOR development effort will adopt, in all probability, one of the simplified models of radionuclide release that is now available. The review then provides a framework for ascertaining what features are included and what features are omitted from the available models.

Calculations produced by the MELCOR model should be, of course, as accurate as is feasible. But, equally important, the model should be capable of examining the sensitivity of the calculated results to assumptions concerning the nature of the plant and the accident in question. The review of the fundamentals of vaporization processes defines several features of release processes that ought to be available in the model used in MELCOR:

1. Release should be constrained by the limits imposed by the thermochemistry of the volatile element.
2. Release rates ought to be sensitive to pressure, flow velocity, and gas composition as well as time and temperature.
3. Release rates should be sensitive to the melting and slumping of reactor fuel.
4. Release rates should be dependent on location in the core.
5. The release model should consider various rate limiting processes such as condensed phase mass transport, surface reactions, and gas phase mass transport rather than just assuming one of these processes is rate limiting.

3.4 Extant Models of In-Vessel Release

In this section the various models of fission product release that have been used in reactor accident analyses are described. Some attempt is made to comment on how well these models fit with the framework of fundamental properties of vaporization processes outline above.

The organization of the section is along the lines of the description of the in-vessel source term developed in the Reactor Safety Study. That is, the discussions are divided into sections dealing with:

A) Gap Release

B) Diffusion Release

C) Meltdown Release

D) Fragmentation Release

Release of materials from the core is a continuous process. The categorization is done merely to mark major phenomenological events in the core degradation process.

A. <u>Gap Release</u>

The first dramatic event in a reactor core following loss of adequate cooling is the pressurization, expansion (called ballooning), and rupture of the fuel cladding. More detailed accounts of this process are to be found elsewhere [126]. Suffice it here to say that cladding on the fuel can be expected to rupture when the clad temperature is between 700 and 1100°C. The precise temperature of clad rupture depends on the rate the clad is heated, the system pressure, and the gas inventory of the fuel rods.

When the clad ruptures there is a rapid expulsion of fission products as the internals of the fuel rod pressure equilibrate with the primary system atmosphere. Estimation of the release of fission products that occurs during this period might at first appear to be fairly simple annular flow problem with serious wall friction. It must be remembered though that a substantial portion of the void structure in a fuel rod is produced by cracks, gaps, and pores in the fuel itself. Fission products in these crevices can also contribute to the release.

Experimental studies of gap release have been conducted at Oak Ridge National Laboratory [59]. Results of these studies have been used to develop empirical descriptions of the gap release. The entire process is divided into two steps. The first step, called burst release, is due to the pressure equilibration with the primary system atmosphere. This step occurs very quickly, so time resolution of release by this process is not necessary for severe reactor accident analyses. The mass of the ith radionuclide released during the pressure equalization was found to be:

$$M_i = \alpha_i V \left[\frac{M_o(i)}{A} \right]^{\alpha_i} \exp\,(-C_i/T)$$

where

M_i = mass of the ith radionuclide released (g)

V = volume of gas expelled (cm^3) calculated at the system pressure and 273 K

$M_o(i)$ = mass of ith radionuclide in the fuel-to-cladding gap

A = internal surface area of the cladding

T = absolute temperature at the clad rupture location.

Parametric values, α_i, a_i, C_i, were obtained by fitting the model to data. These values are listed in Table 3.7. The second step in the gap release can be treated as part of the diffusion release discussed next.

In addition to parametric values, the model also requires that gap inventories of the radionuclides be provided. Gap inventories are not especially certain. Some values recommended in various investigations are shown in Table 3.7.

B. Diffusion Release

During the time between clad rupture and fuel melting, fission products are slowly released from the fuel. They must be conducted along the cladding fuel gap to a site of clad rupture. Early in the accident, the only opening in the clad that will allow fission products to enter the primary system atmosphere is that created by clad ballooning and rupture. As the accident progresses, multiple openings in the clad may develop. It would be expected that release of fission products during this time period would accelerate, not only because of the temperature increases, but also because continued rupture of the cladding would provide some relief to rate-limiting transport of released fission products to a single rupture site.

The early phases of fission product release by diffusion have been described by the empirical model [59]:

$$M(i) = M_o(i) \quad 1 - \exp\,[-R_o(i)t/M_o]$$

where $M(i)$ = mass (g) of the ith fission product released at time t (hrs).

$$R_o(i) = \sigma_i[W/P][M_o(i)/A]^{a_i} \exp\,[-\,\gamma_i/t]$$

W = width of the fuel-to-cladding gap (µm)

P = system pressure (MPa)

Again, the model parameters σ_i, γ_i, and a_i were found by fitting the model to experimental data. Some values of these parameters are shown in Table 3.7.

When this and the gap release model have been used for accident analysis, the results are lower than those estimated in the Reactor Safety Study. For a 10-minute transient to 1200°C, the predicted releases of cesium, iodine, and the fission gases

Table 3.7

Parameters for the Gap Release Model Developed at Oak Ridge

Parameter	Cesium	Iodine
α	3.49	0.163
∂	0.8	0.8
e	7420	3770
σ	1900	122
γ	19800	14800

Recommended Gap Inventories

Element	% of Total inventory in the Gap*		
	Reference 7	Reference 1	Reference 59
Xe	3	8	1.27
Kr	3	8	1.27
Cs	5	5	0.025
I	1.7	3.3	0.053
Te	0.01		
Sb	0.01		
Ba	0.0001		
Sr	0.0001		

* Note: these are the % of the entire rod inventory, not of just the node adjacent to the breach.

were 0.025 percent, 0.053 percent, and 1.27 percent of the respective inventories. The Reactor Safety Study suggests gap releases of 3, 1.7, and 3 percent of the cesium, iodine, and fission gas inventories, respectively. It should be remembered, however, that the Reactor Safety Study definition of gap release continued longer and to higher temperatures than the above diffusion release model and the preceeding gap release model.

It is clear from the model predictions that diffusion release at temperatures less than 1000°C is small, and this is not the release that is the source of greatest concern in severe reactor accidents. Diffusion release at higher temperatures is faster and more important for accident analyses.

Another empirical model, based again largely on correlation of experimental data, is the CORSOR model [60]. This model was first described in conjunction with the U.S. Nuclear Regulatory Commission's "NUREG-0772" effort to assess the technical basis for changing the source term descriptions in the Reactor Safety Study [5]. It has subsequently been used with the MARCH code for accident analyses. The CORSOR model is intended to treat the entire process of fission product release from the time of clad rupture through rapid diffusion release to gross core slumping and release from molten fuel. A more complete discussion of this model is presented in the subsection dealing with Meltdown Release.

Based on the attempts to describe the process empirically, it might be concluded that the state of knowledge concerning fission product release from hot, but still solid fuel is poor. Within the fast reactor safety and development fields, there has, however, been a considerable effort to develop detailed mechanistic understanding of the process. Models developed in the fast reactor field are now being applied to light water reactor severe accident analysis. For the most part, these models were designed for normal operating conditions and must be extrapolated to severe reactor accident conditions.

The earliest mechanistic models of fission product release were dedicated to determining the release of fission gases Xe and Kr from the fuel and have come to be known as "Booth-type" diffusion models [61,62]. These models consider the fuel pellets to consist of grains that are treated as spheres. Each sphere is isothermal, though a pattern of spheres across the fuel pellet can be used to mimic a thermal gradient. Self-consistent temperature profiles can be calculated with the models given a description of the thermal conductivity of the fuel/cladding gap. None of the Booth-type diffusion models appear to have considered heat input to the fuel from clad oxidation, since for fast breeder reactors, this is not a serious problem.

In the simplest models, transport of fission gases to the grain boundaries is assumed to occur by simple diffusion through a homogeneous medium. If fission gas production can be neglected, as would be the case following scram of a light water reactor, then an approximate solution to the diffusion problem for a grain is:

$$J_i = D_o(i) \exp [-E(i)/RT] \frac{C_o(i)}{a} \{[\pi\tau(i)]^{-1/2} - 1\}$$

where J_i = flux of the ith fission gas out of the grain pores

$D_o(i)$, $E_o(i)$ = parameters characterizing the diffusion coefficient of the ith fission product gas in the fuel

$C_o(i)$ = initial concentration of fission gas in the fuel grain

$\tau(i)$ = $D_o(i)[t/a^2] \exp[- E(i)/RT]$

a = the radius of the sphere that has the same surface to volume ratio as the grain.

This solution is usually applicable up to releases of 80-90 percent.

The models can be used by fitting the model to release data to determine the parameters that characterize the diffusion coefficient of the species in question. Some values of the diffusion coefficient parameters are listed in Table 3.8.

Very early in the use of the Booth diffusion models, it was found that diffusion coefficients determined by different methods were not in good agreement. Quite an extensive base of literature exists showing how corrections to the general diffusion model would yield a more correct description of the release process. The possibility that defects introduced by the fission process trap diffusing species is an especially popular explanation of this problem with the simple diffusion models. Models have been formulated to account for these defects [62] and typically involve two additional parameters.

Table 3.8

Parameters for Booth Diffusion Model [65]

Fission Product	$D_o(i)$ (cm/s)	E(i) (Kcal/mole)	Temp Range (°C)
Xe	$3x10^{-6}$ to $8x10^{-3}$	61 to 92	800-1600
Xe	$1.1x10^{-5}$	72	1500-2000
Xe	$1.6x10^{-4}$	67	1500-2000
Xe	$3x10^{-3}$	63	600-2400
I	50	110	900-1500
I	$1.9x10^{-3}$	68	900-1500
I	$3.5x10^{-3}$	87	1500-2000
I	$1.5x10^{-5}$	53.5	1500-2000
I	$1.5x10^{-3}$	59	1400-2500
Te	90	120	1000-1500
Te	0.56	84	1000-1500
Te	$1.5x10^{-3}$	78	1500-2000
Te	$4.2x10^{-5}$	58	1500-2000
Te	$6.6x10^{-3}$	70	1400-2500
Cs	0.04	100	1000-1500
Cs	$4.5x10^{-7}$	40	1000-1500
Cs	$3.8x10^{-3}$	97	1500-2000
Cs	$1.9x10^{-5}$	52	1500-2000
Cs	$8.5x10^{-9}$	6.1	1400-2500
Sr	1600	160	1300-1500
Sr	86	140	1500-2000
Sr	86	140	1500-2000

Table 3.8 (Cont.)

Parameters for Booth Diffusion Model [65]

Fission Product	$D_0(i)$ (cm/s)	E(i) (Kcal/mole)	Temp Range (°C)
Sr	4.5×10^{-7}	24.4	1400-2500
Ru	4.2	95	800-970
Ru	5.0×10^{-7}	175	1200-1500
Ru	0.08	110	1500-2000
Ru	0.09	110	1500-2000
Ru	8.6×10^{-8}	19.2	1400-2500
Zr	1.2×10^{-9}	45.6	800-950
Zr	1.6×10^{-6}	59.2	1120-1410
Zr,Nb	0.167	104	1400-2500
Ce	7.2×10^{-6}	37	1400-2500
La	2.2×10^{-6}	35	1400-2500
Y	6.8×10^{-8}	46.4	1150-1450
Pr	3.5×10^{-6}	56.8	1120-1420
Mo	3.9×10^{-4}	54	1400-2500
Am	0.03	92	1200-1500
Np	2.9	109	1200-1500
Pa	2.5	107.6	1200-1500
Pm	3.5×10^{-6}	56.8	1120-1410
Pu	0.34	97.3	1200-1500
Tn	0.16	98	1200-1500

Booth diffusion type models probably reached their zenith with the publication of the ANS 6.5 Standard Fission Product Release Model [64]. This model took an empirical approach to diffusion by using release data to define "effective" diffusion coefficients. It also took an important step of including a correction term for the effects of irradiation on the diffusion coefficients. Diffusion coefficients for Cs, I, and Te were determined relative to those found for Xe and Kr. The diffusion coefficients specified by the ANS 6.5 Standard are:

$$D_{Kr} = D_{Xe} = \frac{D_o}{a^2} \exp(-Q/RT)\ 100^{(Bu/B)}$$

$$D_I/D_{Xe} = 0.575 \exp(8900/RT)$$

$$D_{cs}/D_{Xe} = 0.078 \exp(12100/RT)$$

$$D_{Te}/D_{Xe} = 1100 \exp(-12500/RT)$$

where $D_o/a^2 = 0.61\ \text{sec}^{-1}$

$Q = 72300$ cal/mole

$B = 28000$ MWd/t

R = gas constant = 1.987 cal/mole-K

Bu = fuel burn up in MWd/t

To summarize, Booth diffusion type models assume the release rate is limited by condensed phase mass transport. No rate limitation arising because vapors must migrate through the pore structure of the pellets or along the fuel-to-cladding gap is recognized. Diffusion coefficients are peculiar to each element and are functions of temperature and, in the case of the ANS 5.4 model, fuel burnup. The operative geometry is the fuel grain which is assumed to be fixed in size.

The difficulties with simple diffusion models of fission gas release prompted a considerable amount of experimental investigation into fission product behavior within the fuel. Improved data led to the definition of "deep" traps and "shallow" traps for fission gases that affected the diffusion process. Eventually, the deep traps were identified as gas bubbles about 10-50 Å diameter.

The more modern of the mechanistic models of fission gas release take into account the behavior of bubbles as well as atomic diffusion, the behavior of grains, and the behavior of bulk fuel. The best known of the modern fission gas release codes is GRASS-SST [63] developed at Argonne National Laboratories. GRASS-SST has been the basis of two other codes that deserve mention:

1. FASTGRASS: A faster running version of GRASS-SST. Speed was achieved largely by using a single, average but time varying, fission gas bubble size.
2. PARAGRASS: A correlational model based on an extensive library of computations with either GRASS-SST or FASTGRASS.

Several other models of the same general type as GRASS-SST have been developed [66].

Much of the modeling in both GRASS-SST and FASTGRASS has been included to describe the dynamic behavior occurring during the fission process. This modeling is, of course, not important for severe light water reactor accidents. In the brief description that follows, the discussions focus on the phenomena germane to accidents in which the reactor has been neutronically shut off.

The grains in the fuel are viewed as polyhedra with faces and edges rather than as spheres. Fission gases can migrate in the grain both as atomic species and as bubbles. The diffusivities of atomic species and gas bubbles are:

$$D_{atomic} = 2.1 \times 10^{-4} \exp(-91000/kT)$$

$$D_{bubble} = D_{atomic} (r_{atom}/r_{bubble})^{1.62} Q$$

where

r_{atom} = radius of the atomic species

r_{bubble} = radius of the bubble

Q = correction factor to account for lattice distortion by the bubble.

The correction factor Q is a function of the bubble size, pressure and UO_2 material properties.

Bubbles collect at the faces of the grains, move about, and coalesce. The surface diffusivity of the bubbles is

$$D_i = (2.4x10^{-25}/r_{bubble})\ \exp(-10800/RT)$$

The migration of bubbles on the surface of the grains can lead the bubbles to the grain edges, which lead to the interconnected network of porosity in the fuel. Bubble density can saturate at the grain surface [N(max) = $6x10^{12}$ bubbles/m^2], which opens the grain surfaces to the network of porosity. The release can also be accelerated by microcracking of the fuel. All three of these processes are considered in the model.

Obviously, GRASS-SST and FASTGRASS are very sophisticated and very complex codes. When compared to experimental data involving normal operating conditions or relatively mixed transient heating conditions, these codes yield high-quality predictions. Among these predictions is the nature of burnup on release. Burnup is found to increase the rate of release for burnups up to about 10000 MWd/t. At higher burnups the effects are less dramatic. At about 30000 MWd/t, all the effects of burnup on release have been realized.

Accentuation in the release caused by fuel burnup is the result of two processes in the GRASS-type models. As the inventory of fission gases builds with burnup, it becomes easier for bubbles of the fission gases to collect and coalesce to form an interconnected network of porosity that provides release pathways from the pellet. Coalescence is enhanced by grain growth, which sweeps bubbles from the interior of grains to the grain boundary. But, grain growth is inhibited by impurities such as radionuclides. Thus, with increasing burnup, it becomes harder for grains to grow. At sufficiently high burnups, a complete network of interconnected porosity may exist in the fuel before an excursion in fuel temperature during an accident begins. Further irradiation will not add to this network of porosity. But, further irradiation will inhibit fission products reaching the porosity because of inhibition to the grain growth process. Thus, there is a limit to the accentuation of release brought on by irradiation.

The severe failing of FASTGRASS, that it only treats fission gases, is being corrected at least to the extent that Cs and I are being included. The way these species are being incorporated is fairly elegant. Both Cs and I are allowed to migrate in the fuel as atomic species:

$$D_I = 2.1\times10^{-4} \exp(-91000/RT)$$

$$D_{Cs} = 8.53\times10^{-9} \exp(-61000/RT)$$

It is also recognized that these species will tend to vaporize into gas bubbles at the fuel temperatures during accident transients [68]. The partial pressures of these species present in the vapor state as Cs(g), I(g), and CsI(g) are calculated. The condensed form of Cs is taken to be Cs_2UO_4 or Cs_2MoO_4, as dictated by the oxygen-partial pressure of UO_{2+x} calculated with the Blackburn model [67]. The gaseous forms of Cs and I are assumed to saturate the fission gas bubbles and to migrate with these bubbles. It should be noted that there are some questions about the vapor equilibration with gases in bubbles.

The chemistry being added to the GRASS-type models is assumed to be dictated by the fuel. Thus, oxygen potential is created by hyperstoichiometric urania. Condensed forms of cesium are uranates and molybdates. Vapor forms of iodine are I(gas) and CsI(gas). In this regard, two experimental observations are noteworthy. Kleykamp [69] has found cesium in the fuel-to-cladding gap to be in an oxide mixture which contains Zr and Sn but neither U nor Mo. Also, a variety of evidence from studies of Zircaloy stress corrosion cracking suggests that iodine reacts with zirconium, probably to form ZrI_2 [70]. The iodides of zirconium appear stable in radiation fields--unlike CsI [71]. Thus, to complete the chemistry in these models may require that clad chemistry as well as fuel chemistry be included.

The GRASS and similar type models assume rate control lies within the condensed phase mass transport to a free surface. The barrier to release caused by transport through the pore structure or along the fuel-to-cladding gap is assumed negligible. The operative geometry for release is, as in the Booth diffusion models, the fuel grain. Unlike the Booth diffusion models grains are allowed to grow. Also, not all grains are equal. Surfaces of the grain must be adjacent to the network of interconnected porosity of the fuel pellet for release to occur. Some chemistry is being incorporated into the models. But, this is chemistry dictated by the fuel and is unrelated to the chemical environment created by the steam and hydrogen atmosphere surrounding the core.

C. Meltdown Release

Meltdown release presumably begins with liquefication of the fuel. Distinguishing this stage of release from release while the fuel is solid makes good physical sense. Mass transport in the condensed phase should greatly accelerate with the formation of liquid. The nonideality of liquid mixtures is typically much less than in solid mixtures, so significant changes in the thermodynamic driving force for release would be expected. Finally, the cladding should have lost its integrity by the time of fuel melting so any rate limitation posed by transport of vapor species to a rupture in the clad has disappeared.

As noted in the discussion of phases present during an accident, there is some ambiguity about when meltdown release should start because of liquified clad attack on the fuel pellets. There is presumably some transient period in which there is the potential of rate limitation by both diffusion from an eroding solid to the liquid phase, and through the liquid phase to a free surface.

Clad attack on the fuel could result in chemical transformations of the radionuclides that could effect release. For instance, noble metals such as Ru, Rh and Pd present in the fuel as isolated nodules might dissolve in the molten clad. Dissolution, as noted in section III-A, ought to reduce the driving force for vaporization of these species. Refractory oxides such as BaO might be reduced to the metallic state by clad attack. Since the metal is more volatile than oxide, release of barium might be accentuated by liquefication.

Experimental evidence on the effect of liquefication is mixed. Apparently, out-of-pile tests with highly irradiated fuel rods reveal no dramatic change in release when liquification occurs [86]. In-pile tests with low irradiation fuel rods show a dramatic effect [87].

Modeling of the meltdown release has been attempted many times. Only a few of these attempts are described here.

<u>The Reactor Safety Study Model</u>. To assess the magnitude of fission product release during the melting phase of a severe reactor accident, a series of thermochemical calculations were done in the Reactor Safety Study to determine the equilibrium partial pressure of fission-product-bearing vapors. The vapor-phase chemistry of the fission products was restricted to simple oxidation-reduction:

$$MO_x + H_2O \rightleftarrows MO_{x+1} + H_2$$

Activity coefficients were taken to be unity and pressure invariant (ideal mixture assumption). Temperatures were fixed at 3100 K. An unlimited supply of 1000 psia steam was assumed.

Rate control was assumed to be due to the limitations of surface vaporization, so:

$$R_i \text{ (g/cm}^2\text{-s)} = 0.01\ P_i(\text{eq})\ [M_i]^{1/2}$$

where M_i = molecular weight of the dominant vapor species of element i

R_i = release rate of element i

P_i = equilibrium partial pressure of the vaporizing species.

The results of these analyses, tempered with some laboratory data, were used in an undetermined way to define release fractions for elements during the meltdown process. Time resolution of the release was obtained by determining, with the antecedent of the MARCH code, when a node within the core melted. Upon melting, this node was assumed to release the entire proportion of the meltdown release fraction that could be ascribed to the node.

The Reactor Safety Study model of release was intended to yield an upper bound. Since behavior of the released material as it passed through the primary system into containment was not carefully treated, release rates were not of great concern. The restrictions on the vapor phase chemistry imposed on this model raise questions as to whether an upper bound release was really determined by this model. Neglect of nonradioactive materials also makes the model useless for modern source term analyses.

The Light Bulb Model. The "Light Bulb" Model of fission product release is mechanistic in the sense that it assumes gas phase mass transport is the rate-controlling process in release [72]. The model could be called semiempirical, in that it does require one experimentally determined release parameter. The rate of release is given by the expression for gas phase mass transport rate control into a bulk gas with negligible fission product content:

$$\frac{1}{A}\frac{dn(i)}{dt} = \frac{K_i P_i(\text{eq})}{RT}$$

where $n(i)$ = moles of the $i^{\underline{th}}$ species released

A = surface area

$P_i(eq)$ = equilibrium partial pressure of the $i^{\underline{th}}$ species.

The rate parameter is specified to be

$$K_i = D_{ig}/\delta$$

$$D_{ig} = \frac{0.001858\ T^{3/2}\ (1/M_i + 1/M_g)^{1/2}}{P[(\sigma_i + \sigma_g)/2]^2}$$

P = total pressure

M_i = molecular weight of the vapor phase fission product

M_g = molecular weight of the ambient gas

σ_i and σ_g = collision parameters for the gaseous molecules

δ = parameter determined from experimental release data.

The empirical parameter is theoretically dependent on the temperature, gas composition and pressure, and the nature of the released species. In practice, δ is determined from one data point in a data set of interest. When this parameter is determined, the model does quite a good job correlating experimental data (see Figure 3.5).

The "light bulb model" presents an alternative to all the previously discussed models. Rate control lies in the gas phase mass transport away from the free-surface rather than condensed phase mass transport to the free-surface.

The IDCOR Model. IDCOR [32] has developed a release model based on a suggestion by Cubicciotti [73] that fission product release is controlled by sintering of UO_2. Sintering of UO_2

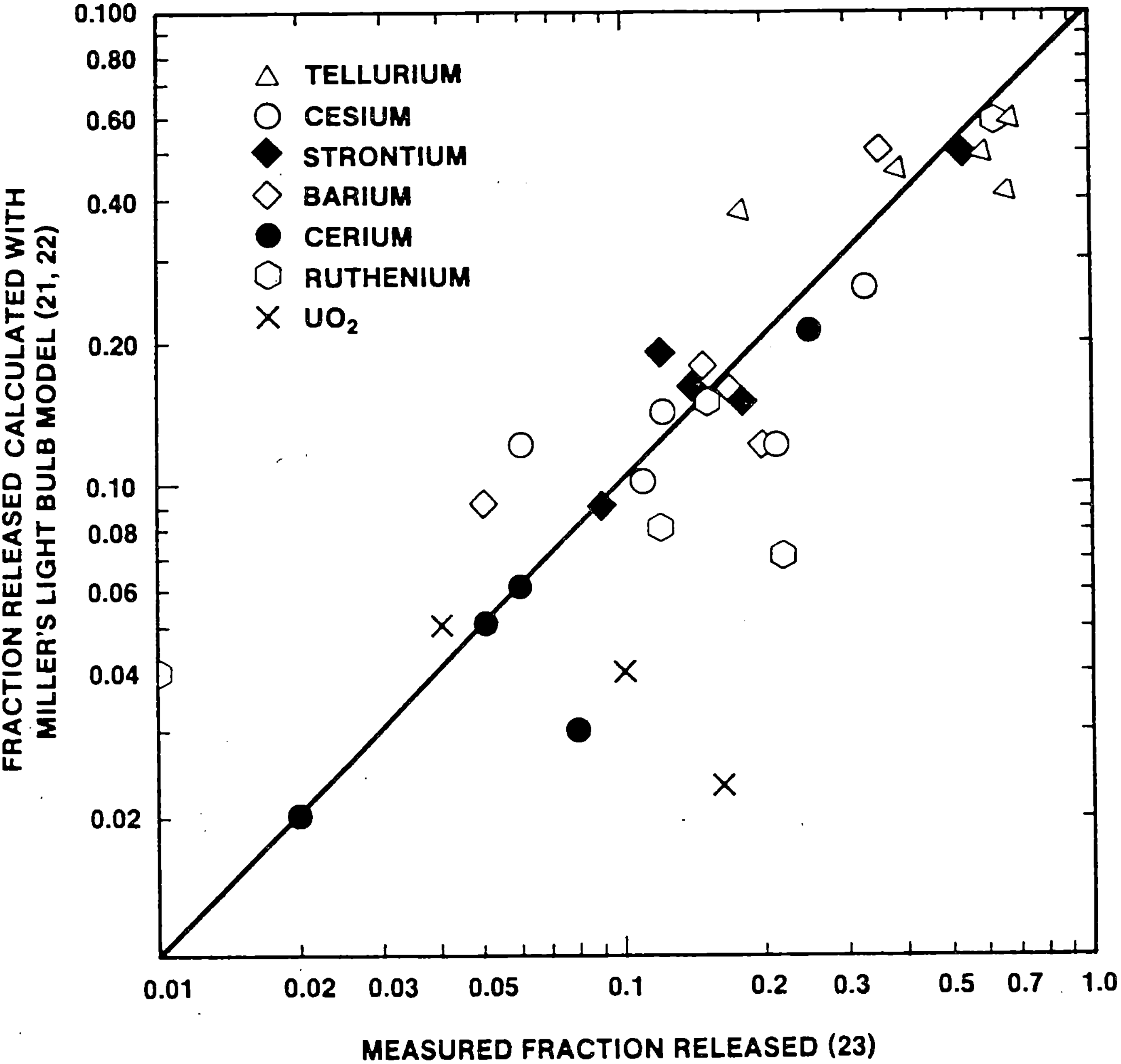

Figure 3.5. Comparison of Observed Releases of Fission Products From UO_2 at Temperatures Between 2273 and 2473 K with Those calculated with the Light Bulb Model.

is accelerated in steam [74, 75]. Cubicciotti argues that the rate of sintering in steam is correlated with the rate of UO_2 oxidation by steam. He then used oxidation rate data by Bittel et al. [76] and Jain's short-cylinder diffusion model [77] to derive a release expression for fuel pellets in steam:

$$F_i(t) = 1 - [1 - 4(\tau_H/\pi)^{1/2}][1 - 4(\tau_\rho/\pi)^{1/2} + \tau_\rho]$$

where $F_i(t)$ = released fraction of the $i^{\underline{th}}$ species

$\tau_H = Dt/H^2$

$\tau_\rho = Dt/r^2$

$D = 0.0099 \exp(-28000/T)\ m^2/s$

T = absolute temperature (K)

H = length of a fuel pellet ~ 13×10^{-3} m

r = radius of a fuel pellet ~ 6.4×10^{-3} m

t = time (s)

When the ambient atmosphere is inert or reducing, Cubiciotti favored use of Malen's UO_2 grain growth model [78] to predict release:

$$F_i(t) = 1 - [1 + 2kt/d_o]^{-3/2}$$

where $k = 1.46 \times 10^{-8} \exp(-32100/T)$
d_o = initial grain size ~ 1×10^{-5} m

Cubiciotti does not provide an indication of how he would alter the grain growth rates with fuel burnup.

A comparison of releases obtained with Cubiciotti's inert and steam atmosphere models is provided in Figure 3.6. The presence of steam accelerates release by about a factor of 100 at temperatures of 1300-1700K. Steam has a decreasing effect on release as temperatures rise.

As written, the models by Cubiciotti really apply only to fission gases. For more refractory species, the release fractions are reduced by a factor of

$$1 - \exp(-P_i/P_T)$$

where P_T = total pressure

P_i = equilibrium partial pressure of the pure species at temperature T.

For the IDCOR implementation of Cubicciotti's model, SOLGASMIX [28,29] was used to calculate the equilibrium partial pressures of the refractory species.

The IDCOR model presents yet another approach to kinetics of vaporization. Here rate control is limited by the diffusion of a reactant into the host material. Release is then independent of the radionuclide in question except for the dependence of the equilibrium partial pressure. The analysis of the equilibrium partial pressure is completely different than that used in connection with the GRASS code. The partial pressure is independent of the fuel and very dependent on the ambient atmosphere composition. The IDCOR model does not provide an explanation of how cladding affects the release.

The IDCOR model ought to be considered a mere hypothesis. When compared to data, the model at best provides an upper bound on these data. Examination of data in detail shows release has not proceeded as has been hypothesized in the model.

3.5 The CORSOR Model

The CORSOR model [5,7] is part of the U.S. NRC's current Accident Source Term Reassessment effort. CORSOR is used in conjunction with the MARCH model of core degradation [78] and an <u>ad hoc</u> model of gap release to predict both radionuclide and nonradioactive species release within the reactor vessel during a severe accident. As currently used, release predictions with CORSOR are made only when the core is intact, though it may be melting or liquefying. Once core material slumps, release calculations are usually terminated. However, in some cases, the release calculations have been continued up to the point of melt penetration of the reactor vessel.

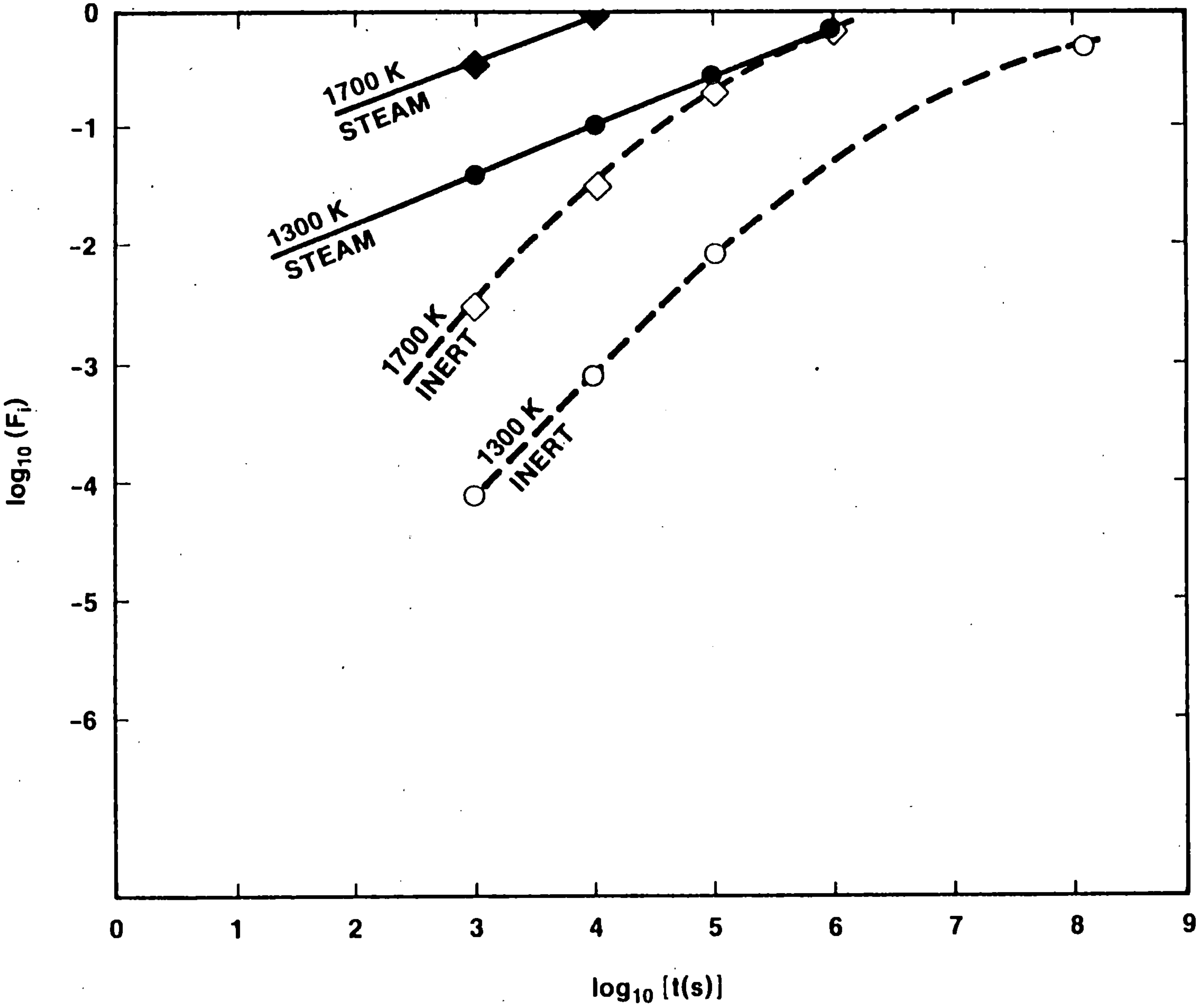

Figure 3.6. Comparison of Cubicciotti's Models of Fission Gas Release in Steam and Inert Environments.

The CORSOR model is an empirical correlation of a variety of experimentally determined release fractions. Most of the data that are the basis for the CORSOR model come from the SASCHA tests at the Kernforschungszentrum in Karlsruhe, West Germany [79-85] and the hot cell tests (HI and HT Series) done at Oak Ridge National Laboratory [86-89,91,92]. The SASCHA tests used simulated fuel doped with fission products to a level expected for fuel with a burnup of 44000 MWd/t. The samples were heated under a variety of atmospheres at pressures up to 2 bars. The Oak Ridge tests used irradiated fuel rods heated in atmospheres initially composed of steam and an inert carrier at a pressure of about 1 atmosphere.

To derive the model it was assumed that release could be described by the first-order rate expression

$$\frac{dF_i}{dt} = - K_i(T)\ F_i(T)$$

where

$K_i(T)$ = temperature-dependent release rate coefficient for the i^{th} element

$F_i(T)$ = fraction of the i^{th} element remaining in the fuel at time t.

The temperature dependence of the release rate coefficient was assumed to be:

$$K_i(T) = A_{ij} \exp(B_{ij}T)$$

where T = temperature in Celsius

A_{ij} and B_{ij} = release rate parameters for the i^{th} species in the j^{th} temperature regime.

Temperature regimes used in CORSOR are:

(1) 900 - 1400°C
(2) 1400 - 2200°C
(3) > 2200°C

The parameters in the release expression were evaluated by comparison to experimental data. These data are, in all cases, the integral release achieved after a protracted exposure of a sample to elevated temperatures. Consequently, it is necessary to integrate the release rate to make the comparison to the data. Where temperature changes are involved in the sample's history, these changes were assumed to proceed at a linear rate:

$$T = \alpha + \beta t$$

Then the release rate expression is easily integrated to:

$$\frac{F_i(0) - F_i(t)}{F_i(0)} = 1 - \exp\{(H_{ij}/G_{ij})(1 - \exp[G_{ij}t])\}$$

where $H_{ij} = A_{ij} \exp(\alpha B_{ij})$

$$G_{ij} = \beta B_{ij}$$

The unusual form of the temperature dependence of the release rate coefficient in the CORSOR model was chosen obviously to facilitate the integration during changes in temperature.

A set of parameter values for the CORSOR model is shown in Table 3.9. CORSOR is being maintained. As new experimental data are obtained, improved parametric values are derived. Consequently, the values listed in Table 3.9 may not be the latest version of the parameter set for CORSOR. One recent modification of the CORSOR model has been made to accommodate the possibility that Te released from the fuel may bind to unoxidized Zr metal and not escape the core. To accommodate this possibility, the release rate coefficient of Te is reduced by a factor of 40 whenever 5 percent or more of the Zircaloy clad has not been oxidized [94].

CORSOR is the only release model that treats all the diverse elements of interest for reactor accident analyses. It is also the only model other than the Reactor Safety Study model that treats release over the entire temperature range of interest. The close relationship between the model and experimental data also provides an attraction. By empirically correlating data, the need to identify and to describe a host of detailed mechanisms is avoided. At the same time the coupling to experimental data limits the applicability of CORSOR without extrapolation. For instance, all data that are the basis for

Table 3.9

Coefficients for the CORSOR Model

Element	1173-1673 K CORSOR		1173-1673 K Arrhenius		1673-2473 K CORSOR		1673-2473 K Arrhenius		2473 K CORSOR		2473 K Arrhenius		Single Arrhenius Coefficient	
	A_i	B_i	K_i	E_i	A_i	B_i	K_i	E_i	A_i	E_i	K_i	E_i	$K_i^o(min^{-1})$	E_i (cal/mole)
Cs	7.53×10^{-12}	0.0142	3.9356×10^{4}	55573	2.02×10^{-7}	0.00607	2.5248×10^{4}	55091	1.74×10^{-5}	0.0046	4.608×10^{5}	68640	3.504×10^{4}	55591
I	7.02×10^{-9}	0.00886	45.042	34674	2.02×10^{-7}	0.00667	2.5248×10^{4}	55091	1.74×10^{-5}	0.0046	4.608×10^{5}	68640	1.108×10^{4}	50371
Xe	7.02×10^{-9}	0.00886	45.042	34674	2.02×10^{-7}	0.00667	2.5248×10^{4}	55091	1.74×10^{-5}	0.0046	4.608×10^{5}	68640	1.108×10^{4}	50371
Kr	7.02×10^{-9}	0.00886	45.042	34674	2.02×10^{-7}	0.00667	2.5248×10^{4}	55091	1.74×10^{-5}	0.0046	4.608×10^{5}	68640	1.108×10^{4}	50371
Te	3.88×10^{-12}	0.01350	3405.7	52833	9.39×10^{-8}	0.00630	2844.2	52035	1.18×10^{-5}	0.00411	2.424×10^{4}	61328	6.085×10^{3}	54590
Sr	2.74×10^{-8}	0.0036	2.6464×10^{-4}	14089	2.78×10^{-11}	0.00853	4319.1	70453	9×10^{-7}	0.0037	217.72	55210	23.786	46717
Ba	7.50×10^{-14}	0.0144	652.626	56356	8.26×10^{-9}	0.00631	259.966	52117	1.38×10^{-5}	0.0029	51.387	43273	524.4	55476
Sb	1.9×10^{-12}	0.0128	280.085	50094	5.88×10^{-9}	0.00708	3534.8	58477	2.56×10^{-6}	0.00426	1.1502×10^{4}	63566	2602.2	56512
Ag	3.88×10^{-10}	0.0135	3405.7	52833	9.39×10^{-8}	0.00630	2844.2	52035	1.18×10^{-5}	0.00411	2.424×10^{4}	61328	6.085×10^{3}	54590
Mo	5.01×10^{-12}	0.0115	26.877	45006	5.93×10^{-8}	0.00523	29.80	43197	3.7×10^{-5}	0.0020	1.2587	29843	24.381	44057
Ru	1.36×10^{-11}	0.00768	0.004312	30056	1.36×10^{-11}	0.00768	81.422	63433	1.4×10^{-6}	0.00248	0.5827	37006	3.776	49402
Zr	6.64×10^{-12}	0.00631	6.409×10^{-5}	24695	6.64×10^{-12}	0.00631	0.209	52117	1.48×10^{-7}	0.00177	1.5164×10^{-3}	26411	0.01374	39977
UO_2	5×10^{13}	0.00768	1.585×10^{-4}	30056	5×10^{-13}	0.00768	2.9935	63433	5×10^{-13}	0.00768	$1.261\times10^{+5}$	114599	1.090	55811
Clad Zr	6.64×10^{-12}	0.00631	6.409×10^{-5}	24695	6.64×10^{-12}	0.00631	0.209	52117	1.48×10^{-7}	0.00177	1.5164×10^{-3}	26411	0.01374	39977
Clad Sn	1.9×10^{-12}	0.0128	280.085	50094	5.88×10^{-9}	0.00708	3534.8	58477	2.56×10^{-6}	0.00426	1.1502×10^{-4}	63566	2602.2	56512
Struct Fe.	6.64×10^{-12}	0.00631	6.409×10^{-7}	24695	6.646×10^{-12}	0.00631	0.00209	52117	1.48×10^{-11}	0.00177	1.516×10^{-5}	26411	0.0001374	39977

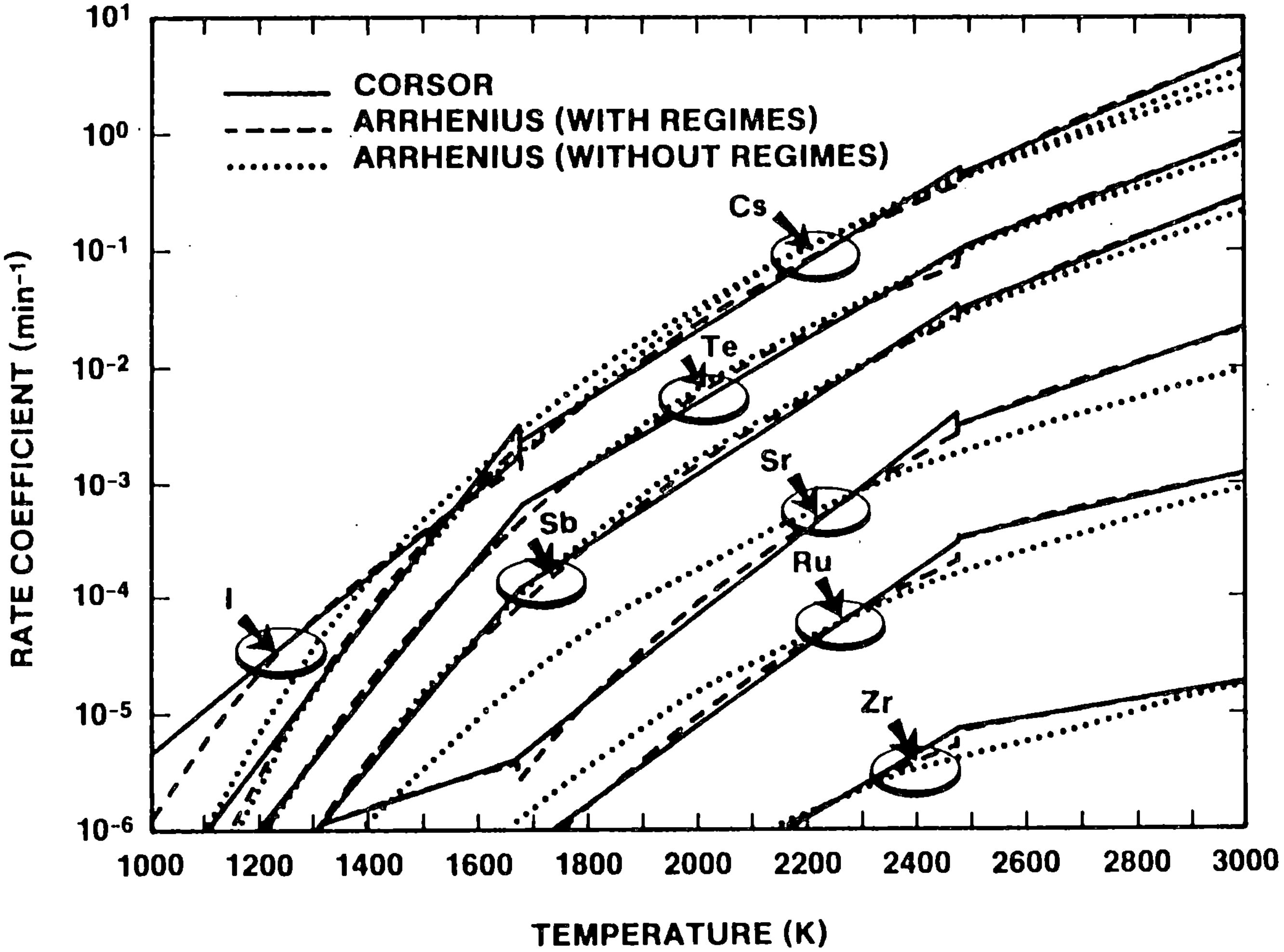

Figure 3.7. Comparison of the Temparature Dependencies of Release Rate Coefficients Calculated with the Original CORSOR Model and with Parameters For the Model Modified to Have an Arrhenius Temperature Dependence.

the reactor core is treated as independent of releases from adjacent nodes. This violates the thermodynamic principle described in Subsection III that release rates ought to be proportional to the difference between vapor concentrations at equilibrium and vapor concentrations in the ambient gas. Releases from a given node ought not to be independent of releases from adjacent nodes.

CORSOR contains no explicit representation of surface area. Minimal changes in the surface areas for release--such as those caused by grain growth, microcracking of the fuel, etc.--may be hidden within the empirical coefficients of the model. More substantive changes in surface area, such as those that accompany fuel melting or liquefaction, cannot be treated easily by altering the release coefficients. No formalism is included in the model to describe dilution of the condensed phase as clad and fuel mix and melt. In many applications to date [7], CORSOR predictions of release have been stopped when core slumping is assumed to begin. Continued application of CORSOR as molten core material begins to slump and the surface-to-volume ratio of the material changes dramatically is clearly in error.

The CORSOR model relies on a lot of physical and chemical processes being adequately represented by the assumed rate expression and empirical parameters. Unfortunately, the first-order rate expression assumed in the model is not a very flexible format for the representation of these processes. Of all the empirical descriptions of heterogeneous processes, some of which are listed in Table 3.10, the hardest to rationalize is the first-order rate description [96]. Data available to date for evaluating the CORSOR model have been integral releases measured, typically, posttest. These data do not test the validity of the first order assumption. Some examination of the first order assumption is made below.

3.6 Discussion of the First Order Assumption

The assumption that the kinetics of radionuclide release from the fuel is dependent to first order on the radionuclide concentration in the fuel is widely accepted. This acceptance arrives despite the fact first order dependence has not been demonstrated experimentally. Sophisticated fuel behavior models do not predict a first order dependence. The assumption of first order behavior is apparently an approximation made to simplify the modeling. Models involving first order composition dependence and Arrhenius-type temperature dependence are notorious for being sufficiently flexible to "fit" data involving radically different mechanisms. It is of interest then to ascertain if the assumption of first order kinetics is likely to have any appreciable effect on predictions of radionuclide release.

CORSOR were acquired at pressures of less than 2 atmospheres whereas reactor accidents can involve pressures in excess of 100 atmospheres. Unappreciable errors may arise then when CORSOR is applied to pressurized accident sequences.

Because CORSOR is the state-of-the-art model for analysis of release during core degradation including melting, it has been examined closely in the past. A variety of criticisms have been formulated.

One of the most frequently raised criticisms is the unusual temperature dependence of the CORSOR release rate coefficients. Most would prefer to see an Arrhenius temperature dependence:

$$K_i(T) = K_o(i) \exp(-E_i/RT)$$

where $K_o(i)$ and E_i are release rate parameters for the ith species and T is the absolute temperature rather than the temperature in Celsius used in CORSOR. First, it must be noted that the Arrhenius form of the temperature dependence is no more "fundamental" nor theoretically sound that the temperature dependence used now in CORSOR. Especially when applied to reactions involving solids or liquids, the Arrhenius temperature dependence is just an empirical correlation of experimental observations. To be sure, this base of experimental observations is quite large.

Second, it should be noted that the CORSOR temperature-dependence can be readily converted to have the Arrhenius form. This can be done retaining the temperature regimes defined by the model (which may indeed have some physical significance) or by fitting to a single Arrhenius expression for the entire temperature range of interest. Results of such a conversion are shown in Figure 3.7. Parametric values derived by the conversion are shown in Table 3.9. Others (127, 128) have made this conversion to the Arrhenius form and have obtained different parametric values.

The activation energies, E_i, available from the Arrhenius expression are sometimes interpreted as physically significant. For instance, Andriesse and Tanke [95] have noted the similarity of the activation energies for Cs, I, Xe, and Kr release to the activation energy for oxygen diffusion in the UO_{2+x} lattice. Such interpretations may be useful for some insights about further experiments. They ought not be the basis for extrapolation of the CORSOR model. The parameters [$K_o(i)$ and E_i] are simply too highly correlated and the data base too sparse to attach much credence to the interpretation of the E_i values.

In application, CORSOR is used on a node-by-node basis in accident analyses. However, the release from a given node in

Ta[illegible]3.10

Some Kinetic Expressions for Solid Decomposition Reactions

	Mechanism	F(f)*	G(f)**
1.	Prout Tompkins	$f(1-f)$	$\ln(f/(1-f))$
2.	Topotactic	$f^{2/3}(1-f)^{2/3}$	
3.	1D Diffusion	$1/2f$	f^2
4.	2D Diffusion	$-1/\ln(1-f)$	$(1-f)\ln(1-f) + f$
5.	3D Diffusion	$3/2((1-f)^{-1/3}-1)$	$(1-2f/3) - (1-f)^{2/3}$
6.	D3	$1.5/((1-(1-f)^{1/3})/(1-f)^{5/3})$	$((1+f)f^{1/2}-1)^2$
7.	D5		$(1/(1-f)^{1/3}-1)^2$
8.	P4	$4(1-f)(-\ln(1-f))^{3/4}$	$(-\ln(1-f))^{1/4}$
9.	P2	$2(1-f)(-\ln(1-f))^{1/2}$	$(-\ln(1-f))^{1/2}$
10.	P3	$3(1-f)(-\ln(1-f))^{2/3}$	$(-\ln(1-f))^{1/3}$
11.	P4/3	$(4/3)(1-f)(-\ln(1-f))^{1/4}$	$(-\ln(1-f))^{3/4}$
12.	P2/3	$1.5(1-f)(-\ln(1-f))^{1/3}$	$(-\ln(1-f))^{2/3}$
13.	First Order	$1-f$	$-\ln(1-f)$
14.	Second Order	$(1-f)^2$	$f/(1-f)$
15.	2D Phase Bound	$2(1-f)^{1/2}$	$1-(1-f)^{1/2}$
16.	3D Phase Bound	$3(1-f)^{2/3}$	$1-(1-f)^{1/3}$
17.	Jander Approx.	$3(1-f)^{2/3}/2(1-(1-f)^{1/3}$	$(1-(1-f)^{1/3})^2$

---

* for df/dt = fractional rate = F(f)k(T)

**for integrated rate expression G(f) = K(T,t)

Data for the release of cesium from irradiated fuel obtained in tests at Oak Ridge National Laboratory are shown in Table 3.11. These data were obtained by heating fuel in flowing steam to an arrest temperature. The sample was held at the arrest temperature for a prescribed length of time and then cooled. At least early in the cooling, temperatures fell at a near constant rate. Heating rates, arrest temperatures, and hold times for the ORNL experiments are shown in Table 3.11.

The heating and cooling ramps of the tests pose an added complexity to analysis of the release data. For some of the tests, the durations of the heating and cooling stages constitute a major portion of the time the irradiated fuel specimen was at elevated temperatures. To properly analyze these test results the release that must have occurred during heating and cooling should be recognized.

Assume the rate of radionuclide release is described by the expression:

$$\frac{df}{dt} = K_o\ F(f)\ \exp\ [-E/RT_a]$$

where f = fraction of the radionuclide that has escaped the fuel

$F(f)$ = function that describes the compositional dependence of the release rate

R = gas constant

t = time

T_a = arrest temperature (K)

K_o and E = parameters to be determined from release data.

If the temperature is fixed, the release rate is easily integrated to yield

$$\int_{F_1}^{F_2} \frac{df}{F(f)} = K_o\ \exp\ [-E/RT_a]\ (t_2 - t_1)$$

where F_1 = release that occurred before the arrest temperature, T_a, was reached

Table 3.11

Some Data From Out-of-Pile Tests of Radionuclide Release From Irradiated Fuel Rods [97]

Test	T_a (K)	Δt (min)	ß (K/s)	ß' (K/s)	Fraction of Cs Released
HI-1	1673	30	0.97	0.6	0.0204
HI-3	2273	20	2.78	1.67	0.577
HI-4	2123	20	1.93	1.58	0.319
HT-1	1598	10	9.9	12.2	0.00224
HT-2	1718	7	11.1	11.1	0.0964
HT-4	1673	0.33	18.5	11.0	0.06108

T_a = Arrest temperature.

Δt = Time the fuel was held at the arrest temperature.

ß = Rate of temperature rise during heatup of the fuel to the arrest temperature.

ß' = Rate of temperature fall during cooling at the fuel from the arrest temperature.

F_2 = release that occurred by the end of the time the sample was held at the arrest temperatures

t_1 = time the arrest temperature, T_a, was reached

t_2 = time when cooling the sample from the arrest temperature began.

To treat the case when the sample is being heated, it is convenient to transform the release kinetics expression. Assume temperature increases at the constant rate, ß, to the arrest temperature T_a. Then,

$$\frac{df}{dT} = \frac{K_o}{\beta} F(f) \exp(-E/RT_a) \; .$$

Integration of this expression yields

$$\int_{F_0}^{F_1} \frac{df}{F(f)} = \frac{K_o}{\beta} \int_{T_o}^{T_a} \exp(-E/RT)dT$$

where F_0 = release that had occurred prior to the start of the experiment which is typically assumed to be zero

T_0 = temperature of the fuel at the start of the experiment.

The integral on the right-hand side of the above equation cannot be reduced to elementary functions. A variety of approximations for this integral have been found. Coats and Redfern [98] described the most popular approximation:

$$\int_{o}^{T} \exp(-E/RT)dT = \frac{RT^2}{E} (1 - 2RT/E) \exp(-E/RT)$$

Gorbaschev [99] has suggested a somewhat more accurate approximation:

$$\int_0^T \exp(-E/RT)dT = \frac{RT^2}{(E + 2RT)} \exp(-E/RT)$$

Van Tets [100] has derived an expansion that allows the integral to be evaluated to any desired level of accuracy.

With expressions for the integral of the temperature dependence during isothermal periods and during periods of heating at a constant rate, it is possible to fit a model to the Oak Ridge data. Here three models of the composition data are considered:

1. First order dependence:

   $F(f) = 1 - f$

2. Three-dimensional phase boundary model:

   $F(f) = 3(1 - f)^{2/3}$

3. Three-dimensional diffusion model:

   $F(f) = 1.5[(1 - f)^{-1/3} - 1]^{-1}$

The first of these models is, of course, the conventional assumption. The motivation for the second model, three-dimensional phase boundary motion, is the suggestion by Cubicciotti that release is controlled by sintering. It must be emphasized, though, that this second model is not either identical to or a reformulation of Cubicciotti's model. The motivation for the third model, three-dimensional diffusion, is the formulation of release processes in the GRASS-SST code where diffusion of radionuclides is heavily emphasized. Again, this third model is not intended to be an approximation or a simplification of the GRASS-SST code.

The parameters K_0 and E were adjusted for each of the three models to get a best fit in the least squares sense to the cesium release data in Table 3.11. The quality of the fit was judged from the chi-squared statistic

$$\chi^2 = \sum_{i=1}^{N} (f_{obs} - f_{calc})^2$$

where: N = number of data points

f_{obs} = observed release fraction

f_{calc} = calculated release fraction.

Parametric values derived in this way and the values of the chi-squared statistic are shown in Table 3.12.

Table 3.12

Kinetic Parameters and the Chi-Squared Statistic for the Quality of Fit of Three Models to the Cesium Release Data

Model	$K_o(S^{-1})$	E(cal/mole)	χ^2
First order	0.855	34,617	0.073
3d phase boundary	1.732	41,513	0.0527
3d diffusion	7869	86,280	0.04297

The first thing to note about results in Table 3.12 is that both the three-dimensional phase boundary model and the three-dimensional diffusion model actually fit the data better than does the first order model. If linear statistics are actually applicable to this least-squares fitting problem, then the quality of the fits are not significantly different. To a relatively high level of confidence it can be said all three models fit the data equally well.

The next feature of the results to note is the value of the parameter E. Values of E, the activation energy, differ by only about 15 percent for the first order and the three-dimensional phase boundary models. But, the three-dimensional diffusion model yields an activation energy nearly twice that obtained with the first order model. This illustrates a very important point. The activation energy for the release of radionuclides cannot be derived from integral release data if the compositional dependence of the release rate is not known. Physical interpretation of activation energies derived from data, assuming a particular compositional dependence of the release rate, is an idle exercise. Activation energies derived in this way are simply empirical parameters and ought not to be used as a basis for extrapolating away from the underlying data base.

So far, it has been shown that alternative models will describe the release data as well as does the assumed first order model. What remains to be done is to show whether the precise form of the model will make any significant difference to release predictions. To do this, a single node of fuel in a degrading core is considered. Release from this node is treated as it is in the CORSOR model. That is, release is strictly a function of time and temperature. It is independent of flow, gas composition, pressure, or release from adjacent nodes. Two situations are considered then:

1. The node heats so that the temperature rises at a constant rate of 4 K/s to 2500 K. The temperature is then fixed at 2500 K.

2. The node temperature rises at 4 K/s to 2000 K and thereafter rises at 0.3 K/s until it reaches 2800 K.

The first of these scenarios is reminiscent of the core heatup predicted with the MARCH code [78]. The alternative scenario reflects somewhat the effects that natural circulation and the like are thought to have on core heatup [101]. Cesium releases predicted with the first order and the three-dimensional diffusion models for the two heating scenarios are shown in Figures 3.8 and 3.9. In general, the diffusion model yields higher release rates early in time and lower releases late in time than does the first order model. The maximum release rate during the MARCH-like heating scenario is nearly 10 times the maximum release rate in the heating scenario based on calculations that include natural circulation. In the natural circulation case, cesium release continues for nearly twice as long by first order kinetics than by diffusion kinetics.

3.7 Modifications of the CORSOR Model for use in the MELCOR Code

None of the models described in the preceding section are entirely satisfactory. Clearly, the GRASS-SST and FASTGRASS

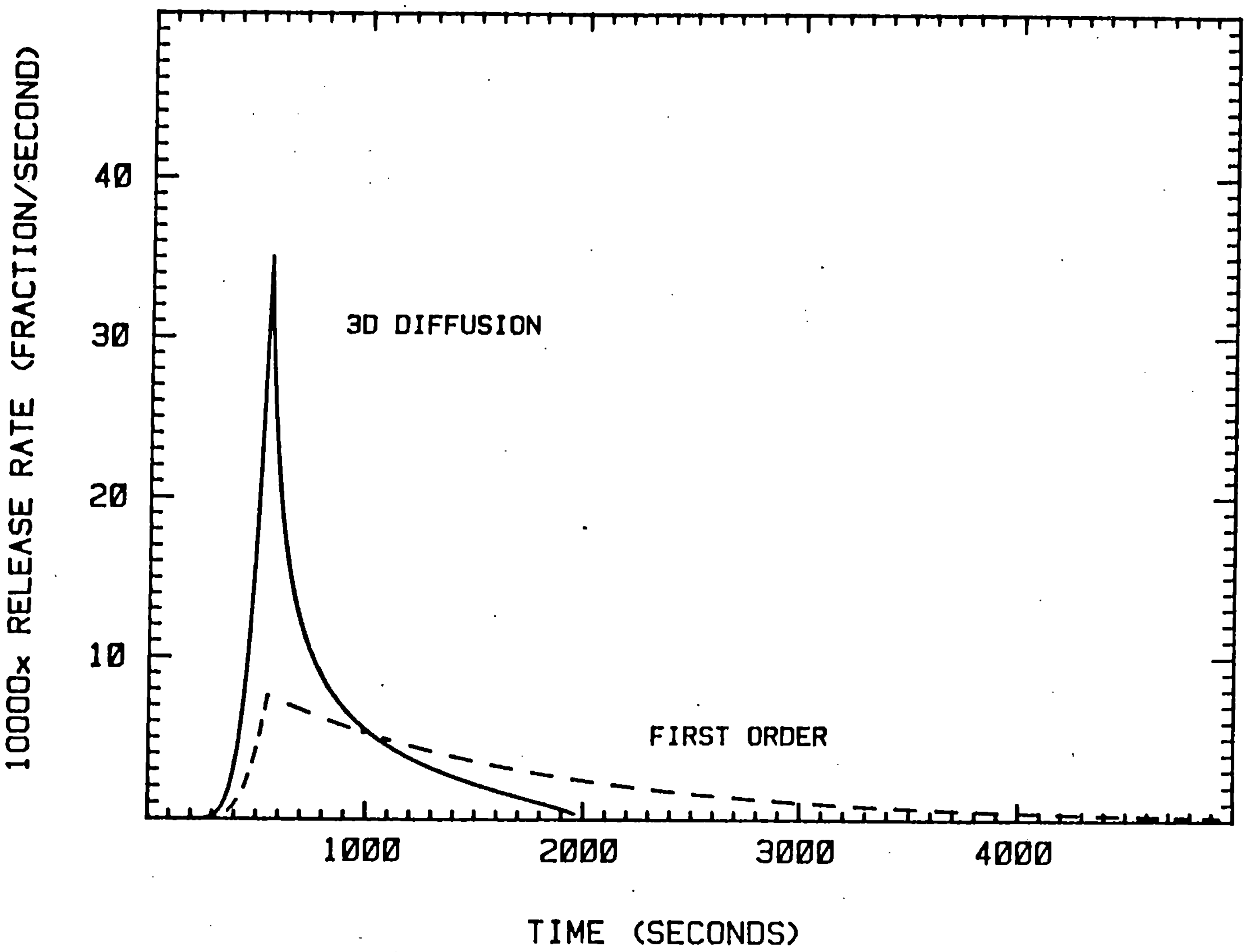

Figure 3.8. Comparison of the Predictions of Cesium Release by Two Models of the Release Kinetics Assuming the Core Heats at 4 K/s to 2500 K.

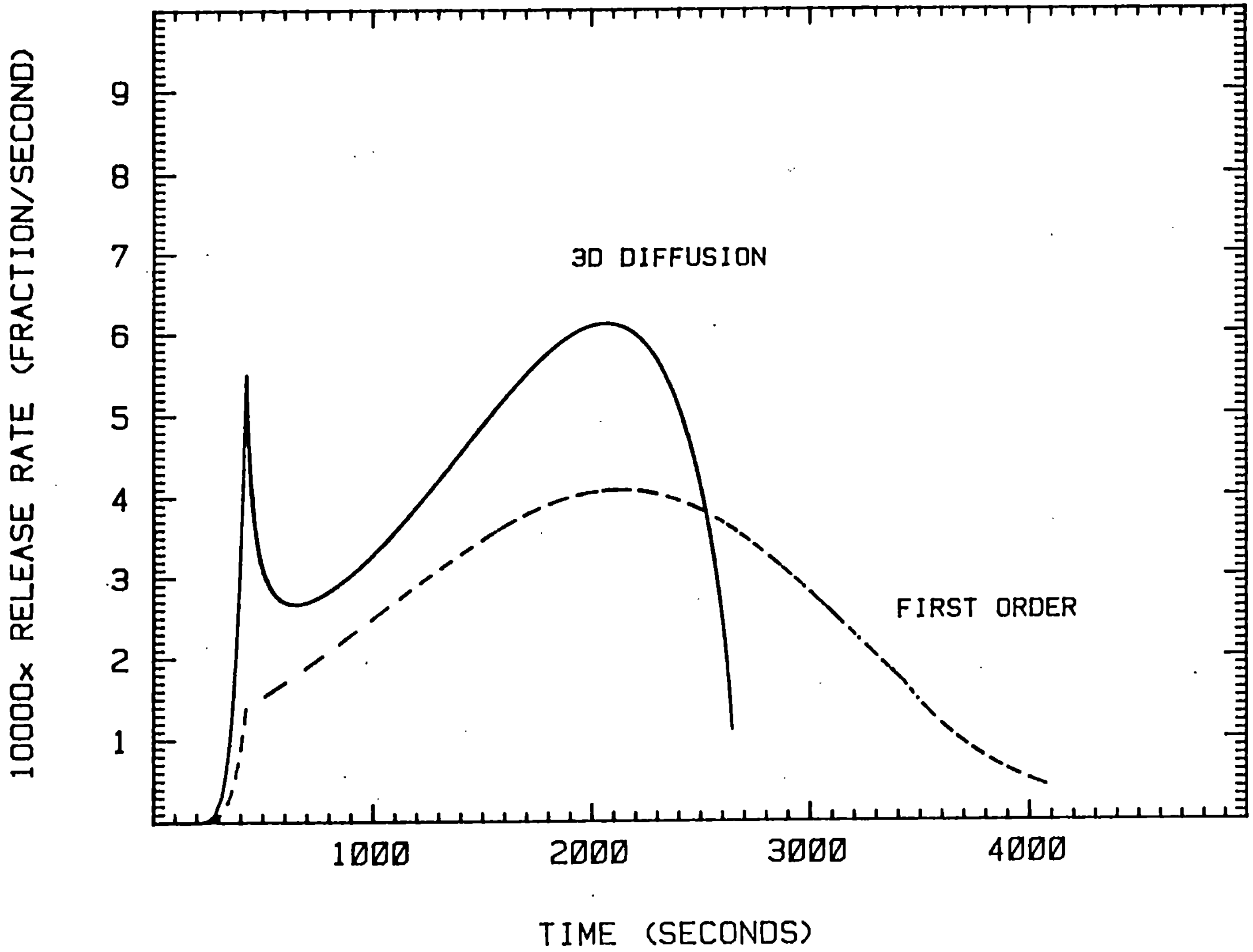

Figure 3.9. Comparison of the Predictions of Cesium Release From Two Models of the Release Kinetics Assuming the Core Heats to 2000 K at 4 K/s and to 2800 K at 0.3 K/s.

models are the most sophisticated. But, they do not treat all the radionuclides of interest and their complexity precludes them from inclusion in a systems code such as MELCOR. The CORSOR model has many attractive features, and it has already been used in reactor analyses [7]. The deficiencies and the virtues of the CORSOR model all stem from its close association with experimental data. The CORSOR model is, essentially, a correlation of experimental data. As such, the effects of many phenomena and processes have been encompassed by the empirical parameters of the model. But, the data base from which these empirical parameters are derived is quite limited. Use of the model for circumstances well removed from those that arise in the experimental data base is a concern. Unfortunately, reactor accident analyses frequently require release estimates for situations in which the CORSOR model extrapolates the data base. For instance, many of the most important reactor accidents involve core degradation within a reactor vessel pressurized to over 150 atmospheres. The CORSOR data base involves tests at pressures no greater than about 2 atmospheres. Gas flows through the core of a reactor can be quite slow--sometimes velocities as low as 1-2 cm/s are estimated. Yet, the CORSOR data base involves tests with gas flows on the order of 30 cm/s. Core degradation eventually leads to melting and slumping of the core materials. In many analyses to date, the CORSOR model has been used only up to the time the core slumps. There has been, recently, a tendency to continue to apply the CORSOR model throughout slumping and collapse of the core.

The CORSOR model can be modified to broaden its range of applicability. In the sections below this is done to take into account the effects:

1. Changes in the surface area and geometry of the core materials,
2. Dilution of the fuel by interaction with the fuel cladding, and
3. The effects of ambient pressure and flow velocities through the core.

In making these modifications, some of the conceptual difficulties with the model are corrected:

4. Release does not exceed the limit prescribed by the thermochemistry of the volatile material,
5. Release becomes reversible,
6. Release at a given location becomes dependent on releases from preceding locations along the flow pathway, and
7. The effects of fuel burn up and initial grain size are explicitly depicted in the model.

The modifications made to the CORSOR model do not include all the phenomena known or suspected to affect radionuclide release. A barrier to broader modification of the model is the limitations on size posed by the systems code. Another barrier is that it is not always clear if processes and phenomena were operative in release experiments and consequently are reflected by the CORSOR release rate expressions.

A. Modifications to Account For Surface Area Changes and Dilution During Core Degradation

The CORSOR release rate expression for the volatile element i, altered to have an Arrhenius temperature dependence but retaining the assumption of first order kinetics, is:

$$\frac{dF_i}{dt} = K_o(i)\ (1 - F_i)\ \exp\ [-E(i)/RT]$$

where F_i is the fraction of the element i that has been released by time t. Suppose attention is focused on a single node of the core which contains a volume V_O of fuel. Let the initial amount of element i present in this fuel be $N_i(0)$ moles. Then, the release rate expression can be rewritten as:

$$-\frac{1}{N_i(0)}\ \frac{dN_i(t)}{dt} = K'_o(i)\ \exp\ [-E(i)/RT]\ \frac{1}{N_i(0)}\ \frac{N_i(t)}{V}$$

where $K'_o\ (i) = V_o K_o(i)$, $N_i(t)$ is the number of moles of the element i still present in the fuel, and V is the volume of core material containing element i.

Suppose now that the free surface through which release takes place has an area ßA where A is the geometric surface area of the fuel and ß is a coefficient that relates the geometric surface area to the actual surface area. Then, the rate expression can be further modified to be:

$$-\frac{dN_i(t)}{dt} = K''_o(i)\ \exp\ [-E(i)/RT]\ \beta A\ \frac{N_i(t)}{V}$$

where $K''_o(i) = \frac{V_o K_o(i)}{\beta A_o}$, and $\frac{A_o}{V_o}$ is the geometric surface area to volume ratio of fuel used in the tests to define the CORSOR release rate coefficients.

The term $N_i(t)/V$ is the concentration of element i in the condensed phase at time t. Initially, element i is dissolved in just a volume V_o of fuel. But, as core degradation progresses, oxidized cladding can be incorporated into the fuel and this will reduce the concentration of the element i and consequently its rate of release. For typical pressurized water reactor fuel, there are 0.56 moles of zirconium clad for each mole of urania fuel. Were all of this clad to be oxidized and incorporated into the fuel, the concentrations of the volatile elements would be reduced by about 30 percent.

Incorporation of clad into the fuel will assuredly occur when the clad and fuel melt. If clad incorporation is complete then the release rate expression would have to be modified to be:

$$-\frac{dN_i(t)}{dt} = K_o''(i) \exp\left[-E(i)/RT\right] \beta A \frac{N_i(t)}{1.44\ V_o}$$

ignoring thermal expansion, the volume change of melting, and any excess volume of mixing fuel and clad.

Dilution of the fuel can also occur prior to melting. In pressurized accident sequences clad collapses onto the fuel and can chemically attack the fuel. This attack has been extensively studied recently [102]. If it is assumed that the volatile element instantaneously redistribute into the zone of fuel/clad interactions then the release rate expression becomes:

$$-\frac{dN_i(t)}{dt} = K_o''(i) \exp\left[-E(i)/RT\right] \beta A \frac{N_i(t)}{[V_o + \nu(t)]}$$

where $\frac{d\nu(t)}{dt} = 0.814 \exp\left[-20{,}785/T\right]\ \mathrm{cm}^3/\mathrm{s}$ and $\nu(0) = 0$.

The coefficient ß also presents some difficulties. Once melting has occurred, the geometric surface area and the actual surface area are the same, so $\beta = 1$.

Prior to melting, ß is more complex because the fuel is not fully dense.

In the Booth-type diffusion models, the solid fuel was hypothesized to consist of spherical grains of diameter "a."

Then

$$\beta = \frac{6}{a}\left[\frac{V_o}{A_o}\right]$$

where V_o/A_o is the fuel volume divided by the geometrical surface area. The hypothesis in the Booth models is that all surfaces of the grains contribute to the release process and that the grains are fixed in size. It is now recognized that neither of these hypotheses are correct. Only the surfaces of grains adjacent to interconnected porosity of the fuel can contribute to the release. The nature of the pore network is affected both by the past irradiation history of the fuel and the behavior of volatile species in the fuel. The FASTGRASS model involves elaborate descriptions of how porosity is affected during normal fuel operation and during the core degradation process. Here, a simpler description is developed.

Assume only a fraction E of the grain surface contributes to the release process. Assume E is a function only of fuel burnup. In examining the effects of fuel burnup on release, authors of the ANS 5.4 model concluded the release rate increased with burnup as

$$E(Bu) = E_o \exp\,[1.6\ Bu/10{,}000]$$

where Bu is the burnup in units of megawatt days per metric ton of uranium.

It is also understood now that the fuel grains will grow in an accident transient. A model by Malen used in Cubicciotti's model is

$$a(t,T) = a_o[1 + (2.92\text{x}10^4 t/a_o^2)\ \exp\,(-32100/T)]$$

where a_o is in units of micrometers.

Time scales for core degradation in a severe reactor accident are estimated typically to be on the order of 1-2 hours [7]. The Malen growth model indicates that temperatures must exceed about 2200 K for grain growth to be significant for such short times. Experiments with solid, irradiated fuel such as those listed in Table 3.11 probably did not involve significant grain growth with the possible exception of test HI-3 [86]. The rate coefficients derived from these tests for the CORSOR model do not reflect, then, any significant grain growth.

Grain growth is treated here simply as a mechanism for reducing the actual surface area available for release. Grain growth can have another effect which enhances the rate of release. As grain boundaries migrate they can sweep impurities to the void structure between the grains. In the case of reactor fuel the impurities can be, of course, volatile radionuclides. When these radionuclides reach to void network they can escape the fuel. No modifications of the CORSOR model is made here to reflect this effect.

The Malen model of grain growth is strictly applicable for urania in inert or slightly reducing circumstances. As noted in the description of Cubicciotti's model grain growth in oxidizing and especially in steam can be very rapid. Following the suggestion made by Cubicciotti, an alternative to Malen's model for grain growth in steam might be constructed assuming growth is proportional to the rate of steam oxidation of urania. Circumstances of fuel degradation in strongly oxidizing environments are rare. Consequently, no such model of the so-called "steam sintering" of UO_2 is developed here.

Incorporating grain growth and burnup effects into the CORSOR model yields the rate expression:

$$-\frac{dN_i(t)}{dt} = 2.75\text{x}10^{-3}\ K_o(i)\ \exp\left\{-\left[\frac{E(i)}{RT} + \frac{1.6\ Bu}{10{,}000}\right]\right\}\left[\frac{10}{d_o}\right]\frac{AN_i(t)}{V(t)\xi(t)}$$

where d_o = initial grain size of the fuel in µm and $\xi(t)$ is defined by:

$$\frac{d\xi(t)}{dt} = \frac{2.92\text{x}10^4}{d_o^2}\exp\left[-32{,}100/T\right]$$

with the initial condition that $\xi(0) = 1$ and T is the absolute temperature. For this incorporation it was assumed that the rate coefficients for the CORSOR model were derived from fuel with a burnup of 28,000 MWd/t and initial grain sizes of 10 µm. In fact, fuel used in tests at lower temperatures had burnups varying between 15,000 and 39,000 MWd/t. Initial grain sizes of the fuel are seldom reported.

When the fuel is liquefied the modified model becomes simpler:

$$-\frac{dN_i(t)}{dt} = \frac{K_o(i)}{4.225}\exp\left[-\frac{E(i)}{RT}\right]\frac{AN_i(t)}{V}$$

Note that the modified CORSOR model developed here has retained the original assumption of first order kinetics. This was not necessary. In fact, an entirely similar development could have been conducted for any one of the other kinetic models mentioned above such as the three-dimensional diffusion or the three-dimensional phase boundary models.

The modified model that has been derived here is still quite crude. In some cases processes and phenomena have been omitted simply because it is unclear whether these processes or phenomena are already reflected in the rate coefficients of the original CORSOR model. There are also cases where significant phenomena known not to be reflected in the coefficients have been omitted. Sweeping of radionuclides by grain boundary migration and the effects of fuel/clad interactions are areas where the model could be refined further.

Though the modified CORSOR model derived here is still crude, it can be used to demonstrate the effects on radionuclide release of fuel and accident features other than just time and temperature. The modifications to CORSOR are arrested here to demonstrate some of these effects.

In Figure 3.10 the extents of cesium release from fuel heated from 700 K at rates of 0.1, 1, and 10 K/s are shown as functions of temperature. Liquefaction and fuel/clad interactions were neglected in preparing this figure. The burnup and initial grain size were assumed to be 28,000 MWd/t and 10 μm, respectively. The effect of heating rate on release is as would be expected. As the heating rate decreases there is an opportunity for more extensive release at any given temperature.

The sensitivity of the extent of release to heating rate shown in Figure 3.10 can be used to evaluate the sensitivity of cesium release to burnup and initial grain size shown in Figures 3.11 and 3.12, respectively. For these plots heating rates were taken to be 1 K/s. From these figures, it is apparent that burnup and initial fuel grain size can have effects on release comparable to the effects of heating rate.

In Figure 3.13 cesium release from fuel during a stylized meltdown sequence is shown. Again, it is assumed the fuel is heated at 1 K/s from 700 K. However, it was assumed that once a temperature of 2200 K was reached clad began to be incorporated into the fuel. After 100 seconds at 2200 to 2300 K all the clad was assumed to have been incorporated in the fuel. Then, it was assumed that the fuel began to slump into a spherical mass. After 400 s it was assumed the fuel was part of an 80 ton spherical mass of fuel and clad. The releases predicted neglecting the fuel/clad interactions, melting, and slumping are shown in the figure for comparison. The comparison shows that fuel/clad interaction of the type hypothesized here has a small but detectable effect. Slumping of the molten fuel has a more dramatic

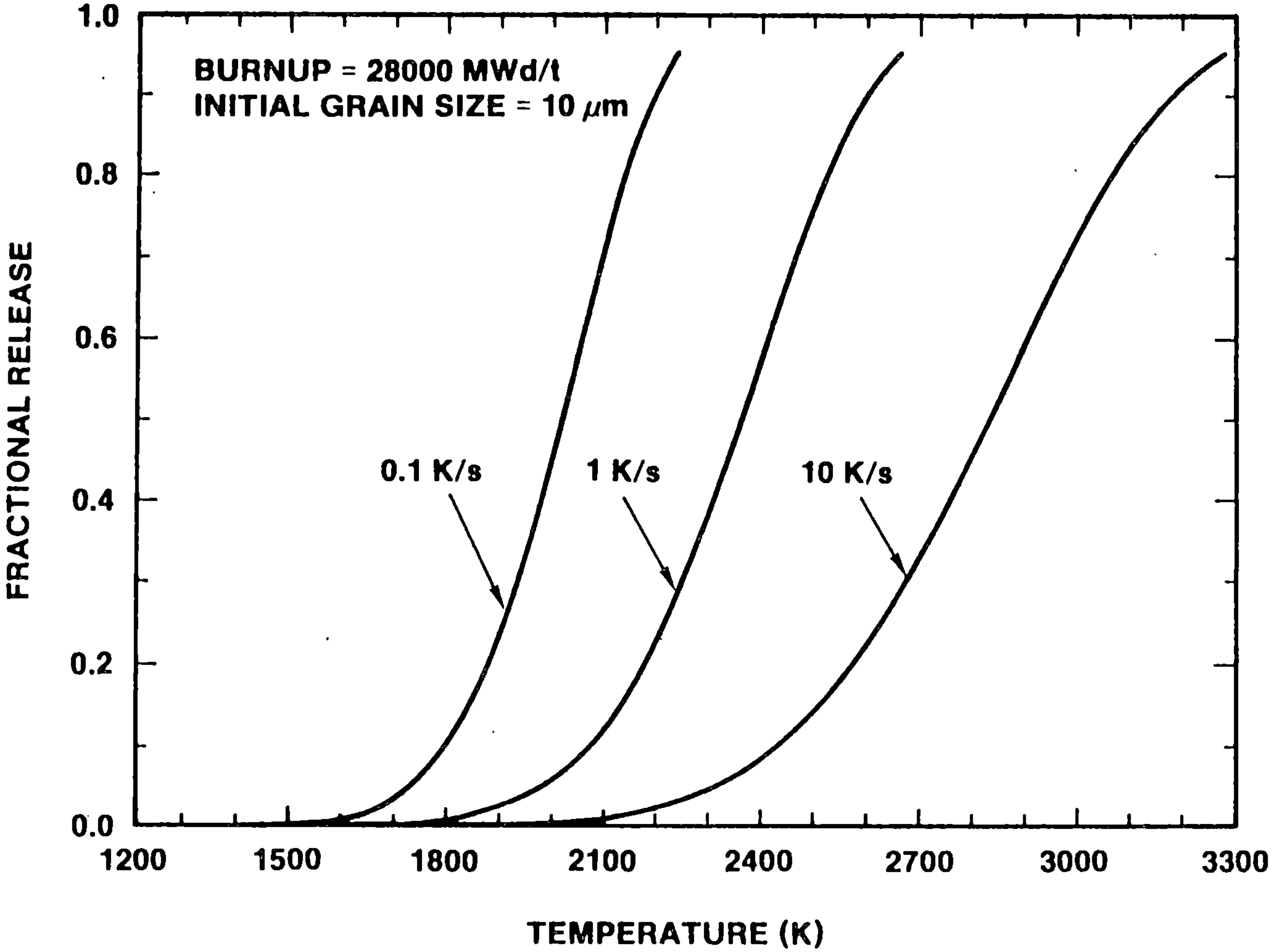

Figure 3.10. Effects of Heating Rate on the Release of Cesium.

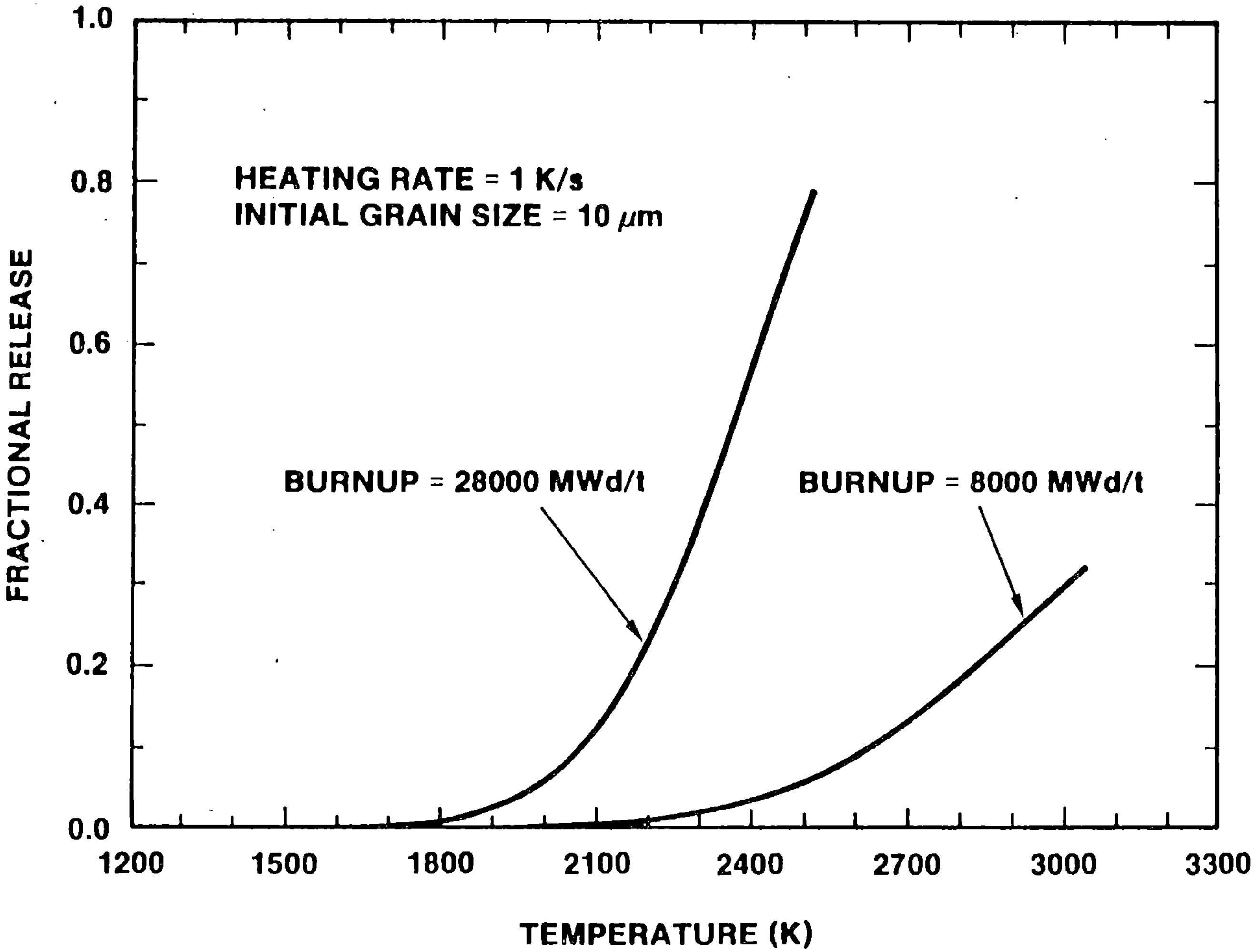

Figure 3.11. Effects of Burnup on Release of Cesium From Fuel Heated From 700 K at 1 K/s.

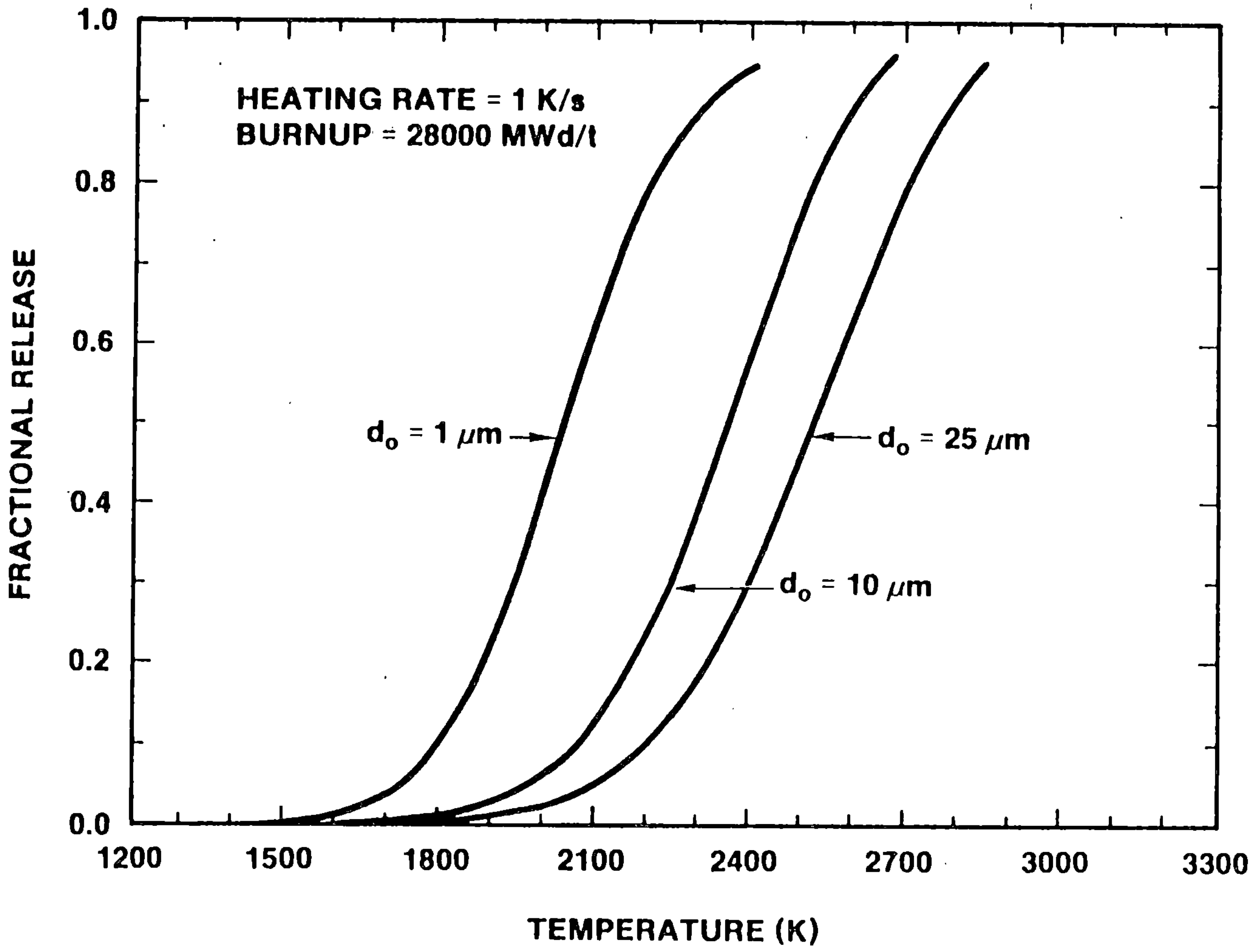

Figure 3.12. Effects of Initial Grain Size on Release of Cesium From Fuel Heated From 700 K at 1 K/s..

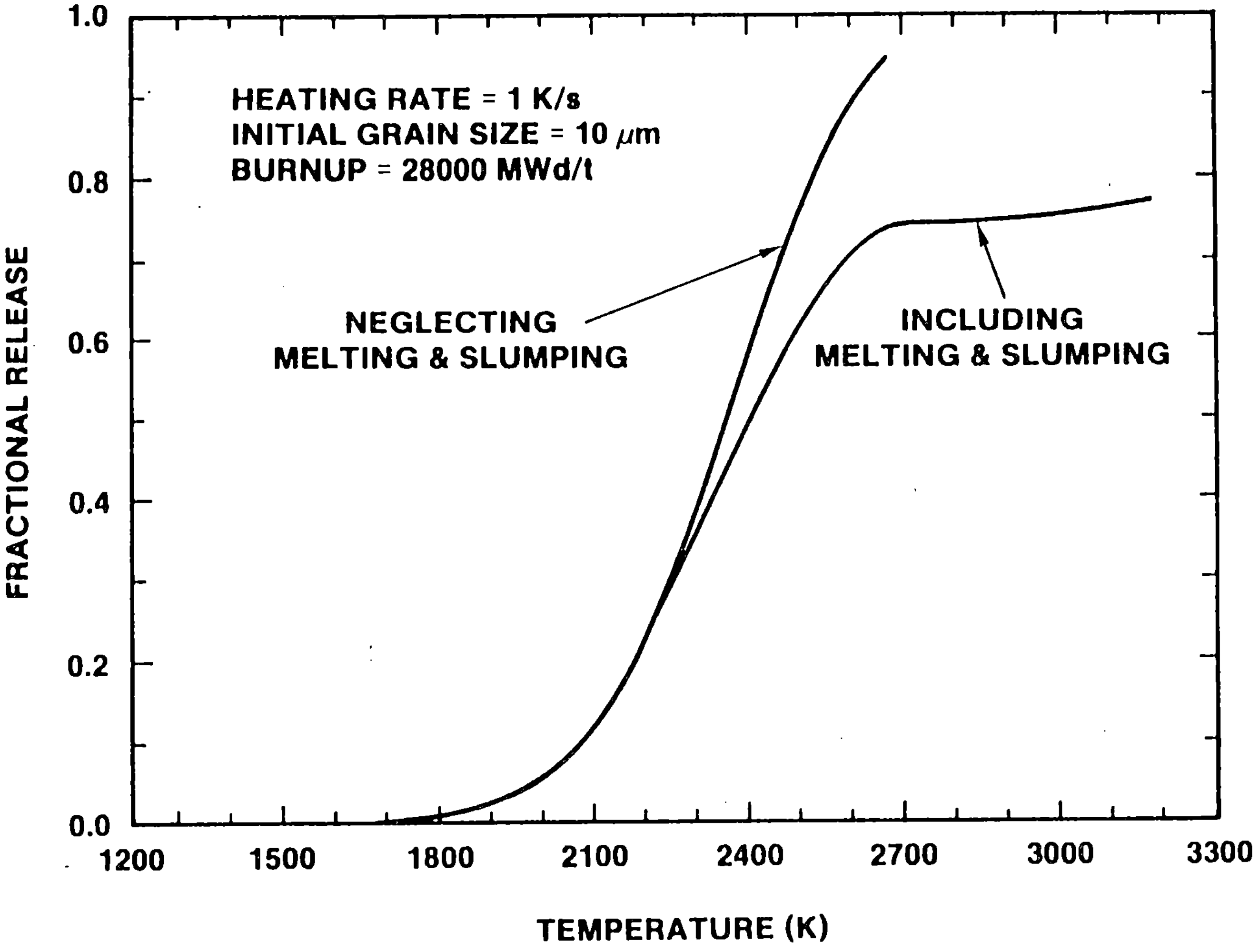

Figure 3.13. Effects of Melting and Slumping of the Fuel on Release of Cesium.

effect. The very small surface to volume ratio that develops as the molten sphere grows leads to very much reduced release rates.

B. Modifications to Account for Gas Phase Mass Transport

The description of radionuclide release from fuel has focused in the past nearly exclusively on the limitations in the condensed phase. Assuredly, this rate limitation is quite important at low temperatures and for the more volatile species such as Cs, I, and the noble gases. The exception to this concentrated attention on condensed phase mass transport is Miller's so-called "light-bulb" model in which condensed phase mass transport is assumed a negligible resistance to release and gas phase mass transport is considered a dominant resistance. The many diverse circumstances that can be hypothesized for severe reactor accidents make it apparent that neither gas phase nor condensed phase mass transport can be exclusively the source of release rate limitations. In this section, the CORSOR model is modified to account for the possibility of gas phase mass transport resistance to release.

Before delving into the modifications of the model, it is important to understand qualitatively how radionuclides will behave once they escape the fuel. Early in an accident radionuclides that emerge from the urania lattice will enter a network of interconnected porosity that provides a pathway to any gap between the fuel and the clad. The radionuclide vapor will have to traverse this pathway in order to reach a breach in the clad from which it can escape into the bulk flow of gas through the reactor core. If the clad has "ballooned" due to internal pressurization during an accident, a substantive gap will exist between the fuel and the clad. In this case, the primary resistances to release of the radionuclide once it has escaped the urania lattice are:

1. Transport through the pore network to the fuel/clad gap, and
2. Possible chromatographic resistance brought on by reaction with the clad and revaporization within the fuel/clad gap.

The low temperature experiments with clad, irradiated fuel that provided the CORSOR release rate coefficients examined this circumstance. That is, there were relative large gaps between the fuel and the clad in these tests. Thus, the CORSOR release rate coefficients fully reflect resistances to radionuclide release in these circumstances.

In a pressurized reactor accident sequence, the clad need not "balloon." Rather, as high temperatures are reached the high, external, pressures could cause the clad to collapse onto the fuel. A very narrow fuel/clad gap would then exist. The gap would be further complicated as chemical interactions between the clad and fuel progress. The nature of resistances to radionuclide release in this circumstance would be qualitatively similar to those arising when the clad balloons. However, the distance a vapor must travel through narrow pore structures to reach a breach in the cladding might be longer. On the other hand, because the clad and the fuel are in intimate contact, and the clad and fuel chemically interact, there may be more frequent breaches in the clad through which radionuclides can escape.

As temperatures rise further, the interaction of the fuel and the clad lead to liquid formation. At this point the clad no longer constitutes a major barrier to release. Experimental studies of fuel rod melting have been conducted extensively by Hagan et al. [105]. If oxidation of the clad by steam has been extensive, there is a tendency for liquid to flow downward in the annular space between the solid fuel and a ZrO_2 shell. Even so, there are frequent breaks in the shell through which radionuclides could escape. If clad oxidation is not extensive, then what little ZrO_2 has been formed dissolves in the liquefied fuel/clad mixture and the melting clad provides little resistance to release.

Once a radionuclide migrates to a free surface adjacent to bulk flow through the core, there is still a resistance to escape that must be negotiated. The radionuclide vapor must traverse a boundary layer between the free surface and the bulk flow.

The gas phase mass transport resistance posed to vaporized radionuclides while the clad is present is complex. Some sort of a model of this process could be formulated assuming, say, that transport through the flow passages was by Knudsen diffusion. Mean pore diameters and transport distances could be hypothesized and an additional release resistance incorporated into the model. These effects will be most important only for the more volatile radionuclides. Vaporization of species such as Sr, La, and the like will not be extensive until liquefaction begins and the resistance to release posed by the clad and the clad/fuel gap has disappeared.

The resistance to release posed by the boundary layer between the condensed phase and the bulk flow through the reactor core is pandemic. It is operative throughout the accident and affects the release of all radionuclides.

Here the complex resistance to release that arises because of the clad is neglected. It is assumed that limitations on the release that arise from such resistances are adequately reflected by the CORSOR release rate coefficients. This assumption is open to doubt simply because the data base used to develop the release rate coefficients does not include the diversity of circumstances that can be hypothesized to arise in reactor accidents. Relief from this assumption is yet another area where the model developed here could be refined further.

The modification of CORSOR to account for gas phase mass transport will be confined here to the examination of the effects of the boundary layer between bulk flow and the condensed phase.

The rate expression for release from the condensed phase derived in the previous section can be written in the form

$$-\frac{dN_i(t)}{dt} = AK(i) \exp\,[-E(i)/RT]\,\frac{dC_i(t)}{dx}$$

where K(i) is a complex function of burnup, grain size, and physical state of the condensed phase and $dC_i(t)/dx$ is the gradient in volatile element concentration in the condensed phase. This gradient can be expressed as:

$$\frac{dC_i(t)}{dx} = \frac{C_i(t) - C_i(\text{surface})}{\delta}$$

where $C_i(t)$ = bulk concentration of the volatile element

$C_i(\text{surface})$ = concentration of the volatile element at the condensed phase surface

δ = length scale.

When resistances other than condensed phase mass transport are neglected, $C_i(\text{surface})$ is assumed to be zero. When these other resistances are to be considered, allowance for a finite surface concentration must be made and the release rate expression becomes:

$$-\frac{dN_i(t)}{dt} = AK'(i) \exp\,[-E(i)/RT]\,[C_i(t) - C_i(\text{surface})]$$

Examination of the other resistances to release must provide an estimate of the unknown surface concentration.

Suppose now that a surface of area A' in a node is exposed to the bulk flow of gases through the core. A general expression for the rate at which a volatile element passes through the exposed surface into the bulk flow is given by:

$$-\frac{dN_i(t)}{dt} = \frac{A'k_g}{RT}[P_i(\text{surface}) - P_i(\text{bulk})]$$

where P_i(surface) = vapor pressure at the surface

P_i(bulk) = partial pressure in the bulk gas phase

k_g = gas phase mass transport coefficient.

If a quasi-steady state has been reached then the rate at which element i is released from the condensed phase must equal the rate at which it passes through the area exposed to the flow. Thus,

$$-\frac{dN_i(t)}{dt} = AK'(i) \exp[-E(i)/RT][C_i(t) - C_i(\text{surface})]$$

$$= \frac{A'k_g}{RT}[P_i(\text{surface}) - P_i(\text{bulk})]$$

To progress in the analysis it is necessary to relate the surface concentration of element i to the partial pressure P_i(surface). It was unnecessary in the development of the condensed phase mass transport equation to specify the chemical form of the migrating species. Specification of the chemical form of the vapor species can be deferred, but not avoided entirely, by recognizing that regardless of the complexity of the chemistry the surface partial pressure can be specified as:

$$P_i(\text{surface}) = \frac{C_i(\text{surface})}{\rho_{\text{molar}}} P_i^o(\text{eq})$$

where ρ_{molar} = moles of condensed species per cubic centimeter of condensed phase

P_i^o(eq) = equilibrium partial pressure that would develop over the pure migrating species i under the ambient conditions.

Similarly, an equilibrium partial pressure can be associated with the concentration of element i in the condensed phase:

$$P_i(t) = \frac{C_i(t)}{\rho_{molar}} P_i^o(eq)$$

Then,

$$-\frac{dN_i(t)}{dt} = \frac{AK(i)\ \exp\ [-E(i)/RT]}{P_i^o(eq)}\ \rho_{molar}\ [P_i(t) - P_i(surface)]$$

$$= \frac{A'k_g}{RT}\ [P_i(surface) - P_i(bulk)]$$

Eliminating the unknown partial pressure $P_i(surface)$ yields:

$$-\frac{dN_i(t)}{dt}\left[\frac{1}{AK'(i)\ \exp\ [-E(i)/RT]\ \rho_{molar}} + \frac{RT}{A'k_g P_i^o(eq)}\right]$$

$$= \left[\frac{P_i(t) - P_i(bulk)}{P_i^o(eq)}\right]$$

or,

$$-\frac{dN_i(t)}{dt} = K_{Total}\left[\frac{N_i(t)}{V\rho_{molar}} - \frac{P_i(bulk)}{P_i^o(eq)}\right]$$

where $$\frac{1}{K_{Total}} = \frac{1}{AK'(i)\ \exp\ [-E(i)/RT]\ \rho_{molar}} + \frac{RT}{A'k_g P_i^o(eq)}$$

or,

$$\frac{dF_i(t)}{dt} = \frac{K_{Total}}{V\rho_{molar}}\left[1 - F_i(t) - \frac{P_i(bulk)}{P_i(o)}\right]$$

where $P_i(o)$ is the partial pressure that would develop over the condensed phase had no release occurred.

Inspection of this revised release model shows that several important effects not available in the original CORSOR model have been introduced. First, the release of volatiles is now reversible. That is, if the vapor concentration in the bulk gas phase is sufficiently high, the flux of element i is back into the condensed phase. The release of element i from a particular node in the core is dependent now on the extent of release from nodes that precede it along the flow path. Chemistry of the element i has been introduced albeit formally at this point. This chemistry will have to be made explicit before the rate expression can be applied. Once the chemistry is explicit, it will be possible to recognize changes that occur in the chemical conditions along the flow pathway. Because the chemistry is included, the revised release model assures that vapor phase concentrations do not exceed the thermochemical limit appropriate for the ambient temperature and chemical conditions.

To apply the model for release developed here, it is necessary to have values of the mass transport coefficient, k_g. It is possible, in principle, to determine k_g in a totally theoretical manner. But, the exercise can be enormously complex. Solution of the equations can be done usually in only a very approximate manner. Consequently, correlations of experimental data are an attractive source of information on the mass transport coefficient. Such correlations are not universal in nature. Separate correlations have been developed for various flow and geometry configurations.

The patterns of gas flow through a degrading reactor core are poorly known. It is likely that the geometry of the core as it degrades evolves in a very complicated fashion. Details of this evolution may not be, however, exceptionally important for the analysis of radionuclide release. Here a stylized description of the degradation process is outlined. This description emphasizes "limiting" core geometries that have at least a transient existence during the degradation process. Though these "limiting" geometries and gas flows may be complicated in detail, they can be idealized to be simple forms for which correlations of experimental data are available.

When the core degradation process begins, the fuel consists of vertical arrays of rods. These rods may be distorted somewhat as a result of clad ballooning and rupture. The simplest description of gas flow through the core during this early stage of an accident is flow parallel to the rod axes. This type of flow has been enforced in out-of-pile release experiments with irradiated fuel rods [86,88-93]. This is also the flow pattern sought in recent in-pile, core degradation experiments [87]. It is the flow pattern allowed by the MARCH model [7] of core degradation. It is probably a particularly accurate description of flow during boil-off of coolant from the core.

Once most of the coolant has boiled from the core, the flux of steam into the core drops sharply [103]. Heatup of the fuel means that a significant temperature difference exists between the core and structures above the core. This temperature difference will induce natural circulation of gases through the core [104]. In pressurized water reactors, the open lattice of fuel will be exposed in some regions to a flow perpendicular to the rod axes. Fuel in boiling water reactors is unlikely to be exposed to such perpendicular flows since fuel bundles are shielded in channel boxes.

As the degradation process proceeds, cladding will interact chemically with the fuel and liquid will be formed. Here, it is supposed that liquefied clad and fuel drains down the rod. This draining has been observed in out-of-pile experiments [105] and is described in greater detail elsewhere [103,106]. The flow is not necessarily continuous. Rather, liquid forms first in an especially warm region, flows downward until it freezes temporarily. It then remelts, as does some of the underlying material of the rod. This combined mass then flows down along the rod until it is again frozen.

Not all the fuel in a particular location need be liquefied as a result of interaction with the clad. That which is not may remain in place until much higher temperatures are reached. It is more likely though that once the cladding is lost, the fuel that is not liquefied will collapse into a debris bed composed of coarse particles. Temperatures in this debris bed may become high enough that the bed material melts and flows down through the core.

As more liquefied material forms, the individual streams of melt flowing down the rods coalesce into a single mass of liquid. This mass is characterized here as a sphere though it is undoubtedly a far more complex shape. Initially, the flow pattern around a sphere can be used to determine the mass transport coefficient. As the mass becomes a significant fraction of the core mass the geometry might better be characterized as one consisting of a downward facing surface and an upward facing surface. At low flows, the mass transport in the gas phase from these surfaces is determined by natural convection.

In summary, the stylized description of core degradation presented above requires that mass transport coefficients be known for the following geometries and flow patterns:

Longitudinal flow parallel to the axes of the rods with and without discontinuities created by clad ballooning or fuel liquefaction.

1. Transverse flow perpendicular to the axes of the rods.

2. Flow around a spherical mass.

3. Flow through a debris bed.

4. Natural convection flow from a downward facing surface and from an upward facing surface.

Experimental data are available in greater abundance for convective heat transport than for convective mass transport. A conventional approach is to draw an analogy between heat and mass transport. Then correlations of data for heat transfer can be used to estimate the mass transfer coefficients.

The mass transfer coefficients for the geometries and flows that arise in the simplified description of core degradation presented above are summarized in Table 3.13. The bases for these values are discussed below.

Flow Around a Sphere. Heat and mass transport around a sphere has been much studied. The correlations shown in Table 3.13 provide values averaged over the surface of a sphere. As such, the correlations are most useful when the sphere is small. As the sphere diameter increases, local variations in the mass transport become important. Schutz [109] has studied the local mass transport under natural convection conditions. He finds the minimum mass transport occurs at an angle of about 135° to the direction of the flow. Mass transport at angles less than 90° and larger than 140° is relatively insensitive to the angle. Mass transport coefficients from surfaces bounded by angles greater than 140° can be as much as two times the mass transport from surfaces bounded by an angle of 90°.

The natural convection regime of flow can be characterized in greater detail than shown in the table:

$$N_{Sh}(\text{natural convection}) = 2 + K(N_{Gr}N_{Sc})^{1/4}$$

$K = 0.3$ for $0 < N_{Gr}N_{Sc} < 50$

$K = 0.4$ for $50 < N_{Gr}N_{Sc} < 200$

$K = 0.5$ for $200 < N_{Gr}N_{Sc} < 10^6$

$K = 0.6$ for $10^6 < N_{Gr}N_{Sc} < 10^8$

Table 3.13

Mass Transfer Coefficients for Configurations That Develop During Core Degradation

Geometry, Flow, and References	Sherwood Number	Limitations
Flow around a sphere [107,108]	$Sh = 2 + K(N_{Gr}N_{Sc})^b + 0.347(N_{Re}N_{Sc}^{1/2})^{0.62}$	$N_{Gr}N_{Sc} < 10^8$, $K = 0.569$, $b = 0.25$
	$Sh = k_g d/D$	$N_{Gr}N_{Sc} > 10^8$, $K = 0.0254\ N_{Sc}^{0.244}$, $b = 0.5$
	d = diameter of sphere	
	$N_{Sc} = \mu/\rho D_{AB}$	
	μ = gas viscosity	
	ρ = gas density	
	$N_{Re} = dv\rho/\mu$	
	v = gas velocity	
	$N_{Gr} = \frac{g\rho^2 d^3}{\mu^2}\frac{\Delta T}{T}$	
Natural convection from a downward facing surface	$Sh = 0.27(N_{Gr}N_{Sc})^{1/4}$	$3\times10^5 < N_{Gr} < 3\times10^{10}$
	$N_{Gr} = \frac{g\rho^2 L^3}{{}^2\mu}\frac{\Delta T}{T}$	
	L = characteristic length of surface	

Table 3.13 (Continued)

Geometry, Flow, and References	Sherwood Number	Limitations
Natural convection from an upward facing surface	$Sh = 0.54(N_{Sc}N_{Gr})^{1/4}$	$10^5<N_{Gr}<7x10^7$
	$Sh = 0.12(N_{Sc}N_{Gr})^{1/3}$	$N_{Gr}>7x10^7$
	$N_{Gr} = \frac{g\rho^2L^3}{\mu^2}\frac{\Delta T}{T}$	
	L = characteristic length of surface	
Flow parallel to rod axis [114,115,118,119]	$Sh = Nu(laminar) + A\ N_{Re}^{0.8}\ N_{Sc}^{1/3}$	
	$Nu(laminar) = [7.55x - 6.3x^{-b}]\ [1 - 3.6x/(3.2+x^{20})]$	
	$b = 17x(x - 0.81)$	
	$x = S/D$	
	$A = [0.042x - 0.024][1.103x^2 - 1]^{-0.2}$	triangular arrays
	$A = [0.026x - 0.006][1.273x^2 - 1]^{-0.2}$	square arrays
	The length dimension in Sh and N_{Re} is the rod diameter	

Table 3.13 (Continued)

Geometry, Flow, and References	Sherwood Number	Limitations
Effects of a discontinuity in flow [121]	$\frac{Sh}{Sh(*)} = \min \left\{ N_{max},\ K\left[\frac{y}{D_h}\,\frac{1}{N_{Re}N_{Pr}}\right]^m \right\}$	N_{max} defined in text
	$K = 4.42 - 1.05\ \log_{10}(N_{Re}) - 2.25\varepsilon$ $m = -\ 0.001855\ N_{Re}\ \varepsilon^2$	$N_{Re}<3000$
	$K = 0.426 + 0.113\ \log_{10}(N_{Re}) - 2.25\varepsilon$ $K > 0.895 - 2.25\varepsilon$ $m = -\ 30.34\ N_{Re}^{-0.253}\ \varepsilon^2$ $m > -\ 4\varepsilon^2$	$N_{Re}>3000$ and smooth tubes
	$K = \min \left\{ \begin{array}{l} -\ 0.344 + 0.35\ \log_{10}(N_{Re}) - 2.25\varepsilon \\ \text{and} \\ -\ 1.8478 + 1.2466\ \log_{10}(N_{Re}) \\ -\ 0.1298\ [\log_{10}(N_{Re}0)]^2 - 2.25\varepsilon \end{array} \right.$ $K \geq 0.885 - 2.25\varepsilon$ $m = -\ (1 + 4.9\text{x}10^4\ N_{Re}^{-1.2})\varepsilon^2$ $m \geq -\ 4\varepsilon^2$	$N_{Re}>3000$ and rough tubes

Table 3.13 (Concluded)

Geometry, Flow, and References	Sherwood Number	Limitations
	where $Sh(*)$ = Sherwood number for undisturbed flow ε = blockage factor which is the fraction of the flow occluded by rods and the obstacle y = distance from the front edge of the flow discontinuity along the rod	
Flow through a debris bed [122]	$Sh = \frac{k_g d_p}{D_{AB}} = \frac{2}{1 - (1-\varepsilon)^{1/3}} + \frac{2}{3\varepsilon} N_{Re}^{n} N_{Sc}^{1/3}$ d_ρ = particle diameter ε = porosity of the bed $\frac{2-n}{3n-1} = 4.65 N_{Re}^{-0.28}$	$N_{Re} > 80$ and isothermal debris beds
Flow perpendicular to the axes of the rods	$Sh = a + (0.5 N_{Re}^{1/2} + 0.2 N_{Re}^{2/3}) N_{Sc}^{1/3}$ $a = 2/[\ell n\{1 + 2/[0.468(N_{Gr}N_{Sc})^{1/4}]\}]$ $N_{Gr} = \frac{g\rho^2 D^3 \Delta T}{\mu^2 T}$ D = diameter of a rod $N_{Re} = \frac{Dv\rho}{\mu}$	

Natural Convection From Upward and Downward Facing Surfaces. The correlations shown in Table 3.13 are actually for natural convection from upward and downward facing squares. The correlations were developed from correlations of natural convection heat transfer by replacing the dimensionless Prandtl number ($C_p\mu/k$) with the dimensionless Schmidt number ($\mu/\rho D_{AB}$). Density differences that drive natural convection are assumed the result of temperature differences between the bulk gas and the condensed phase surface temperature with no contribution from the vaporizing material.

Based on Schutz's data for natural convection from a sphere the length scales in the correlations can be taken to be:

$$L(\text{upward}) = 0.7\ D(\text{equivalent})$$

$$L(\text{downward}) = 1.6\ D(\text{equivalent})$$

where D(equivalent) is the diameter of the sphere containing an equivalent amount of mass as the body in question.

Flow Perpendicular to the Rod Axes. The correlation in Table 13 for mass transfer during flow perpendicular to the axes of the rods was developed from a correlation proposed by Whitaker for heat transfer from staggered tube arrays [110]. The transformation to mass transfer was accomplished by replacing the Prandtl number and Nusselt numbers in Whitaker's correlation with the Schmidt and Sherwood numbers, respectively. A natural convection correlation appropriate for a single cylinder was then added to the expression. Again, density differences that drive natural convection were assumed to be the result of temperature differences between the bulk gas phase and the condensed phase surface with no contribution from the changing composition of the gas.

Whitaker's correlation was developed to comply with the theoretical condition that in the absence of natural convection the convective heat transfer from a single cylinder should go to zero as velocity goes to zero. Correlations of experimental data at low flow rates such as that obtained by Collis and Williams [111]:

$$Nu = 0.24 + 0.56\ N_{Re}^{0.45}$$

for air and $0.02 < N_{Re} < 44$ support this condition.

An alternate correlation found from actual mass transport studies of flow perpendicular to the axes of tubes is [112]:

$$Sh = 0.169\ [1-0.5\ \exp(-0.69\ N)]\ N_{Re}^{0.68}\ N_{Sc}^{0.33}$$

where N is the number of rows of tubes.

Whitaker's correlation does not describe data for in-line tube arrays as well as data for staggered tube arrays.

Flow Parallel to the Rod Axes. Investigations of flow parallel to the axes of the rods have concentrated on situations in which the Reynolds number is high. Weisman [113] derived the following correlations for water flow through bundles:

$$Nu = C\ N_{Re}^{0.8}\ Pr^{1/3}$$

where $C = 0.042\ S/D - 0.024$ for square arrays with $1.1 < S/D < 1.3$

$C = 0.026\ S/D - 0.006$ for triangular arrays with $1.1 < S/D < 1.5$

S = center-to-center rod separation

D = rod diameter.

Dingee and Chastain [114] found adequate correlation of data for water flow through various types of arrays with a Dittus-Boelter type equation:

$$Nu = 0.023\ N_{Re}^{0.8}\ N_{Pr}^{1/3}$$

in which the dimension for the Nusselt and Reynolds numbers is the equivalent hydraulic diameter.

Sparrow et al. [115] have analyzed the problem for triangular arrays and laminar flows. They present a nomograph for the average Nusselt number which can be approximated by the expressions:

$$Nu = 3.6 + 16.25(S/D) \quad \text{for } 1 < S/D \leq 1.4$$

$$Nu = 10 + 9.23(S/D) \quad \text{for } S/D > 1.4$$

The dimension for the Nusselt number is the rod diameter in this case.

Gimble et al. [120] have examined parallel flow in a configuration proposed for early nuclear power plant fuel. Their experimental data were obtained with air and for Reynolds numbers between 8000 and 30,000. Heat transfer data were correlated by the expression

$$Nu = (0.040 + 5.96x^{-1/2})N_{Re}^{1-\beta}\ N_{Pr}$$

where $\beta = \dfrac{0.00104 + 0.347/x}{0.00434 + x}$

$x = S/D$

The length scale for the dimensionless parameters is the rod diameter.

There have been several studies of parallel flow for liquid metals. Dwyer [116,117] presents the correlations:

$$Nu = 6.66 + 3.126x + 1.184x^2 + 0.0155\ (\bar{\psi}RePr)^{0.86}$$

for $100 < RePr < 10^4$

$$Nu = 7 + 3.8x^{1.52} + 0.027\ (\bar{\psi}RePr)^{0.8}\ x^{0.27}$$

for $0 < RePr < 10^5$ and where

$x = S/D$

$$\bar{\psi} = 1 - \frac{1.82}{Pr\ (\varepsilon_M/V)_{max}^{\ 1.4}}$$

and $(\varepsilon_M/V)_{max}$ values are presented in a graph. Dwyer recommends for the low turbulence regime the correlation for molecular conduction:

$$Nu = -2.79 + 3.97x + 1.025x^2 + 3.12 \log_{10}N_{Re} - 0.265 (\log_{10}N_{Re})^2$$

Ushakov et al. [118] cite the following correlations:

$$Nu = Nu(laminar) + \frac{3.67}{90x^2} (N_{Re}N_{Pr})^a$$

where $a = 0.56 + 0.19x$

$$Nu(laminar) = 7.55x - 6.3x^{-b}$$

$$b = 17x (x - 0.81)$$

$$x > 1.3$$

and

$$Nu = Nu_o + \beta N_{Re}^{0.87} N_{Pr}^m$$

where $m = 0.4 + (2 + 4N_{Pr})^{-1}$

$$\beta = 0.0083\{1-\exp[-10.4(x-1)-0.1 \alpha]\} + 0.008(x - 1)$$

$$\alpha = 1 + 4/(1 + 10N_{Pr})$$

for $0 \leq Pr < 10$ and $10^4 < N_{Re} < 10^5$. Values of Nu_o are reported to be tabulated, but this author could not retrieve the document. Some values Nu_o from Reference 118 are:

x	Nu_o
1.5	14
1.4	13
1.32	12

1.15	8.2
1.113	8
1.01	1.7

The recommended correlation for the Sherwood number is derived from the correlation by Ushakov et al. [118] of Nu(laminar) and Weisman's [113] description of turbulent flow. Values of the Nusselt number for laminar conditions match well tabulated values in Reference 119.

Effects of Discontinuities. In the stylized description of core degradation outlined above, melt flowing down a rod would freeze temporarily on the rod. This introduces a discontinuity in an otherwise smooth rod. Discontinuities could also be created by clad ballooning and rupture. The mass transport and heat transport consequences of melt formation and freezing have apparently not been investigated. It is readily apparent that the efficiency of mass and heat transport should go up when flow encounters a discontinuity such as melt frozen on a rod.

Hassan and Rehme [121] have investigated the effects on heat transfer caused by a grid spacer. They found that the increase in the local Nusselt number could be correlated in terms of the Reynolds number and some geometric factors. The "blockage factor" created by an obstacle is an important geometrical quantity in the correlation. This blockage factor is just the fraction of the flow area occluded by the rods and the obstacle.

The Hassan and Rehme model asserts that about one hydraulic diameter ahead of a blockage the local Nusselt number begins to rise to a maximum. The rise rate is given by

$$\frac{\mathrm{Nu(y)}}{\mathrm{Nu(undisturbed)}} = 1 + \frac{\left[\frac{\mathrm{Nu(max)}}{\mathrm{Nu(undisturbed)}}\right]\left[\frac{y}{D_h} + 1\right]}{A + 1}$$

where D_h = hydraulic diameter

y = distance from the leading edge of the obstacle

$A = L_A/2D_h$ for $N_{Re} < 3000$ or for rough surfaces

$A = L_A/D_h$ for smooth surfaces and $N_{Re} > 3000$

L_A = obstacle length

After passing the obstacle the disturbance caused by the obstacle begins to decay. The relative Nusselt number is then given by

$$\frac{\mathrm{Nu(y)}}{\mathrm{Nu(undisturbed)}} = \min \left\{ \mathrm{Nu(max)},\ K\left[\frac{y}{D_h}\,\frac{1}{N_{Re}N_{Pr}}\right]^m \right\}$$

where values of K and m are given in Table 3.13 and Nu(max) is given by

$$\mathrm{Nu(max)} = \min \left\{ \begin{array}{l} 1 + 0.174\ \varepsilon^2 N_{Re}^{1/2} \\ \quad \text{and} \\ 1 + \left[3.3 + 72{,}700\ N_{Re}^{-1.2}\right] \varepsilon^2 \end{array} \right. \qquad \text{for rough surfaces}$$

$$\mathrm{Nu(max)} = \min \left\{ \begin{array}{l} 1 + 0.174\ \varepsilon^2 N_{Re}{}^{1/2} \\ \quad \text{and} \\ 1 + \ 6.38 + 4550\ N_{Re}{}^{-0.8}\ \varepsilon^{2.4} \end{array} \right. \qquad \text{for smooth surfaces}$$

Of course, Nu(y)/Nu(undisturbed) is never allowed to be less than one.

The correlation for the increase in the Sherwood number caused by a flow discontinuity was created from the Hassan and Rehme correlation by assuming the relative effects on mass transport and heat transport were the same. Based on the simplified description of core meltdown outlined above, slumping melt or local clad ballooning creates a local increase in the rod diameter. Blockage factors are then, for triangular arrays:

$$\varepsilon = \frac{0.907\ D_{max}^2}{S^2}$$

and for square arrays

$$\varepsilon = \frac{0.785\ D_{max}^2}{S^2}$$

where D_{max} is the maximum rod diameter at the discontinuity. The correlations also account for surface roughness of the rods. Surface roughness has an effect only at Reynolds numbers greater than 3000. For the purposes here, it is recommended that the correlation for rough surfaces be used when the flow discontinuity is created by melting. Otherwise, the smooth rod correlation should be adequate.

Plots of the effects of discontinuities on local Sherwood numbers as functions of distance and Reynolds numbers are shown in Figure 3.14.

A somewhat simpler expression for the effects of discontinuities can be derived from correlations of heat transfer data by Gimble et al. [120]. These investigators examined the effects of a transverse grid spacer and correlated their data in the turbulent regime ($8000 \leq N_{Re} < 30{,}000$) with the expression:

$$\frac{Nu}{N_{Re} N_{Pr}} = (0.0850 + 0.612/x^{1/2}) N_{Re}^{-\alpha}$$

$$\alpha = \frac{0.00780 + 0.350/x}{0.00257 + x}$$

Then, in the turbulent regime

$$Sh = A\, N_{Re}^{1-\alpha}\, N_{Pr}^{2/3} Sc^{1/3}$$

where $A = (0.0850 + 0.612x^{-1/2})$

$$\alpha = \frac{0.00780 + 0.350/x}{0.00257 + x}$$

This correlation yields an overall effect rather than a local effect. Because of the way data were obtained by Gimble et al. the correlation applies only to regions beyond the location of the obstacle in the flow path.

<u>Flow Through a Debris Bed</u>. The recommended correlation in Table 3.13 is one provided by Rowe and Claxton [122]. It is for fixed, isothermal beds with $N_{Re} > 80$. For low Reynolds numbers, correlations appropriate for flow over single sphere should be used.

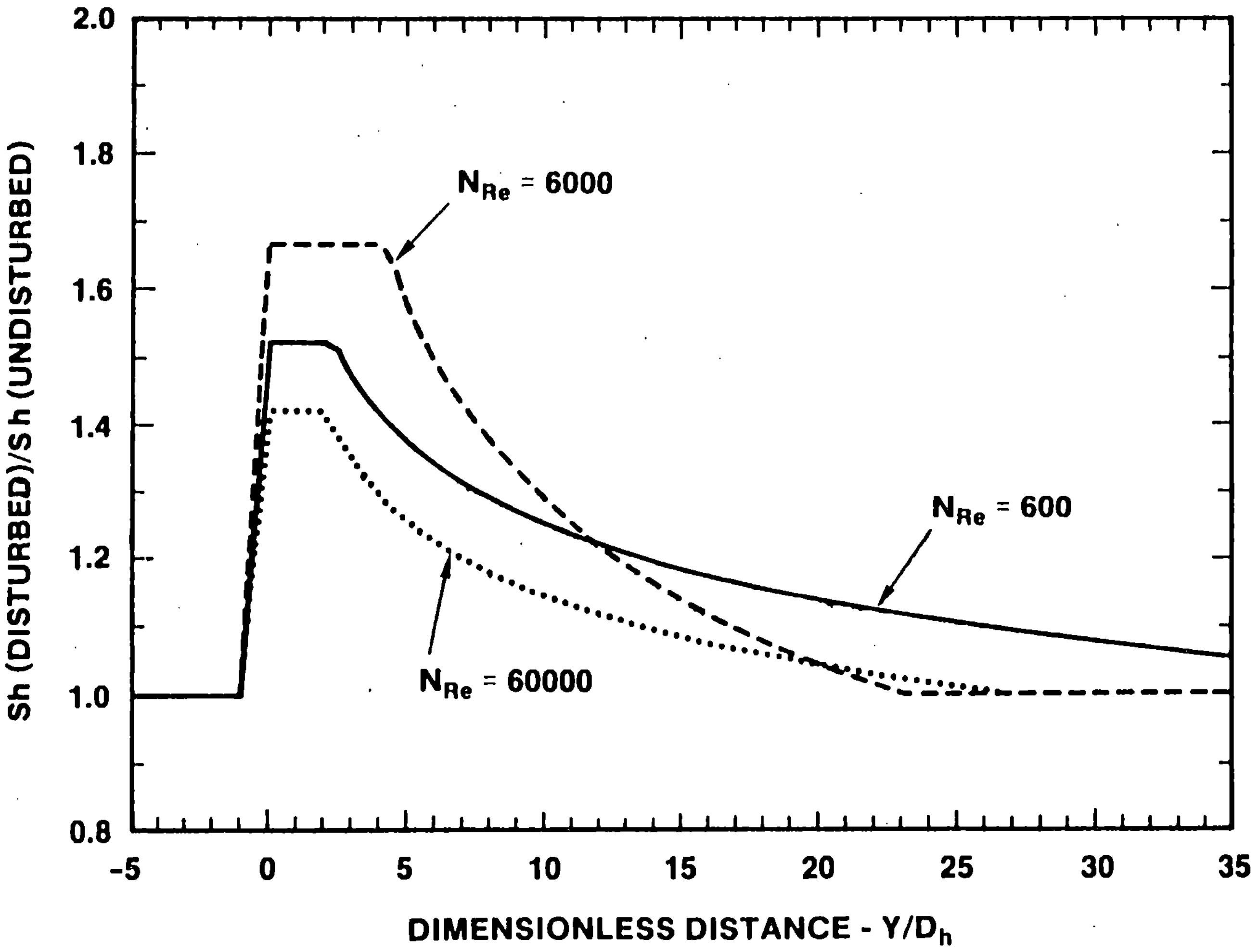

Figure 3.14. Effects of an Obstacle 1 Hydraulic Diameter Wide on the Relative Sherwood Number. Flow blockage was taken to be 0.35 and formulae for rough tubes were used to prepare this figure.

Whitaker [110] has offered an alternate correlation of heat transfer data that appears adequate to Reynolds numbers of up to 10:

$$Nu = (0.5 N_{Re}^{1/2} + 0.2 N_{Re}^{2/3}) N_{Pr}^{1/3}$$

Should gas velocities become high enough to fluidize the debris bed, then the following correlation [123] may be used to obtain gas phase mass transport coefficients:

$$Sh = 0.374 N_{Re}^{1.2} N_{Sc}^{1/3} \quad \text{for} \quad 0.1 < N_{Re} < 15$$

$$Sh = 2.01 N_{Re}^{1.5} N_{Sc}^{1/3} \quad \text{for} \quad 15 < N_{Re} < 250$$

where $N_{Re} = d_p v \rho / \mu$.

Correlations for Steel Structures. Vaporization of constituents of steel can be important for some accidents. A major fraction of the steel in a reactor core is configured as long vertical surfaces. The Sherwood number and consequently the gas phase mass transport coefficient for this type of surface subjected to forced convection can be found from correlations for flow along a flat plate:

1. Laminar flow: $Sh = 0.646 N_{Re}^{1/2} N_{Sc}^{1/3}$

2. Turbulent flow: $Sh = 0.0365 N_{Re}^{08}$

The length dimension used for both the Sherwood and Reynolds numbers is the length of the structure.

To evaluate the gas phase mass transport coefficient, it is necessary to have the diffusion coefficient of the volatile species in the ambient gas. The ambient gas is, to a first approximation, a mixture of steam and hydrogen. Especially at higher temperatures, the ambient gas becomes more complex since species such as H(gas), OH(gas), and O(gas) become more prevalent. If this complexity is neglected, then the diffusion coefficient of a volatile species in the ambient gas mixture, D_{Am}, is given by

$$D_{Am} = (P_{H_2}/D_{A,H_2}P_T + P_{H_2O}/D_{A,H_2O}\ P_T)^{-1}$$

where D_{A,H_2} = diffusion coefficient of A in hydrogen

D_{A,H_2O} = diffusion coefficient of A in steam

$$P_T = P_{H_2} + P_{H_2O}$$

The binary diffusion coefficients

$$D_{A,H_2} \text{ and } D_{A,H_2O}$$

can be found from:

$$D_{A,H_2} = \frac{3.2x10^{-4}\ T^{1.622}}{P_T}$$

$$D_{A,H_2O} = \frac{1.2x10^{-4}\ T^{1.622}}{P}$$

where P is in atmospheres.

The viscosity of the ambient gas, which is assumed to be predominantly steam and hydrogen, can be found from the Herning-Zipperer equation [124]:

$$\mu_{mix} = \frac{4.24\ P_{H_2O}\ \mu_{H_2O} + 1.41\ P_{H_2}\mu_{H_2}}{4.24\ P_{H_2O} + 1.41\ P_{H_2}}$$

where $\mu_{H_2} = 1.9x10^{-6}\ T^{0.674}$

$\mu_{H_2O} = 0.179x10^{-6}\ T^{1.106}$.

C. Radionuclide Release From Fragmented Core Debris

The preceding discussions have addressed release as the core degrades from intact fuel rods to a slumped molten pool. Once the molten pool has been formed, some hypothesized accident scenarios assert that the pool cascades from the core region into a water pool in the lower plenum of the reactor vessel. Sudden quenching of the core debris causes it to fragment into particles. Formation of a particle bed could also occur if water were sprayed onto overheated core materials during the core degradation process.

Once a particle bed is formed, it may not be coolable. The supply of coolant might be insufficient to keep the debris quenched. Or, the particle size and the bed structure may be such that coolant cannot flood the bed and keep the core debris particles quenched. If the bed is not coolable, it will heat to sufficient temperatures that the release of radionuclides and other volatiles can resume. The CORSOR model can be modified to predict this release from a debris bed.

Assume the debris has been fragmented into particles which if deformed into spheres would have diameters d_p. Assume the particles are packed so that the porosity of the debris bed is E. The rate of release of the volatile element i from the bed is given then by:

$$\frac{dF_i}{dt} = \frac{6K_{bed}}{d_p \rho_{molar}} \left[1 - F_i(t) - \frac{P_i(bulk)}{P_i(o)} \right]$$

where $$\frac{1}{K_{bed}} = \frac{1}{K_b(i) \exp[-E(i)/RT] \, \rho_{molar}} + \frac{RT}{k_g P_i^o(eq)}$$

$$K_b(i) = 2.75x10^{-3} \; K_o(i) \; \exp \; [1.6 \; Bu/1000) \left[\frac{10}{d_o}\right]^{\frac{1}{\xi}}$$

if burnup and porosity have not been annealed from the fuel or

$$K_b(i) = K_o(i)/4.225$$

if fuel melted prior to quenching.

If the bed is assumed isothermal and that the gas flow through the bed is not sufficient to levitate the particles, then the gas phase mass transport coefficient is given by [122]:

$$K_g = \frac{D_{AB}}{d_p}\left\{\frac{2}{1-(1-\varepsilon)^{1/3}} + \frac{2}{3\varepsilon}\left[\frac{d_p U_o \rho_g}{\mu}\right]^n \left[\frac{\mu}{\rho_g D_{AB}}\right]^{1/3}\right\}$$

where U_o = superficial velocity of gas through the bed

ρ_g = gas density in g/cm^3

μ = gas viscosity

and n is defined by the equation

$$\frac{2-n}{3n-1} = 4.65\left[\frac{d_p U_o \rho_g}{\mu}\right]^{-0.28}$$

Inspection of the release rate expression shows that for any severe comminution of the debris and if volatile concentrations are not too small, release is controlled almost exclusively by mass transport in the gas phase. When this is the case, greater attention to the mass transport coefficient may be needed. In particular, the assumption that the bed is isothermal may be removed. Heat and mass transport in the bed are then coupled and a substantially more complicated release expression is derived [123].

3.7 Recommendations for MELCOR

1. The MELCOR model should include models of gap release, release during heating, melting, and slumping of the core, and release from fragmented debris.

2. The ORNL gap release is recommended to MELCOR. Inventories of the fuel/clad gap that participate in the gap release are not certain. The inventories used in Reference 7 are recommended to MELCOR. Some care in selecting the gap inventories may be merited since conclusions drawn in severe accident analyses have a tendency to "creep" into design basis considerations where they may not be applicable.

3. The modified CORSOR model derived in this chapter is recommended to MELCOR. Unlike the original form of CORSOR, this modified version can be applied during

melting and slumping. The modified model also allows the effects of fuel burnup, initial grain size of the fuel, ambient pressure, gas flow velocities, and gas composition to be recognized in the analyses. Recommended default values for burnup and initial grain size are 28,000 MWd/t and 10 μm, respectively.

4. If MELCOR will permit core debris to quench and fragment then a model of release from the fragmented debris is needed. The model outlined here is recommended. If release from the debris in this state is significant, an improved model may be needed.

REFERENCES

1. USNRC, Reactor Safety Study: An Assessment of Accident Risks in US Commercial Nuclear Power Plants, WASH-1400, October 1975 and especially R. L. Ritzman et al. "Release of Radioactivity in Reactor Accidents," Appendix VII to the report.
2. Report of the President's Commission on the Accident at Three Mile Island, J. G. Kemeny, Chairman, August 1979 and also the Reports of the Te. Library of Congress Card Number 79-25694 ISBN 0-935758-00-3
3. D. O. Campbell, A. P. Malinauskus, and W. R. Stratton, Nucl. Tech. 53, p. 111 (1981).
4. USNRC, Fission Product Release and Transport Research: Existing Experimental and Analytical Program Needs, NUREG-1053, to be published.
5. USNRC, Technical Bases for Estimating Fission Product Behavior During LWR Accidents, NUREG-0772, June 1981.
6. S. J. Niemczyk and L. M. McDowell-Boyer, Interim Source Term Assumptions for Emergency Planning and Equipment Qualification, NUREG/CR-2629, ORNL/TM-8274, and Technical Considerations Related to Interim Source Term Assumptions for Emergency Planning and Equipment Qualification, ORNL/TM-8275, September 1982 Oak Ridge National Laboratory, Oak Ridge, TN.
7. J. A. Gieske, et al. Radionuclide Release Under Specific LWR Accident Conditions-Volumes 1-6, BMI-2104, Batelle Columbus Laboratory, Columbus, OH.
8. IDCOR, Industry Degraded Core Rule Making Program, Subtasks 11.1, 11.3, 11.4, and 11.5.
9. G. J. Kolb et al., Reactor Safety Study Methodology Applications Program: Oconee #3 PWR Power Plant, NUREG/CR-1659, SAND80-1897, Rev; Sandia National Laboratory, Albuquerque, NM, May 1981.
10. Commonwealth Edison, Inc., Zion Probabilistic Safety Study, 1981.
11. P. Baybutt, "Radionuclide Release and Transport," Chapter 8, PRA Procedures Guide, Volume 1, NUREG/CR-2300, January 1983.
12. C. Politus, KfK-2167, 1975.

REFERENCES (Continued)

13. D. A. Powers, Transactions American Nuclear Society, 34, p. 563 (1980).

14. Y. B. Katayama, "Leaching of Irradiated LWR Fuel Pellets in Deionized and Typical Ground Water," BNWL-2057, Pacific Northwest Laboratory, July 1976.

15. T. T. Vandergraaf, L. H. Johnson, and D. W. P. Lau, Leaching of Irradiated CANDU UO_2 Fuel," Scientific Basis for Nuclear Waste Management, p. 335.

16. U. B. Ekland and R. Forsyth, Leaching of Irradiated UO_2 Fuel, KBS Report 70, February 1978.

17. R. A. Lorenz, J. L. Collins, and A. P. Malinauskus, Nuclear Technology, 46, p. 404 (1979).

18. J. Brockmann and T. Stalker, Sandia National Laboratories, Albuquerque, NM, unpublished results.

19. G. Parker, G. E. Creek, and A. L. Sutton, Jr., "Influence of Variable Physical Process Assumptions on Core Melt Aerosol Release," Proc. Int'l Mtg. on Thermal Reactor Safety, Chicago, IL, NUREG/CP-0027, Volume 2, p. 1078, 1983.

20. J. P. Mitchell, A. L. Nichols, and J. A. H. Simpson, "The Characterization of Ag-In-Cd Control Rod Aerosols Generated at Temperatures Below 1900 K," CSNI Specialists Meeting on Nuclear Aerosols in Reactor Safety, Karlsruhe, West Germany, September 1984.

21. Major sources of data necessary to calculate $\Delta G_i(T)$ are:

    a. D. R. Stull and H. Prophet, JANAF Thermochemical Tables, 2nd edition, NSRDS-NBS37, June 1971.

    b. M. W. Chase et al. "JANAF Thermochemical Tables 1974 Supplement," J. Phys. Chem. Ref. Data 3, pp. 311-480 (1974).

    b. M. W. Chase et al. "JANAF Thermochemical Tables 1975 Supplement," J. Phys. Chem. Ref. Data 4, pp. 1-175 (1975).

    c. M. W. Chase, Jr. et al. "JANAF Thermochemical Tables 1978 Supplement," J. Phys. Chem. Ref. Data 7, pp. 793-940 (1978).

d. M. W. Chase, Jr., et al. "JANAF Thermochemical Tables 1982 Supplement," J. Phys. Chem. Ref. Data 11, pp. 695-940 (1982).

e. I. Barin and O. Knacke, Thermochemical Properties of Inorganic Substances, Springer-Verlag, 1973.

f. I. Barin, O. Knacke, and O. Kubachewski, Thermochemical Properties of Inorganic Substances, Supplement, Springer-Verlag, 1977.

g. K. C. Mills, Thermodynamic Data for Inorganic Sulphides, Selenides and Tellurides, Butterworths, London, 1974.

h. R. A. Robie et al. Thermodynamic Properties of Minerals and Related Substances at 298.15 K and 1 Bar (10^5 Pascals) Pressure and at Higher Temperatures, Geological Survey Bulletin 1452.

i. D. D. Jackson, Thermodynamics of Gases Hydroxides, UCRL-51137, 1971.

j. P. E. Blackburn and C. E. Johnson, ANL-82-42, Argonne National Labs, 1982.

k. F. Garisto, Thermodynamics of Iodine, Cesium, and Tellurium in the Primary Heat Transport System Under Accident Conditions, Atomic Energy of Canada, Ltd., AECL-7782.

l. D. D. Wagman, et al. "The NBS Tables of Thermodynamic Properties," J. Phys. Chem. Ref. Data 11 (1982) Supplement 2.

m. R. Hultgren, R. L. Orr, P. D. Anderson, and K. K. Kelley, Selected Values of Thermodynamic Properties of Metals and Alloys, J. Wiley and Sons.

22. D. A. Powers, Control Rod Behavior During Core Degradation I: Pressurization of Ag-In-Cd Control Rods, NUREG/CR-4401, SAND85-0469, Sandia National Laboratories, Albuquerque, NM. September, 1985.

23. D. A. Powers and J. E. Brockmann, VANESA: A Mechanistic Model of Radionuclide Release and Aerosol Generation During Core Debris/Concrete Interactions, NUREG/CR-4308, SAND85-1370, Sandia National Laboratories, Albuquerque, NM, July 1986.

24. J. F. Muir, et al., CORCON-MOD1: An Improved Model for Molten-Core/Concrete Interactions. NUREG/CR-2142, SAND80-2415, Sandia National Laboratories, Albuquerque, NM, 1981.

25. W. R. Smith, Industrial and Engineering Chemistry, Fundamentals 19, p. 1 (1980).

26. W. B. White, S. M. Johnson, and G. B. Dantzig, J. Chem. Phys. 28, p. 751 (1958).

27. T. Gerlach, FLUEQU, unpublished code used in the calculations for Reference 5.

28. G. Eriksson and E. Rosen, Chem. Scripta 4, p. 193 (1973).

29. G. Eriksson, Acta Chem. Scand. 25, p. 2651 (1971).

30. S. R. Brinkley, Jr., J. Chem. Phys. 15, p. 107 (1947).

31. D. A. Powers in Advanced Reactor Safety Research Quarterly Report April-June, 1979, NUREG/CR-0984 SAND79-1597, Sandia National Laboratories, Albuquerque, NM, November 1979.

32. Electric Power Research Institute, Technical Reports 11.1, 11.4 and 11.5 Estimation of Fission Product and Core Material Characteristics, Atomic Industrial Forum, October 1983.

33. K. Konashi, T. Yato, and H. Kaneko, J. Nucl. Mat'ls 116, p. 86 (1983).

34. G. A. Somorjai, "High Temperature Vaporization Mechanisms," p. 73 in High Temperature Technology Proceedings of the 3rd International Symposium, Asilomar, CA, 1967.

35. J. P. Hirth and G. M. Pound, Condensation and Evaporation, (Pergamon Press, New York, 1963).

36. S. E. Ziemniak, "A Study of Interfacial Resistance to Mass Transfer at High Evaporation Rates," Thesis, Rensselaer Polytechnic Institute, August 1968.

37. R. G. Ward, J. Iron and Steel Institute, 201, p. 11 (1963).

38. R. A. Lorenz, "The Vaporization of Structural Materials in Severe Accidents," Proc. Int'l Mtg. on Thermal Nuclear Reactor Safety, Chicago, IL, NUREG/CP-0027, 1983.

REFERENCES (Continued)

39. E. A. Mason, A. P. Malinauskus, and R. B. Evans, J. Chem. Phys. 46, p. 3199 (1967).

40. S. Chapman and T. G. Cowling, Mathematical Theory of Non-uniform Gases, 2nd edition, Cambridge Press, 1961.

41. E. R. Gilliland, Ind. Eng. Chem. 26, p. 681 (1934).

42. P. C. Singh and S. Singh, Int. Comm. Heat Mass Transfer 10, p. 123 (1983).

43. E. T. Turkdogan, P. Grieveson, and L. S. Darken J. Metals 5, p. 21 (1962).

44. A. W. D. Hills and J. Szekeley, Int'l J. Heat and Mass Transport 12, p. 111 (1969).

45. E. T. Turkdogan and K. C. Mills, Trans. AIME 230, p. 750 (1964).

46. F. F. Abraham, Homogeneous Nucleation Theory, Academic Press, 1974.

47. R. Becker and W. Döring, Ann. Phys. (Leipzig) 24, p. 719 (1935).

48. J. Lothe and G. M. Pound, J. Chem. Phys. 36, p. 208c (1962).

49. W. Camp, Sandia National Laboratories, unpublished results.

50. B. M. Jeffery, J. Nucl. Mat'l. 22, p. 33 (1967).

51. J. I. Bramman, et al., J. Nucl. Mat'l 25, p. 201 (1968).

52. F. Schmitz, et al, Int'l Mtg. on Fast Reactor Fuel and Fuel Elements, p. 336 (1970).

53. K. C. Russel, J. Chem. Phys. 50, p. 1809 (1969).

54. M. W. Mallett, A. F. Gerds, A. W. Lemmon, Jr., and D. L. Chase, BMI-1028 (1956).

55. P. Hofmann, D. Kerwin-Peck, and P. Nikolopoulos, Physical and Chemical Phenomena Associated with the Dissolution of Solid UO_2 by Molten Zircaloy-4, PNS-Nr 675812, Kernforschungszentrum Karlsruhe, 1982.

56. C. Politus, KfK 2167 (1975).

57. D. A. Powers, "Chemical and Physical Processes of Reactor Core Meltdown, Chapter 4 in Core Meltdown Experimental Review, SAND74-0382 (Revision) NUREG-0205, Sandia National Laboratories, Albuquerque, NM, March 1979.

58. J. Fischer, J. D. Schilb, and M. G. Chasanov, J. Nucl. Mat. 48, p. 233 (1973).

59. R. A. Lorenz, J. L. Collins, and A. P. Malinauskus, Nuclear Technology, 46, p. 404 (1979).

60. R. A. Lorenz, "Status of Validation of the CORSOR Computer Code Used for the Accident Source Term Reassessment Study," in Review of the Status of Validation of the Computer Codes Used in the NRC Accident Source Term Reassessment Study (BMI-2104), ORNL/TM-8842, Oak Ridge National Laboratory.

61. A. H. Booth, AECL CRDC-721, Atomic Energy of Canada, Ltd. 1954.

62. D. R. Olander, Fundamental Aspects of Nuclear Reactor Fuel Elements, UC 736 TID 26711, 1975.

63. J. Rest, GRASS-SST: A Comprehensive, Mechanistic Model for the Prediction of Fission-gas Release in UO_2-Base Fuels During Steady-State and Transient Conditions, NUREG/CR-0202, ANL78-53, Argonne National Laboratory, June 1978.

64. S. E. Turner, et al., Background and Derivation of ANS5.4 Standard Fission Product Release Model, NUREG/CR-2507, January 1982.

65. D. M. Haaland, "Release of Radioactivity from the Core," Chapter 7 in Core Meltdown Experimental Review, SAND74-0382 (Revision), NUREG-0205, Sandia National Laboratories, Albuquerque, NM, 1977.

66a. W. Herning, J. Nucl. Mat'ls. 114, p. 41 (1983).

66b. I. R. Brearly and D. A. MacInes, SINGAR-A Model to Examine Fission Product Release in Accident Studies, SRD R-258, Safety and Reliability Directorate, UK Atomic Energy Authority, June 1983.

66c. K. Malen, AFISS-A Computer Code for Calculation of Accident Fission Product Release from Fuel Rods, Studsvik/NF(p)-81/62, 1981.

67. P. E. Blackburn, J. Nucl. Mat'ls. 46, p. 244 (1973).

68. S. W. Tam, P. E. Blackburn, and C. E. Johnson, "Effect of Core Chemistry on Fission Product Release," Proc. Int'l Mtg. on Thermal Nuclear Reactor Safety, Chicago, IL, NUREG/CP-0027, Vol. 1, pp. 101-110, February 1983.

69. H. Kleykamp, J. Nucl. Mat'ls. 84, p. 109 (1979).

70. O. Gotzmann, J. Nucl. Mat'ls. 107, p. 185 (1982).

71. D. Cubicciotti and J. H. Davies, Nucl. Sci and Eng. 60, p. 314 (1976).

72. C. E. Miller, Jr., Nuclear Applications 5, p. 1 (1968).

73. D. Cubicciotti, Nuclear Technology 53, p. 5 (1981).

74. W. I. Stuart and R. B. Adams, J. Nucl. Mat'ls. 58, p. 201 (1975).

75. M. J. Bannister and W. J. Buykx, J. Nucl. Mat'ls. 64, p. 57 (1977).

76. J. T. Bittel, L. H. Sjodakl, and J. F. White, J. Am. Ceram. Soc. 52, p. 446 (1969).

77. S. C. Jain, Proc. Roy. Soc. (London) A 243, p. 359 (1957).

78. R. O. Wooton and H. I. Avci, MARCH 1.1 (Meltdown Accident Response Characteristics) Code Description and User's Manual, NUREG/CR-1711, October 1980.

79. H. Albrecht, V. Matschoss, and H. Wild, "Experimental Investigation of Fission and Activation Product Release from LWR Fuel Rods at Temperatures Ranging from 1500-2800°C," Proc. Specialists Mtg. on the Behavior of Defected Zr Alloy Clad Ceramic Fuel in Water Cooled Reactors, CONF-790935-3 (1979).

REFERENCES (Continued)

80. H. Albrecht and H. Wild, "Investigation of Fission Product Release by Annealing and Melting LWR Fuel Pins in Air and Steam," Proc. Topical Mtg. on Reactor Safety Aspects of Fuel Behavior, Sun Valley, ID, August 1981.

81. H. Albrecht, "Out-of-Pile Release Tests Under Core Melting Conditions," OECD-NEA-CSNI/IAEA Specialists Mtg. on Water Reactor Safety and Fission Product Release in Off-Normal and Accident Conditions, 1983.

82. H. Albrecht and H. Wild, "Behavior of I, Cs, Te, Ba, Ag, In, and Cd During Release from Overheated PWR Cores," Proc. Int'l Mtg. on LWR Severe Accident Evaluation, August 1983 Cambridge, MA, paper TS4.2.

83. H. Albrecht, K. Nolte, and H. Wild, Project Nukleare Sicherheit, KfK 2950, Kernforschungszentrum Karlsruhe, West Germany, 1980.

84. H. Albrecht, K. Nolte, V. Prech, K. H. Simon, and H. Wild, Project Nukleare Sicherheit, KfK-3250, Kernforschungszentrum Karlsruhe, West Germany, 1981.

85. H. Albrecht, V. Matschoss, K. Nolte, and H. Wild, Project Nukleare Sicherheit, KfK-2750, Kernforschungszentrum Karlsruhe, West Germany, 1978.

86. M. F. Osborne, R. A. Lorenz, K. S. Norwood, J. R. Travis, and C. S. Webster, Data Summary Report for the Fission Product Release Test HI-3, NUREG/CR-3335 ORNL/TM-8783, Oak Ridge National Laboratory, Oak Ridge, TN.

87. D. J. Osetek, K. Vinjamuri, D. E. Kuders, and R. R. Hobbins, "Iodine and Cesium Behavior During the First PBF Severe Fuel Damage Test," Proc. Int'l Mtg. on LWR Severe Accident Evaluation paper TS 4.3, Cambridge, MA, 1983.

88. R. A. Lorenz, et al., Fission Product Release from Highly Irradiated Fuel Heated to 1300-1600°C in Steam, NUREG/CR-1386, ORNL/NUREG/TM-346, Oak Ridge National Laboratories, Oak Ridge, TN, December 1980.

89. R. A. Lorenz, et al., Fission Product Release from BWR Fuel Under LOCA Conditions, ORNL/NUREG/TM-388, Oak Ridge National Laboratories, Oak Ridge, TN, July 1981.

90. R. A. Lorenz, J. L. Collins, and A. P. Malinauskus, Fission Product Source Terms for the LWR Loss-of-Coolant Accident, NUREG/CR-1288, ORNL/NUREG/TM-321, July 1980.

91. M. F. Osborne, R. A. Lorenz, J. R. Travis, and C. S. Webster, Data Summary Report for the Fission Product Release Test HI-1, NUREG/CR-2928, ORNL/TM-8500, Oak Ridge National Laboratories, Oak Ridge, TN, December 1982.

92. M. F. Osborne, R. A. Lorenz, J. R. Travis, C. S. Webster and K. S. Norwood, Data Summary Report for the Fission Product Release Test HI-2, NUREG/CR-3171, ORNL/TM-8667, Oak Ridge National Laboratory, Oak Ridge, TN.

93. M. F. Osborne, R. A. Lorenz, K. S. Norwood, and R. P. Wichner, "Fission Product Release Under LWR Accident Conditions," Proc. Int'l Mtg. on LWR Severe Accident Evaluation paper TS 4.1, Cambridge, MA, 1983.

94. R. A. Lorenz, E. C. Beahm, and R. P. Wichner, "Review of Tellurium Release Rates from LWR Fuel Elements Under Accident Conditions," Proc. Int'l Mtg. on LWR Severe Accident Evaluation, paper TS 4.4, Cambridge, MA, 1983.

95. C. D. Andriesse and R. H. J. Tanke, Nuclear Technology 65, p. 415 (1984).

96. D. A. Young, Decomposition of Solids, Pergamon Press, 1966.

97. R. A. Lorenz, "Status of Validation of the CORSOR Computer Code Used for the Accident Source Term Reassessment Study," in Review of the Status of Validation of the Computer Codes Used in the NRC Accident Source Term Reassessment Study (BMI-2104), T. S. Kress, editor, ORNL/TM-8842, Oak Ridge National Laboratory, Oak Ridge, TN.

98. A. W. Coats and J. P. Redfern, Nature 201, p. 68 (1964).

99. V. M. Gorbaschev, J. Thermal Analysis 8, p. 349 (1975).

100. A. Van Tets, Thermochemical Acta 17, p. 372 (1976).

101. V. Denny and B. Raj Schgal, "Analytical Predictions of Core Heatup/Liquefaction/Slumping" paper TS-5.4 in Proc. Int'l Mtg. LWR Severe Accident Evaluation Vol. 1, August 28-September 1, 1983, Cambridge, MA.

102. B. D. Johnston, The Zircaloy-Uranium Dioxide Reaction, SRD R294, Safety and Reliability Directorate, United Kingdom Atomic Energy Authority, Culcheth Warrington, Great Britian, September 1984.

103. J. Rivard, Review of In-vessel Meltdown Models, NUREG/CR-1493, SAND80-0455, Sandia National Laboratories, Albuquerque, NM, July 1980.

104. D. Williams and J. B. Rivard, "Range of Possible Net Release from the RCS," Appendix B in R. J. Lipinski, et al. Uncertainty in Radionuclide Release Under Specific LWR Accident Conditions, Volume 2, SAND84-0410/2, Sandia National Laboratories, Albuquerque, NM, February 1985.

105. S. Hagan, et al. Projekt Nuklease Sicherheit, KfK-2750 4300-62, Kernforschungszentrum Karlsruhe, West Germany, November 1978.

106. J. Rivard, "RCS Assessment for MELCOR," Chapter 2 in Thermal-Hydraulic Process Modeling in Risk Analysis: An Assessment of The Relevant Systems, Structures, and Phenomena, NUREG/CR-3986, SAND84-1219, Sandia National Laboratories, Albuquerque, NM, August 1984.

107. R. L. Steinberger and R. E. Treybal, AICHE J. 6, p. 227 (1960).

108. D. C. T. Pei, C. Narasimham, and W. H. Gauvin, Proc. Symp. on Interactions between Fluids and Particles, Institute of Chemical Engineering, London, June 1962.

109. G. Schütz, Intern J. Heat and Mass Transfer 6, p. 873 (1963).

110. S. Whitaker AIChE J. 18, p. 361 (1972).

111. D. C. Collins and M. J. Williams, J. Fluid Mechanics 6, p. 357 (1959).

112. H. Smyczek and J. Zablocki, Pr. Nauk Inst. Inz. Chem. Urzadzen Cielplnych Politech. Wroslaw 24, pp. 261-266 (1974); CA:82:142094a.

113. J. Weisman, Nucl. Sci. and Eng. 6, p. 78 (1959).

114. D. A. Dingee and J. W. Chastain, "Heat Transfer from Parallel Rods in Axial Flow," Reactor Heat Transfer Conference of 1956, J.E. Viscardi, editor, TID-7529 pt. 1, p. 462, 1957.

115. E. M. Sparrow, A. L. Loeffler, Jr., and H. A. Hubbard, Trans. ASME J. of Heat Transfer, pp. 415-422, November 1961.

REFERENCES (Continued)

116. O. E. Dwyer, Nucl. Eng. Design 10, p. 3 (1969).

117. O. E. Dwyer, AIChE J. 9, p. 261 (1963).

118. P. A. Ushakov, A. V. Zhukov and N. M. Matyukhin, Teplofizika Vysokikh Temperatur 15, p. 1027 (1977).

119. R. K. Shah and A. L. London, "Laminar Flow Forced Convection in Ducts," Advances in Heat Transfer Supplement 1, Academic Press, 1978.

120. R. E. Gimble, W. H. Bell, and S. L. Fawcett, Heat Transfer and Friction-Flow Characteristics of Cylindrical Parallel Rods with Transverse Cylindrical Spacers, AECD-3975, Batelle Memorial Institute, Columbus, OH, 1954.

121. M. A. Hassan and K. Rehme, Nucl. Technology 52, p. 401 (1981).

122. P. N. Rowe and K. T. Claxton, Trans. Inst. Chem. Eng. 43, p 10 T321 (1965).

123. O. Mathews, Trans. Can. Inst. Min. Met. 52, p. 97 (1939).

124. F. Herning and L. Zipperer, Gas Wasserfach. 73, p. 49 (1936).

125. C. F. Clement, Aerosol Growth in Vapour-Gas Mixtures Cooled Through Surfaces, TP. 897, AERE Harwell, May, 1982.

126. A. D. Emery, D. B. Scott, and J. R. Stewart, Nucl. Technology 11 (1971) 474.

127. M. R. Kuhlman, D. J. Lehmicke and R. O. Meyer, CORSOR User's Manual, NRC Report NUREG/CR-4173, BMI-2122, Battelle Columbus Laboratory, Columbus, OH, March, 1985.

128. J. L. Kelly, A. B. Reynolds, and M. E. McGown, Nuclear Science and Engineering 88 (1984)184.

CHAPTER 4

FISSION PRODUCT RELEASE AND AEROSOL GENERATION WITHIN THE REACTOR CONTAINMENT

4.1 Introduction and Definitions

An accident severe enough to melt the reactor fuel in a light water reactor will lead to release of radioactive material from the fuel. This released material, primarily in the form of aerosols, may escape into the reactor containment and, perhaps, from there into the environment. The nature of radioactive material released from the fuel--its composition, form, release rate, and integral release fraction--is called the "source term."

Radioactive material released from fuel that has penetrated the reactor pressure vessel is the "ex-vessel source term". Ex-vessel release of radioactive material is one of the four release processes considered in the Reactor Safety Study [1]. At the time of the Reactor Safety Study, little was known about any of the release processes. Approximate calculations, possible then, placed the greatest emphasis on release from fuel within the reactor primary system. The relatively volatile species emitted from the fuel during the early stages of a severe reactor accident were assumed to pose the greatest radiological threat. In an effort to provide bounding estimates of released radioactivity that would be applicable to the severest accident at a wide variety of nuclear plants, the analyses in the Reactor Safety Study [2] neglected many processes that mitigate the source term. One consequence of the conservative approach was to make the ex-vessel source term appear less significant than the source terms from in-vessel processes.

The more sophisticated understanding of severe accident source terms that has developed since the Reactor Safety Study has kindled a greater interest in ex-vessel release processes. Modern treatments of source terms distinguish between radioactive material released from the fuel--the "phenomenological source term"--and the radioactive material that escapes from a reactor plant--the "radiological source term". Much of the new interest in the ex-vessel source term arises because of the mechanistic relationship between the phenomenological and the radiological source terms, as well as the inherent nature of ex-vessel release of radioactive material. Some specific reasons for this interest
are:

1. Ongoing studies of fission product behavior under reactor-accident conditions have shown that much of the radioactive material released in-vessel may not escape

the reactor primary system and contribute to the inventory of material in the containment available for the radiological source term. Proportionately, the contribution of material released ex-vessel to this inventory may be greater than heretofore supposed because ex-vessel releases are less susceptible to mitigation during transport from the point of release to the reactor containment.

2. Radioactive material released ex-vessel includes more refractory isotopes than does the in-vessel release. The qualitative nature of the radiological source term may be changed if the ex-vessel release contributions are greater than expected.

3. Aerosol processes naturally mitigate the phenomenological source term. Significant delays between in-vessel emissions of radioactivity from the fuel and gross containment failure are possible and provide an opportunity for great reduction in the amount of material released in-vessel that will escape into the environment. The ex-vessel sources are likely to be operative even after gross containment failure has occurred. Then the ex-vessel sources are less susceptible to mitigation by aerosol processes.

4. The aerosol processes that can cause such mitigation of the in-vessel source proceed among particles whether they are radioactive or not. The copious emission of non-radioactive materials typically associated with the ex-vessel sources provides a means to greatly enhance mitigation of the phenomenological source term, particularly, that portion of the source term created of the ex-vessel source term could lead to both quantitative and qualitative changes in the perceived radiological consequences of severe reactor accidents.

The second of the above points deserves some elaboration. Fission product releases during the ex-vessel debris interactions do involve the more refractory elements since volatile species would escape the fuel before the onset of ex-vessel phenomena. The radiological effects of refractory fission products have not received a great deal of attention in the past: first, because the releases of these elements were deemed small, and second, because the effects would be swamped by the releases of large amounts of cesium and iodine from fuel in the vessel. If the volatile species such as iodine do not escape the reactor coolant system, then the radiological consequences of releasing refractory fission product species need further examination. Results of a first attempt to do so are assembled in Table 4.1. To prepare this table, the radiological consequences of the

Table 4.1

Radiological Effects of Refractory Fission Products in Comparison to Cesium and Iodine [6]

Element	Relative Early Bone-Marrow Dose
I	1.0
Cs	0.1
Te	0.6
La	0.8
Ce	0.2
Pr	0.0001
Nd	0.3
Np	1.2
Pu	1×10^{-6}
Mo	0.1

Element	Relative Long Term Dose
Cs	1.0
Ce	0.21
Nb	0.7
Zr	1.4
Ru	0.7

release of 10 percent of the cesium inventory and 10 percent of the iodine inventory were normalized to unity. The consequences of the release of 10 percent of the inventory of other, selected, isotopes were then determined on this relative scale. It is apparent from these results that the refractory isotopes can be every bit as consequential as the volatile isotopes that have received so much attention in the past.

In the sections that follow, the current state-of-the-art in predicting the ex-vessel phenomenological source term is described. To present this discussion, it is convenient to divide the topic into two categories--primary ex-vessel source processes and secondary source process. The primary source processes give rise to release as a direct consequence of the ex-vessel behavior of the fuel. Release of radioactivity during (1) ejection of fuel from the primary system into the reactor containment, (2) interaction of fuel and core debris with concrete, and (3) ex-vessel interaction of molten material with water are all primary source processes. Leaching of radioactive materials from core debris by groundwater should the reactor basemat be penetrated is considered also to be a primary process.

Secondary source processes are those that arise because of the behavior of materials previously released from the fuel whether this release occurred during the in-vessel or ex-vessel stages of an accident. Resuspension of deposited aerosols and radiolytic release of iodine in sump waters are examples of secondary processes.

The focus of the discussions below is on the release of radioactivity from the fuel ex-vessel. Mitigation of this phenomenological source term by the presence of nonradioactive aerosols and enhancement of the source by secondary processes have become quite important aspects of severe reactor accident analyses [3]. To meet the needs of these analyses, release of nonradioactive materials from concrete and structural materials in a reactor containment are also discussed. The processes by which the phenomenological ex-vessel source term is converted into a radiological source term are reserved for treatment elsewhere [4].

4.2 Primary Fissions Product Release

A. Release Associated with Melt Ejection

The ex-vessel phase of a severe reactor accident begins with the expulsion of core debris from the reactor coolant system. Most previous analyses of severe reactor accidents have devoted little attention to the details of the expulsion process. Reactor accident phenomena have been described in these previous studies as though the coolant system were depressurized--a situation appropriate for accidents initiated by large breaks in the coolant system. Consequently, expulsion of the molten core material from the primary system was considered to be driven by gravity. Some small amount of fission product and aerosol release could come from the core debris as it fell from the primary system into the reactor cavity. But, any error caused by neglecting this release has been judged small in comparison to uncertainties concerning aerosol generation and fission product release associated with the behavior of the core debris once it has been expelled. This judgement is supported by the results of recent tests with large-scale UO_2 melts expelled under the force of gravity from a furnace [4].

The past systematic analyses of severe reactor accidents have concluded unanimously that accidents initiated by large breaks in the primary coolant system do not dominate the risk associated with the commercial use of nuclear power (for examples, see References 1 and 7). Accidents initiated by small breaks in the coolant system or transient events are more frequent. Descriptions of the phenomena during accidents initiated by small breaks or transients assuming a depressured primary system have been criticized [5]. It is expected that prior to melt expulsion in these more frequent accidents, the primary system would be at or near operating pressure. Even in boiling water reactors where operation procedures dictate primary system depressurization during off-normal events, the system would be at an elevated pressure (> 200 psig) throughout the process of core melt formation and up to the time of melt expulsion.

Henry has attempted to determine how the process of melt expulsion might be affected if the reactor coolant system were pressurized [7]. His analysis concluded that hydrodynamic phenomena exist which could disperse the core debris broadly if it were expelled from a pressurized system. The fraction of the core so broadly distributed (nominally 50 percent) could easily be quenched and kept cool so it would not further interact with materials outside the coolant system. Consequently, this debris would not be a continuing source of fission product release or aerosol generation.

These first attempts to ascertain how expulsion of the core debris from a pressurized primary system might affect the course of ex-vessel phases of a severe reactor accidents have not considered fission product release and aerosol production during melt expulsion. Early attempts to study melt ejection from pressurized systems have demonstrated that the ejection process can be a formidable source of aerosols [8]. Figure 4.1 is a series of photographs taken of an experiment in which a thermitically generated melt weighing 2.5 kg was ejected from a vessel pressurized to 40 atmospheres. Aerosol production begins

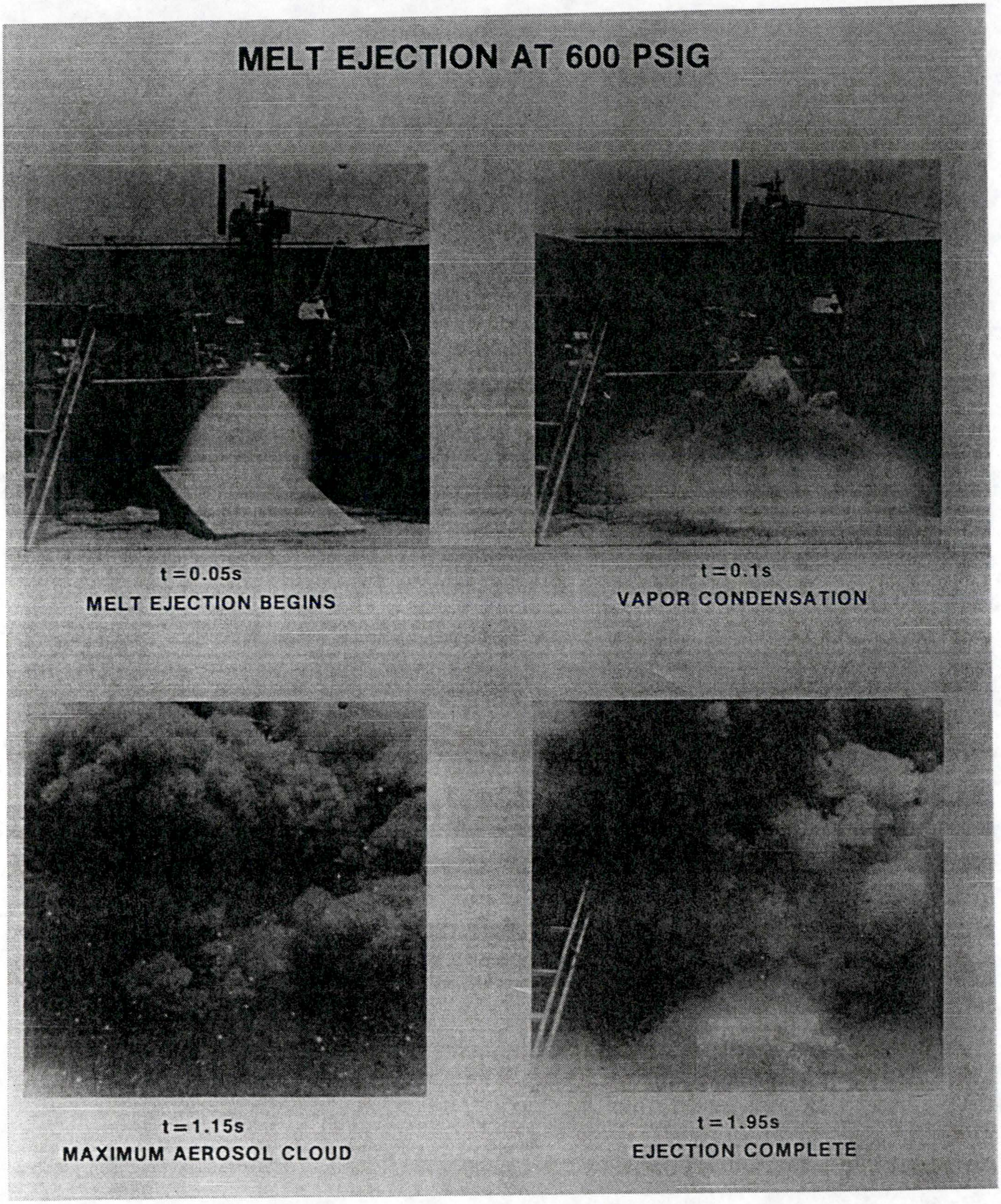

Figure 4.1. Sequence of Photographs Taken During Expulsion of 2.5 Kg of Melt From a Vessel Pressurized to 40 Atmospheres.

in this experiment with the initial emergence of melt and continues throughout the expulsion process. The aerosol production becomes so intense, the experimental apparatus is completely obscured about one second after the start of the test.

Samples taken during this and similar tests show a size distribution that may be trimodal (see Figure 4.2). Modes appear at 0.5 µm, 5 µm and at a larger size--nominally 65 µm [8]. The finest particles seem to be composed of compact agglomerates of 0.1 µm particles. The material of size near 5 µm is composed of nearly spherical particles that have the appearance of frozen liquid. The coarse mode material consists of both spherical and granular shapes. These particles, too, may have been liquid droplets once. The irregular shapes of some of the particles may have been caused by shrinkage during solidification or because the particles were broken during sampling. These coarse particles may not represent a mode in the aerosol size distribution. They may, in fact, be the "tail" of the distribution of very coarse particulate debris produced by the pressurized melt ejection. The aerosol sampling equipment was used in tests to date does not provide a very accurate characterication of the coarser material.

Pressurized melts have also been expelled into scaled models of reactor cavities. Aerosols collected during these tests have size distributions with only two modes. The fine material (<1 µm) is similar to that described above. There is no indication of aerosol material concentrations in the 3-8 µm size range. There is a significant amount of coarse material. Again, this coarse material collected with the aerosol sampling equipment is probably the "tail" of the size distributed debris particulate produced during expulsion from the reactor cavity model. This debris has been characterized by flash x-rays as it emerged from the cavity and by post-test sieve analyses. The material has been found to be log-normally distributed in size with mean particle sizes of 0.4 to 0.8 mm and a geometric standard deviation of about 3.4 (see Figure 4.3). This size distribution implies that less than 4 percent of the mass expelled from the cavity would have particle sizes of less than 50 µm.

Few measurements of the mass of expelled melt converted into aerosols have been reported. In tests involving melt expulsion into a reactor cavity, 0.5-1 percent of the melt mass aerosolized. About half of this material was smaller than 10 µm and about 35 percent was smaller than 1 µm. In tests involving melt expulsion into a gravel bed, 0.3 to 6 percent of the melt mass was estimated to be in the form of aerosols.

Several mechanisms of aerosol generation may be operative in the pressurized melt ejection tests:

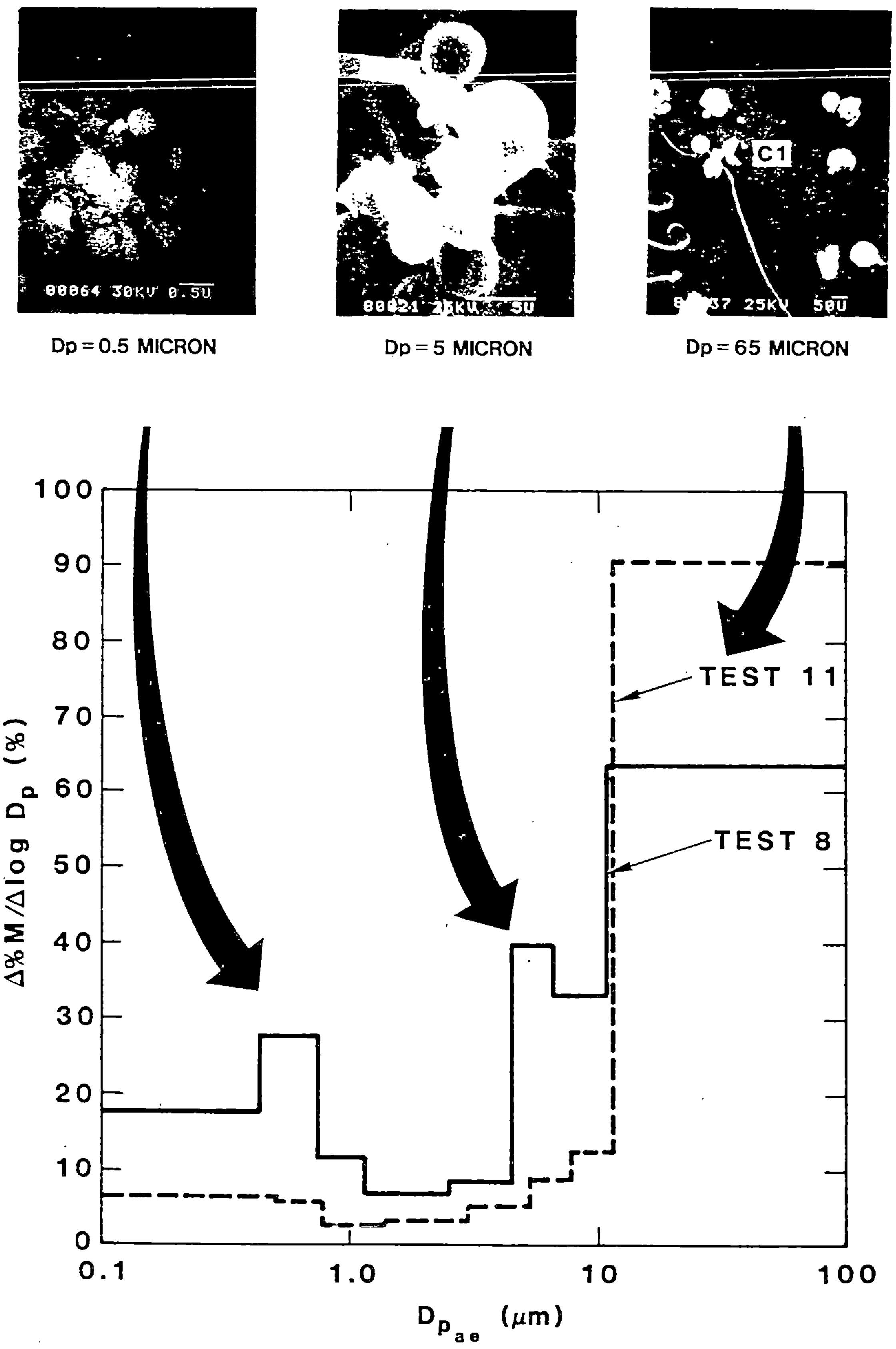

Figure 4.2. Size Distribution of Aerosols Produced During Pressurized Ejection of Melts. Test 11 was done with CO_2 as the pressurizing gas, and test 8 was done with N_2 as the pressurizing gas.

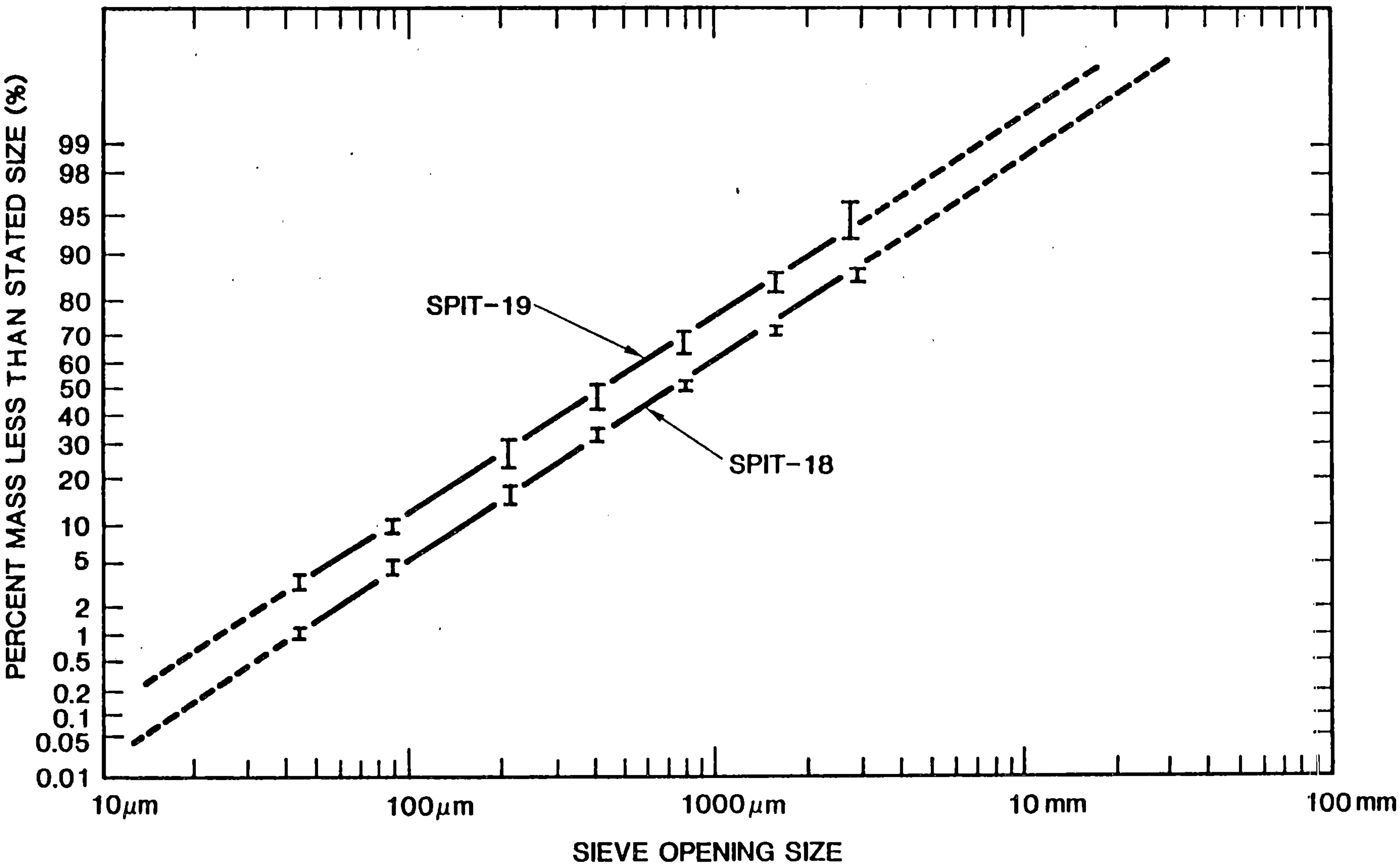

Figure 4.3. Size Distribution of Debris Produced When Melt is Ejected From a Pressurized Vessel into Scaled Models of a Reactor Cavity (SPIT Test Series).

1. simple vaporization of volatile species from the melt,
2. disruption of the jet of melt by hydrodynamic processes or by effervescence of gases dissolved in the melt,
3. pneumatic atomization of the melt at the point of discharge from the pressure vessel, and
4. chemical reaction of coarse debris lofted into the atmosphere by the expulsion process.

Vaporization of melt constituents followed by condensation of these vapors is the most obvious means of aerosol production. Photographic records of pressurized melt ejection suggest this mechanism is operative in the tests (see Figure 4.1). The finest particles observed in the pressurized melt ejection tests have been attributed to this vaporization process. Microscopic examination of the 0.5 µm particles shows that these particles are probably agglomerates of yet finer particles. The sizes of these finer particles, 0.05-0.1 µm, are consistent with a nucleate condensation mechanism of formation.

The vaporization process should yield particles whose compositions reflect the relative volatility of melt constituents rather than the bulk melt composition. In reactor accident situations, this aerosol could be enriched in fission products relative to the bulk melt. The vaporization aerosol could be enriched in steel constituents because of the high vapor pressures of these constituents relative to reactor fuel oxides.

The rate of aerosol formation by vaporization depends on the melt surface area. If the melt stream is compact as depicted in the analyses to date, the fractional aerosolization of the melt will vary with the reciprocal of the diameter of the melt stream. If, on the other hand, the melt stream disintegrates because of aerodynamic forces or other processes to create more surface area, the aerosolization by vapor formation will become invariant with respect to scale. X-ray photographs of melt jets emerging from pressurized vessels show the melt to be very disrupted and not compact [8].

Disintegration of the melt jet can lead to aerosol formation because melt droplets streaming at high velocities through the nearly stagnant atmosphere are unstable. These droplets will disintegrate until surface tension forces can balance the inertial forces on the droplets. Pilch [9] has investigated this process and has found that the criterion for droplet stability is:

$$We = \rho_g \frac{V^2 D}{\sigma} > 12$$

where ρ_g = density of the atmosphere gas
V = droplet velocity
D = diameter of the melt droplet, and
σ = surface tension

Pilch's analysis suggests that disintegration of melt droplets will yield an aerosol with a mass mean diameter of 60-70 µm. This aerosol is consistent with the coarsest aerosol observed in the pressurized melt ejection tests. Unfortunately, sampling such coarse aerosols is difficult, so it has not been possible to verify all of Pilch's predictions with the test data.

Aerosols produced by the aerodynamic mechanism will have compositions similar to those of the bulk melt. The fraction of melt aerosolized by this process depends on how disrupted is the melt jet. If melt jets are as disrupted as observed in tests of pressurized melt ejection, then the fraction of melt aerosolized will be scale independent. If the jet remains compact, then droplets of melt that disintegrate to form the aerosol are produced by Helmholtz instabilities at the melt stream surface. In this case, the fraction of the melt converted to aerosols will vary with the reciprocal of the stream diameter.

The stability of the melt jet is obviously a critical feature of pressurized melt ejection. Powers [10] has suggested that melt jets under accident conditions will not be stable because of gas effervescence. Gases in the primary system of a nuclear reactor during a severe accident are predominantly steam and hydrogen. Steam and hydrogen will dissolve in molten core debris. Some estimates of the solubilities of these gases in the oxidic and metallic phases of core debris under severe accident conditions are listed in Table 4.2. The solubility of the H_2 in iron was obtained from the correlation [11]:

$$\log_{10} (\xi 10^4) = -1637/T + 2.1326 + 0.5 \log_{10} P_{H_2}$$

where ξ = atomic fraction hydrogen in solution
T = absolute melt temperature (K)
P_{H_2} = partial pressure of hydrogen (atms)

Solubilities for hydrogen and steam in UO_2 were obtained with Blander's correlation for gas solubility in molten salts [12]:

$$\ln (RTC/P) = - 9.104\times10^{16} \, r^2\sigma/T$$

where
σ = surface tension of the melt (dyne/cm)
C = concentration of the gas in solution (moles/cm^3)
R = gas constant (cm^3-atmospheres/K)
r = radius of the dissolved gas molecule (cm)
P = partial pressure of the dissolving gas in the atmosphere surrounding the melt prior to ejection (atms)

Blander's correlation probably produces a lower bound on the true solubility of steam in UO_2 since it ignores chemical effects known to greatly increase the solubility of steam in high temperature melts [13].

Table 4.2

Solubilities of Steam and Hydrogen in Core Debris

Temperature (°K)	Partial Pressure (atm)		Solubility (liter gas-STP/liter melt)			
			Oxide		Metal	
	H_2	H_2O	H_2	H_2O	H_2	H_2O
2800	75	75	0.43	0.62	39.55	-
	15	135	0.086	1.10	17.71	-
	1.5	-	0.009	-	5.6	-
1800	75	75	0.132	0.24	18.97	-
	15	135	0.026	0.42	8.47	-
	1.5	-	0.003	-	2.66	-

Inspection of the variation in gas solubility with ambient pressure shows that there will be a tremendous driving force to desorb gas when molten material emerges from a pressurized vessel into an environment of near normal atmospheric pressure. This is especially true for the metallic phase in which the volume of gas that must desorb is many times the volume of melt. The desorption process should radically disrupt the melt stream.

Tarbell [14] has verified the disruptive effect of effervescing gases in tests that compare melt ejection from vessels pressurized with nitrogen or with carbon dioxide. In tests with nitrogen, which is quite soluble in high temperature melts, the emerging jets disintegrated into fine droplets. In tests with the vessel pressurized with CO_2, which is much less soluble than nitrogen, the melt stream remained compact as it emerged though some surface disruption due to Helmholtz instability was evident.

Effervescence of gas can also be a source of aerosols. Bursting gas bubbles will throw off aerosol particles 1 to 10 µm in diameter [15]. These aerosols will have the bulk melt composition. The fraction of melt aerosolized in this way should be approximately scale-independent.

Another mechanism of aerosol formation during melt ejection arises if both gas and melt can emerge from the breach in the vessel simultaneously. This pneumatic atomization is likely to develop during later stages of melt ejection of a reactor accident but may not have been operative in tests to date. Analysis of this process by Pilch [16] showed that it can yield UO_2 aerosols 1-10 µm in size and steel aerosols 2-60 µm in size. The fraction of melt aerosolized by this process will depend critically on the details of the breach in the vessel and the melt ejection process. Simple, scoping calculations indicate up to 10 percent of a core melt could be converted into aerosols this way.

Most of the aerosols produced by melt ejection processes are quite unlike aerosols produced by other severe reactor accident phenomena. With the exception of those aerosols generated as a result of vaporization, the aerosols produced during melt ejection have the bulk melt composition.

Both the oxide and the metallic phases of a core melt are quite reactive in the steam and air atmospheres likely to be present in reactor containments. If aerosol emissions are as intense under accident conditions as in the tests, cloud effects will prevent the aerosols from cooling rapidly. The hot, perhaps molten, aerosols produced by melt ejection would be expected to react rapidly once they emerge from the reactor cavity into the reactor containment.

The air oxidation of UO_2 has been studied extensively (see for example References 17 and 18). Bittel [19] has examined steam oxidation of solid UO_2. Oxidation of UO_2 appears to be a two step process in which first U_4O_9 or U_3O_7 is formed which subsequently reacts to form U_3O_8. Both reaction steps are mildly exothermic. Substantial structural change brought on by the oxidation causes the condensed material to fragment.

Cubaciotti [20] has argued that sintering and oxidation of UO_2 will allow fission products to escape the UO_2 matrix and, presumably, form new aerosols. Cubaciotti has formulated a rate expression for this type of release based on Bittel's rate of steam oxidation of UO_2.

The high potential reactivity of metallic melt ejection aerosols is worrisome not only from concerns over the release of radioactivity but also concerns of containment integrity. Recent reactor accident analyses have indicated that much of the zirconium clad from the reactor core will not have been oxidized at the time melt penetrates the primary vessel [7]. The rapid, exothermic, oxidation of fine particles of metal containing zirconium could be a dramatic event in the containment. It could influence hydrogen generation and deflagration. The ability of equipment to survive the rapid oxidation reaction is an interesting question.

Nelson [21] has studied the nature of metal particle oxidation in air. Particles of zirconium 250 µm in diameter ignite spontaneously when dropped into an air column. After these particles have burned for about 0.23 s, they disintegrate in a brilliant flash to yield finer rapidly burning particles. Such behavior is also observed in pure nitrogen, except the reaction is nitriding instead of oxidation.

Nelson's experiments did not address the behavior of zirconium diluted in either steel or UO_2. Nelson does suggest iron, chromium and manganese will combust in air and emit finer aerosol particles.

Experimental studies of other metals burning in oxygen suggest that the deflagration process may also generate aerosols and release fission products [22].

Recommendations For MELCOR Development Concerning the Source Term From Pressurized Melt Ejection. The information available concerning aerosol formation during pressurized melt ejection is not adequate for defining a highly mechanistic model of the process. The duration of the process is quite short, amounting to only a few seconds. Consequently, a detailed model of the process may not be important for a comprehensive code such as

MELCOR. Until further evidence from experimental studies becomes available, the following approximate description of the high pressure melt ejection source term developed for a study of source term uncertainties [23] may be adequate:

1. 1 percent of the mass expelled from the reactor coolant system is assumed to be instantly converted into aerosol.

2. The size distribution of the aerosol is described by two log-normal distributions. Mean sizes are 0.7 and 30 µm. The geometric standard deviations are 1.6 and 2, respectively. Half the mass of aerosol is apportioned to each of the distributions.

3. The composition of the coarser mode material is taken to be the bulk melt composition.

4. The composition of the finer mode in the size distribution is taken to be:

(a) alkali metals as Cs	0.8 w/o
(b) alkaline earths as BaO	3.6 w/o
(c) halogens as I	0.2 w/o
(d) chalcogens as Te	0.3 w/o
(e) platinoids as Ru	$3\text{x}10^{-5}$ w/o
(f) early transition as FeO	17 w/o
(g) tetravalents as CeO_2	4 w/o
(h) trivalents as La_2O_3	2.7 w/o
(i) uranium as UO_2	balance
(j) volatile main group as Cd	20 w/o
(k) main group as Sn	18 w/o

A check must be made in the code to assure that the emissions of an element do not exceed the inventory. If the inventory is exceeded, the composition numbers above would have to be re-normalized.

The energetic effects on the containment atmosphere produced by high pressure melt ejection constitute a serious threat to the containment integrity. Though not considered in detail in this chapter, these effects should be considered in the MELCOR code. Approximate models for these effects have been formulated by Pilch [24].

B. Release Associated with Core Debris Interactions with Coolant.

For many types of accidents, in most reactors, the cavity below the reactor pressure vessel may contain water at the time melt penetrates the vessel. Even if water is not present in the cavity initially, it could possibly be poured onto the melt later, either as a natural consequence of the accident progression or as result of some accident mitigation strategy. In any case, it is very likely that ex-vessel core debris interactions with water will occur.

The subject of core debris interactions with water has occupied a great deal of attention in the past. The concerns over these interactions have focused on the possibility of steam explosions that rupture the primary vessel or the reactor containment building. To a lesser extent, there has been concern that the quasi-static pressurization of containment brought on by steam generation during the interactions might exceed the capabilities of reactor containments.

The structural consequences of violent core debris interactions with water are not at issue here. The question addressed in this section is the fission product release that should accompany core debris interactions with water, particularly when those interactions take the form of a steam explosion. The Reactor Safety Study did associate a release with steam explosions and this release is listed in Table 4.3. Rather large release fractions are associated with the volatile halogens and noble gases in this release estimate. The estimate is, however, based on the inventory of the element present in the melt participating in the explosion. Whether the explosion took place in-vessel or ex-vessel, most of the noble gases and the halogens would have already escaped the fuel. The steam explosion release fractions for these elements estimated in the Reactor Safety Study are not especially significant.

A high release fraction is associated also with tellurium. Again, this release estimate is not especially significant. Were the steam explosion not to occur, tellurium release from the melt would still be nearly complete because of releases associated with other in-vessel and ex-vessel processes.

Omissions in the Reactor Safety Study estimate of steam explosion release might be significant. No releases of the alkali metal group elements (Cs, Rb), alkaline earth group elements (Sr, Ba), and the lanthanide group elements (La, Ce, U, Zr, Nb, Pm) are considered.

The Reactor Safety Study estimate of nearly complete ruthenium release, and by implication nearly complete release of the analogous metals Mo, Pd, Tc, and Rh, is significant. The combination of all other events in a severe reactor accident would release 8 percent of the ruthenium inventory according to the Reactor Safety Study. Participation of only 10 percent of the reactor core in a steam explosion would yield an equivalent release of ruthenium.

The Reactor Safety Study estimate of steam explosion release was prepared under the handicap of a total lack of pertinent,

Table 4.3

Radionuclide Release Associated with Steam Explosions in the Reactor Safety Study [1]

Element	Release* (%)
Xe, Kr	80-100
I, Br	80-100
Te, Se, Sb	40-80
Ru**	80-100

* Percent released of the inventory of the indicated element remaining in the melt involved in the explosion.

** Also stands for Mo, Tc, Pd and Rh

nuclear-reactor-related data. The rather dire structural consequences of steam explosions predicted in the Reactor Safety Study have prompted considerable research into the fundamentals of the steam explosion process. Unfortunately, none of these research efforts directed their attentions to the fission product release caused by steam explosions. The research has provided a good physical portrait of steam explosions and enough information to permit a limited re-evaluation of the Reactor Safety Study release estimate.

There appear to be two steps essential to the steam explosion process:

1. When molten core debris enters water, the melt coarsely fragments into droplets about 1 cm in diameter, intermixed and surrounded by coolant in film boiling.

2. The steam film surrounding the coarse fragments collapses permitting efficient transfer of heat from the melt into the coolant and consequently, rapid steam formation.

Thermal shock, quench fragmentation, or mechanical shock by the rapid steam generation reduces the debris to fine particulate material which is ejected into the atmosphere. Within the primary system, this atmosphere is a mixture of steam and hydrogen. Within the containment, air may also be present.

The considerations that led to the Reactor Safety Study estimate of steam explosion release were directed toward the behavior of the fine particulate debris thrown into the atmosphere. Experiments by Parker [25] have shown remarkable ruthenium release when irradiated fuel pellets are heated in air. The speciation of ruthenium vapors in air as a function of temperature shown in Figure 4.4 suggests the high release rates are probably due to formation of $RuO_4(g)$ or $RuO_3(g)$. The rate of ruthenium release observed in Parker's experiments followed different kinetic paths above and below 800°C which parallels the kinetics of UO_2 oxidation in air [13,14]. In this, Parker's results are consistent with Cubaciotti's argument that oxidation of the UO_2 is a key first step in the release of fission products [20].

In the current position of superior, but still far from adequate, information, it is possible to critique the Reactor Safety Study analysis of the steam explosion release on several grounds:

1. Whereas in irradiated fuel rods ruthenium may be present as isolated alloy nodules containing 20-25 percent Ru [26], by the time a steam explosion can occur, the

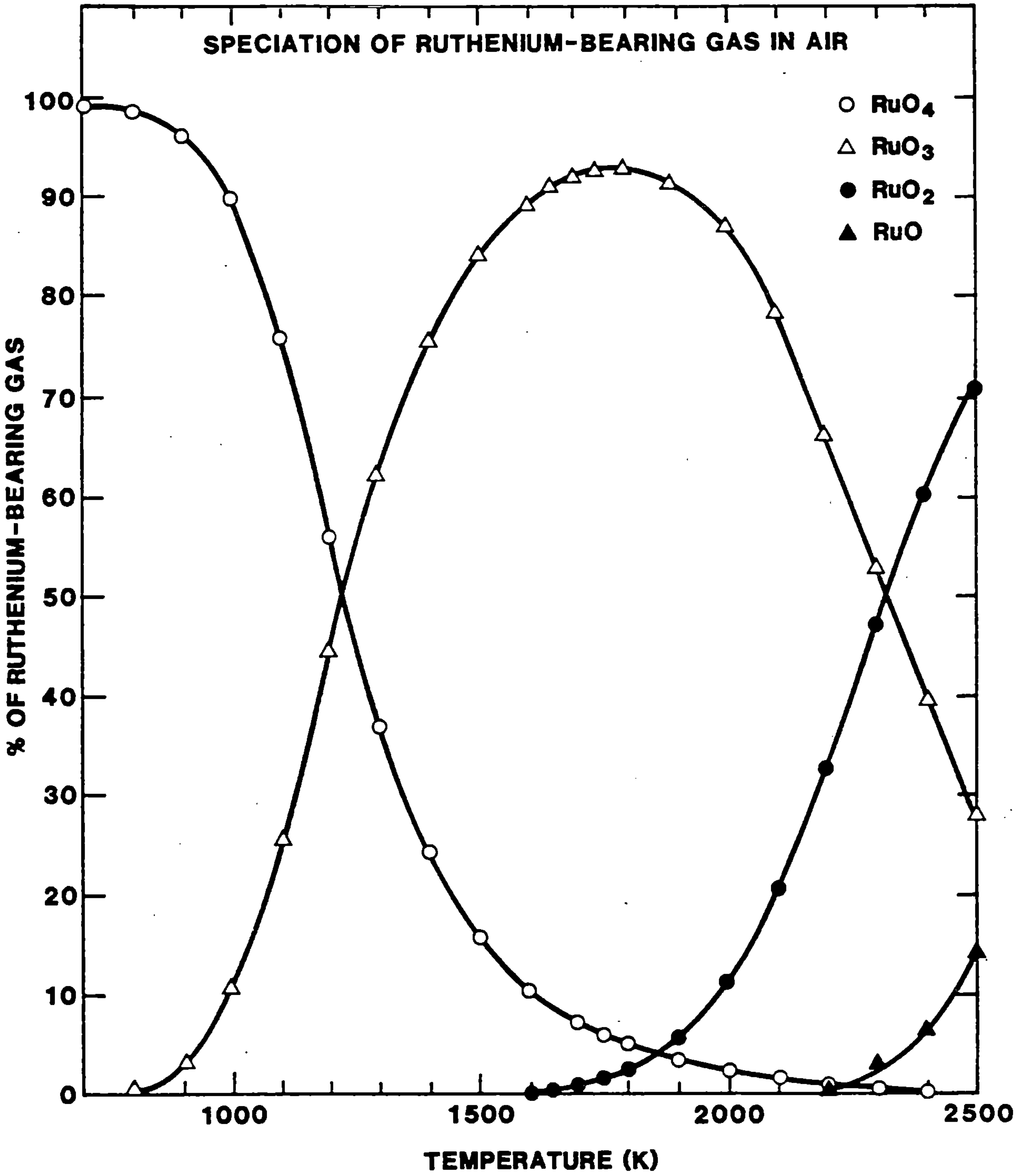

Figure 4.4. Speciation of Ruthenium Vapors in Air as a Function of Temperature.

ruthenium will probably have been incorporated as a very dilute constituent of the metallic phase of the core melt. In this dilute alloy, reaction of ruthenium to form a volatile oxide should be greatly slowed relative to the rates observed in Parker's experiments since the mechanism hypothesized by Cubaciotti is unavailable.

2. Even if the ruthenium is isolated in a urania matrix as in Parker's experiments, the time the urania particles remain suspended in the containment atmosphere may be too short to achieve the very high release rates implied by the release estimated in the Reactor Safety Study. Chemical conditions to which fragmented debris is exposed may not be conducive to high releases.

3. If release of ruthenium does occur as expected in the Reactor Safety Study, the other fission products notably the alkali metals, alkaline earths and the lanthanides should also be released.

The second of these points is most critical to the re-assessment of the steam explosion source term.

In the first step of the steam explosion process, the coarse, very hot, fragments are immersed in a strong oxidant, water. As shown by Corradini [27] this strong oxidant also attacks the bulk debris to form significant amounts of hydrogen. The vapor film surrounding the coarse fragments at this state is not steam, but rather a mixture of steam and hydrogen.

The sum of the partial pressures of ruthenium-bearing gases in equilibrium with pure ruthenium or ruthenium dioxide is shown in Figure 4.5 as a function of temperature for several values of the ratio of hydrogen partial pressure to steam partial pressure. Also shown is the partial pressure of ruthenium-bearing gases when the atmosphere is air. Clearly, when even small hydrogen partial pressures exist, the partial pressure of ruthenium-bearing gases is significantly depressed relative to the partial pressure in the air. Because hydrogen is formed, the volatility of ruthenium must be quite low during the first stage of the steam explosion process. Total release of ruthenium during this stage must also be low since the volatility is low and the duration of the coarse fragmentation and intermixing process is short (~0.2 s).

The steam explosion comminutes the debris into fine particles. These particles have been characterized in some of the steam explosion research programs. In general, the characterization has been by sieve analysis over the size range of 10^4 to 45 µm. Some typical size distribution data are shown in Figure 4.6. No characterizations of the debris in the size

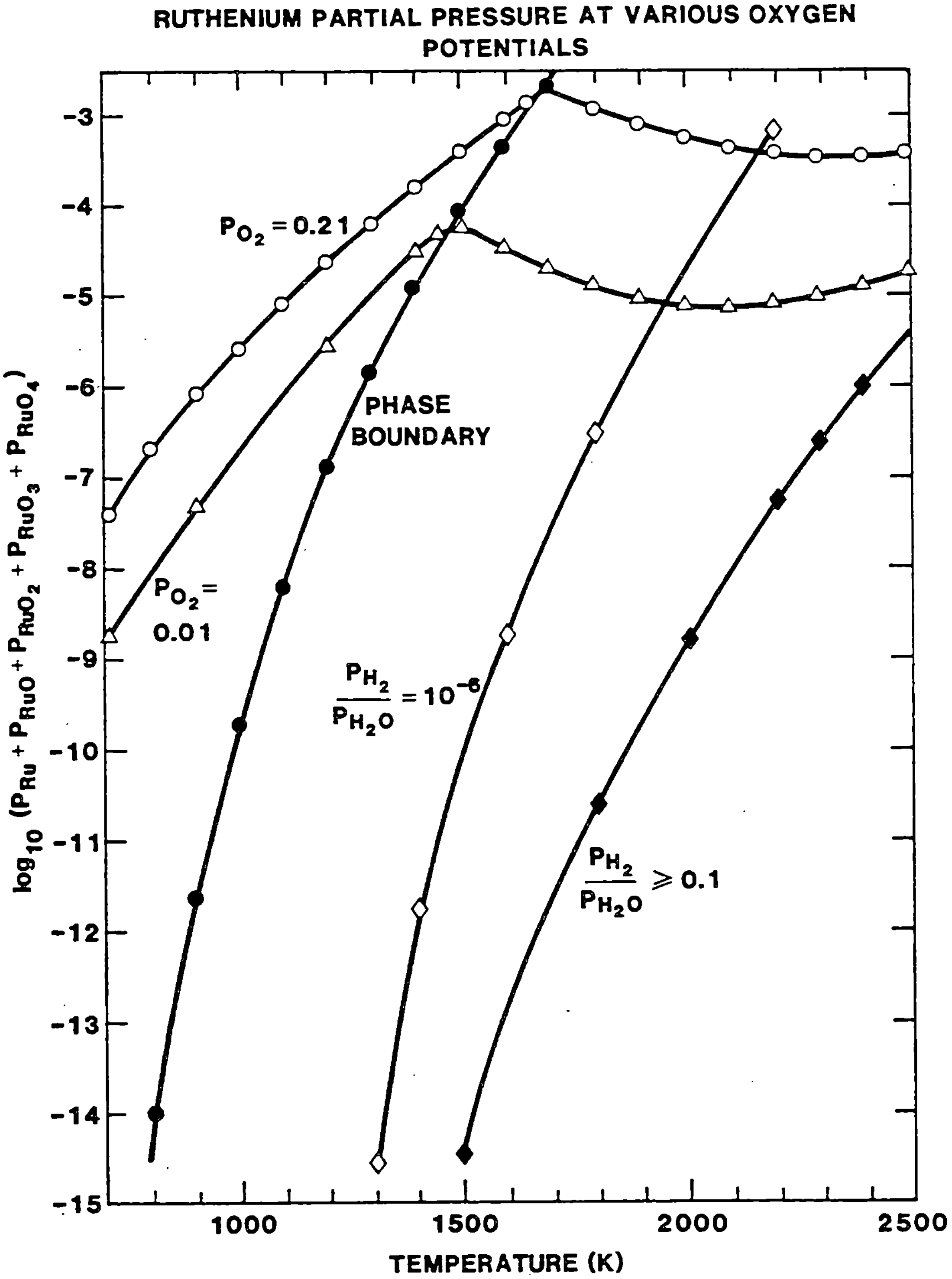

Figure 4.5. The Sum of the Partial Pressures of Ruthenium-Bearing Vapors in Various Atmospheres as a Function of Temperature.

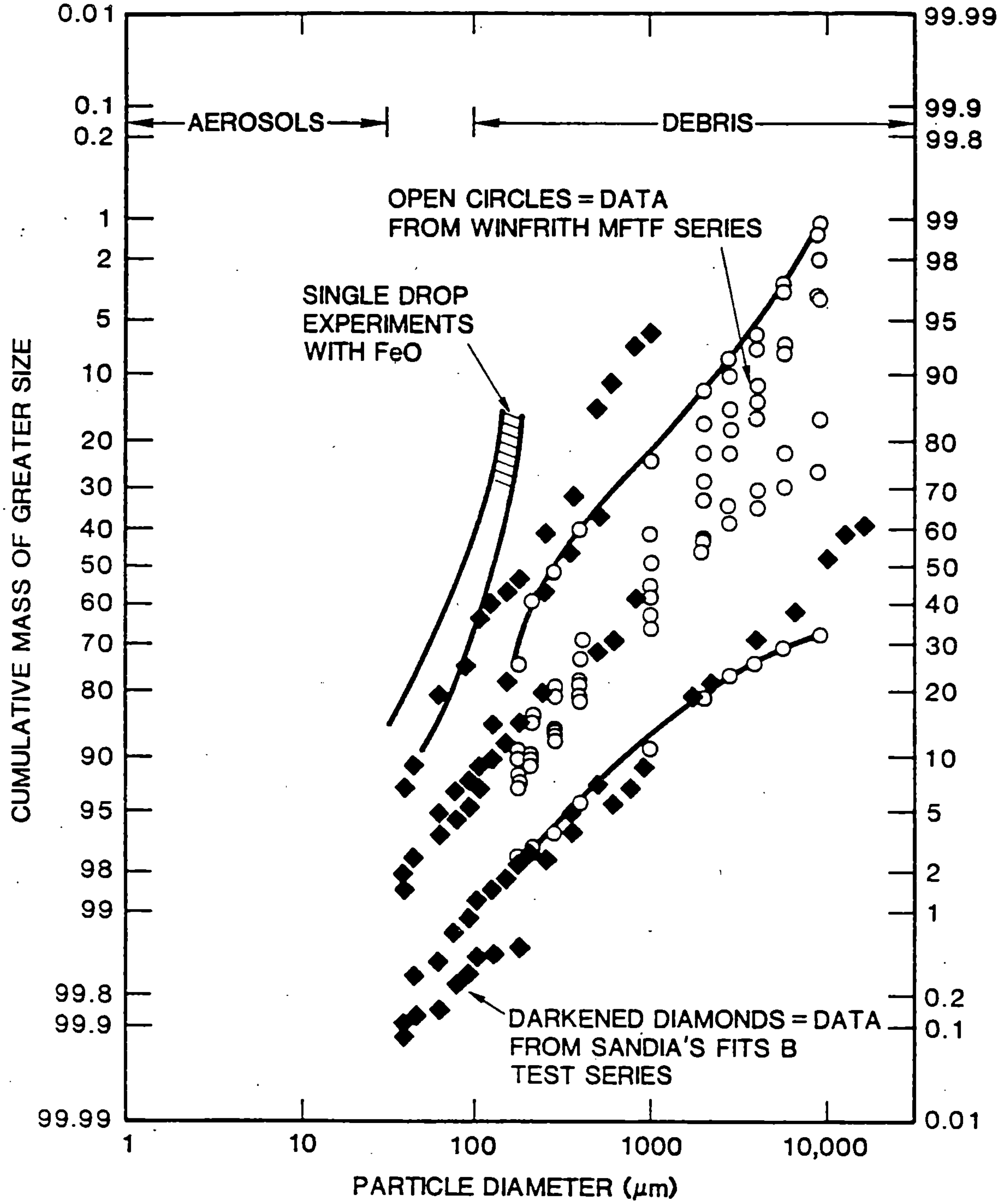

Figure 4.6. Size Distribution of Debris Formed by Melts Involved in Steam Explosions.

interval typical of aerosols that will remain suspended for long periods of time have been reported. If the characterization of the debris size distribution as log-normal is accepted, then it is possible to estimate the amount of material in the aerosol size range (taken here, arbitrarily, to be < 38 µm). It is apparent from such estimates that aerosol formation by steam explosions is an insignificant contributor to fission product release.

The route to significant ruthenium release from debris formed by steam explosions lies through chemical reaction of the debris to form volatile ruthenium oxides. If the steam explosion takes place within the reactor pressure vessel and the vessel does not rupture, the atmosphere encountered by the ejected debris is a mixture of steam and hydrogen. The suppression of release described above for the first stage of the steam explosion process will also be operative for debris in the vessel atmosphere. The suppressive effect of the atmosphere is likely to be stronger since the debris will, of necessity, be cooler than the coarse fragments formed in the first stage of a steam explosion.

When the steam explosion takes place ex-vessel, the chemical constraint on ruthenium release is not present. To estimate the release possible when debris is injected into an air atmosphere, it is necessary to consider the kinetics of release. The kinetics will depend on the temperature of the debris and the surface area of the debris. Total release will depend on these factors and the time the particles are suspended in the containment atmosphere.

Recent analyses of the steam explosion process show that the time particles are suspended in the containment atmosphere is a critical factor that controls the release of ruthenium [28]. The mass weighted mean residence time of the particles of fuel is only a few seconds. Unless a strongly exothermic reaction can be triggered when these particles are injected into the containment atmosphere, there is insufficient time to achieve releases exceeding a few percent.

The likelihood of causing the particulate material ejected during a steam explosion to burn is much less than the likelihood of igniting aerosol particles produced by pressurized ejection. The steam explosion particles are much coarser than the pressurized ejection particles; they have been cooled to lower temperatures because of their interaction with water; and they have already been extensively oxidized during early stages of the steam explosion process [27].

Though these arguments cannot be considered definitive in the absence of supporting experimental data, they are cause for questioning the rather high ruthenium release fractions cited in the Reactor Safety Study.

Recommendations for MELCOR Development of a Source Term Associated with Steam Explosions. The following recommendations are made concerning the treatment of the steam explosion source term in the MELCOR code:

1. The generation of aerosols during a steam explosion takes place over such a small period of time that the MELCOR model need not include a highly mechanistic description of the process.

2. Aerosols produced by the steam explosion can be assumed to amount to a constant fraction of the melt mass participating in the explosion. This fraction should be user adjustable. A default value of 0.2 percent would be appropriate.

3. The size of the aerosol should be user selected with a default value of 10 μm. The composition of the aerosol may be assumed to be the bulk melt composition.

4. There is no need to consider the aerosol produced by steam explosions to be enriched in volatiles. In latter versions of MELCOR, a more sophisticated treatment of aerosol composition may be adopted if ongoing research indicates a need.

C. Release During Core Debris/Concrete Interactions

The most frequently mentioned source of aerosols and fission products outside the reactor coolant system is that associated with core debris/concrete interactions. This source was recognized in the Reactor Safety Study. Experimental studies have verified the existence of the core debris/concrete interactions source term and established some important features of the source.

The Reactor Safety Study analysis of the core debris/concrete interaction source term considered only the release of radioactive constituents that were present in the debris when it penetrated the reactor vessel. Qualitative thermochemical arguments were used to define ultimate release fractions for various categories of fission products. These release fractions are listed in Table 4.4. The time-dependencies of fission product release were assumed to be the same for all fission products and to be of the form

$$\mathrm{VRF}_i(t) = \begin{cases} \mathrm{VRF}_i(\infty)\,[1 - \exp(-0.0231t)] \text{ for } & 0 \text{ min} \leq t \leq 90 \text{ min} \\ \mathrm{VRF}_i(\infty)\,[0.87 + \frac{0.13}{30}(t-90)] & \text{for } 90 \text{ min} < t \leq 120 \text{ min} \end{cases}$$

Table 4.4

Release During Core Debris Interactions with Concrete as Estimated in the Reactor Safety Study

Fission Product	Release*
Xe, Kr	100
I, Br	100
Cs, Rb	100
Te, Se, Sb	100
Ru, Rh, Pd, Mo, Te	5
Ba, Sr	5
La, Nb, Eu, Y, Ce, Pr Pm, Sm, Np, Pu, Zr, Nb	1

* % of the amount remaining in the core debris at the start of interactions with concrete

where $VRF_i(t)$ = release fraction of the i^{th} element at time t(min.).

$VRF_i(\infty)$ = release fraction of the i^{th} element listed in Table 4.4.

Authors of the Reactor Safety Study were aware that materials other than fission products would vaporize to form aerosols during core debris interactions with concrete. Experimental investigations of these interactions have yielded some information both on fission product release and the formation of aerosols by constituents of concrete, steel and UO_2 [29]. The total aerosol production rate has been found to vary from about 5-10 g/m^3 of gas (STP) evolved from the interaction of concrete with melts at 1500-1700°C (see Figure 4.7) to over 150 g/m^3 when melts in contact with concrete are at about 2400°C. Aerosol generation has been found to correlate with the superficial velocity of gas sparging through the melt. The contribution of non-fuel species to the aerosol has been observed to be 60-90 percent of the total aerosol in experiments with compositionally prototypic melts.

Murfin and Powers [30] developed an empirical correlation of the experimental data for total aerosol production during melt/concrete interactions:

$$[A] = 10^4 (24V_s + 3.3) \exp [-19000/T(K)]$$

where [A] = mass concentration (g/m^3 STP) of aerosol in gas evolved during core debris/concrete interactions

T = absolute temperature (K)

V_s = superficial velocity of gas sparging through the melt (m/s)

When this correlation and an experimentally determined aerosol composition are applied to a reactor accident, 1-10 tons of aerosol are predicted to form. Release fractions for some fission product isotopes (La, Ce, Ba, Sr, and Mo) are predicted to be much higher than estimated in Reactor Safety Study.

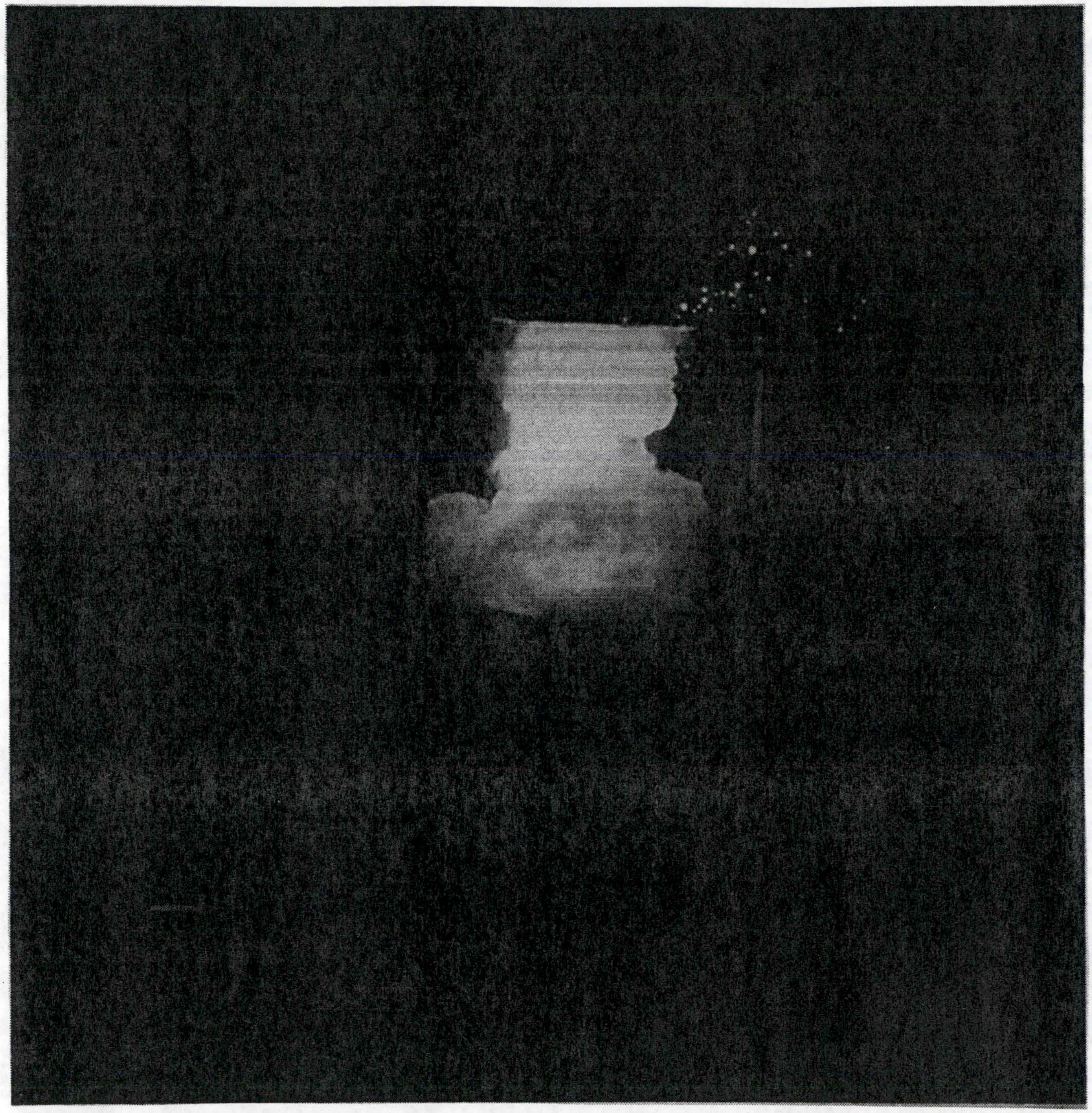

Figure 4.7. Aerosol Production During Interaction of 200 Kg Molten Steel at 1700°C With Concrete.

Application of the empirical correlation to accident situations involves such strenuous extrapolation that it is difficult to attach much confidence to the resulting predictions. The predictions do form a basis for questioning the Reactor Safety Study estimates of the release to associate with core debris/concrete interactions.

Powers and Brockmann [31] have attempted to formulate a mechanistic model of aerosol formation during core debris interactions with concrete. The operative physics embodied in their model includes:

1. release is assumed to occur both by vapor formation processes and by the mechanics of bubbles breaking at the surface of a melt.
2. the rate of vapor formation depends on the amount of free surface available, mass transfer in the liquid phase, surface vaporization, and gas phase mass transport.
3. the amount of surface available for vaporization is dominated by that created by gases sparging through the melt.
4. vapor formation processes are considered for species in ternary M-O-H systems where M is the fission product of interest.
5. gases and liquid mixtures are assumed to be ideal.
6. the model recognizes 250 chemical species made from 27 elements. The elements recognized in the model are shown in Table 4.5.

Examples of the predictions from the mechanistic model called "VANESA" are shown in Figure 4.8, which is a plot of the estimated rate of aerosol production against the time from the start of core debris interactions with concrete. The calculations were done for the Surry Nuclear Power Plant. The reactor cavity concrete was assumed to be siliceous in nature. The molten core debris was assumed to have spread over an area of 55.7 m^2 at the start of the core debris/concrete interactions. The nature of the core debris interactions in the cavity were estimated with the CORCON code [32]. For the aerosol production rate designated "ANS-Surry-NoZr", it was assumed that all the Zircaloy clad in the reactor core had been oxidized to ZrO_2 prior to the onset of core debris interactions with concrete. For the estimate designated "ANS-Surry-1/2Zr", it was assumed that only half the Zircaloy was oxidized. Also shown in the figure are aerosol generation rates predicted for the Surry plant with the

Table 4.5

Elements and Vapor Species Considered in the VANESA Code

Element	Vapor Species
Hydrogen	H, H_2, OH, H_2O
Oxygen	O, O_2, OH, H_2O, CO, CO_2
Carbon	CO, CO_2
Iron	Fe, FeO, FeOH, $Fe(OH)_2$
Chromium	Cr, CrO, CrO_2, CrO_3, H_2CrO_4
Nickel	Ni, NiO, NiOH, $Ni(OH)_2$
Molybdenum	Mo, MoO, MoO_2, MoO_3, H_2MoO_4, $(MoO_3)_2$, $(MoO_3)_3$
Ruthenium	Ru, RuO, RuO_2, RuO_3, RuO_4
Tin	Sn, SnO, SnOH, $Sn(OH)_2$, SnTe
Antimony	Sb, SbOH, $Sb(OH)_2$, Sb_2, Sb_4, SbTe
Tellurium	Te, TeO, TeO_2, Te_2O_2, H_2TeO_4, Te_2, H_2Te, SnTe, SbTe, AgTe
Silver	Ag, AgOH, $Ag(OH)_2$, AgTe
Manganese	Mn, MnOH, $Mn(OH)_2$
Calcium	Ca, CaO, CaOH, $Ca(OH)_2$
Aluminum	Al, AlO, AlOH, Al_2O, AlO_2, Al_2O_2, $Al(OH)_2$, AlO(OH)
Sodium	Na, Na_2, NaOH, $(NaOH)_2$, NaO, NaH
Potassium	K, K_2, KOH, $(KOH)_2$, KO, KH
Silicon	Si, SiO, SiO_2, SiOH, $Si(OH)_2$, $Si(OH)_4$
Uranium	U, UO, UO_2, UO_3, H_2UO_4
Zirconium	Zr, ZrO, ZrO_2, ZrOH, $Zr(OH)_2$
Barium	Ba, BaO, BaOH, $Ba(OH)_2$
Strontium	Sr, SrO, SrOH, $Sr(OH)_2$
Cesium	Cs, Cs_2, CsOH, $Cs_2(OH)_2$, Cs_2O, CsO, CsI
Lanthanum	La, LaO, LaOH, $La(OH)_2$
Cerium	Ce, CeO, CeOH, $Ce(OH)_2$
Niobium	Nb, NbO, NbO_2, NbOH, $Nb(OH)_2$
Iodine	CsI, HI, I_2, I

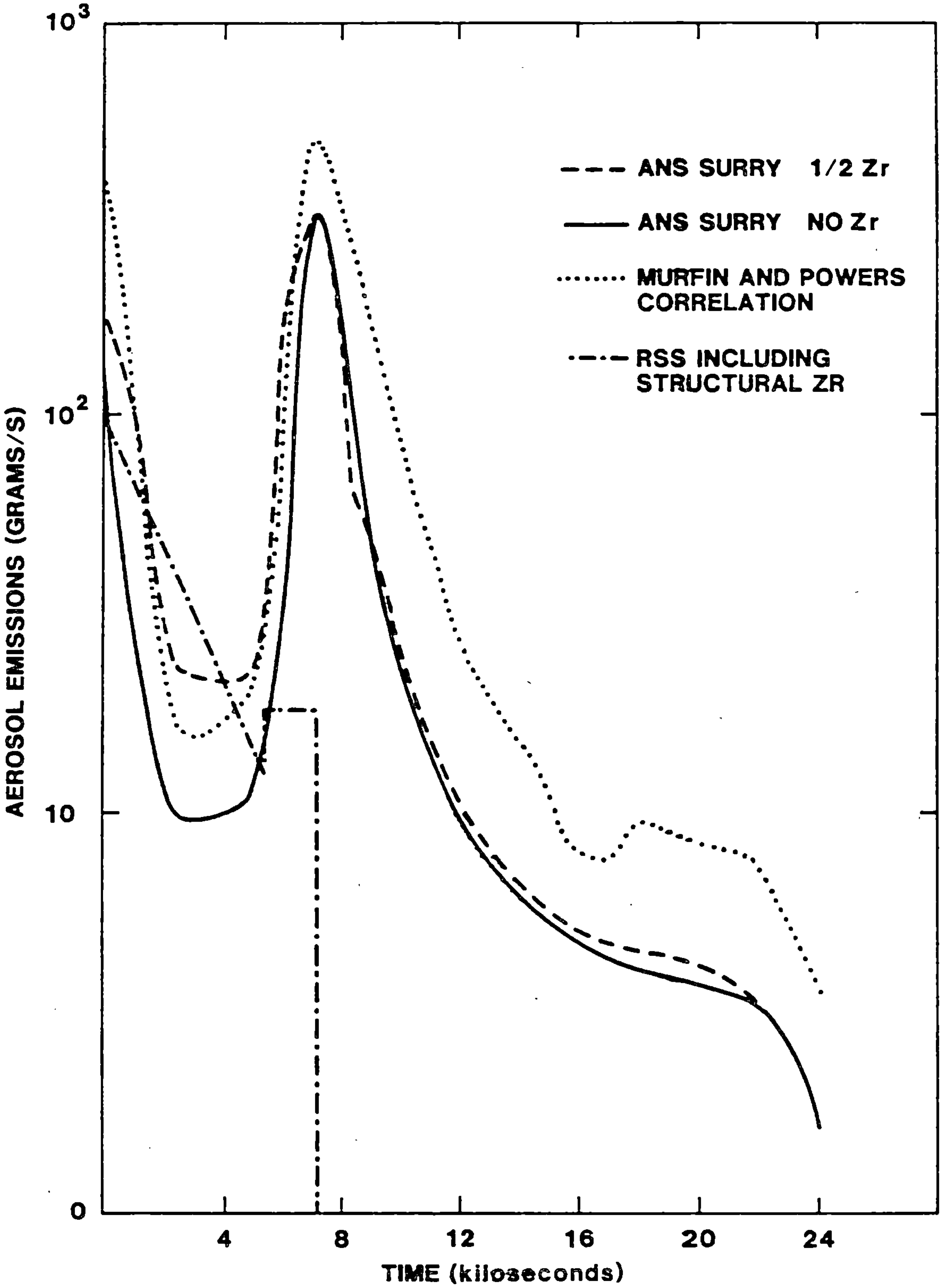

Figure 4.8. Aerosol Production Rates Estimated for Core Debris/ Concrete Interactions at the Surry Plant.

empirical correlation mentioned above and with the release model used in the Reactor Safety Study. Zirconium from the fuel cladding, as well as fission product zirconium, were considered in making the release rate estimate with the Reactor Safety Study model. Otherwise, structural or concrete materials were neglected in estimates with this model.

The mechanistic model predicts that initially high aerosol generation rates arise. These rates fall because the melt is quenched somewhat after entering the reactor cavity. Fission product decay heating and, especially in the "ANS-Surry-1/2Zr" case, heat generated as the metallic phases of the melt are oxidized by gases from the decomposing concrete, cause the melt temperature to rise. Aerosol generation increases with melt temperature. Eventually, a maximum melt temperature and maximum aerosol generation rate are reached. Following this maximum, the temperature of the melt slowly decreases. Aerosol generation also decreases but much more dramatically because of the inherently exponential dependence of vaporization on temperature.

The mechanistic model predicts that core debris containing metallic zirconium will produce aerosols at greater rates than does core debris in which all zirconium has been oxidized. The effect arises both because the oxidation of zirconium keeps the melt hotter and because metallic zirconium chemically reduces some melt species to more volatile oxidation states. Oxidation of residual zirconium by steam from the concrete is complete at about the time of maximum aerosol generation rate. Once the zirconium has been completely oxidized, predictions for the "ANS-Surry-NoZr" and "ANS-Surry-1/2Zr" cases are quite similar.

The mechanistic model of aerosol generation and fission product release during core debris/concrete interactions is of too recent a vintage to have been subjected to extensive validation by comparison with experimental results. It is encouraging that there is generally good agreement between the estimates of aerosol generation for the Surry case obtained with the Murfin and Powers correlation and the mechanistic model predictions. Nowhere do estimates obtained with this correlation differ by more than about a factor of two from the model predictions. At early times, estimates obtained with the empirical correlation are bracketed by the two mechanistic predictions. At late times, when aerosol generation rates are low, the empirical correlation yields higher estimates than does the mechanistic model.

Estimates of aerosol generation obtained with the mechanistic model or the empirical correlation are unlike predictions obtained with the Reactor Safety Study model. The most important difference is that these more recent descriptions of the process show aerosol generation to continue far longer than is predicted by the Reactor Safety Study model. In fact, aerosol generation predicted by the Reactor Safety Study model has stopped when mechanistic predictions indicate the aerosol generation rate has reached a maximum. Predictions of the amount of aerosol suspended in the reactor containment atmosphere and the amount of aerosol that escapes should the containment rupture will differ dramatically depending on which of these models is used to estimate the aerosol source term from core debris interactions with concrete.

Other differences arise between the mechanistic model and the Reactor Safety Study model with regard to the releases of individual elements. The fraction of tellurium remaining in the core debris as predicted by the two models is shown as a function of time in Figure 4.9. The Reactor Safety Study model predicts the release of this relatively volatile element to be more extensive and more rapid than does the mechanistic model. The extents of Sr and Ba release predicted by the mechanistic and Reactor Safety Study models are shown as functions of time in Figure 4.10. For these elements, assumed to be present in the core debris as relatively non-volatile oxides, the mechanistic model predicts more rapid and more extensive release than does the Reactor Safety Study model.

Experimental studies necessary to validate and to improve these and other predictions of the mechanistic model are underway.

The mechanistic model includes a description of the effect an overlying pool of water would have on the source term of aerosols to the containment caused by core debris interactions. Such an effect was neglected in the Reactor Safety Study. The model, essentially a modification of the description of aerosol entrapment from bubbles passing through water formulated by Fuchs [33], is based on the following assumptions:

1. The overlying water pool is in film boiling over the core debris/concrete mixture. The water affects in no way the generation of aerosols from the melt. The aerosols evolve from the melt into the gas film between the melt and the water pool.

2. Aerosol-laden gas thermally equilibrates with the water pool in vapor film between the pool and the melt. The gases are assumed to be non-condensible.

3. The bubbles enter the pool at an initial size of 1 cm. There are no bubble-bubble interactions.

4. Entrapment of aerosols is by inertial deposition from internally circulating flows, diffusion of aerosols to the bubble walls and by sedimentation.

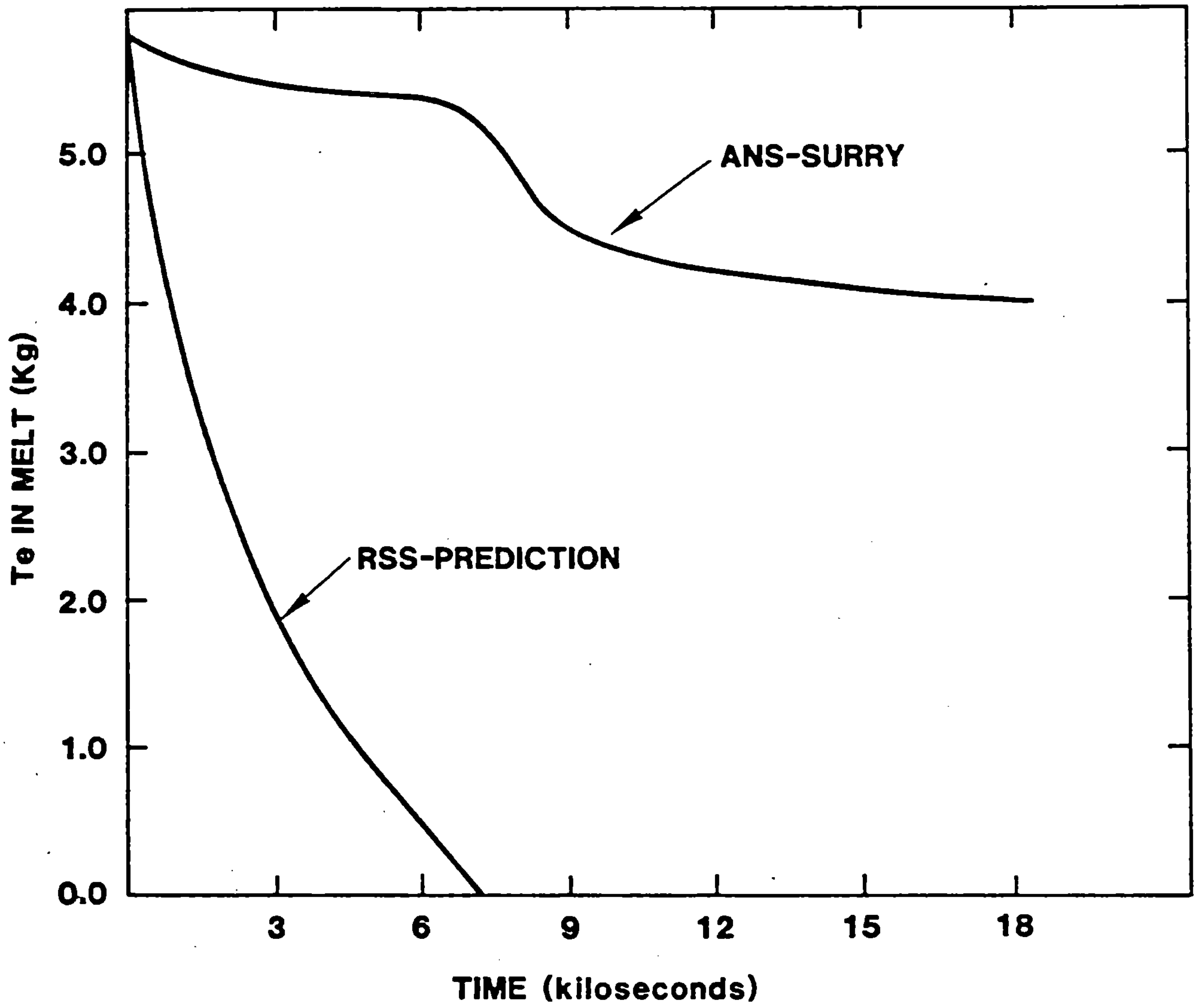

Figure 4.9. Estimates of the Amount of Tellurium Remaining in the Core Debris During Interactions with Concrete.

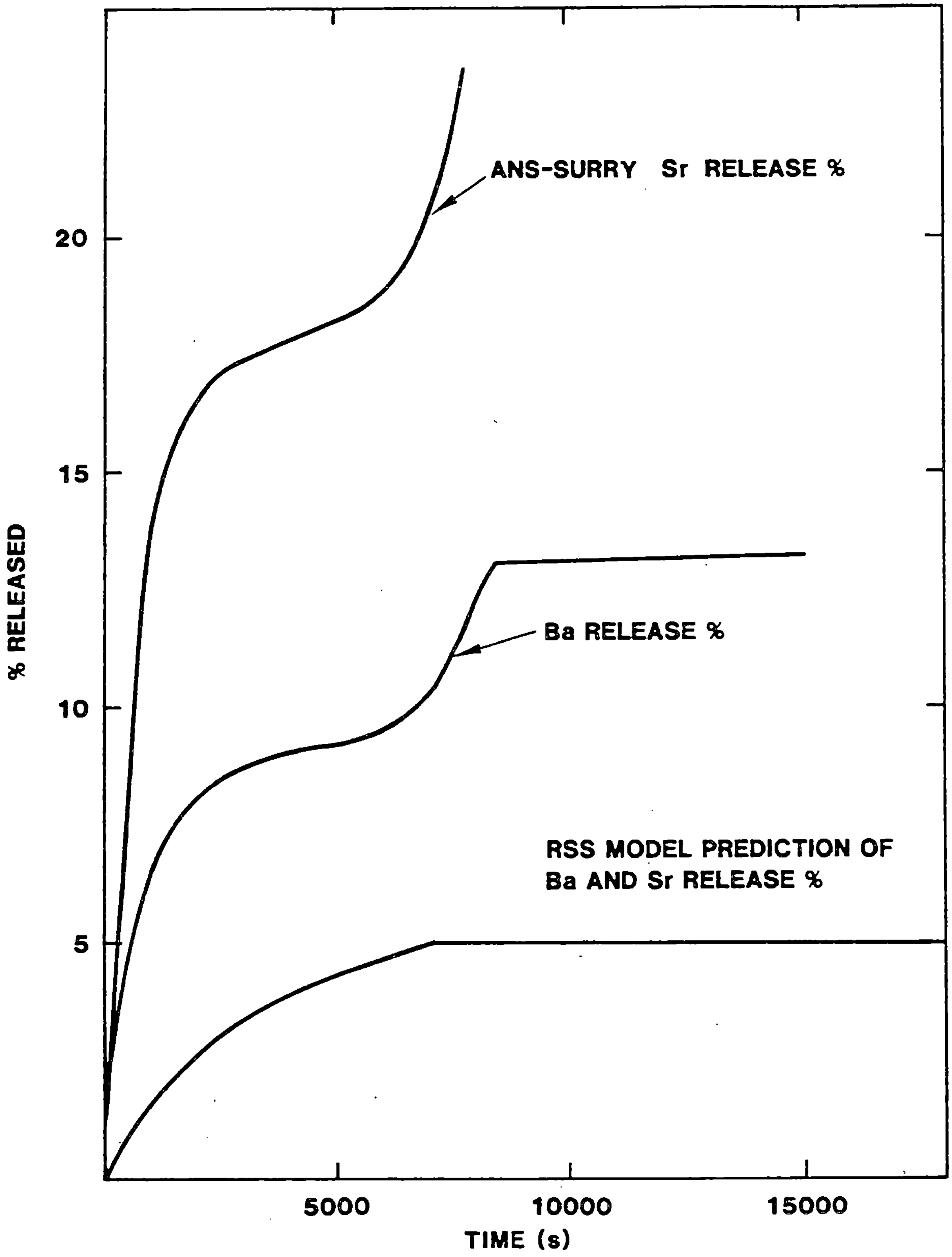

Figure 4.10. Estimates of the Release of Ba and Sr During Core Debris/Concrete Interactions.

The expansion of the bubble caused by the loss of hydrostatic head as the bubble rises is taken into account:

$$\frac{V(x)}{V_o} = P_{atms} + \frac{x}{1033.6}$$

where

$V_o = \frac{4}{3} \pi R_o^3$

$R_o = 0.5$ cm

P_{atms} = absolute pressure of the containment atmosphere (atms)

x = distance from the top of the water pool (cm)

$V(x)$ = volume of the bubble at $x = \frac{4}{3} \pi R(x)^3$

Then, if n is the number of aerosol particles within the bubble,

$$\frac{dn}{dt} = -(\alpha_i + \alpha_s + \alpha_d)n$$

where t = time

α_i = impaction coefficient = $\frac{9V\tau}{2R^2}$

α_s = sedimentation coefficient = $\frac{3g\tau}{4RV}$

α_d = diffusion coefficient = $1.8\ (D/VR^3)$

V = bubble rise velocity

g = gravitational constant

τ = relaxation time = $\pi \, Dp^3 \rho_p B/6$

ρ_p = particle material density

D = kTB

k = Boltzmann's constant

T = absolute temperature

B = $C(D_p)/3\pi\mu_g D_p$

D_p = particle diameter

μ_g = gas viscosity

$$C(D_p) = 1 + \frac{2\lambda}{D_p}\,[1.257 + 0.4 \exp(-0.55\, Dp/\lambda)]$$

λ = molecular mean free path in gas

Examples of the decontamination of the aerosol-laden gas by an overlying pool as a function of particle size and as a function of pool depth are shown in Figures 4.11 and 4.12. Log-normally distributed particle sizes were assumed to make the decontamination calculations shown in these figures. Decontamination factors used in these figures are defined as the ratio of mass input to mass that passes through the pool. Note that a minimum occurs in the decontamination factor when plotted against particle size. Diffusion is predominantly responsible for the removal of particles of sizes less than this minimum. Particles larger than the minimum decontamination efficiency size are removed predominantly by impaction and sedimentation. The particle size range where little decontamination occurs broadens as the geometric standard deviation of the log-normal size distribution increases.

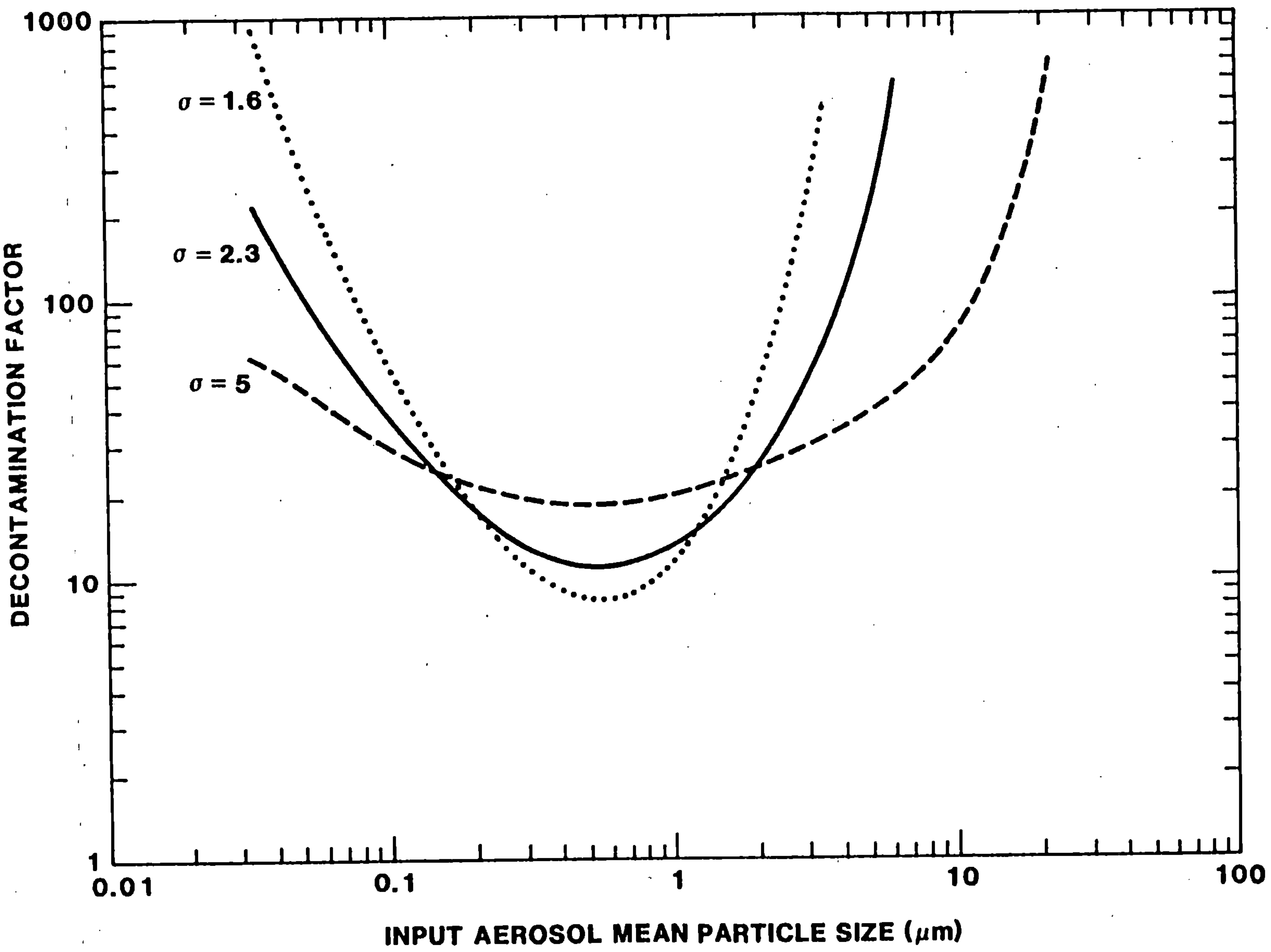

Figure 4.11. Decontamination of Aerosol-laden Gas by a Saturated Water Pool Seven Meters Deep as a Function of Mean Particle Size.

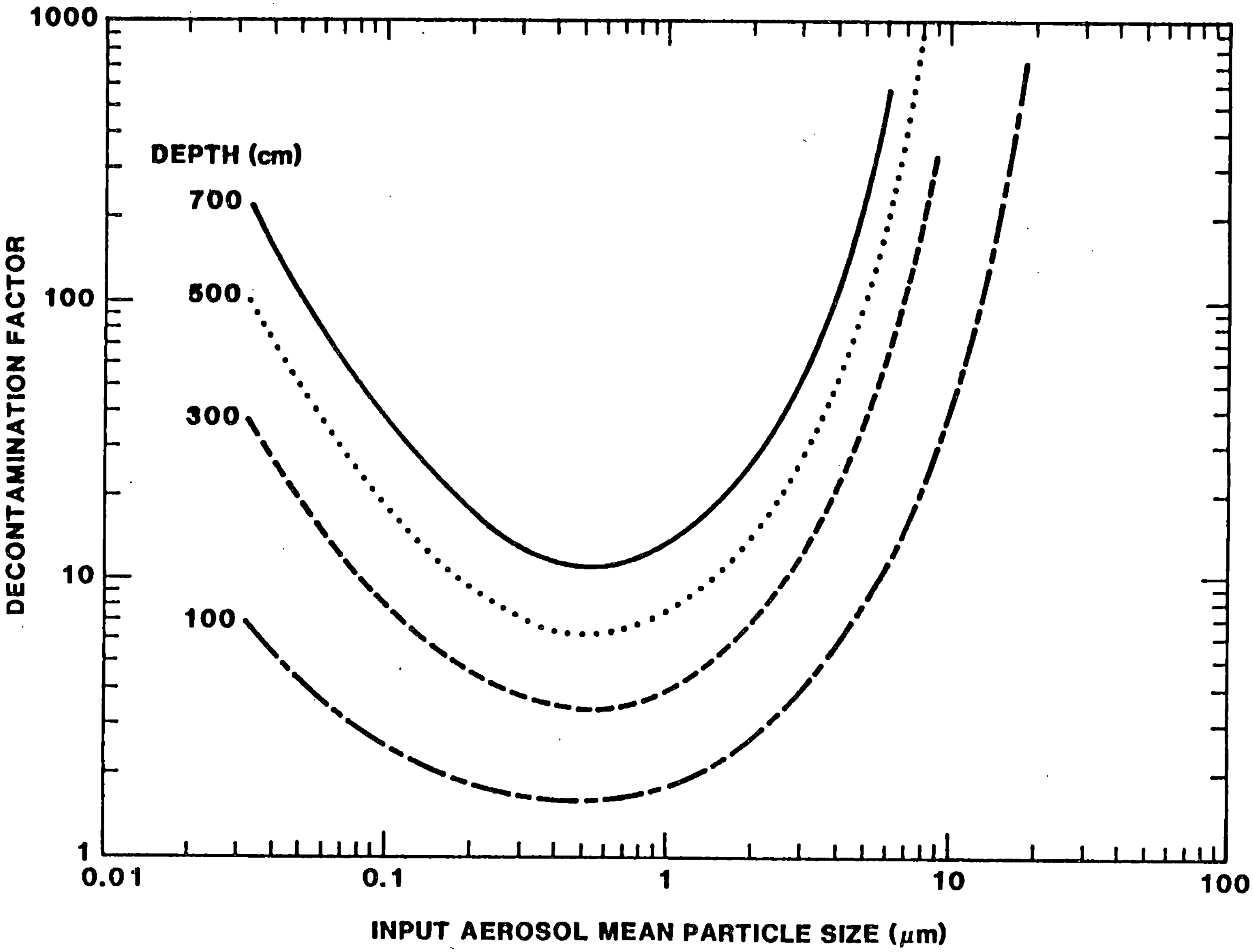

Figure 4.12. Decontamination of Aerosol-laden Gas by a Saturated Water Pool of Various Depths.

Recommendation for the MELCOR Model of the Source Term From Core Debris/Concrete Interactions. At this stage in development, the MELCOR code can use a relatively crude model of the source term associated with core debris interactions with concrete. To this end, the following recommendations are made:

1. The rate of aerosol mass generation should be obtained from the Powers-Murfin correlation.

2. The aerosol size distribution can be taken a log-normal with a geometric standard deviation of 2.3 and a mean size given by the Brockmann equation:

$$D_p = 0.266\ (A/\rho)^{1/3}$$

   where D_p is the particle diameter in micrometers, A is the aerosol concentration is g/m^3-STP, and ρ is the material density of the aerosol in g/cm^3.

3. Aerosol compositions can be provided by the user. Default compositions are shown in Table 4-6. These compositions change with melt temperature and the time after the start of core debris interactions with concrete. A check will have to be made in the code to assure inventories are not exceeded. Eventually these default compositions will have to be replaced with more smoothly varying functions of the melt properties.

4. The effect of an overlying water pool can be satisfactorily described by the modified Fuchs model.

D. Fission Product Release by Leaching

The duration of vigorous core debris interactions with concrete is uncertain. Eventually, these interactions must stop and further erosion or thermal decomposition of the concrete cease. If the core debris has eroded through the basemat, then the core debris is susceptible to leaching by groundwater. Fission product release by this leaching process* is a long-term, low-level source of radioactivity that is probably much less a threat to the public than the intense, airborne sources discussed above [34].

---

* Basemat penetration may allow coolant waters containing radioactive material to drain from the plant into the groundwater system. This source of radioactivity is not considered here. It may, however, far exceed in importance to risk the in-plant radioactivity release by leaching.

Table 4.6

Default Compositions for Aerosol From Core Debris Interactions with Concrete

	Early in Time after start of core debris interactions with concrete	Late in Time after start of core debris interactions with concrete
	High Melt Temperature ($T > 2200K$)	
alkali metals	0.8 w/o as Cs	0
alkaline earths	3.6 w/o as BaO	3.3 w/o as BaO
halogens	0.2 w/o as I	0
chalcogens	0.3 w/o as Te	1.0 w/o as Te
Platinoids	3×10^{-5} w/o as Ru	1×10^{-5} w/o as Ru
early transition	17 w/o as FeO	12.6 w/o as FeO
tetravalents	4 w/o as CeO_2	1.6 w/o as CeO_2
trivalents	2.7 w/o as La_2O_3	1 w/o as La_2O_3
uranium	1.6 w/o as UO_2	0.8 w/o as UO_2
volatile main-group	20 w/o as Cd	0
main group	18 w/o as Sn	16 w/o as Sn
concrete	balance	balance
	Low Melt Temperature ($T < 2250K$)	
alkali metals	9 w/o as Cs	0
alkaline earths	3.3 w/o as BaO	0.2 w/o as BaO
halogens	8.5 w/o as I	0
chalcogens	0.3 w/o as Te	0.5 w/o as Te
platinoids	0	0
early transition	8.1 w/o as FeO	24 w/o as FeO
tetravalents	0.01 w/o as CeO_2	0.001 w/o as CeO_2
trivalents	4×10^{-6} w/o as La_2O_3	2×10^{-6} w/o as La_2O_3
uranium	0.06 w/o as UO_2	0.04 w/o as UO_2
volatile main group	10 w/o as Cd	0
main group	4 w/o as Sn	9.2 w/o as Sn
concrete	balance	balance

There have been few systematic studies of leaching of core debris/concrete mixtures expected at this final stage in a severe reactor accident. The core debris is usually considered a single phase solid in analyses of leaching. Recent work by Westrich [35] suggests that this would not be the case. Westrich found that when mixtures of UO_2, ZrO_2 and siliceous materials analogous to concrete were slowly cooled (<2 K/s), phase separation took place. The crystalline precipitates from the melt consisted of UO_2, MgU_2O_5, and ZrO_2, but not $ZrSiO_4$. The silica-rich liquid phase would eventually solidify as a glass. Plagioclase solid solutions ($NaAlSi_3O_8$ - $CaAl_2Si_2O_8$) were observed in high silica content systems.

Westrich examined the partitioning of fission products among the solid phases. He finds the fission products whose oxides favor the cubic fluorite structure, such as cerium and zirconium, preferentially partition into the cubic MgU_2O_5 phase. Alkaline earths remain in the glass phase. Fission products that as oxides form hexagonal structures enter both phases though concentrations are usually higher in the glass.

Braithwaite and Johnson [36] have examined the leaching of cesium and strontium from mixtures of "corium" and basaltic concrete. Leaching was done with distilled water and a saline solution to simulate sea water. Samples were leached for 3 days at 25 and 90°C. Over the leaching period 0.1-0.85 percent of the cesium was removed from the corium-concrete mixture and 0.68-2.55 percent of the strontium was removed. The temperature dependence of leaching was small, suggesting liquid phase diffusion was the rate controlling process.

Powers [37] conducted scoping studies of Mo, U, Zr, Th, Nb, La, Ce, Sr, and Cs leaching from mixtures composed of 34 percent UO_2, 5.1 percent Fe_3O_4, 5.1 percent Cr_2O_3 and 48 percent dehydrated basaltic concrete. Samples were leached in bombs for 1.5-200 hours at temperatures of 80-200°C. Leaching solutions of various compositions were used to simulate different groundwater chemistries. Conclusions from this scoping work included:

1. Cs, La, Ce and U were the most easily leached elements. Only upper bounds on Sr and Th leaching based on the detectability limits could be determined.

2. Solutions containing NaCl and saturated with $CaCO_3$ were not more effective leachants than distilled water.

3. Solutions containing sodium phosphate were very effective leachants especially for zirconium.

4. Ferric ion appeared to accentuate leaching. This could be because of the oxidation reaction:

$$UO_2 + 2Fe^{3+} \text{ â } UO_2^{2+} + 2Fe^{2+}$$

or the low pH created by the hydrolysis reaction:

$$Fe^{3+} + 2H_2O \text{ â } FeO(OH) + 3H^+$$

5. Chromate-containing solutions were not especially effective leachants, which suggests that oxidation of the UO_2 to soluble uranyl ions is not the primary leaching mechanism.

6. Colloidal suspensions were formed during many of the leaching experiments.

7. The surface area of the solid mixture increased during leaching due to the Zwiebelschale effect [38].

It is apparent, then, that slow leaching of a core debris-concrete mixture that has penetrated the reactor basemat is possible. The leaching may involve subtleties not considered in past analyses. It remains to be demonstrated, however, that leached fission products pose a sufficient threat to merit a more thorough study of the leaching process.

Recommendations to MELCOR Concerning the Treatment of Ex-vessel Leaching. At this juncture, there appears to be no generally satisfactory model for leaching core debris by groundwater. Nor does there appear to be a critical need to consider this process in MELCOR.

4.3 Secondary Fission Product Release in Containment

The term "secondary fission product release" is used here to signify the generation of airborne fission product vapors or aerosols by processes not directly connected to the behavior of the core debris. One such process, the combustion of debris to form aerosols in the reactor containment atmosphere, has been discussed above in connection with release associated with pressurized melt ejection. Three other, secondary, fission product release processes discussed here are:

1. resuspension of deposited or sedimented aerosols,
2. vapor partitioning of dissolved fission products, and
3. mechanical resuspension of fission products trapped in water.

There may be other important secondary mechanisms of fission product release to the containment atmosphere.

Grouping resuspension of aerosols and vapor partitioning of dissolved fission products under the heading secondary processes is not an assessment of the relative importance of these processes. Resuspension reverses the natural mitigation of the severe reactor accident source term brought on by the agglomeration, deposition and sedimentation of aerosols. Vapor partitioning reverses the natural or engineered mitigation of the source term brought on by water scrubbing of the containment aerosols. The secondary release processes, then, may play a critical role in determining the severe reactor accident source term. These processes may well undo much of the mitigation expected by many to substantially reduce the severe accident source term to levels well-below those estimated in the Reactor Safety Study.

A. Resuspension of Deposited Aerosols

Detailed, mechanistic treatments of the processes leading to the deposition and sedimentation of aerosols have proliferated in recent years. Treatments of the reverse process, aerosol resuspension, have not been attempted to a similar level of detail. This may be because resuspension involves analysis of both the aerosol particles and the surfaces to which they adhere whereas attention concentrates on only the aerosol particle in the analysis of aerosol deposition. It is likely that in any real situation, a dynamic equilibrium between aerosol deposition and resuspension develops. Throughout most phases of a reactor accident, the rate of resuspension is sufficiently small that it can be neglected or accounted for in an approximate manner as an inefficiency in the deposition process.

There are a few instances in hypothesized nuclear reactor accidents in which wholesale aerosol resuspension must be considered:

1. blowdown of the reactor coolant system
2. in-vessel fuel/coolant interactions that lead to high steam generation rates
3. catastrophic depressurization of the containment building.

In these instances, high gas velocities arise near aerosol-coated surfaces. The surfaces may experience sudden accelerations. High gas velocities and sudden surface acceleration are conducive to efficient particle re-entrainment. Such re-entrainment could reverse temporarily the natural mitigation of the source term produced by aerosol agglomeration, settling and deposition processes.

Aerosol particles are held to surfaces by Van der Walls forces, electrostatic forces, and the surface tension forces of liquid films. It is useful to distinguish between aerosols bound to dry surfaces and aerosols bound to wet surfaces because of the radical differences in adherence forces. The adhesive force between a particle and a surface can be defined as:

$$F_{ps} = H\ D_p$$

where H is a constant and D_p is the particle diameter. For dry aerosols, H is on the order of 1-60 dyne/cm (see Table 4.7). The adherence force does vary over at least 2 orders of magnitude, depending on the peculiar nature of the particle and the surface (see Table 4.8). The irregularity of the surface may contribute to some of this variability (see Table 4.9). When the particle is bound to a surface by a liquid film, H is on the order of 400 dyne/cm.

There is a gradation between the extremes posed by the classification of systems as either "dry" or "wet". As shown in Figure 4.13, the adherence of a particle to a surface increases with relative humidity once a critical humidity (65 percent relative) is exceeded.

Some data for the resuspension of glass spheres on stainless steel exposed to flowing gas are shown in Figure 4.14. At low gas velocities (< 5 m/s) some small resuspension occurs. The extent of resuspension does not increase much with gas velocity until a critical velocity is achieved. Then entrainment increases sharply with flow velocity to 40-70 percent. Once this plateau in the entrainment efficiency is reached, entrainment is again relatively insensitive to gas velocity. It appears then that sudden increases in flow velocity will produce some entrainment, but complete entrainment of all deposited aerosols will be difficult to achieve.

The force on deposited aerosols produced by flowing gas is given by:

$$F = 1/2\ \rho_g\ U_\ell^2\ C\ A_p$$

where ρ_g = gas density

U_ℓ = local gas velocity

$A_p = \pi Dp^2/4$

$C = [2.87 + 1.58 \log_{10} (x/D_p)]^{-2}$ for $10^2 < x/D_p < 10^6$

Table 4.7

Comparison of Air Flow and Acceleration as Mechanisms for Aerosol Removal [40]

Particle Size (μm)	Force (dynes) Required to Achieve 75% Removal by	
	Air Flow	Centrifugation
10.6 - 21.2	0.0195	0.016
21.2 - 31.8	0.056	0.060
31.8 - 42.4	0.11	0.21
42.4 - 53	0.11	0.26

Table 4.8

Effects of Particle Composition and Surface Characteristics on Particle-Surface Adherence [41]

50μ Particles of	Force (dynes) Required to Remove 98% of the Particles from a Surface of			
	Aluminum	Brass	Glass	Enamel
glass	0.5	2.85	1.83	3.63
sand	6.60	0.45	0.06	6.34
charcoal	0.57	0.32	0.94	2.30

Table 4.9

Effect of Surface Roughness on Particle Adherence [39, 42]

Mean Height of Surface Irregularities (Å)	Relative Particle Adhesion
150	100 (a)
1000	79 (a)
4000	51 (a)
100000	0 (a)
2160	100 (b)
2920	67 (b)
3430	59 (b)
4826	45 (b)

(a) Adhesion of glass particles to a glass surface at 100% relative humidity.

(b) Adhesion of quartz particles to Pyrex glass.

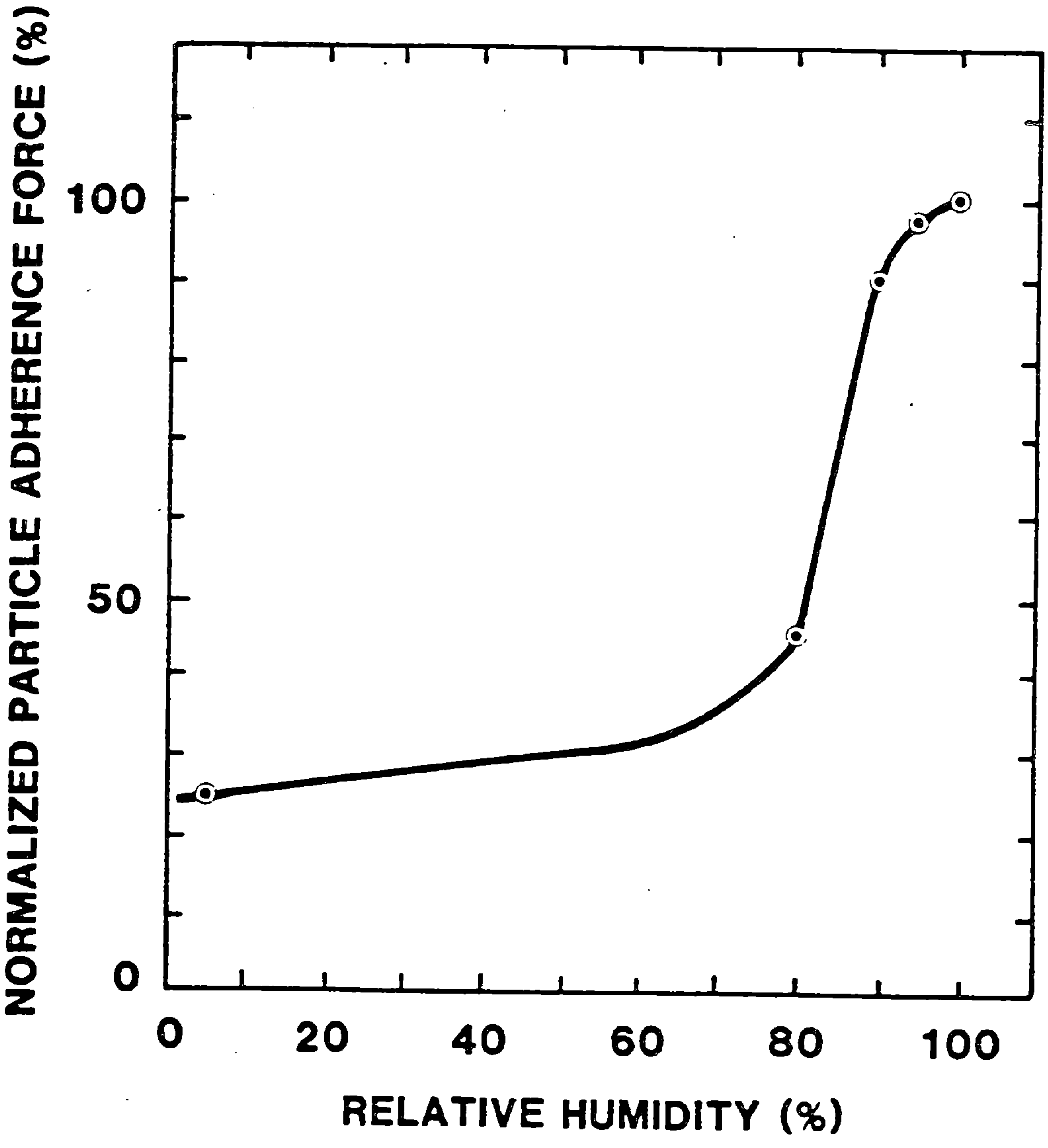

Figure 4.13. Dependence of Normalized Particle Adherence Force on Relative Humidity.

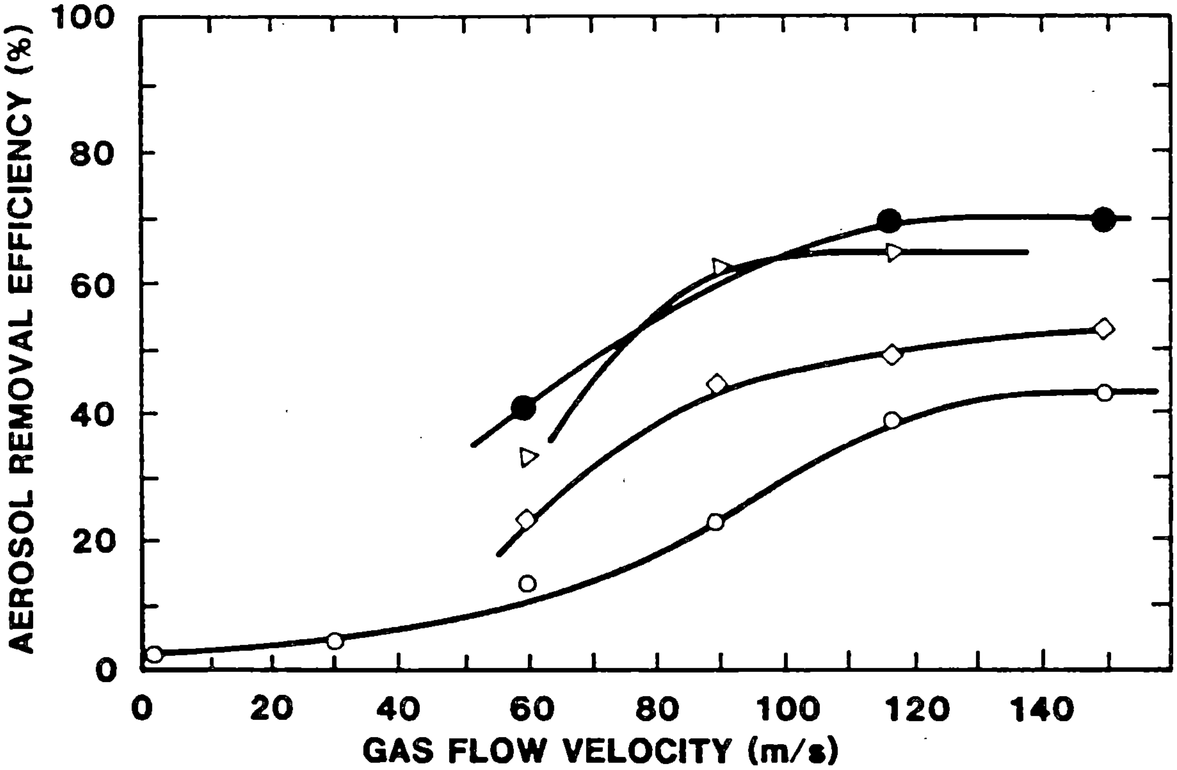

Figure 4.14. Resuspension of Glass Particles From a Stainless Steel Plate as a Function of Gas Velocity and Particle Size (• = 3 µm, Δ = 4 µm, □ = 1.2 µm, o = 20 - 40 µm).

x = distance along a surface where re-entrainment begins.

Notice that the local gas velocity, as opposed to the free-stream or bulk velocity is used in this description of the forces. Because this local velocity will depend on both the surface geometry and the aerosol deposit geometry, it is most difficult to estimate for reactor accident situations.

Brockmann [23] has advocated using an equation derived by equating binding forces between the surface and aerosol and the flow forces on the aerosol as a criterion for re-entrainment:

$$U_{Re-ent} > \frac{8H}{\pi\rho_g D_p C} + \frac{4f\rho_p g D_p}{3C\rho_g}$$

where f = friction factor = 0.2; C has a typical value of 0.01 and U is the free stream velocity. This criterion indicates re-entrainment of dry, 1 µm particles occurs at flow velocities of about 2 m/s. Brockmann asserts that once the criterion is met, re-entrainment will be 90 percent complete. The criterion also indicates that wet aerosols are unlikely to be entrained by gas flows arising in nuclear reactor accidents.

Particle removal by acceleration of surface has received some study in nonnuclear contexts. This mechanism of particle resuspension is often overlooked in the analysis of severe reactor accidents. In view of the many dynamic events postulated to occur during severe reactor accidents, this is likely to be an important process. Where comparisons have been made, the forces to remove particles by gas flow entrainment or by acceleration agree to within about a factor of two (see Table 4.7)

Recommendations to MELCOR Concerning Aerosol Particle Re-entrainment

1. MELCOR should allow for re-entrainment of aerosol particles during blowdown of the reactor coolant system.

2. Since particle deposits in the reactor containment are wet it is probably unnecessary to treat particle re-entrainment during pressurization of the containment.

3. The criterion for re-entrainment during vessel depressurization is:

$$U > \frac{258H}{\rho_g D_p} + \frac{26\rho_p g D_p}{\rho_g}$$

where H is a user supplied force constant with a default value of 1 dyne/cm.

4. The extent of re-entrainment is also a user supplied constant with a default value of 90 percent.

5. No recommendation is made concerning particle resuspension caused by surface acceleration save that it should be noted as a possibility.

B. Secondary Release From Water

One of the most important causes of source term mitigation is the entrapment of radioactive species in water. Mitigation of this sort can arise at many points in a severe reactor accident. Effluent from the core may have to pass over or through water as it is carried through the primary system; thus, an opportunity to partition between the liquid and the vapor is presented. For boiling water reactors, radioactive species may have to pass through the steam suppression pool before they can enter containment. Once in containment, there will very likely be large bodies of water to absorb radioactive species. Operation of containment sprays can sweep the containment atmosphere of suspended vapors or particles.

The mitigation of the source term that can be provided by water depends not only on the efficiency with which water can entrap radioactive species, but also the permanence of the entrapment. In this section, some of the mechanisms available to reverse water entrapment of radioactive materials are described.

Iodine Partitioning. Modern perceptions concerning the severe reactor accident source term hold that fission product iodine is liberated from the core and carried through the reactor primary system as iodide--probably cesium iodide--rather than as iodine gas. With few exceptions, iodides are quite soluble in water. Dissolution of any iodides in water would mitigate possible airborne release of the iodine from containment.

Iodide (I^-) in aqueous solution can be oxidized to volatile iodine (I_2) or to another soluble anion, iodate (IO_3^-). Some of the relevant chemical reactions and their associated equilibrium constants at 298K are shown in Table 4.10.

Table 4.10

Some Relevant Solution Phase Equilibria

Reaction	Equilbrium Constant
$2H^+ + 2I^-(aq) + 1/2\ O_2 \rightleftarrows I_2(aq) + H_2O$	$[I_2]/[H^+]^2[I^-]^2\ P_{O_2}^{1/2} = 2.6x10^{23}$
$2I_2(aq) + 2H_2O + 5O_2 \rightleftarrows 4IO_3^-\ (aq) + 4H^+$	$[IO_3^-]^4\ [H^+]^4/[I_2]^2\ P_{O_2}^5 = 9.4x10^{16}$
$I_2(aq) + H_2O \rightleftarrows H^+ + I^-(aq) + HOI\ (aq)$	$[H^+]\ [I^-]\ [HOI]/[I_2] = 4.04x10^{-13}$
$HOI(aq) \rightleftarrows H^+ + OI^-$	$[OI^-]\ [H^+]/[HOI] = 5x10^{-13}$
$H_3BO_3 \rightleftarrows H^+ + H_2BO_3^-$	$[H^+]\ [H_2BO_3^-]/[H_3BO_3] = 6.4x10^{-10}$
$I_2(aq) \rightleftarrows I_2(g)$	$P_{I_2}/[I_2] = 0.303$
$5Ag^+ + 3I_2 + 3H_2O \rightleftarrows 5AgI(s) + IO_3^- + 6H^+$	$[IO_3^-]\ [H^+]^6/[Ag^+]\ [I_2]^3 = 1.68x10^{33}$
$I_2(aq) + I^- \rightleftarrows I_3^-$	$[I_3^-]/[I_2]\ [I^-] = 710$
$AgI(s) \rightleftarrows Ag^+ + I^-$	$[Ag^+]\ [I^-] = 8.32x10^{-17}$
$Ca(OH)_2 \rightleftarrows Ca^{2+} + 2OH^-$	
$Ca(OH)_2 \rightleftarrows CaOH^+ + OH^-$	$[CaOH^+]\ [OH^-] = 1.7783x10^{-4}$

Because there is the potential for iodide in solution to form volatile species, there is the potential for iodide to escape the solution. The tendency for iodine to escape the solution is measured by a partition coefficient which is defined as:

$$\text{Partition Coefficient} = \frac{\text{moles of iodine in solution}}{\text{moles of iodine in vapor}}$$

Estimates of this partition coefficient have appeared in the literature [43].

Quantitative analysis of the hydrolysis and vaporization equilibria listed above leads to the conclusions:

1. with increasing acidity of the water, the partition coefficient decreases,

2. the partition coefficient increases with dilution of the iodine solution, and

3. the variation of the partition coefficient with temperature depends on the acidity and iodine concentration of the aqueous phase.

Equilibrium analysis of the behavior of iodine species and the partitioning of iodine between the aqueous and vapor phases is not likely to be entirely satisfactory because:

1. radiolysis will affect the partitioning,

2. the gas phase in reactor containment is not at equilibrium especially whenever both O_2 and H_2 are present, and

3. other species dissolved in the water--such as Cd^{2+} or Ag^{+}--can alter the partitioning by reacting with iodide to form insoluble precipitates.

The vapor-liquid partitioning of iodine can be responsible for long-term, low-level release of iodine. This, of course, is quite different than the prompt, intense release of iodine envisaged by the Reactor Safety Study. The radiological consequences of slow iodine release from aqueous solutions are very much mitigated by the rapid radioactive decay of iodine.

Other fission product species, nominally quite soluble in water, will partition between the aqueous and the gas phases. For instance, ruthenium tetroxide engages in such a process:

$$RuO_4(g) \rightleftarrows RuO_4(aq)$$

Quantitative evaluations of the partitioning of these other radionuclides between the aqueous and vapor phases under reactor accident conditions have not been reported.

Recommendation to MELCOR Concerning Iodine Partitioning. It is recommended that MELCOR allow for iodine partitioning between water and the containment atmosphere. The equilibrium partial pressure of I_2 in the atmosphere can be defined as

$$P_{I_2}^{eq} = C_I/K$$

where $P_{I_2}^{eq}$ = equilibrium I_2 partial pressure

C_I = total iodine concentration in water pools (moles/liter)

K = user-supplied partition coefficient with a default value of 1×10^4

The approach to equilibrium can be calculated knowing the surface area of water pools in the containment, A, and a mass transport coefficient, K_m, appropriate for the flow conditions over the water pools:

$$\frac{dN_{I_2}}{dt} = \frac{K_m A}{RT} [P_{I_2}^{eq} - P_{I_2}(t)]$$

where N_{I_2} = moles of I_2 in the containment atmosphere

R = gas constant

$P_{I_2}(t)$ = I_2 partial pressure in containment at time t

There appears at this time to be no need to recognize partitioning of other fission products between water and the containment atmosphere.

Mechanical Release From Water. Water pools within the containment will contain, for the reasons outlined above, fission products. These fission products will be dissolved or present as particulate. The decay heat from the fission products will tend to keep the water pools at or near the boiling point as the reactor containment pressurizes. Should the containment suddenly depressurize, the superheated water pools will boil spontaneously. If the depressurization is rapid, vigorous boiling will entrain water droplet laden with dissolved and particulate fission products. That is, sudden depressurization can reverse the mitigation of the severe accident source term provided by water entrapment of fission products. The extent of water entrainment by flash boiling depends on (1) the rate at which the containment depressurizes and (2) the geometry of the water pool.

Brockmann [23] has formulated a model of liquid entrainment caused by the boiling of water pool during depressurization of containment. The pressure within the containment during depressurization is given by:

$$\frac{dP}{dt} = -\frac{PQ}{V}$$

where
P = pressure
t = time
V = containment volume
Q = volumetric flow rate

The volumetric flow rate depends on the size of the hole in the containment. When the flow is choked:

$$Q = 0.65\, A_o C_D\, (RT/MW)^{1/2}$$

where
A_o = hole area
R = universal gas constant
T = absolute temperature of the containment atmosphere
MW = mean molecular weight of the containment atmosphere
C_D = orifice drag coefficient = 0.61

When the flow out of the containment is subcritical:

$$Q = 4.19\ A_o\ C_D\ (RT/MW)^{1/2}\ [(P_a/P)^{1.77} - (P_a/P)^{1.89}]^{1/2}$$

where P_a is the pressure of the atmosphere surrounding the containment.

The temperature of the water is assumed to adjust to the saturation temperature of water throughout the depressurization

$$T(K) = \frac{3576}{11.342 - \ln P(\text{atms})} + 57.8$$

The rate at which mass evaporates from the water pools is given by:

$$m_v = - \frac{C_p}{h_f} m_f \frac{dT}{dt}$$

where m_v = mass evaporation rate
C_p = specific heat of water
h_f = enthalpy of vaporization of water
m_f = mass of water in the pool

The evaporating water entrains liquid:

$$E = \frac{m_e}{m_v} = 3.8\text{x}10^{-5}\ (K^{1/2} + 530K^{2.1})\ [(\rho_f - \rho_g)/\rho_g]^{1/2}$$

where m_e = mass rate of entrainment

ρ_f = density of water

ρ_g = density of water vapor

$K = D_c\ j_c$

$j_c = U_v\ (\rho_g)^{1/2}/[g\sigma(\rho_f - \rho_g)]^{1/4}$

$D_c = 4U_V\ [n_g\rho_g/g(\rho_f - \rho_g)]^{1/3}\ [\sigma/g(\rho_f - \rho_g)]^{-1/2}$

U_V = superficial velocity of water vapor off the pool surface

g = gravitational acceleration

n_g = viscosity of water vapor

σ = surface tension of water

The size distribution of water droplets entrained by evaporating water is assumed by Brockmann to be lognormal with a geometric standard deviation of 2.3 and a geometric mass mean diameter, DGM, of

$$\mathrm{DGM} = \begin{cases} D_s/2 & \text{if} \quad D_c > D_s \\ D_c/2.3 & \text{if} \quad D_s > D_c \end{cases}$$

where $D_s = 12\sigma/\rho_f U_v^2$

$$D_c = 4U_v n_g \sigma_g/(\rho_f g)^2$$

Some results for a specific accident at the Surry reactor obtained with Brockmann's model are shown in Figures 4.15 and 4.16. The mass geometric mean particle size increases with the area of the hole in containment to a plateau of 50-3000 µm for a hole area of about 100 m^2. The entrained mass increases sharply with hole area. Significant entrainment is obtained only when holes sizes are large (10-100 m^2).

Recommendation to MELCOR Concerning Re-entrainment from Water. Re-entrainment during containment depressurization should be recognized by MELCOR. The model developed by Brockmann is sufficiently simple. It can be implemented in MELCOR. The containment hole size may have to be a user-supplied value. A default value of 1 m^2 would allow a rather modest amount of release by re-entrainment from water pools.

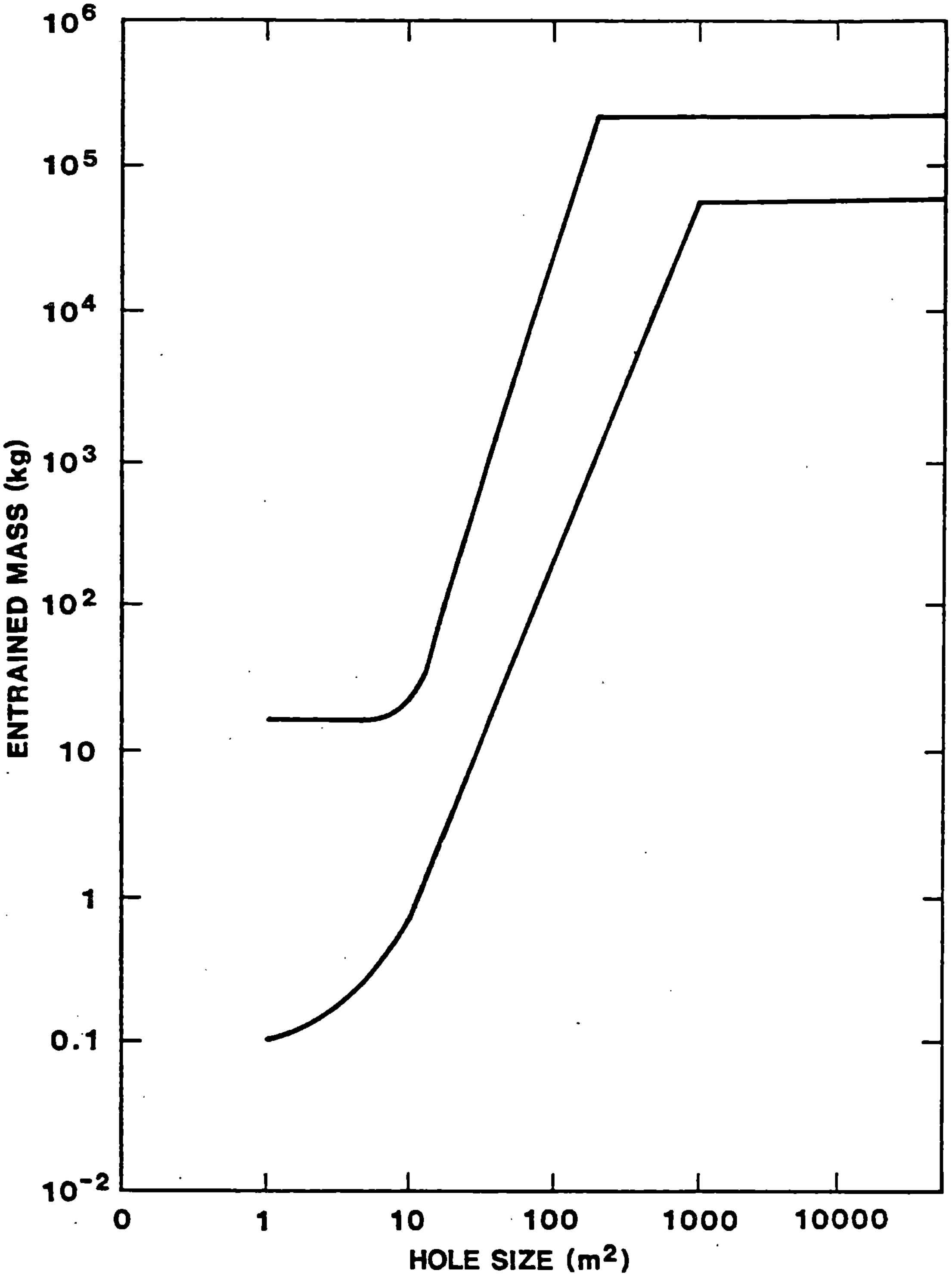

Figure 4.15. Bounding Estimates Obtained with the Brockmann Model of Entrainment of Water During Containment Depressurization as a Function of the Containment Hole Size [23].

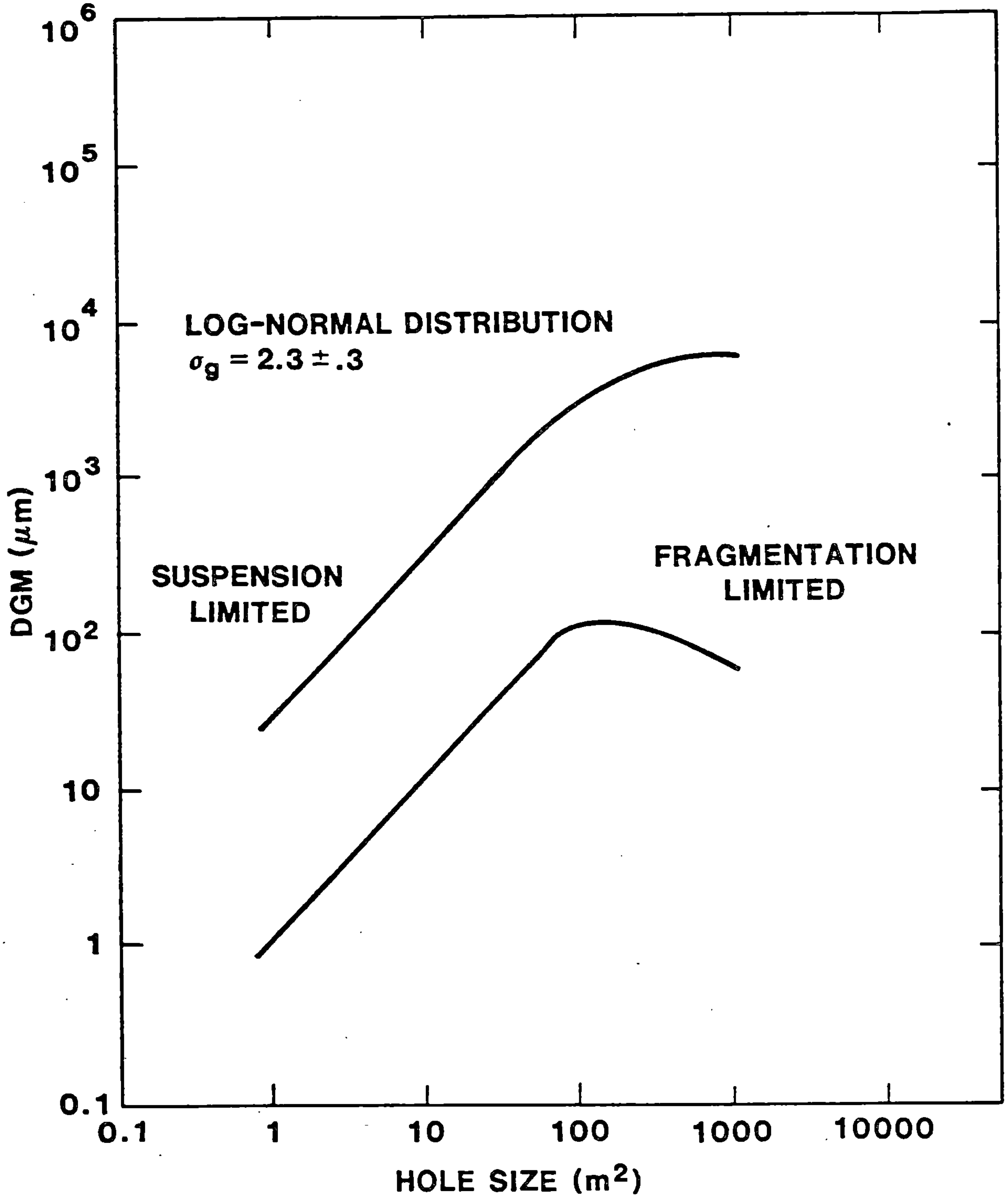

Figure 4.16. Mean Particle Size Predicted With the Brockmann Model of Entrained Water During Containment Depressurization as a Function of the Size of the Hole in Containment [23].

4.4 Conclusions

The ex-vessel sources of fission product release may be categorized as "primary processes" involving the core debris and "secondary processes" that involve resuspension of material that had previously escaped the core debris. Releases of aerosols and fission products associated with melt ejection from the primary system, core debris-coolant interactions, core debris-concrete interactions and groundwater leaching are the most important primary mechanisms. Resuspension of aerosols, vapor partitioning of fission products dissolved in water, and mechanical release of dissolved or suspended material from water are the most important secondary release processes.

Aerosol and fission product release that occurs when a melt is ejected from pressurized primary system was not recognized in the Reactor Safety Study. Recent analyses of the fission product source term associated with steam explosions suggest the Reactor Safety Study estimate of this source may have been too high. Significant improvements have been made in the capabilities to model fission product and aerosol releases during core debris concrete interactions. The effects of coolant waters on this source term can be estimated. Scoping studies support the contention that fission product release by groundwater leaching is not as significant an effect as intense, airborne release of fission products except when very specialized circumstances are present.

Secondary release process can reverse or certainly limit the effectiveness of natural or engineered source term mitigation features of a nuclear power plant. Of the secondary processes, only vapor phase partitioning of dissolved iodide has received great attention. Qualitative indications from a nonnuclear data base suggest there are many instances in a severe reactor accident in which resuspension of deposited or sedimented aerosols would be a serious concern. Data are available to qualitatively assess the likelihood of aerosol resuspension to occur in severe accidents. Similarly, resuspension of dissolved or entrapped material in pools of water by the mechanical action of sparging bubbles or boiling can be quantified. It is apparent that this effect poses a limit to the decontamination that can be achieved with water during a severe accident.

References

1. U. S. Nuclear Regulatory Commission, Reactor Safety Study: An Assessment of Accident Risks in U. S. Commercial Nuclear Power Plants, NUREG-75/014, WASH-1400, Washington, DC, October 1975.

2. R. L. Ritzman, et al., "Release of Radioactivity in Reactor Accidents," Appendix VII to Reactor Safety Study - Reference 1.

3. J. Gieseke, et al., Radionuclide Release Under Specific Accident Conditions, Volume I: A PWR Analysis, BMI-2104 (Draft), Battelle Columbus Laboratory, Columbus, OH, January 1983.

4. T. Y. Chu, J. H. Bentz, F. E. Arellano, J. E. Brockmann, M. E. Field, and J. D. Fish, Report on Large-Scale Molten Core/Magnesia Interaction Test, NUREG/CR-3438, SAND83-1692, Sandia National Laboratories, Albuquerque, NM.

5. J. B. Rivard, "Review of In-Vessel Meltdown Models," Sandia National Laboratories, Albuquerque, NM, July 1980.

6. D. Alpert, unpublished results, 1983.

7. R. Henry, Section 3 in Zion Probabilistic Safety Study, Commonwealth Edison Co., 1982.

8. W. W. Tarbell, J. E. Brockmann, M. Pilch, High Pressure Melt Streaming (HIPS) Program Plan, NUREG/CR-3025, SAND82-2477, Sandia National Laboratories, Albuquerque, NM, June 1983.

9. M. Pilch, Advanced Reactor Safety Research Quarterly Report, January-March 1982, NUREG/CR-2679 (1 of 4), SAND82-0904 (1 of 4), Sandia National Laboratories, ALbuquerque, NM.

10. D. A. Powers, "Gas Solubility in SPIT Melts," Memorandum, Sandia National Laboratories.

11. M. Weinstein and J. F. Elliott, Trans. Met. Soc. AIME 227 (1963) 382.

12. M. Blander, W. R. Grimes, N. V. Smith and G. M. Watson, J. Phys. Chem. 63 (1959) 1164.

13. J. Nichols, Contrib. Mineral. Petrol. 74 (1980) 211.

14. W. W. Tarbell, Technical Highlights/Administrative Report for the Nuclear Regulatory Commission Advanced Reactor Safety Reseach Program, March, 1983, Sandia National Laboratories, Albuquerque, NM, May 1983.

15. M. Tomaides and K. T. Whitby, "Generation of Aerosols by Bursting of Single Bubbles," in Fine Particles: Aerosol Generation, Measurements, Sampling, and Analysis, B. Y. U. Liu, Ed., Academic Press, Inc., New York, New York.

16. M. Pilch, unpublished results.

17. K. A. Peakall and J. E. Antill, J. Nucl. Materials 2, (1960) 194.

18. M. Iwasaki, T. Sakukrai, N. Ishikawa, and Y. Kobayashi, J. Nucl. Sci. Tech 5, (1968) 652.

19. J. Bittel, L. H. Sjodahl and J. F. White, J. Am. Ceramic Society 52, (1969) 446.

20. D. Cubicciotti, Nuclear Technology 53, (1981) 5.

21. L. S. Nelson, Pyrodynamics 3, (1965) 121.

22. D.G.C. Robertson and A. E. Jenkens, in Heterogenous Kinetics at Elevated Temperatures, G. R. Belton and W. L. Worrell, eds., Plenum Press, 1970.

23. R. J. Lipinski, et al., Uncertainty in Radionuclide Release Under Specific LWR Conditions Volume II: Analyses, SAND84-0410/2, Sandia National Laboratories, Albuquerque, NM.

24. M. Pilch, "Direct Heating of Containment Atmosphere by Airborne Core Debris," contribution to the Containment Loads Working Group final report, dated May 3, 1984.

25. G. W. Parker, et al., ORNL-3319, Oak Ridge National Laboratory, Oak Ridge, TN, August 1962.

26. B. M. Jeffrey, J. Nucl. Materials 22, (1967) 33.

27. M. Corradini, "Hydrogen Generation During Molten-Fuel-Coolant Interactions," Second Workshop on the Impact of Hydrogen on Water Reactor Safety.

28. D. A. Powers, "A Re-Examination of the Steam Explosion Source Term During Severe Accidents," paper IAEA-SM-281/34, Intl. Symp. on Source Term Evaluation for Accident Conditions, 28 Oct. to 1 Nov., Columbus, OH, IAEA, 1986.

29. D. A. Powers, "Aerosol Generation During Core Debris Interactions with Concrete," 7th International Light Water Reactor Safety Information Exchange, Gaithersburg, MD.

30. W. B. Murfin and D. A. Powers, Report of the Zion Indian Point Study: Volume I, NUREG/CR-1410, SAND80-0617/1, Sandia National Laboratories, Albuquerque, NM, August 1980.

31. D. A. Powers and J. E. Brockmann, "Release of Fission Products and Generation of Aerosols Outside the Primary System," Appendix C in J. Gieseke et al., Radionuclide Release Under Specific LWR Accident Conditions, Volume 1: PWR Analyses, BMI-2104, Battelle Columbus Laboratory, Columbus, OH, January 1983.

32. J. F. Muir, et al., CORCON-MOD1: An Improved Model for Molten/Core Concrete Interactions, SAND80-2415, NUREG/CR-2142, Sandia National Laboratories, Albuquerque, NM, July 1981.

33. N. A. Fuchs, The Mechanics of Aerosols, Pergamon Press, 1964.

34. Office of Nuclear Reactor Regulation, U.S. Nuclear Regulatory Commission, Liquid Pathways Generic Study, NUREG-0440, February 1978.

35. H. Westrich, J. Nucl. Materials 110, (1982) 324.

36. J. W. Braithwaite and J. K. Johnson, Light Water Reactor Safety Research Quarterly Report, October-December 1977, NUREG/CR-0307, SAND78-0600, Sandia National Laboratories, Albuquerque, NM, June 1978.

37. D. A. Powers, Advanced Reactor Safety Research Quarterly Report, January-March 1980, NUREG/CR-1594 (1 of 4), SAND80-1646 (1 of 4), Sandia National Laboratories, Albuquerque, NM.

38. H. J. Matzke, "Actinide Diffusion in Waste Glasses," Thermodynamics of Nuclear Materials, Vol. 1, IAEA, Vienna, Austria, 1980, p. 311.

39. M. Corn, J. Air Poll. Control Assoc. 11, (1961) 566.

40. M. Corn and F. Stein, Amer. Ind. Hyg. Assoc. J. 26, (1965) 26.

41. M. C. Kordeki and C. Orr, Arch. Env. Health 1, (1960) 1.

42. F. P. Bowden and D. Tabor, The Friction and Lubrication of Solids, Clarendon Press, Oxford (1954).

43. J. T. Bell, et al., "Chemistry of Cesium and Iodine," Chapter 5 in Technical Bases for Estimating Fission Product Behavior During LWR Accidents, NUREG-0772, U.S. Nuclear Regulatory Commission, June 1981.